DISSERTATION

STAKEHOLDER VALUE BASED OPTIMIZATION OF HYBRID PROPULSION SYSTEMS FOR MID-SIZED REGIONAL AIRCRAFT

Submitted by

Todd Spierling

Department of Systems Engineering

In partial fulfillment of the requirements

for the Degree of Doctor of Philosophy

Colorado State University

Fort Collins, Colorado

Spring 2026

Doctoral Committee:

Advisor: Thomas Bradley

Daniel Herber
Kamran Shahroudi
John Williams

ABSTRACT

STAKEHOLDER VALUE BASED OPTIMIZATION OF HYBRID PROPULSION SYSTEMS FOR MID-SIZED REGIONAL AIRCRAFT

Electrified propulsion is increasingly recognized as a key solution to address the sustainability challenges of the growing air transport sector. Traditional studies have often focused on specific configurations of electrified aircraft, analyzing their aerodynamic performance or environmental benefits. However, a comprehensive methodology to evaluate and optimize powertrain configurations based on a deep understanding of customer objectives has been lacking. This research has aimed to fill this gap by developing an analysis and evaluation methodology that captures and quantifies the most important customer requirements. This methodology utilizes physics-based characteristics and penalty factors related to changes in powertrain configuration and optimizes the overall system according to the specified concept of operations. It also includes sensitivity evaluations to assess the robustness of the system to variations in operating needs or technological advancements. The design methodology outputs were validated by comparing them with previous point designs, ensuring the reliability of the characterization and calculation methods. The optimization functionality was then tested to confirm the potential economic benefits for customers. This approach enables faster and more robust exploration and optimization of hybrid electric powerplants, reducing concept design cycle times and enhancing aircraft performance and economic attractiveness. Consequently, it is expected to lead to

increased airframer adoption and implementation, bringing significant environmental benefits.

ACKNOWLEDGEMENTS

I would like to thank the following people who have helped me on this research journey:

- My advisor Dr. Thomas Bradley for his assistance, encouragement, and enthusiasm for this project. He kept me focused and inspired me to drive through to the end.
- My PhD committee (Dr. Daniel Herber, Dr. Kamran Shahroudi, Dr. John Williams) for their time and valuable feedback.
- My colleagues at Collins Aerospace and Pratt & Whitney for their knowledge and advice on this topic and my approach to it. My time with the company guided me to my research topic and my research has brought benefit back into the corporation.
- My wife Kara for her endless patience and support. It was a long journey and I couldn't have done it without her.

DEDICATION

I dedicate this research to all of those in industry, academia, and government who have spent their careers advancing the aviation industry. They have not only brought it to where it is today but are positioning it as a valuable and responsible element of society for future generations to come.

TABLE OF CONTENTS

LIST OF FIGURES

LIST OF TABLES

LIST OF SYMBOLS

$C_{battery}$	Battery cycles to replacement
d_p	Propellor diameter (m)
e_{bat}	Specific energy of battery (w-hr/kg)
e_f	Specific energy of fuel (w-hr/kg)
E_{bat}	Battery energy (w-hr)
E_f	Fuel energy (w-hr)
g	Gravity (m/s^2)
L/D	Lift to drag ratio
L_D	Propellor disc loading (w-m/kg)
n	Propellor rotational speed (revolutions/sec)
n_{DEP}	Depreciation period (years)
OEW	Operating empty weight (kg)
P_{bat}	Battery power (kW)
P_{engine}	Thermal engine power (kW)
P_f	Fuel power (kW)
R	Range (km)
u	Propellor tip speed (m/s)
V_{TAS}	Aircraft true airspeed (m/s)
W_{bat}	Weight – battery (N)
W_f	Weight – fuel (N)
W_{OE}	Weight – operating empty (N)
W_{PL}	Weight – passengers +payload (N)
η_{gt}	Gas turbine efficiency
η_m	Motor/motor drive efficiency
η_p	Propellor efficiency
λ	Propellor advance ratio
ρ	Density (kg/m^3)
Φ	Power ratio

Chapter 1 - Introduction and Background

Aviation Megatrends

Aviation has long been an area where worldwide forces and technology innovations have come together to drive fundamental changes within the industry. Some have argued that we are now in the “Third Era of Aviation” – the first being the original piston engine aircraft, the second being gas turbine powered aircraft, and the third being the introduction of Electrification to aircraft propulsion [1].

There are several forces that are driving the innovation of this new era. The trends of population growth/urbanization and increased focus on sustainability and environmental issues have resulted in new and increasing demands on the aviation sector. Continuing commercial pressures on airlines cause challenges to airline profitability and motivation to provide affordable air service in many areas, particularly in the absence of government incentives and/or mandates.

The first major force is the growth in world population which, along with increasing affluence, result in the continuing growth of travel demand and aviation. World population has doubled in the last 50 years, with most of this growth (at least in absolute terms) occurring in Asia. Much of this growth has occurred in urban areas. While annual population growth rate has slowed in recent years, it has maintained at 1-2% for much of the latter 20th and early 21st centuries [2].

The growth rate of air travel, however, has exceeded that of the population at large. Air travel has grown at an annual rate of 4-5% over the last 25 years, and it is expected to continue at almost this rate for at least the next 25 years as illustrated in Figure 1 [3], with Airbus predicting a growth rate in the large commercial aircraft sector of approximately 4.4% [4].

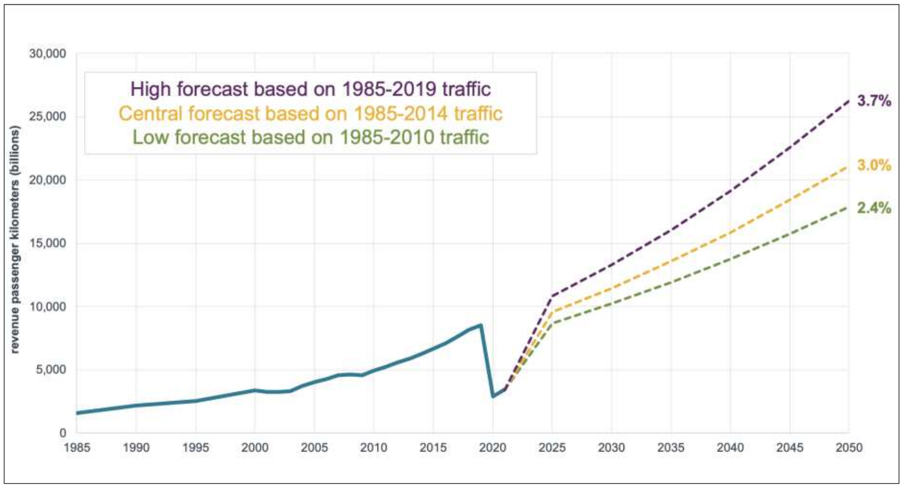

Figure 1 Historical and Projected Future Air Traffic Levels – All Markets [3]

If you only focus on the regional aircraft market, ATR projects an annual traffic growth rate of approximately 4.9%, greater than the overall commercial airline market as shown in Figure 2 [5].

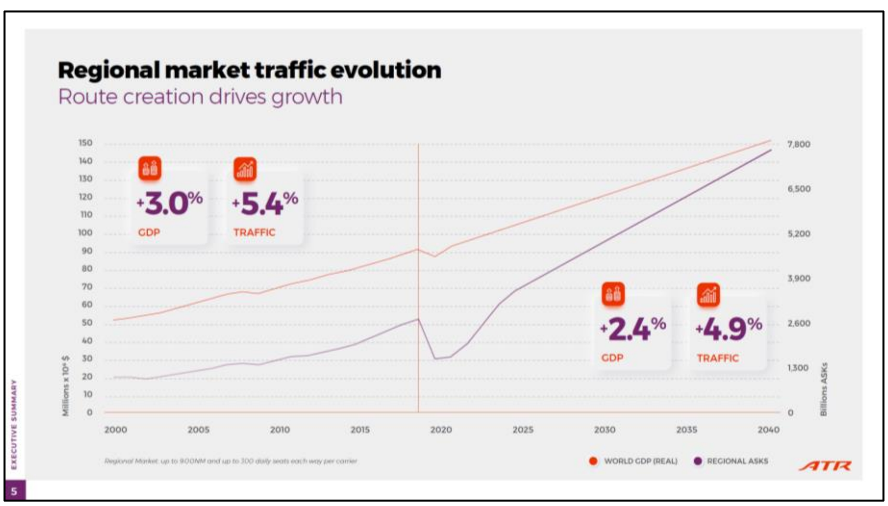

Figure 2 Historical and Projected Future Air Traffic Levels - Regional Markets [5]

This growth is due not only to more traffic on existing routes, but also due to an increase in the number of routes. This route growth is geographic region sensitive as illustrated in Figure 3, ranging from 5% in Africa to 34% in the Asia Pacific region, which aligns with greater population growth and urbanization in that region [5].

Figure 3 New Route Creation by World Region [5]

This increased air traffic, however, comes at an environmental price, which is related to the second trend of environmental sustainability. While carbon emissions due to aviation have held steady at approximately 2.5% of overall carbon emissions worldwide, the absolute level of aviation carbon emissions has steadily increased, and now stands at approximately 1 billion tons/year [6, 7]. This is despite an average yearly increase in aircraft fleet fuel efficiency of 1.3% in the years between 1960 and 2014 [8]. This carbon footprint has become more of a social issue in recent years, and “flight shaming” threatens to impact future airline growth, most pointedly in European and North American markets [9].

The last trend driving change is the commercial pressure on airlines, impacting the routes that they can profitably serve. Currently, 0.6% of US airports support over

70% of US domestic air travel [10], resulting in large numbers of locations that are not being served to their full potential. The number of US regional domestic routes has decreased by more than 30% since the year 2000 [5]. As illustrated in Figure 4 below, the airline industry is intensely competitive, with very small (sometimes negative) margins between revenue and cost [11]. As the pace of new aircraft introduction has slowed, and fuel economy improvements to traditional gas turbines are beginning to plateau [12], it can be seen that airline cost structures have remained relatively constant over the last twenty years, This has led to investigation of nontraditional propulsion configurations such as hybrid electric that have the potential to continue the downward cost progression.

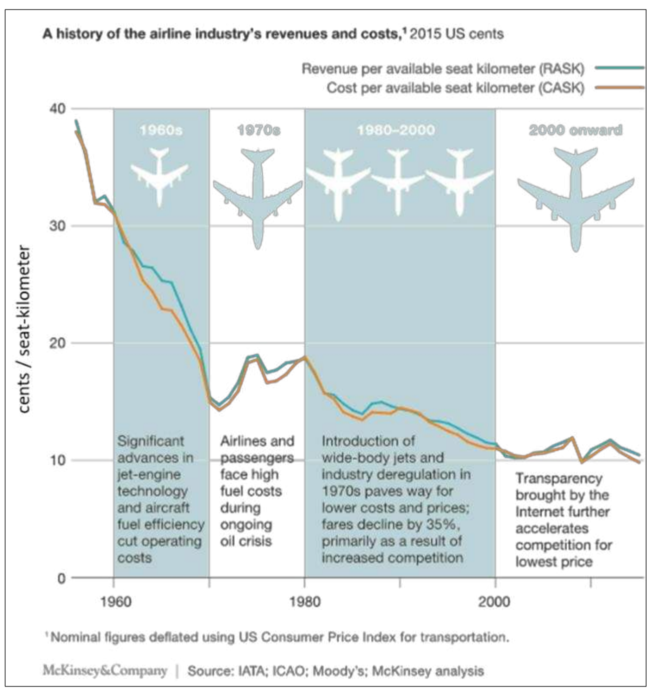

Figure 4 Commercial Airline Revenue/Cost History [11]

In combination, these trends illustrate that aviation needs to become bigger (in terms of greater seat-km per year), cleaner (in terms of absolute greenhouse gases despite rising seat-km), and more economically attractive (in terms of $ per seat-km). This is a substantial, complex technological/economic problem that needs to be addressed through the application of advanced systems engineering approaches.

Background Information

A variety of aviation groups have studied these trends, and presented industry with a series of challenges, particularly around carbon emissions. Various stakeholders have started programs aimed at mitigating aviation's climate change impact, such as ACARE's Flightpath 2050 [13]. Comparable actions have been announced by IATA [14], ICAO [15], and NASA [16], committing the commercial aviation industry to the ambitious goal of achieving "net-zero' carbon emissions by the year 2050 [17]. One of these groups, the Air Transport Action Group (ATAG), has published a widely cited study [18] of projected aviation carbon emissions with no changes, as well as anticipated effects from various technology and operational improvements as illustrated in Figure 5.

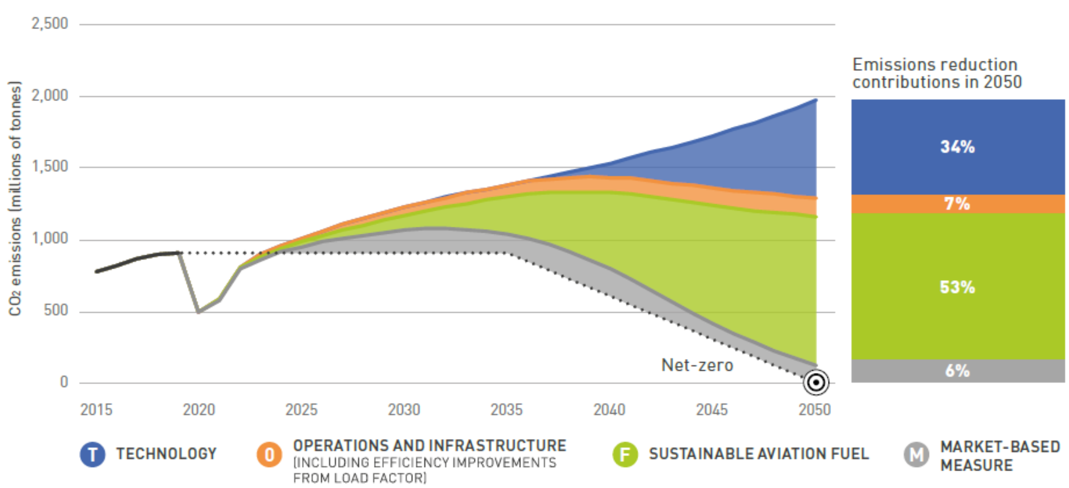

Figure 5 ATAG Carbon Emissions Projections [18]

Hybrid electric aircraft have been widely studied as one of the referenced technological advancements, with the promise of significant reduction in fuel burn, energy consumption and CO_2 emissions compared to conventional aircraft. There are a wide variety of potential electric or hybrid electric propulsion system configurations, with several of the most popular illustrated below in Figure 6 [19].

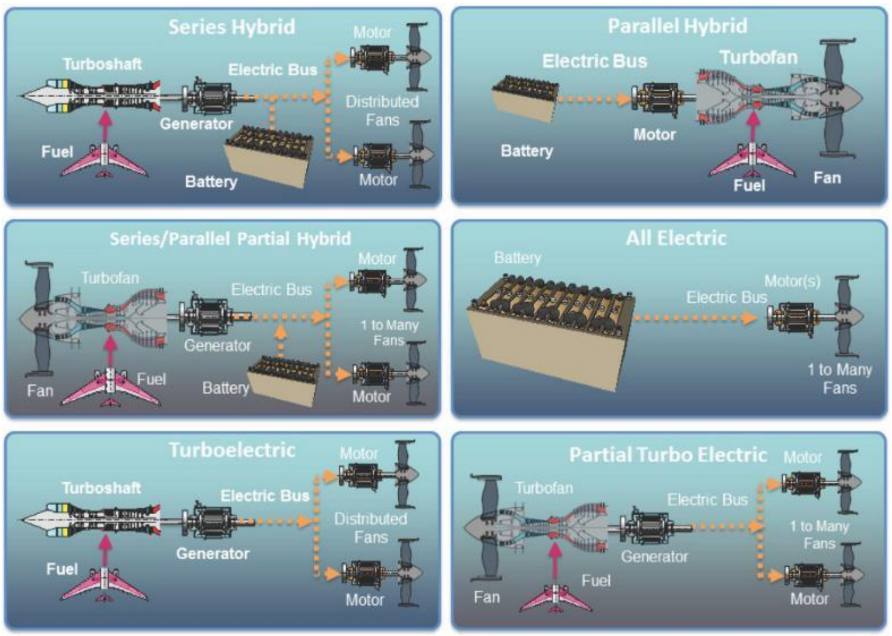

Figure 6 Examples of Electric Propulsion Architectures [19]

In comparing the performance of the powertrain architecture options, researchers have developed an understanding of the benefits and drawbacks of each. The series or turbo-electric architectures in which a prime mover drives a generator to create electric power distributed to electrically driven propulsors have been shown to provide little to no fuel burn benefit due to the electric drivetrain weight and losses [20, 21]. Even with the potential for improved propulsive efficiency and aircraft L/D with distributed propulsion and propulsion airframe integration, there have been few concepts proposed that could provide an overall aircraft-level benefit. Jansen [22, 23] provides a parametric study showing the electrical drivetrain power density and efficiency necessary for a single-aisle aircraft turbo-electric [22] or partial turbo-electric [23] (gas turbine provides direct propulsion plus electric power) based distributed propulsion system to provide an overall aircraft energy consumption reduction. This work shows that very high electric drivetrain power density and efficiency will be required compared to a traditional under-wing gas turbine if there is no efficiency improvement in the electric drivetrain gas turbine prime mover.

In contrast, several studies have shown the potential benefits of a parallel hybrid propulsion system [24, 25, 26, 27, 28], in which the propulsor is powered by a combination of a gas turbine core and an electric motor. These previous studies have focused on single aisle class aircraft. Motivated by these benefits, the author’s current research has investigated the parallel hybrid architecture for a turboprop 30-50 passenger class aircraft. As shown in Figure 7, the parallel hybrid turboprop propulsion system is comprised of a combustion engine and an electric motor integrated on a combining gearbox that drives a common propeller. Fuel and a fuel system feed the combustion engine, while an electric drive train comprised of a battery pack, distribution system (Dist) and motor drive (MD) feed the motor.

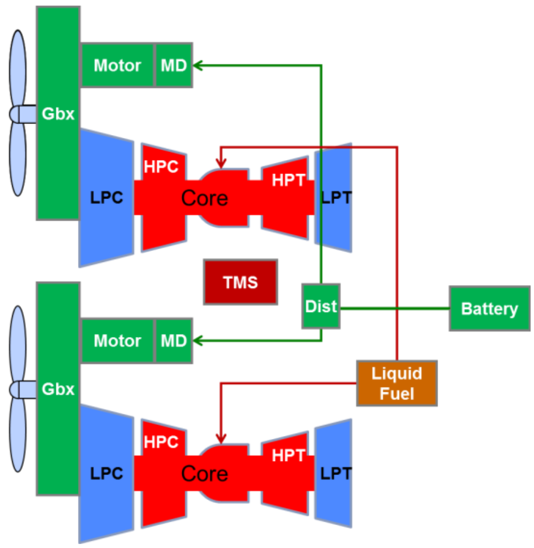

Figure 7 Parallel Hybrid Turboprop Architecture

The studies and methodologies presented to date [29, 30, 31, 32, 33, 34, 35, 36, 37, 38, 39], however, are not amenable to the regional aircraft design/optimization/commercialization problem that would enable the future implementation of commercially viable sustainable aviation. Previous work has focused on pure aerodynamic performance, assessing attributes such as range, speed, climb rate, fuel burn, etc., has been performed for vehicles (either significantly smaller or larger) outside of the range of interest, or has only considered fuel and battery costs in their cost assessments. These attributes are important to determine gross technical viability of a given configuration, but do not address the economic attractiveness of a particular solution relative to existing legacy regional aircraft, which is of primary importance to the ultimate customer for this technology, the regional commercial airlines.

The operating economics of commercial airline operations are complex and consist of multiple cost elements. A Direct Operating Cost (DOC) breakdown of a typical regional airline is shown in Figure 8 below [40].

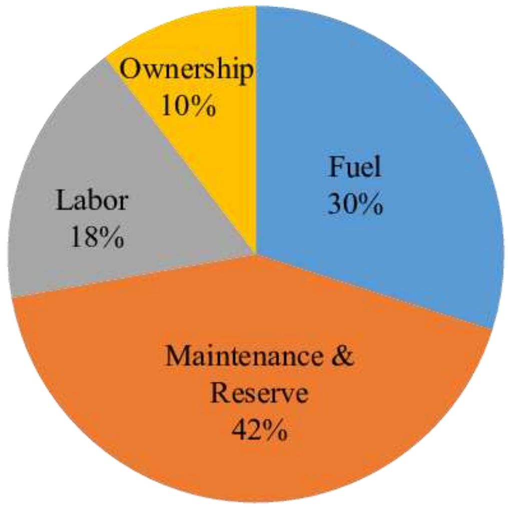

Figure 8 Typical Airline Direct Operating Costs

As this chart illustrates, fuel, crew, and maintenance costs are the largest cost drivers for daily operations. Fuel costs (either jet fuel or electricity) will be influenced by the amount of energy consumed on a given flight, and the relative costs of each energy type. Crew costs will be impacted by flight speeds and refueling/recharging times (how many flights can be completed in each crew shift) if those turn times increase beyond legacy aircraft. Maintenance costs will be driven by part/repair costs, reliability, and need for scheduled maintenance. Ownership costs will be impacted by the initial purchase price of the aircraft and its expected useful life. The remaining costs are largely independent of propulsion system configuration and can be considered as constant in this research activity.

Revenue will also be a key element of the overall economic picture. The number of flights per day that can be conducted by a given aircraft and the average per-seat price will determine daily revenue. Possible price premiums for flights on "green" aircraft will need to be considered to determine if there is market potential for increased revenues.

Aircraft Segment of Interest

The focus of this research is stated as "mid-sized regional aircraft". For purposes of clarity, this segment is categorized as twin-engine turboprop aircraft, with passenger capacity of approximately 30-50 seats. Examples of aircraft in this category are illustrated in Figure 9 below.

Figure 9 Typical Mid-Sized Regional Aircraft

Mid-sized turboprop aircraft continue in wide use across the world, with Table 1 illustrating the breakdown of the roughly 2000 aircraft in revenue airline service. Most operators are small airlines that operate fleets of less than 20 aircraft, although there are a few notable exceptions such as Wideroe with 46 DeHavilland Dash 8, or IndiGo with 50 ATR42/72 [41].

Table 1 Commercial Revenue Fleet by Aircraft Type

Aircraft Type	Number Built to Date	Number of Commercial Airlines Currently Operating	Number of Aircraft in Commercial Airline Service
ATR 42/72	1736	152	965
DeHavilland Dash 8	1258	108	687
Saab 340	459	31	144
Fokker F27/50	799	28	81
Embraer 120	358	38	69
Dornier 328	107	6	16

Ultimately, due to the number of aircraft in service, as well as the fact that it is still in production, the ATR42/72 family was chosen as the use case for this evaluation method.

Chapter 2 - Research Agenda

Based on the above reflections on the state of the field, we can identify a set of key research gaps in the field of electrified aviation. In particular, the research on electrified aviation that exists in the literature today concentrates on an aircraft-centric and technology-centric viewpoint of the purpose, value and considerations for electric aviation. This dissertation and associated research effort will seek to develop a more comprehensive and system-level approach to electric aviation system design including considerations such as customer preferences, operational costs and benefits, and optimal powerplant designs that are sited within real-world operational contexts.

To develop the new systems engineering knowledge that can fill those knowledge gaps, this dissertation proposes a research agenda in the form of 5 research questions, as follows.

Research Question 1) What are the prioritized weighted metrics important to regional airline customers? Understanding what is important to customers is key to optimizing a system to meet that need.

The results of activity will be a consolidated input dataset of airline operator preferences to be considered, expected limits on those preferences, and default starting values to be used in lieu of specific requirements for a given use case. These will be compared and contrasted to the design metrics that have been proposed in previous environmentally improved aircraft design literature to resolve the differences between the regional aircraft manufacturer requirements and those that have informed the field to date.

Research Question 2) How can systems designers determine and characterize important hybrid electric configuration elements through empirical and physics-based models? Optimizing the system will require an understanding of how physical and performance characteristics of the key elements change as configurations and power ratings as modified as a part of that higher level optimization.

The results of this activity will be a set of simulation, equation-based, or empirical models that can be incorporated into the analysis/optimization framework that will be defined as a part of research question 3. These models will be multi-dimensional in nature (specific power versus reliability versus efficiency versus cost are interrelated and can be traded against each other) and will be validated against in service or development test data. This will be a significant advancement over current models that do not readily allow tradeoffs between multiple aspects of performance. They will also be based on near full-scale products and will not be a scaling of vastly different products or power ratings.

Research Question 3) How do systems designers identify and create suitable analysis and optimization methods and tools? An analysis methodology must be defined to determine the performance of a particular configuration, and then to also be able to optimize the configuration if desired to maximize the customer value.

The result of this activity will be a functional analysis and optimization tool that will incorporate the weighted customer metrics from task 1 and the component characteristic models from task 2. At this stage, the validity of the models will not be asserted, only the base functionality of the toolset in enabling the definition of verifiable, optimal configurations.

Research Question 4) How can the analytic tools and methodologies be validated for known configurations? Few examples of hybrid electric regional platforms will have flown prior to this research being completed, but the tools will need to be validated based on flight testing or predictive analyses performed by other researchers.

The results of this activity will be a validated analytic tool that will provide trusted results for a given set of inputs across the defined range of applicability. This tool will not yet have demonstrated the optimization efficiency or effectiveness.

Research Question 5) What needs to be done to perform optimization exercises on a variety of use cases to demonstrate the costs and benefits of the proposed optimization approach? The significant value of the tool is not just to analyze for a given set of inputs and configurations, but to optimize the configuration based on a particular set of inputs to maximize customer value.

The results of this activity will be a full demonstration of the optimization capability of the toolset and its value to the aircraft and powertrain designer compared to legacy point design or heuristic methods.

Summary) Taken together, these research questions seek to understand what is important to the airline customer and to the tool's user (aircraft/powertrain designer), and to create an analysis and optimization tool that satisfies those needs. The tool will be fully validated across a defined range of applicability and will have demonstrated outputs to build confidence and show value to the designer.

Collectively, there is an identified industry need for a methodology and toolset to be able to consider this wide range of system-level airline operator metrics, and to be able to assess the comparative values of these metrics to determine the relative value of differing potential configurations. The ability of the toolset to perform optimization functions in addition to evaluation would be valued to reduce the design time needed to converge on a preferred solution subject to a particular unique set of input and weightings. This is a current gap in industry and forms the value statement for the research results that are outlined in more detail in the following chapters.

Chapter 3 - Derivation of Metrics of Importance to Airline Operators

This chapter seeks to address the research problem identified as research question 1, which is repeated below:

Research Question 1) What are the prioritized weighted metrics important to regional airline customers?

To answer this question, this chapter presents a literature search of existing industry and academic work to identify key metrics and data related to economics, operational desires, and sustainability goals for current and future regional aircraft operators, and the organizational motivations impacting adoption of new technologies. While electrified propulsion has not been implemented yet in revenue service, there has been legacy work to understand the justifications for other technology changes (such as the A320 CEO to NEO) that impact similar elements as electrified propulsion. This chapter will review and synthesize existing academic and industry studies and methods to set a baseline for the current state and identify gaps in this area that need to be complemented with further research. A targeted interview of airline operators will complement existing data. The incorporation of electrified propulsion may result in the creation/expansion of new airline operators, routes, and operating models, resulting in additional data that needs to be collected to properly address the future state of the industry instead of the legacy/current state.

Introduction / Literature Search

This section presents a literature search of existing industry and academic work to identify key metrics and data related to economics, operational desires, and sustainability goals for current and future regional aircraft operators, and the organization motivations impacting adoption of new technologies. This search reviewed and synthesized existing academic and industry studies and methods to set a baseline for the current state and identified gaps in this area that need to be complemented with further research.

There has been a range of work performed in the regional aircraft space, focused on either airline or government/societal expectations for future aircraft and regional operations. A comprehensive airline-based study was performed by Guzhva et.al. [42] which surveyed 31 operators of regional aircraft in the 20-50 seat size class. While this study focused solely on non-electrified fuel burning aircraft, it highlighted the acceptable airline tradeoffs between aircraft list price and other economic considerations such as fuel consumption, maintenance costs, and operational characteristics such as range, speed, and turnaround time. In this case, airlines were willing to trade a 5-10% new aircraft list price for 10-20% reductions in fuel consumption and maintenance costs, highlighting these elements as key measures of importance when assessing the operational value of new aircraft.

The features highlighted by regional aircraft manufacturers when promoting their aircraft also provide insight into the characteristics that they feel are of greatest importance to their potential customers. Deutsche Aircraft (Dornier) [43] highlights their D328(eco) aircraft has having “better economics (trip cost, breakeven point, fuel economy, DMC), better performance (climb/ceiling, STOL, unpaved runway), most modern turboprop (flight deck/cabin), the eco leader (CO_2 emissions)". Avions de Transport Regional (ATR) [102] similarly highlights "unbeatable economics (fuel burn, cash operating cost, direct maintenance costs, resale value), outstanding comfort, superior airport accessibility (hot/high, short, unpaved runway)". As Embraer has discussed the desired attributes of their proposed E3 turboprop aircraft, they particularly highlight cash operating costs but recognize the sensitivity of the typical turboprop customer to aircraft acquisition costs [44].

An example of a study that highlights governmental/societal expectations for future sustainable regional aircraft was the one performed by Eisenhut et.al. [45] as a part of a Horizon Europe sponsored activity. This work sets forth requirements for CO_2/NOX/Noise emissions reductions of 75%, 90%, and 65% respectively, with no CO_2 or NOX emissions during ground operations. While most performance requirements such as speed, climb rate, and takeoff field length were held comparable to the current ATR42, a major compromise was made related to range, reducing from the current maximum (with full passenger load) from 1,556 km [49] to 800 km. This is reflective of the shorter distances common to European regional operations and provides an indication of where compromises could be made to achieve economic or sustainability goals, although this activity did not include direct regional airline operator input.

A large research activity currently underway in Europe is being led by the Clean Aviation Joint Undertaking (CAJU). This is a multiyear government/industry/academia effort with approximately 1.7B euros of funding. In their Strategic Research and Innovation Agenda (SRIA), CAJU laid out a series of targets for future Regional and

Short-Medium Range commercial aircraft. While lifecycle costs were recognized as an airline consideration, this activity intentionally focused on CO_2 emissions as the primary requirement moving forward. Table 2 is from the SRIA, illustrating the CAJU target goals compared to current in-service aircraft. Similar syntheses of R&D and adoption timelines and sustainability targets have also been performed by NASA in the USA [47] as well as researchers in China [48], with a similar emphasis on climate and noise emissions as opposed to economic considerations.

Table 2 Clean Aviation Regional Aircraft Targets [46]

Aircraft Category	Key technologies and architectures to be validated at aircraft level in roadmaps	Entry Into Service Feasibility	CO_2 Emissions reduction (technology based)[28]	Net CO_2 Emissions reduction (i.e. including SAF effect)[29]	Current share of air transport system emissions
Regional Commercial Aircraft	> Hybrid-electric (SAF + Batteries) coupled with highly efficient aircraft configuration	~2035	-30%	-86%	~5%
	> Same with H2-electric power injection (Fuel Cells electric generation)	Beyond 2035	Up to -50%	Up to -90%	
Short-Medium Range Commercial Aircraft	Advanced ultra-efficient aircraft configuration and ultra-efficient gas turbine engines	~2035	-30%	-86%	~50%
Hydrogen-Powered Commercial Aircraft	Full hydrogen-powered aircraft (H2 Fuel Cells or H2-combution)	~2035	-100%	N/A	N/A

In summary, the aviation industry and associated government and private researchers have developed a broad series of sustainability goals that can inform the industry and public as to the opportunities for more fuel efficient and sustainable aviation. In general, however, these studies do not include operational considerations in their roadmapping process. The dynamics of acquisition, operations and operational changes, and economic/environmental tradeoffs are not well represented in the literature to date and point to the need for additional information gathering.

Industry Survey Methods

This review of the literature reveals a lack of direct operator feedback on regional airline needs and preferences applicable to future hybrid-electric aircraft. The incorporation of electrified propulsion may result in significant changes to legacy airline operators, routes, and operating models. This resulted in additional data that needed to be collected to properly address the future state of the industry instead of the legacy/current state. Therefore, a targeted airline operator survey/interview was conducted to expand our understanding of future anticipated industry needs.

Based on the previously cited research, interviews with Mr. Marc Kirner (Vice President of Engineering for Bangkok Airlines 1995-2004), as well as internal discussions with stakeholders at Pratt & Whitney Canada, the predominant supplier of engines to the regional aircraft market, the following questionnaire was created to assess airline ranking of performance, environmental, and economic considerations important to future aircraft configuration choices. A copy of the request letter that was sent to the airlines requesting their participation is provided as Figure 10 below.

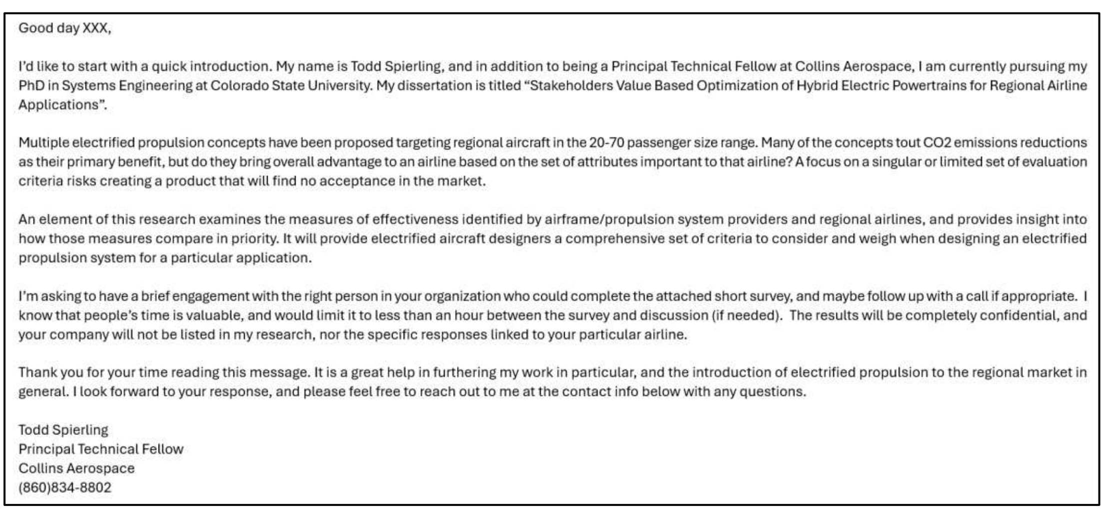

Good day XXX,

I'd like to start with a quick introduction. My name is Todd Spierling, and in addition to being a Principal Technical Fellow at Collins Aerospace, I am currently pursuing my PhD in Systems Engineering at Colorado State University. My dissertation is titled "Stakeholders Value Based Optimization of Hybrid Electric Powertrains for Regional Airline Applications".

Multiple electrified propulsion concepts have been proposed targeting regional aircraft in the 20-70 passenger size range. Many of the concepts tout CO2 emissions reductions as their primary benefit, but do they bring overall advantage to an airline based on the set of attributes important to that airline? A focus on a singular or limited set of evaluation criteria risks creating a product that will find no acceptance in the market.

An element of this research examines the measures of effectiveness identified by airframe/propulsion system providers and regional airlines, and provides insight into how those measures compare in priority. It will provide electrified aircraft designers a comprehensive set of criteria to consider and weigh when designing an electrified propulsion system for a particular application.

I'm asking to have a brief engagement with the right person in your organization who could complete the attached short survey, and maybe follow up with a call if appropriate. I know that people's time is valuable, and would limit it to less than an hour between the survey and discussion (if needed). The results will be completely confidential, and your company will not be listed in my research, nor the specific responses linked to your particular airline.

Thank you for your time reading this message. It is a great help in furthering my work in particular, and the introduction of electrified propulsion to the regional market in general. I look forward to your response, and please feel free to reach out to me at the contact info below with any questions.

Todd Spierling
Principal Technical Fellow
Collins Aerospace
(860)834-8802

Figure 10 Copy of Survey Request Letter Sent to Airlines

Table 3 below provides an illustration of the questionnaire that was included in the request. This questionnaire included a variety of potential criteria for consideration, with a yes/no question on whether that is applicable to a particular airline, and if so, the numeric importance of those criteria.

Table 3 Regional Airline Feedback Survey

METRIC	Would you consider this criteria when making a decision to upgrade or retrofit your fleet to electric or hybrid electric propulsion? (yes/no)	If the powertrain designer had the opportunity to tailor a propulsion system specifically to your airline needs, who would you prioritize the criteria? (1-9, 9 most important)
ENERGY USE/COSTS		
Total Energy Use/Revenue Seat Kilometer		
Total Energy Cost/Revenue Seat Kilometer		
Electricity Use/Revenue Seat Kilometer		
Electricity Cost/Revenue Seat Kilometer		
Jet Fuel Use/Revenue Seat Kilometer		
Jet Fuel Cost/Revenue Seat Kilometer		
ENVIRONMENTAL IMPACT		
CO_2 Emissions/Revenue Seat Kilometer		
Noise (on/near airport)		
MAINTENANCE		
Direct Maintenance Cost - planned		
Direct Maintenance Cost - unplanned		
OPERATIONAL EFFICIENCY		
Dispatch Reliability		
Turnaround Time		
Aircraft Downtime - spare aircraft needs		
AIRPORT INFRASTRUCTURE		
Airport Infrastructure upgrades		
AIRCRAFT PURCHASE/RETROFIT COST		
Acquisition Cost		
Resale Value		
AIRCRAFT PERFORMANCE		
Aircraft Range (within current route structure)		
Aircraft Range (charters, ferry for maintenance actions, etc)		
Balanced Field Length		
Cruise Speed		
Passenger Count		
Payload Capacity (weight/volume)		
TRAINING/CERTIFICATION		
Ground Crew Training		
Pilot Training/Certification		
Maintenance Training/Capitalization		

This survey was provided to 28 major regional operators who either currently operate (or have on-order) large fleets of turboprop aircraft (of any of the aircraft types meeting the definition of mid-sized regional aircraft provided earlier), asking for confidential feedback on the characteristics of interest. These airlines operate a variety of turboprop aircraft, which are of similar characteristics but from a variety of manufacturers. No specific change in weightings could be attributed to operation of a specific aircraft type, suggesting that the weightings are broadly applicable across the regional aircraft space and not just limited to ATR operators, although that is the most widely used aircraft in this space. Additionally, results should be applicable for either new or existing aircraft, unless that aircraft is of a dramatically different configuration (such as eVTOL or hydrogen fueled) that would significantly disrupt the operating model and could result in entirely new considerations. Note that this survey targeted a specific subset of operators using mid-sized regional aircraft and may not apply to airlines with other types of aircraft, route structures, or organizational models. These operators were located across Asia, Europe, and North America, providing a wide cross section of operating markets. 10 operators provided feedback on this request. This survey was sent out to the candidate airlines in October 2022, with responses received over the period of November 2022 through May 2023.

Survey Results

The results of this survey were collated into a listing that includes the characteristics that were considered and the statistical range of the customer responses related to those characteristics. The percentage of respondents who consider a particular characteristic is shown in Figure 11, while the range of the perceived importance of each of the identified characteristics is provided in Figure 12.

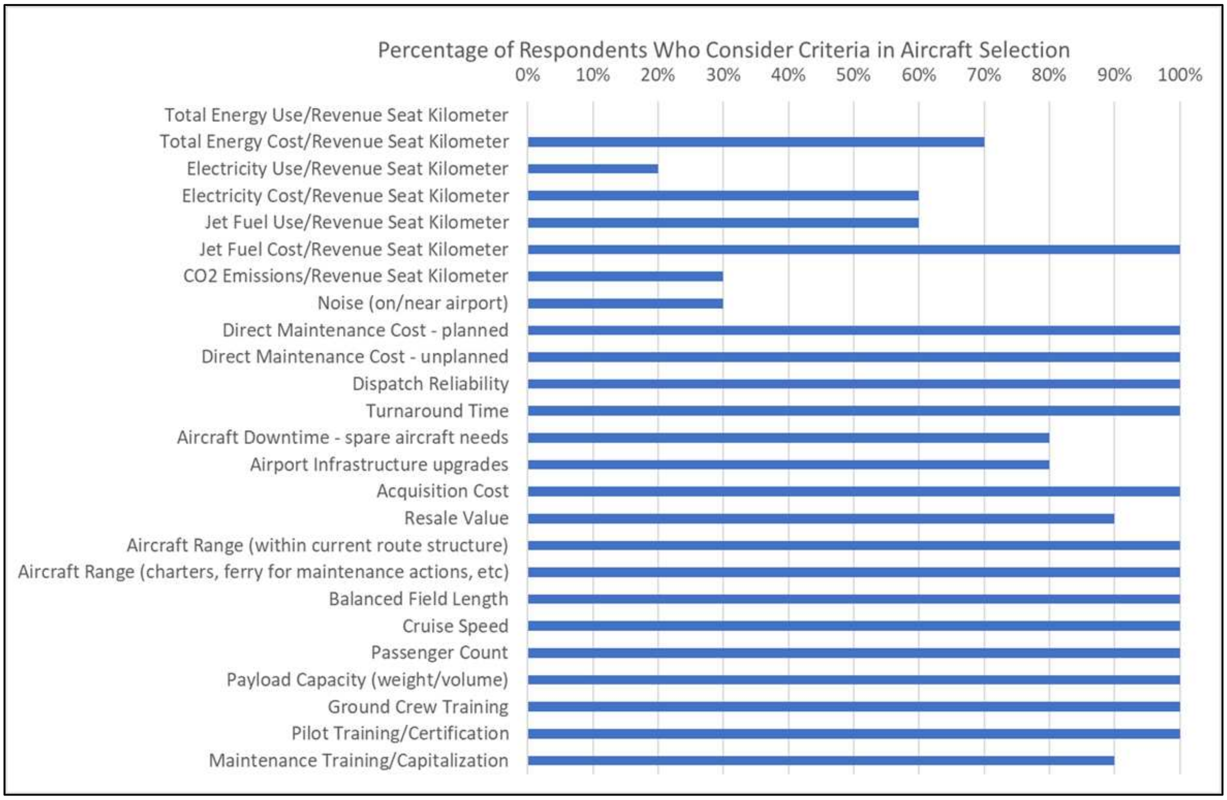

Figure 11 Percentage of Respondents Who Consider a Particular Characteristic in Aircraft Selection

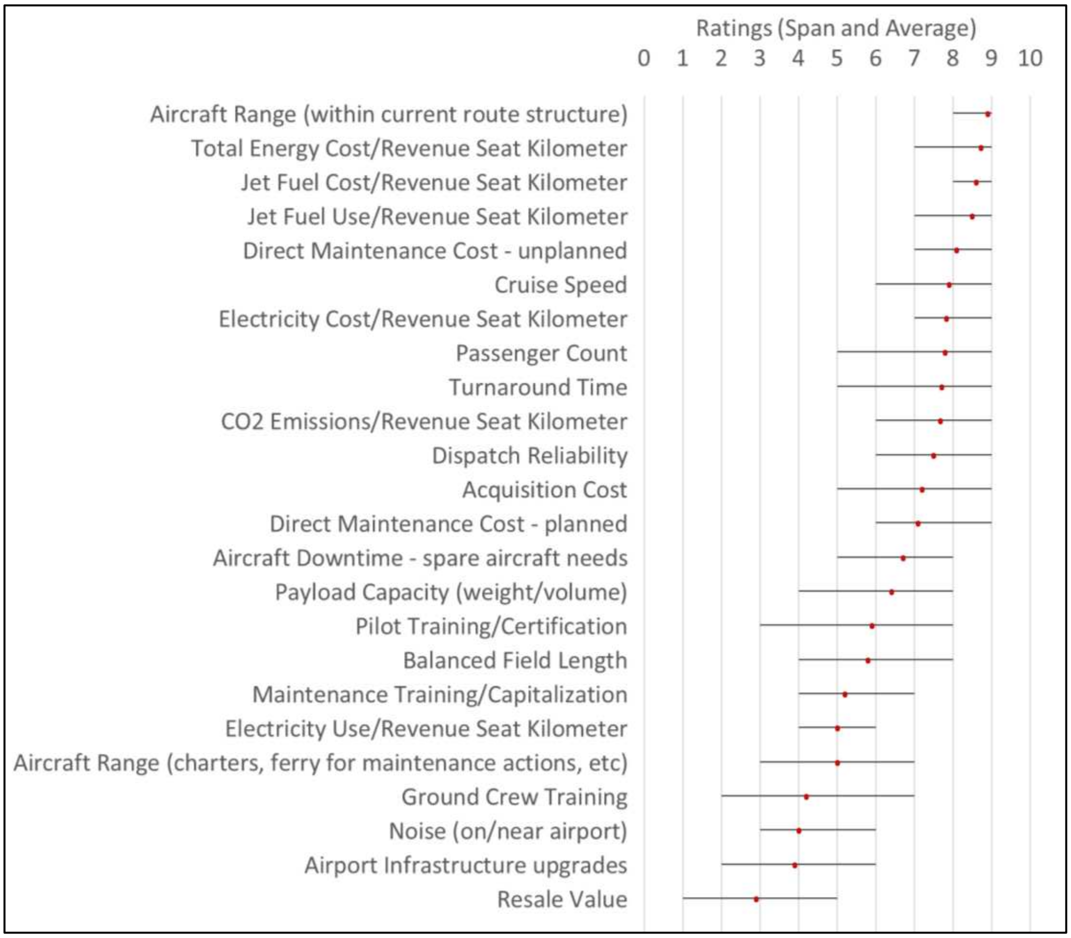

Figure 12 Airline Survey Importance Ranking Results

This survey highlighted some key trends that existed across the range of respondents. Energy costs (whether fuel or electricity) were universally important to all operators, while the amount of energy used was of relatively less importance. CO_2 emissions were also highly ranked in importance, although follow up conversations with several respondents indicated that, in some cases, the concern was an economic one due to “carbon taxes” on conventional fuel, or relatively higher costs of a more carbon-neutral fuel such as SAF. Other economic metrics such as maintenance cost and operational metrics such as turnaround time also score high, providing a more holistic view on the characteristics of most importance to regional operators.

The literature search and subsequent airline survey confirmed that elements of Direct Operating Costs and CO_2 emissions are the key elements that should be evaluated in the overall aircraft model.

Conclusions

This chapter sought to address the research problem identified as research question 1, which is repeated below:

> **Research Question 1) What are the prioritized weighted metrics important to regional airline customers?**

Now having performed the research activities documented in the above sections, we can answer the research question. The results of the survey of operators have developed a list of prioritized metrics that illustrate that operational costs are the primary concern for this type of operator, followed by a concern for environmental impact of their operations. It also highlights that a number of basic aircraft performance characteristics such as range do not necessarily need to remain at their current value but must maintain above a minimum threshold value for particular airlines with their specific route structures.

Chapter 4 - Hybrid Electric Aircraft and Powertrain Component Models

This chapter seeks to address the research problem identified as research question 2, which is repeated below:

Research Question 2) How can systems designers determine and characterize important hybrid electric configuration elements through empirical and physics-based models?

To answer this question, this chapter presents a definition of the library of aircraft, thermal engine, and electrical component information needed to holistically characterize aircraft performance. Based on the characteristics that have been determined to be important to the customer, a variety of models were needed to analyze those metrics. Examples include payload/range estimation, lifecycle costs, etc. This identified the elements and the characteristics of those elements that needed to be modelled to determine the desired results. This was followed by a literature search and industry survey of available characterization models. This surveyed the current state of the art in aircraft and powertrain models and identified where gaps currently exist. The addition of electrified elements to the aircraft configuration required some models that did not yet exist and required added capabilities to existing models.

Introduction / Literature Search

The work described in the previous chapter described how Direct Operating Costs (DOC) were the prime consideration of regional airline operators. DOC as illustrated in Figure 13 is comprised of Cash Operating Costs (COC) which are expenses related to daily aircraft operation, and Cost of Ownership (COO) which accounts for the financial obligation of aircraft ownership or leasing.

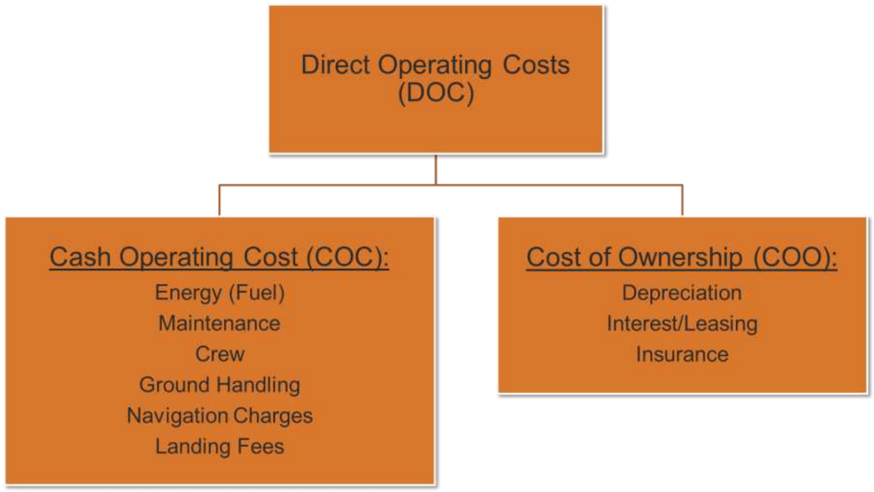

Figure 13 Direct Operating Cost Elements

A diagram of a generic hybrid electric powertrain is illustrated in Figure 14. While each aircraft will not include all these elements, this illustration serves as a superset of the catalog of components that must be addressed to build an appropriate powertrain evaluation library.

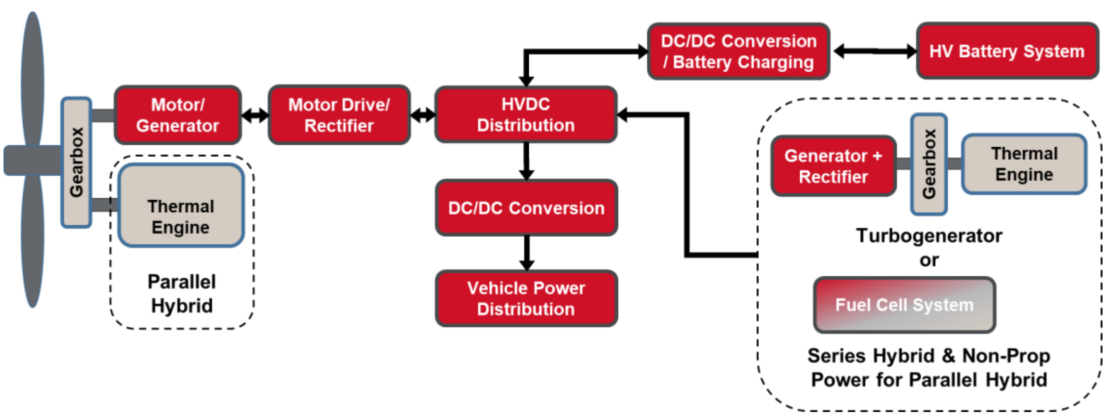

Figure 14 Generic Hybrid Powertrain Configuration

A necessary step was to characterize these hybrid electric configuration elements through empirical and physics-based models. Evaluating and optimizing the system required an understanding of how physical and performance characteristics of the key elements change as configurations, power ratings and usage conditions are modified as a part of that higher level optimization.

Legacy aircraft analysis using traditional powertrains has previously identified a series of necessary propulsion level characteristics such as specific fuel consumption, specific thrust/power, and thermal/propulsion efficiency. To accommodate the addition of new electrical elements into the hybrid powertrain, similar characteristics are also needed for equipment such as electric motors, power electronics, and batteries. Additionally, as opposed to a conventional powertrain where the thermal engine is providing the full propulsive power needs, the hybrid system allows for a new set of operating options where the propulsive need can be met in multiple ways. This requires the modelling of new types of characteristics such as the impact of usage profiles on durability and resulting maintenance costs of both existing and new powertrain elements. Also, a more comprehensive emissions lifecycle analysis requires characterization of manufacturing carbon footprints for added elements such as batteries, which can require frequent replacement over the life of the aircraft.

The first step was to perform a literature search to understand the point design information and parametric models that existed for each of these elements and the specific performance and economic measures of interest. This literature search revealed that this data existed in widely scattered form, with no individual source addressing all the required information. As an example, thermal engines for commercial aircraft are certified by EASA and documented by a Type Certificate Data Sheet (TCDS). An example of this TCDS for the PW100 engine family is illustrated in Figure 15 [50]. Other certification authorities such as the FAA also have comparable documentation.

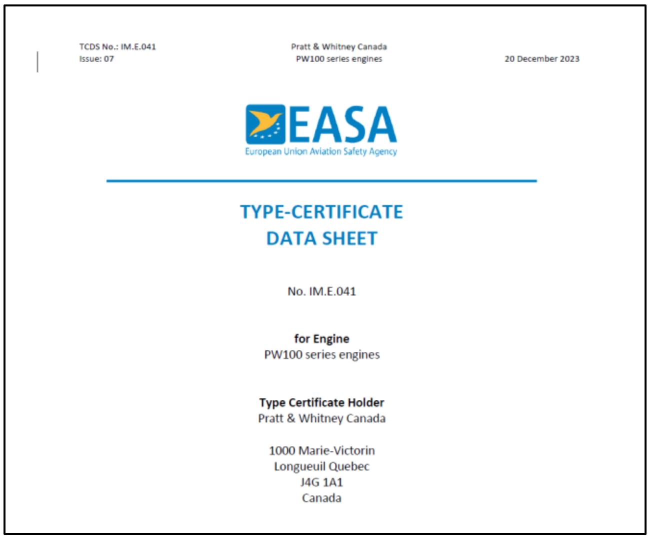

TCDS No.: IM.E.041
Issue: 07

Pratt & Whitney Canada
PW100 series engines

20 December 2023

EASA
European Union Aviation Safety Agency

TYPE-CERTIFICATE
DATA SHEET

No. IM.E.041

for Engine
PW100 series engines

Type Certificate Holder
Pratt & Whitney Canada

1000 Marie-Victorin
Longueuil Quebec
J4G 1A1
Canada

Figure 15 Type Certificate Data Sheet, PW100

This data sheet includes some elements such as power rating and engine mass, but does not include other key performance data such as efficiency, or economic data such as product cost or reliability. Also, this data provides information on only a single engine type, or at best, on a few models of an engine family.

Manufacturer websites and promotional materials can also provide product information. An example of this would be the Pratt Whitney Canada Engine Card shown in Figure 16 [54].

Figure 16 Pratt Whitney Canada Engine Card

Overall, this literature search provided a large quantity of individual data points, but no sources were found that had consolidated this data into a parameterized model that could be directly used in evaluation and optimization studies. Because of this, an effort was undertaken to create those parameterized models for both the powertrain and aircraft.

Model Results

The results of this activity were collated by topical area and are presented in the following sections. It should be noted that these models are based on nominal values, and do not include error bands due to insufficient statistical data to properly characterize the uncertainty. Understanding the potential impacts of uncertainty or of future improvements to these characteristics can be addressed through the addition of scaling factors when the models are implemented in the evaluation tool.

Thermal Engine

Modern turboprop aircraft in the 30-50 seat class have traditionally used gas turbine engines in the 1800-2800 SHP sea level static power range [54]. For purposes of this work, the aperture was widened to include other engine types that, although they were previously discounted, may bring advantage when used in a hybrid electric configuration. Aircraft internal combustion engines may be either intermittent combustion (piston or rotary) or continuous (gas turbine types). Gas turbines generally exhibit higher specific power (particularly at sea level) but have higher specific fuel consumption (less efficient) as shown in Figure 17 below.

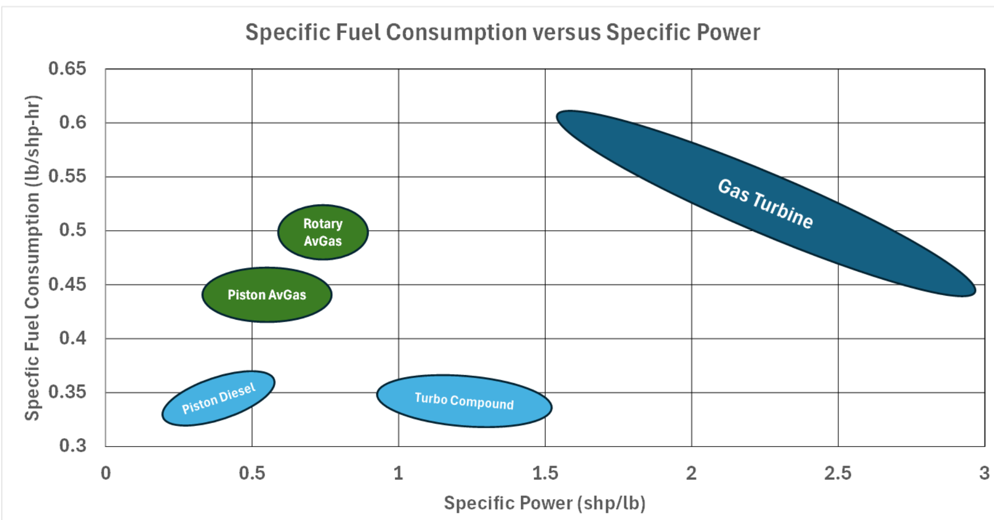

Figure 17 Comparative Performance of Various Aircraft Engine Types

The engine models created for this work include gas turbines and turbo-compounded engines, as these engine types were both believed to have the performance needed by the aircraft operating in this regional market.

Gas Turbines

The primary gas turbine used for this modeling was the Pratt & Whitney Canada PW100 family. This is the most common engine used in this class of aircraft. Over its 40-year history, there have been 30 PW100 engine models certified, and 9,000 engines built to date. Today, there are close to 3,000 PW100-powered aircraft in service with over 600 operators in 128 countries and these engines have logged approximately 200 million flight hours [51]. Both external and internal views of this engine are provided in Figure 18.

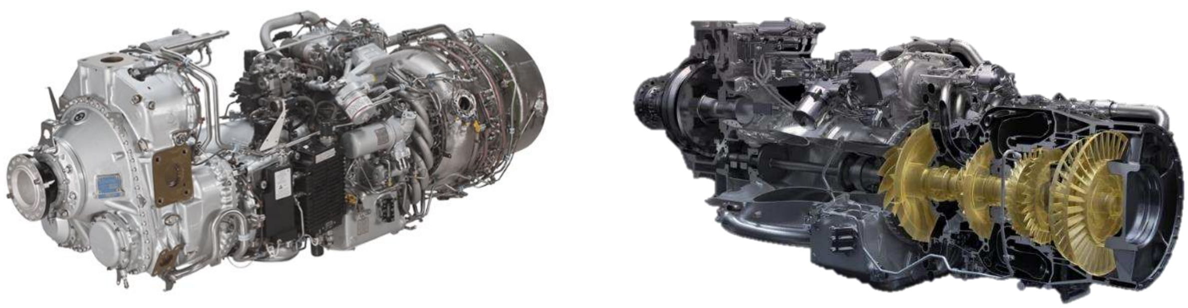

Figure 18 External and Internal Views, PWC PW100

Additionally, information was modelled for the PWC PT6 family of engines. More than 64,000 PT6 engines have been produced since its introduction in 1963, and it powers over 155 different aviation applications, with 500 million flying hours [52]. This engine is slightly too small for this size regional aircraft, with a power rating up to 1,900 SHP [54], but it was modelled in case a variant of parallel hybrid could use an engine of that power class. This engine family includes three variants – “small”, “medium” and “large”. Both external and internal views of this engine are provided in Figure 19.

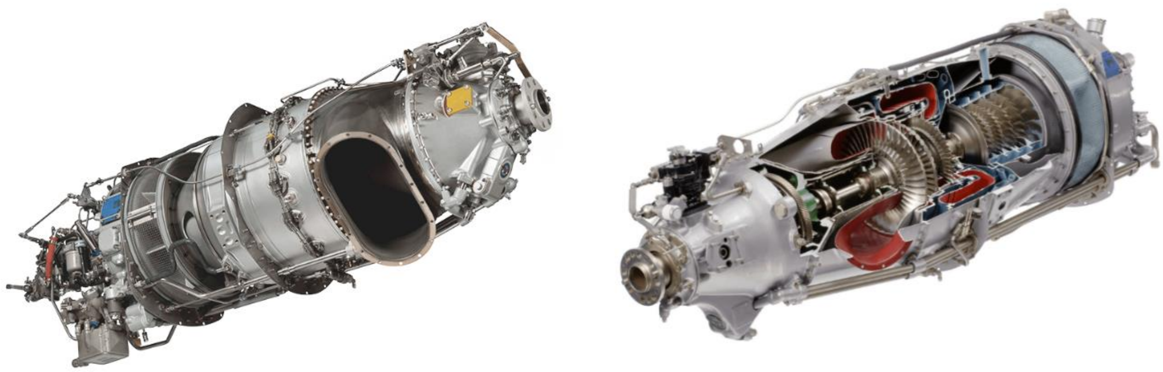

Figure 19 External and Internal Views, PWC PT6

Specific Power

The specific power of a thermal engine is defined as the takeoff power at Sea Level Static (SLS) operating conditions divided by the engine mass. Depending on the particular engine design, the takeoff power limit could be due to either thermodynamic limits of the engine cycle, or mechanical limits of the propellor gearbox or airframe mounting structure. Pertinent details of a variety of PT6 and PW100 engines are included as Table 4 below [53, 54].

Table 4 PWC Turboprop Specific Power Characteristics

	Thermodynamic Rating (KW)	Mechanical Rating (KW)	Mechanical / Thermodynamic Ratio	Shaft Speed (RPM)	Mass (kg)	Specific Power Thermal (kW/kg)	Specific Power Mechanical (kW/kg)	Advertised BSFC (kg/kW-hr)
Small PT6 Family								
PT6A-21 663 550 2200	494	410	83%	2200	153	3.231	2.681	
PT6A-11AG 668 550 2200	498	410	82%	2200	155	3.214	2.646	0.393
PT6A-15 AG 751 680 2200	560	507	91%	2200	153	3.660	3.314	0.366

	Thermodynamic Rating (KW)	Mechanical Rating (KW)	Mechanical / Thermodynamic Ratio	Shaft Speed (RPM)	Mass (kg)	Specific Power Thermal (kW/kg)	Specific Power Mechanical (kW/kg)	Advertised BSFC (kg/kW-hr)
PT6A-27 751 680 2200	560	507	91%	2200	153	3.660	3.314	0.366
PT6A-25C 886 750 2200	661	559	85%	2200	161	4.104	3.474	0.362
PT6A-34 886 750 2200	661	559	85%	2200	155	4.263	3.608	0.362
PT6A-34/AG 886 750 2200	661	559	85%	2200	155	4.263	3.608	0.362
PT6A-35 927 750 2190	691	559	81%	2190	152	4.548	3.679	0.359
PT6A-135A 927 750 1900	691	559	81%	1900	158	4.375	3.540	0.356
PT6A-114A 940 675 1900	701	503	72%	1900	163	4.300	3.088	0.389
PT6A-140 1075 867 1900	802	647	81%	1900	189	4.241	3.421	0.356
PT6A-140AG 1104 867 1900	823	647	79%	1900	175	4.704	3.694	0.356
PT6A-140A 1161 900 1900	866	671	78%	1900	175	4.947	3.835	0.356
Medium PT6 Family								
PT6A-41 1089 850 2000	812	634	78%	2000	190	4.274	3.336	0.359
PT6A-42/42A 1090 850 2000	813	634	78%	2000	190	4.278	3.336	0.365
PT6A-60A/AG 1218 1050 1700	908	783	86%	1700	221	4.110	3.543	0.333
PT6A-61 1218 850 2000	908	634	70%	2000	201	4.519	3.153	0.359
PT6A-52 1346 850 2000	1004	634	63%	2000	204	4.920	3.107	0.365
PT6A-62 1365 950 2000	1018	708	70%	2000	206	4.941	3.439	0.345
Large PT6 Family								
PT6A-65AG 1461 1300 1700	1089	969	89%	1700	228	4.778	4.252	0.309
PT6A-65SC 1514 1110 1700	1129	828	73%	1700	235	4.804	3.522	
PT6A-65B 1548 1100 1700	1154	820	71%	1700	225	5.130	3.646	0.326
PT6A-66 1572 850 2000	1172	634	54%	2000	207	5.663	3.062	0.377
PT6A-64 1583 700 2000	1180	522	44%	2000	207	5.703	2.522	0.427
PT6A-66A 1583 850 2000	1180	634	54%	2000	207	5.703	3.062	
PT6A-67AG 1634 1350 1700	1218	1007	83%	1700	236	5.163	4.266	
PT6A-67B 1703 1200 1700	1270	895	70%	1700	235	5.404	3.808	0.336
PT6A-67D 1703 1200 1700	1270	895	70%	1700	234	5.427	3.824	0.322
PT6A-67R 1754 1424 1700	1308	1062	81%	1700	234	5.590	4.538	0.316
PT6A-68 1805 1250 2000	1346	932	69%	2000	260	5.177	3.585	
PT6A-67T 1807 1424 1700	1347	1062	79%	1700	234	5.758	4.538	
PT6A-66D 1825 850 2000	1361	634	47%	2000	207	6.574	3.062	
PT6A-67A 1825 1200 1700	1361	895	66%	1700	230	5.917	3.891	0.334
PT6A-66B 1844 850 2000	1375	634	46%	2000	207	6.643	3.062	
PT6E-66XT 1844 895 1925	1375	667	49%	1925				
PT6A-67P 1845 1200 1700	1376	895	65%	1700	251	5.481	3.565	

	Thermodynamic Rating (KW)	Mechanical Rating (KW)	Mechanical / Thermodynamic Ratio	Shaft Speed (RPM)	Mass (kg)	Specific Power Thermal (kW/kg)	Specific Power Mechanical (kW/kg)	Advertised BSFC (kg/kW-hr)
PT6E-67XP 1845 1200 1700	1376	895	65%	1700	270	5.096	3.314	
PT6A-67F 1868 1700 1700	1393	1268	91%	1700	259	5.378	4.895	
PT6A-68B 1927 1600 2000	1437	1193	83%	2000	269	5.342	4.435	
PT6A-68C 1962 1600 2000	1463	1193	82%	2000	272	5.379	4.386	
PW100 Family								
PW118 2286 1800 1300	1705	1342	79%	1300	391	4.360	3.433	0.303
PW120 2390 2000 1200	1782	1491	84%	1200	417	4.274	3.576	0.295
PW120A 2416 2000 1200	1802	1491	83%	1200	423	4.259	3.526	0.295
PW118A 2450 1800 1300	1827	1342	73%	1300	393	4.649	3.415	
PW121 2497 2150 1200	1862	1603	86%	1200	423	4.402	3.790	0.289
PW123C 2522 2150 1200	1881	1603	85%	1200	450	4.179	3.563	0.294
PW119B 2658 2180 1300	1982	1626	82%	1300	411	4.823	3.955	0.298
PW119C 2791 2180 1300	2081	1626	78%	1300	411	5.064	3.955	
PW123 2950 2380 1200	2200	1775	81%	1200	450	4.888	3.944	0.286
PW123AF 2950 2380 1200	2200	1775	81%	1200	450	4.888	3.944	0.286
PW123B 2950 2500 1250	2200	1864	85%	1250	450	4.888	4.143	0.282
PW123D 2950 2150 1200	2200	1603	73%	1200	450	4.888	3.563	0.294
PW123E 3113 2380 1200	2321	1775	76%	1200	450	5.159	3.944	0.294
PW127E 3295 2400 1200	2457	1790	73%	1200	481	5.108	3.721	0.279
PW127H 3341 2750 1200	2491	2051	82%	1200	482	5.169	4.255	
PW127XT-M 3360 2750 1200	2506	2051	82%	1200	495	5.062	4.143	
PW127F 3365 2750 1200	2509	2051	82%	1200	481	5.217	4.263	
PW127J 3365 2750 1200	2509	2051	82%	1200	482	5.206	4.255	
PW127M 3515 2750 1200	2621	2051	78%	1200	482	5.438	4.255	
PW127G 3546 2920 1200	2644	2177	82%	1200	484	5.463	4.499	
PW127N 3673 2750 1200	2739	2051	75%	1200	482	5.682	4.255	
PW150A 6680 5071 1020	4981	3781	76%	1020	717	6.947	5.274	0.263

Plotting this data to illustrate the impact of power rating on specific power shows the strong relationship between these parameters as illustrated in Figure 20 below. It is apparent that as engine power rating increases, the specific power also increases, and that differing families of engines exhibit overlapping specific power behaviors.

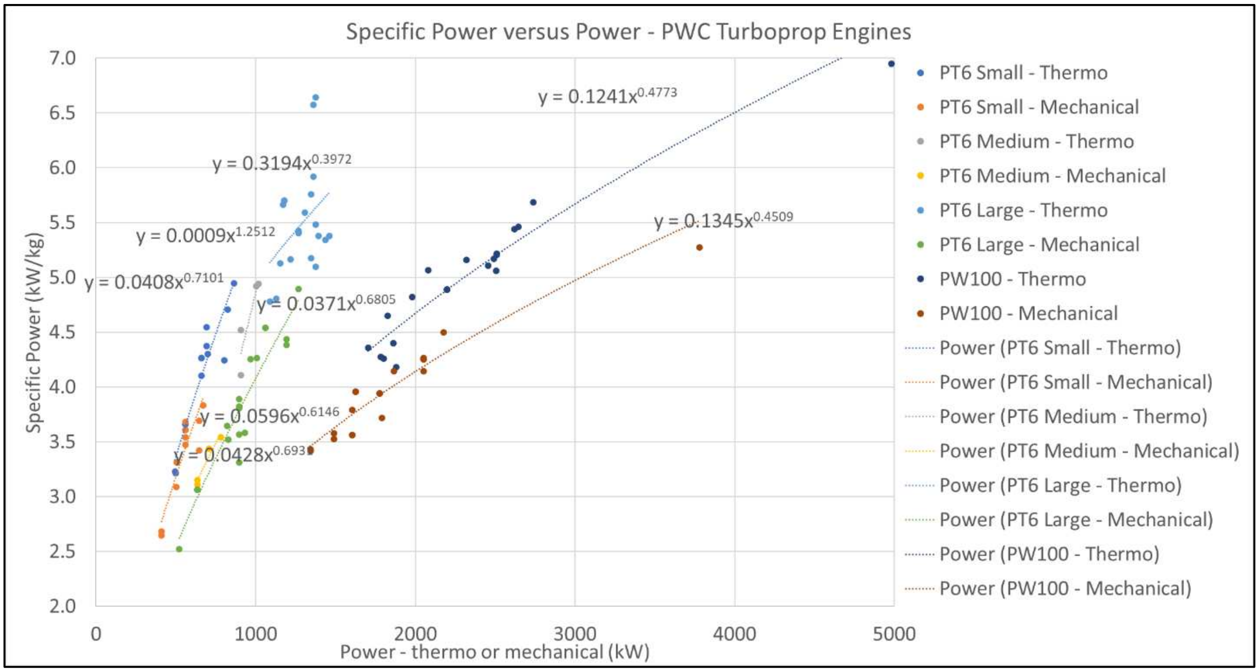

Figure 20 Specific Power versus SLS Power Rating

Thermal Efficiency

The second major thermal engine characteristic is its thermal efficiency. Engine datasheets for turboprop engines typically express this characteristic as Brake Specific Fuel Consumption (BSFC), which is a measure of fuel mass consumed per unit power per unit time (kg/kW-hr). This parameter for operating at SLS ratings is provided in Figure 21 below and illustrates strong dependence on engine power rating, with engines becoming more efficient as their power rating increases [53].

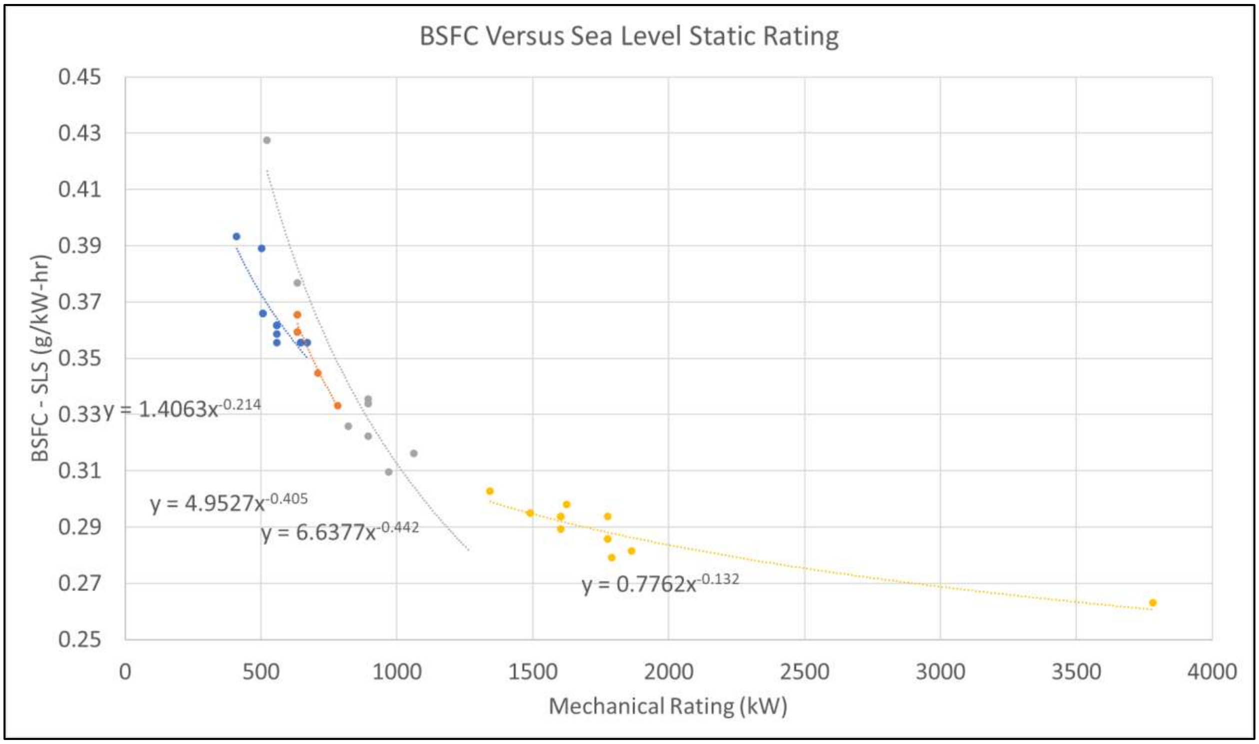

Figure 21 Brake Specific Fuel Consumption versus Sea Level Static (SLS) Rating

Engine thermal efficiency for a given engine, however, changes as the engine is operated at power ratings other than 100% power. As seen in Figure 22 below, the thermal efficiency worsens as the engine operates at less than 100% power levels, [61].

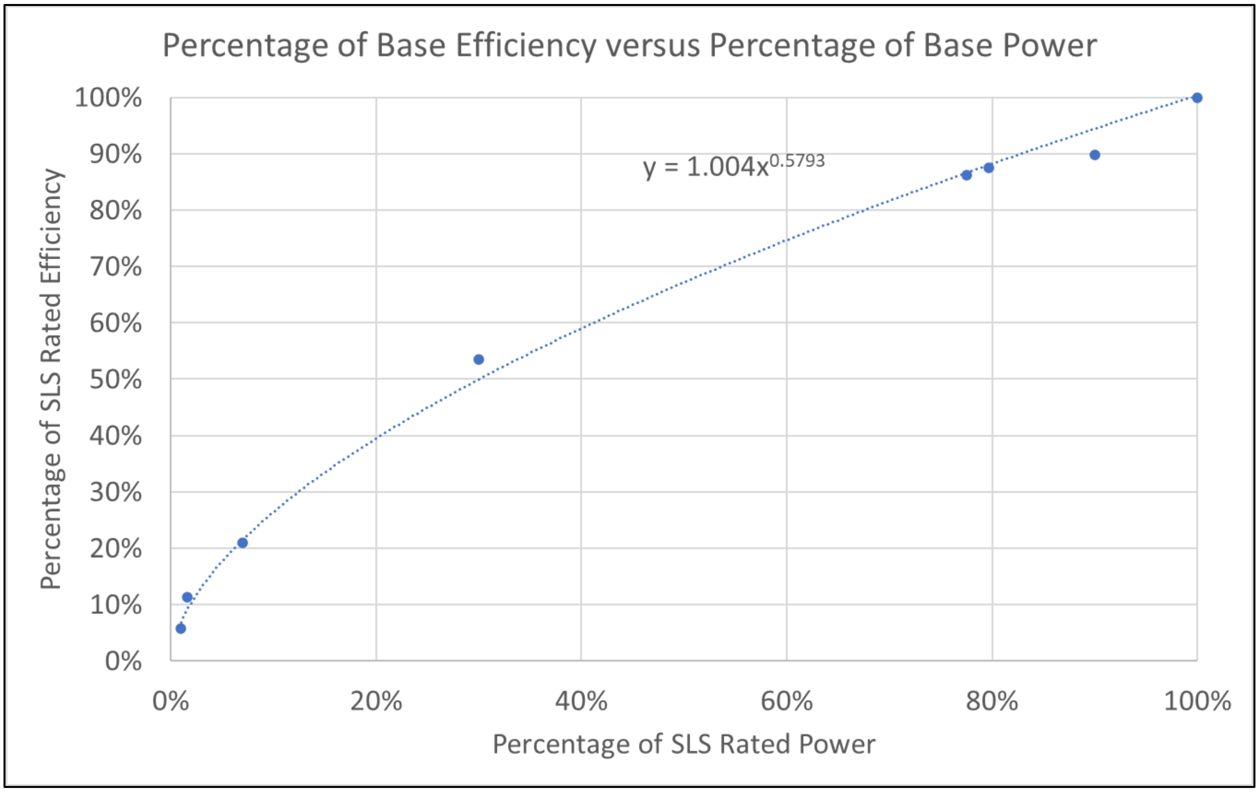

Figure 22 Thermal Efficiency at Varying Power Levels

Available Power During Flight

As the operating altitude increases, the air density decreases. Since the gas turbine engines of this power class operate with fixed geometry, this air density decrease results in reduced engine power. The density used for this altitude lapse calculation is the total stagnation air density, accounting for pressure, temperature, and aircraft speed effects. Additionally, consideration must be made for the varying operating conditions (takeoff, climb, cruise) and how that impacts the available engine power. Shorter flight conditions such as takeoff typically can be operated at higher power levels than the longer-term climb and cruise segments.

These considerations are captured in an available power equation of the following form that is presented as Equation 1.

$$Power\ (Cl, Cr) = Power\ (SLS\ Thermo) * Derate\ (Cl, Cr) * \left(\rho\ (\mathrm{Cl}, \mathrm{Cr}) / \rho\ (\mathrm{SLS})\right)^{Density\ derate} \quad \text{(Eq. 1)}$$

PWC engine power charts from the ATR42-500 Flight Crew Operating Manual [56] were used to determine the coefficients for this equation with the following results:

Table 5 Engine De-Rate / Lapse Rate Coefficients

Parameter	Value
Derate (Cl) - climb	0.92
Derate (Cr) - cruise	0.84
Density derate exponent	0.885

Product Cost

A key product attribute for any economic based analysis is the cost of the product. Data was collected from a wide number of sources [57, 58, 59, 60] to understand how engine cost varies as a function of engine size (which impacts both material quantity and mechanical complexity) with results illustrated in Figure 23 below.

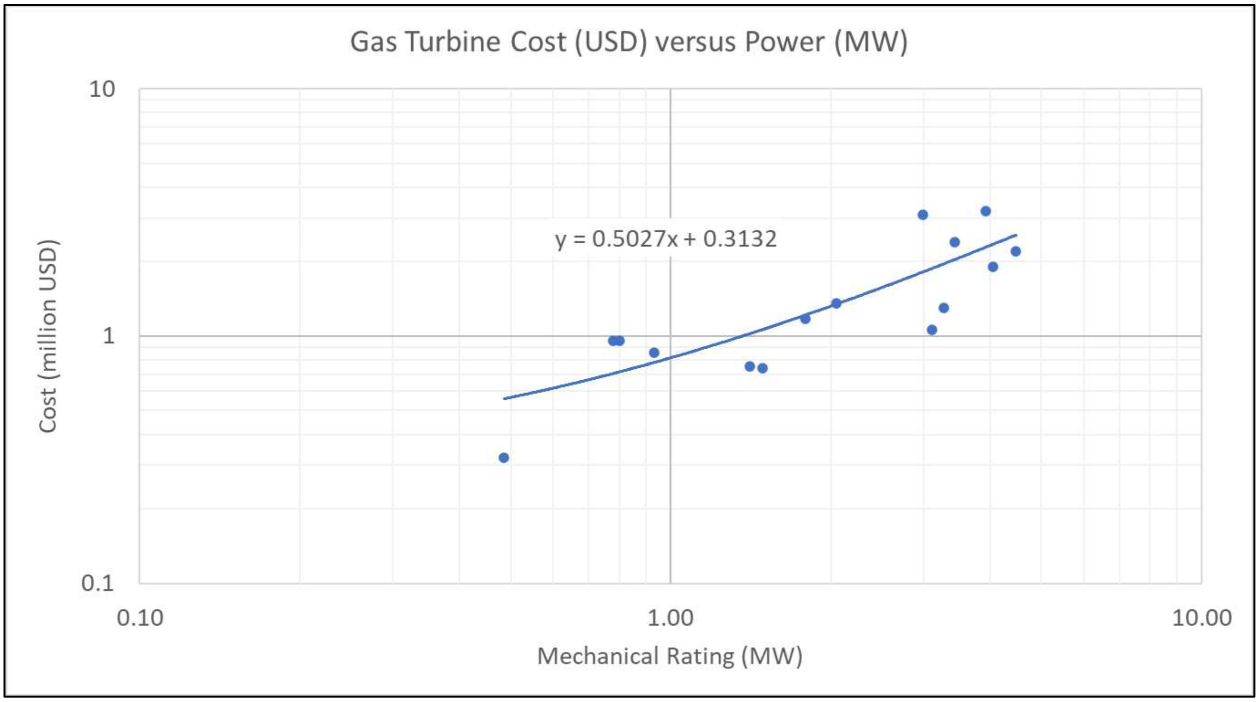

Figure 23 Gas Turbine Cost versus SLS Power Rating

Maintenance Costs

Gas turbine engines have a maintenance schedule that is based on a combination of fixed hours/cycles (life limited parts) and on-condition monitoring (exhaust temperature margin or oil/bearing debris). For the PW120 engine most used on mid-sized regional turboprops, the major maintenance events are hot section inspections (HSI), which occur roughly every 5,000 engine flight cycles, and overhauls, which occur every 15,000 cycles. Additionally, history shows that there is typically also one other shop visit for unscheduled maintenance within that 15,000-cycle interval [61]. Collectively, the total cost of the material and labor for these maintenance actions is roughly equal to the initial purchase price of a new engine [62], so that is the value that is assumed for economic modeling, which is then further modified by the severity factor discussed in more detail in the next section. Equation 2 illustrates this relationship.

$$Cost\ (maintenance, per\ hr, modified) = Cost\ (maintenance, per\ hr, base) * Severity\ Factor \quad \text{(Eq. 2)}$$

Severity Factor

The durability of a gas turbine engine is strongly impacted by how the operator uses the engines. A gas turbine has many life drivers, which may be either temperature based, or cycle based. With this concept, the maintenance costs are estimated for a baseline operating case (typically 10% thrust derate, 2 hr flight cycle) and then those maintenance costs are ratioed up or down based on the actual expected usage. Most publicly available severity curves are based on turbofan engines instead of turboprop, but the failure mechanisms and behaviors were assumed to be the same between engine types [63, 64, 65, 66]. These sources were consolidated to create a generic surface fit for severity factor based on thrust derate and flight length as shown in Figure 24. The equation related to that surface fit is given as Equation 3:

$$Severity\ Factor = 3.86 + 5.00x - 2.53y + 7.06x^2 + 0.73y^2 - 1.87xy + 7.14x^3 - 0.072y^3 + 0.21xy^2 - 1.16x^2y \quad \text{(Eq. 3)}$$

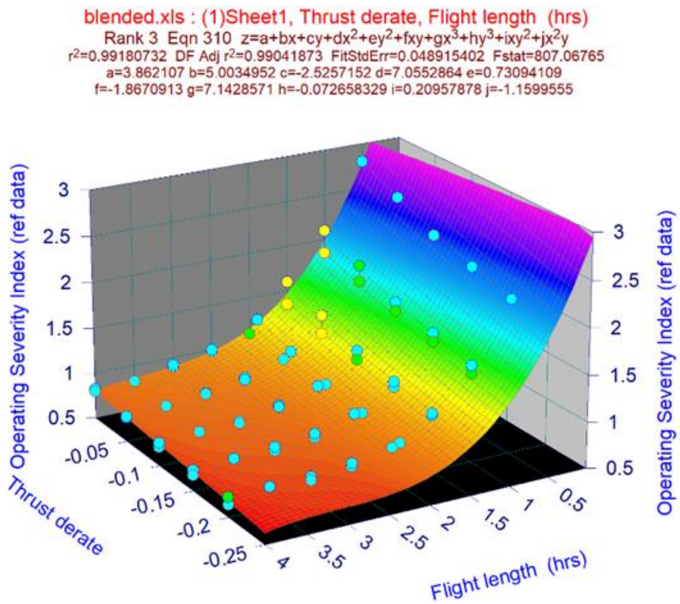

Figure 24 Gas Turbine Operating Severity Curve

This data illustrates that reducing thrust results in longer engine life, and that longer flights have the same effect.

Turbo-compounded Engines

A compounded engine is an arrangement that combines two or more power producing units into a single integrated power plant. As applied to aircraft engines, this takes the form of a combination of an internal combustion engine (either reciprocating or rotary) with a compressor/turbine (turbo) assembly. This arrangement combines the airflow capacity and light-weight pressure rise features of a gas turbine with the highly efficient, although heavier, diesel. A schematic diagram of this engine concept is illustrated in Figure 25 below [67].

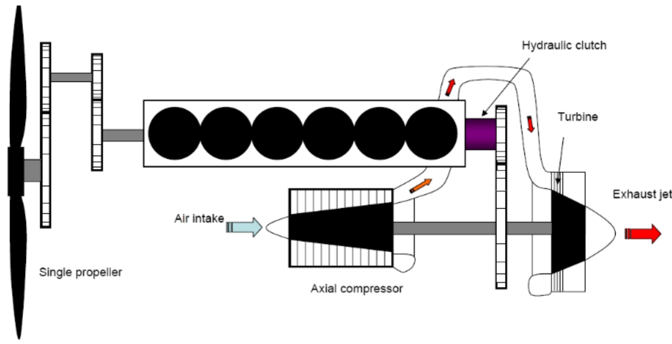

Figure 25 Turbo Compound Engine Schematic

A key feature of this approach, as compared to a traditional turbocharged engine, is that the compressor/turbine assembly is mechanically coupled to the internal combustion engine, allowing excess mechanical power that is harvested by the turbine to contribute to the total mechanical power output of the overall powerplant. While the exact power ratios vary slightly between various engine designs and operating conditions, the internal combustion engine typically provides 70-80% of the total shaft power, while the compressor/turbine provides the remaining 20-30% [67].

Turbocompounded engines were first researched during World War 2 as a potential method to Increase the power levels and efficiency of piston engine aircraft. At that time, the Wright Aeronautical Division of Curtis-Wright in the United States and D. Napier & Son Limited in the United Kingdom were leaders in this technology [67, 68]. Turbocompounded engines saw both military and commercial usage in the 1950's but became obsolete with the increased performance of gas turbine based powerplants, coupled with the low cost of fuel at the time and the drive toward faster aircraft speeds. Turbocompounded technology stagnated while gas turbines flourished, although in recent years, interest has revived in this type of powerplant due to its superior fuel efficiency.

Wright Turbo-Cyclone 18R-3350-TC Radial Engine

The most commercially successful example of a Turbocompounded engine has been the Wright Turbo-Cyclone 18R-3350-TC and is illustrated in Figure 26. Studies began on this engine in 1942, resulting in a demonstration engine in 1946, and an entry into series production in 1950 [68]. Throughout its 10-year production history, approximately 16,000 of these engines were produced in various models for both military and commercial use [69].

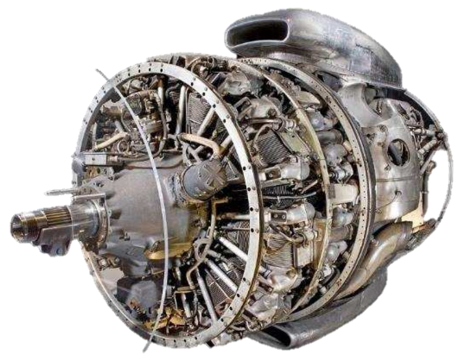

Figure 26 Wright Turbo-Cyclone 18R-3350-TC Radial Engine

This engine was an 18-cylinder radial piston engine configuration, displacing 3,350 cubic inches (54.9 L), and used three power recovery turbines, each being fed by 6 cylinders [70, 71]. A cutaway view of the power turbine (in red) can be seen in Figure 27 below.

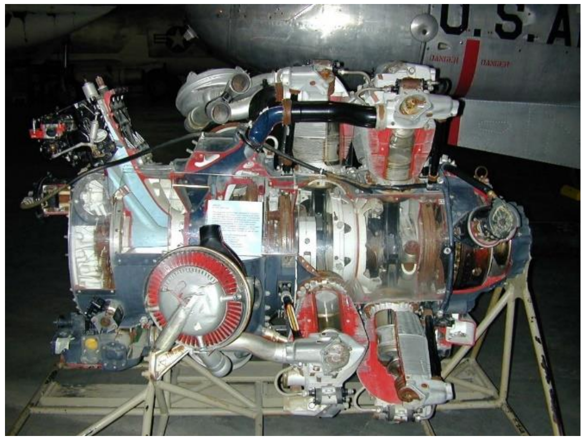

Figure 27 Turbocompounded Engine with Cutaway Power Turbine (in red)

Napier Nomad 2

A different approach to turbocompounding was pursued by D. Napier and Son Limited in the United Kingdom. This engine was based on a two-stroke diesel cycle, with the engine having a horizontally opposed cylinder configuration. While this engine only reached the flight demonstration stage and never entered production, it was considered the most fuel-efficient aircraft engine ever built and the peak of piston engine development [72, 73]. An illustration of the development engine is shown as Figure 28.

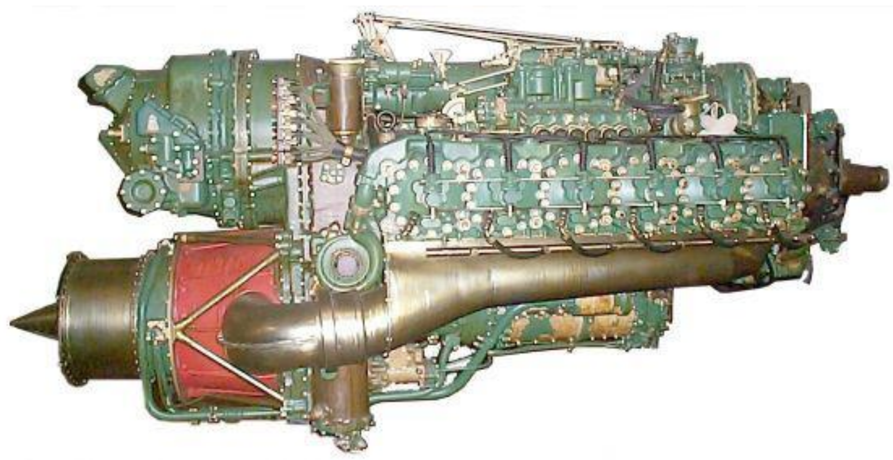

Figure 28 Napier Nomad 2

This engine was a 12-cylinder horizontally opposed piston engine configuration, displacing 2,505 cubic inches (41.1 L), and used a single power recovery turbine [72]. A cutaway view of the engine can be seen in Figure 29 below.

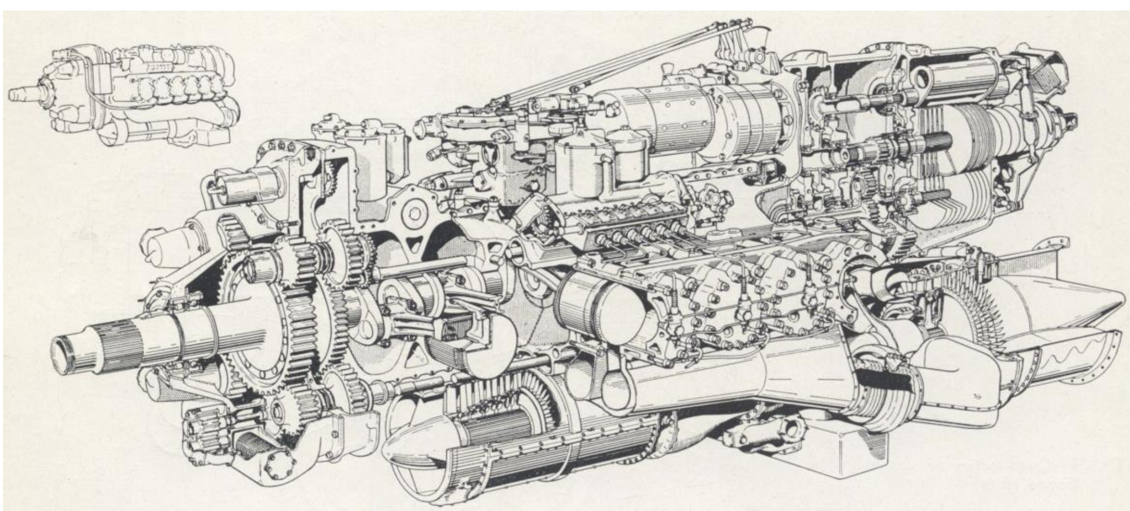

Figure 29 Napier Nomad Cutaway View

Modern Study Engines

In the early 1980's, the oil crisis and subsequent rise in jet fuel prices reinvigorated interest in more fuel-efficient aircraft engine technologies. NASA sponsored design investigations with the Garrett Turbine Engine Company as well as Teledyne Continental Motors for engines in the 1,000 to 2,000 horsepower class. These engines are both piston diesel cycles, with displacements between 200 and 800 cubic inches [74, 75]. Drawings of these concept engines are provided as Figures 30 and 31 below.

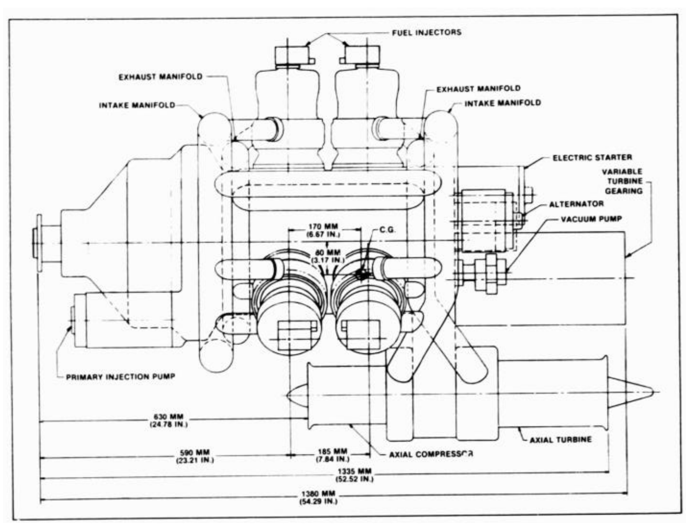

Figure 30 Teledyne Turbocompound Concept

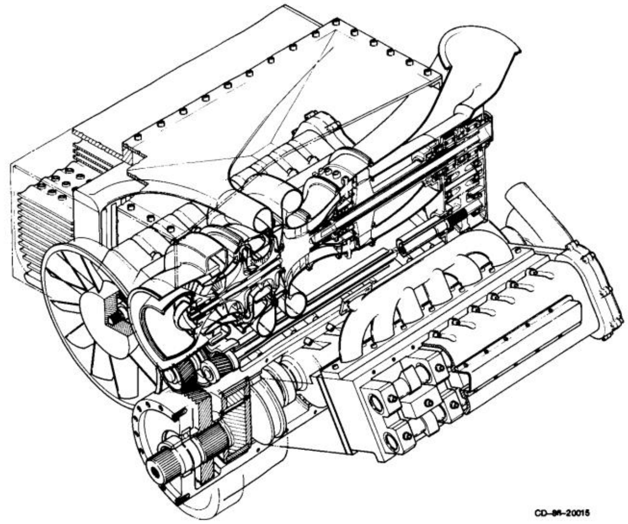

Figure 31 Garrett Turbocompound Concept

High level performance data was gathered for each of the referenced engines and plotted as Figure 32 below. The more modern study engines show both specific power and Brake Specific Fuel Consumption (BSCF) that is superior to the engines from the 1950's, although whether that is due to better materials and analytical methods or estimates prior to potential development weight growth is unknown.

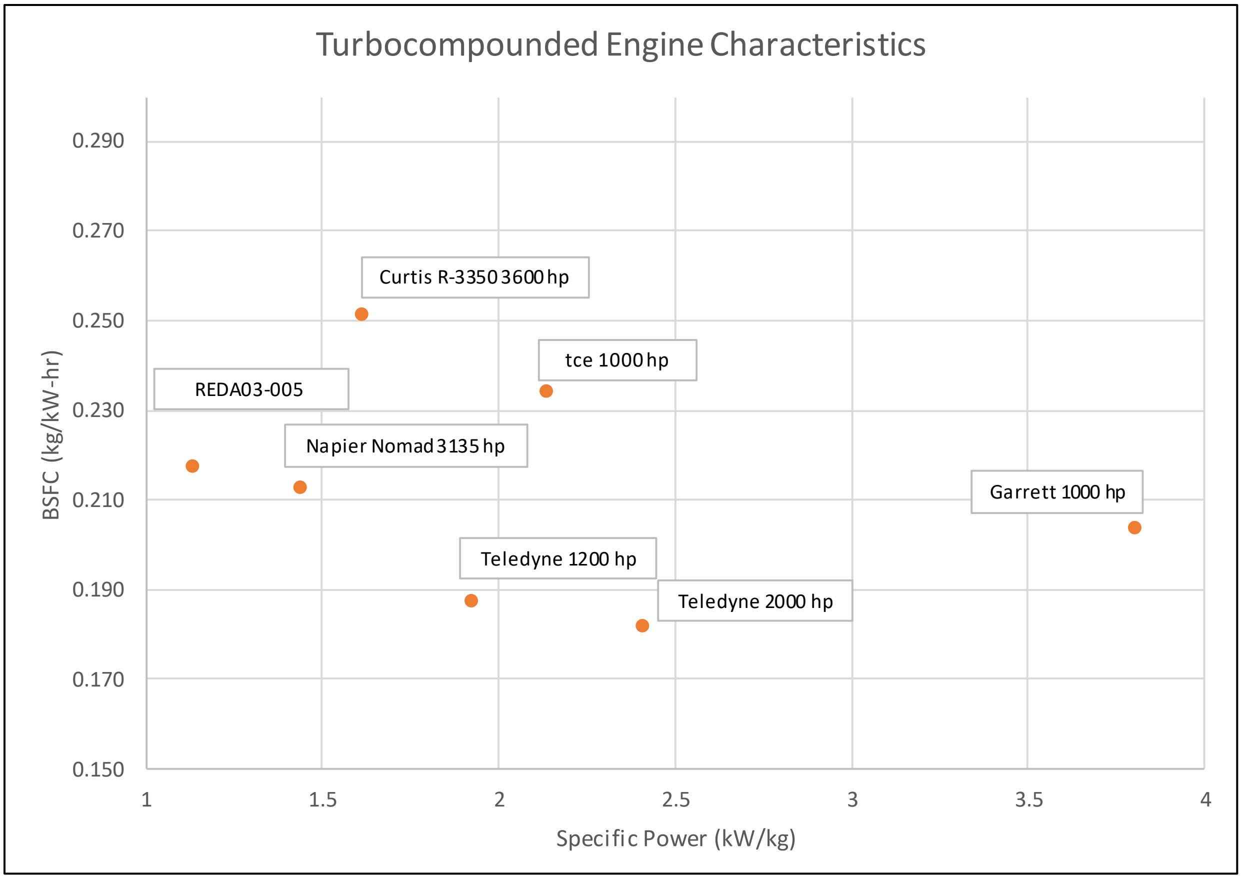

Figure 32 Turbocompound engine characteristics

The following sections address the model characteristics for the turbocompound engine for a variety of measures of interest.

Specific Power

The specific power of the Turbocompounded engine as a function of takeoff power is illustrated in Figure 33 below. These data are for standard day, sea level static operating conditions. Similar to the gas turbine, the specific power increases with an increase in thermal engine power rating. Note that the specific power is significantly less than a gas turbine of comparable takeoff power rating, but difference in the lapse rate behavior with altitude (discussed below) results in both engine types having comparable specific power at cruising altitudes.

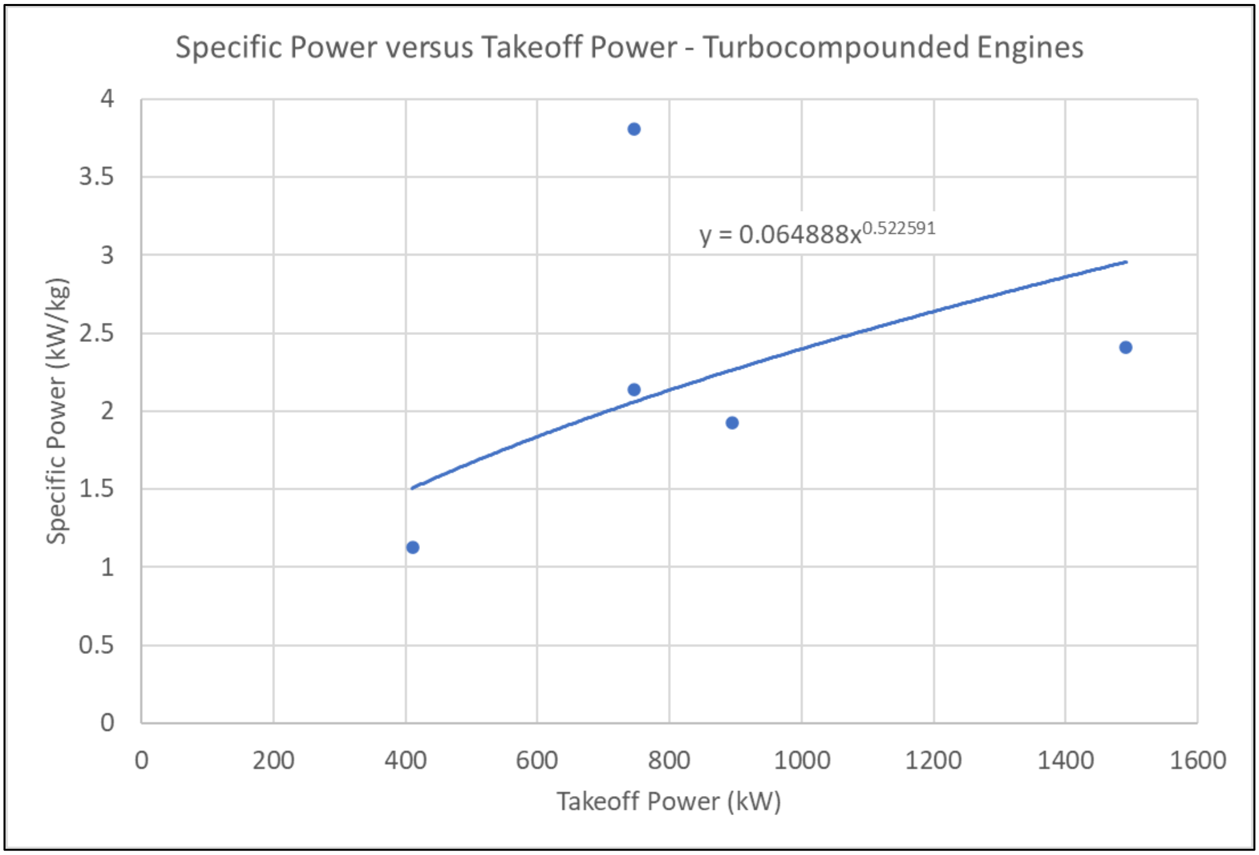

Figure 33 Turbocompound Specific Power vs Takeoff Power

Altitude Power Lapse

The previous data for a traditional gas turbine engine revealed that the engine power decreased with increasing altitude. The turbocompound engine, however, does not reveal this same behavior, due to the ability to independently control the speed of the compressor/turbine section through the use of a variable ratio transmission. This results in constant manifold pressure into the internal combustion engine that is independent of altitude, resulting in a constant power level. This behavior is illustrated in the power curve for a Napier Nomad [72] as shown in Figure 34. Limitations of antiquated control systems resulted in a slight increase in available power with altitude, but for purposes of this analysis the behavior was assumed to be altitude independent.

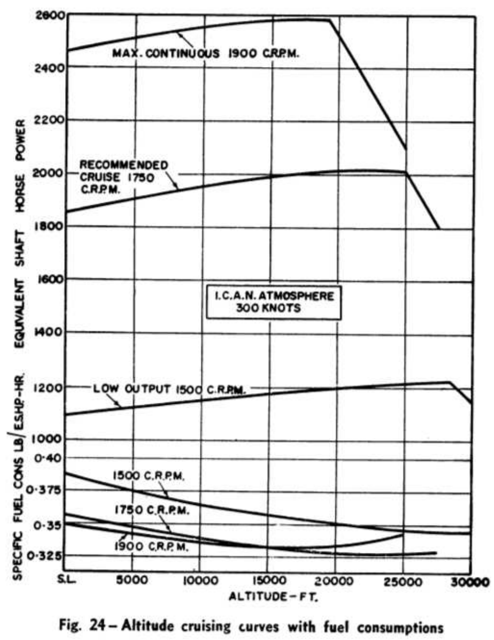

Figure 34 Turbocompound Power and BSCF vs Altitude

Thermal Efficiency

A low BSFC compared to small gas turbine engines is a known advantage of the turbocompound engine cycle. The rated power thermal efficiency versus takeoff power levels is provided as Figure 35. Again, similar to a gas turbine, the thermal engine becomes more thermally efficient as power rating increases.

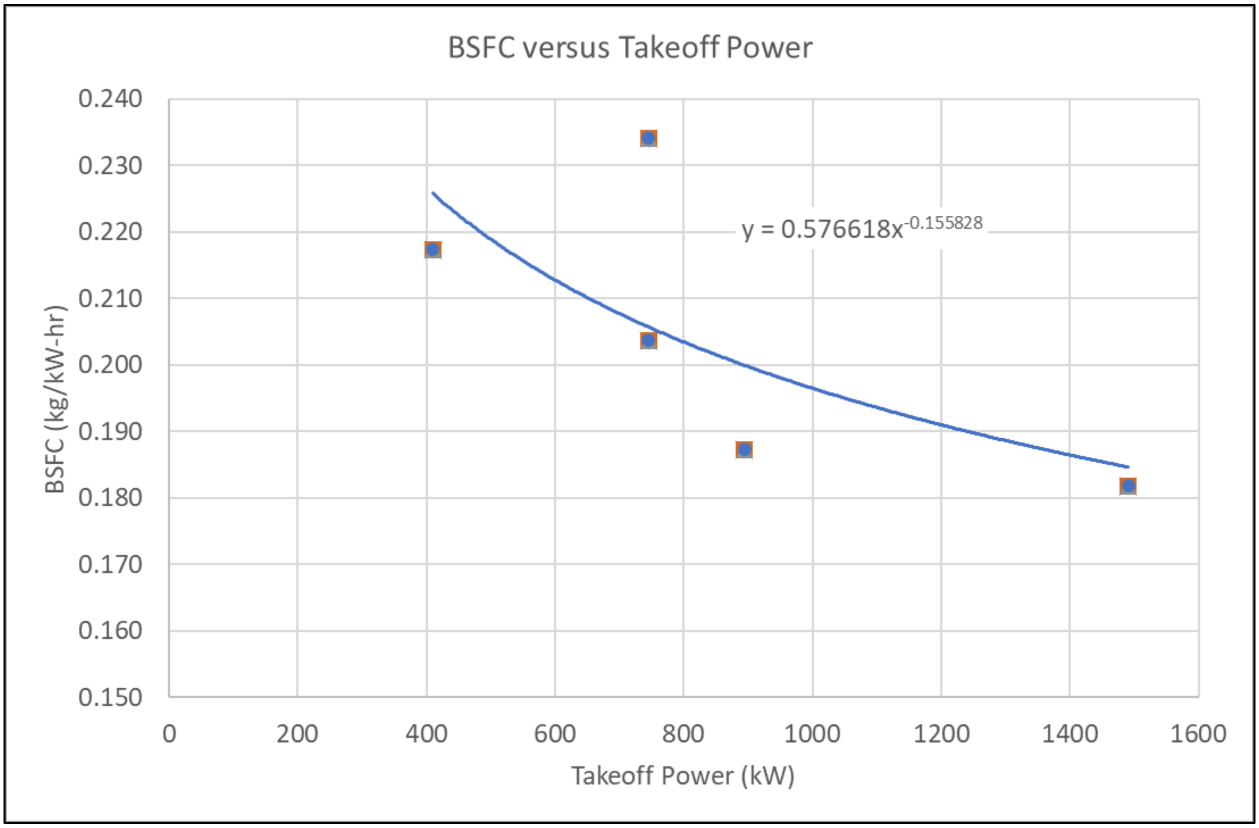

Figure 35 Rated Power BSCF vs Takeoff Power

As the engine operates at part throttle condition, however, the thermal efficiency drops, with slightly different behaviors at sea level versus at altitude. This behavior is provided as Figure 36.

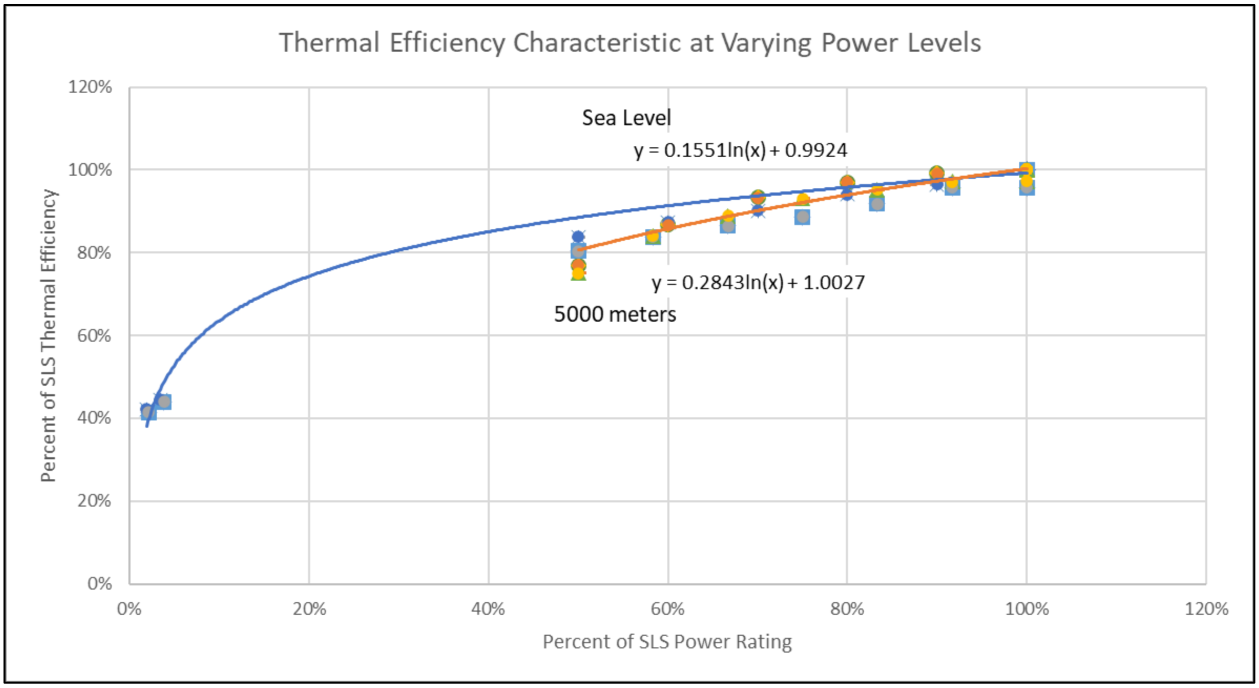

Figure 36 Thermal Efficiency at Varying Power Levels

Product Cost

Production costs of high power turbocompounded engines are difficult to determine since the only high-volume example (Wright 3350) was last produced in the 1950's. In 1957, the production cost of this engine was $88,000 (approximately $997,000 in 2025 dollars) [69].

To provide a more modern comparison of costs for this engine type, a survey was performed on a variety of lower powered aircraft turbocharged diesel engines from manufacturers such as Lycoming [76] and Raikhlin Aircraft Engine Developments (RED Aircraft) [77]. The resulting relationship between engine cost and takeoff power is provided in Figure 37.

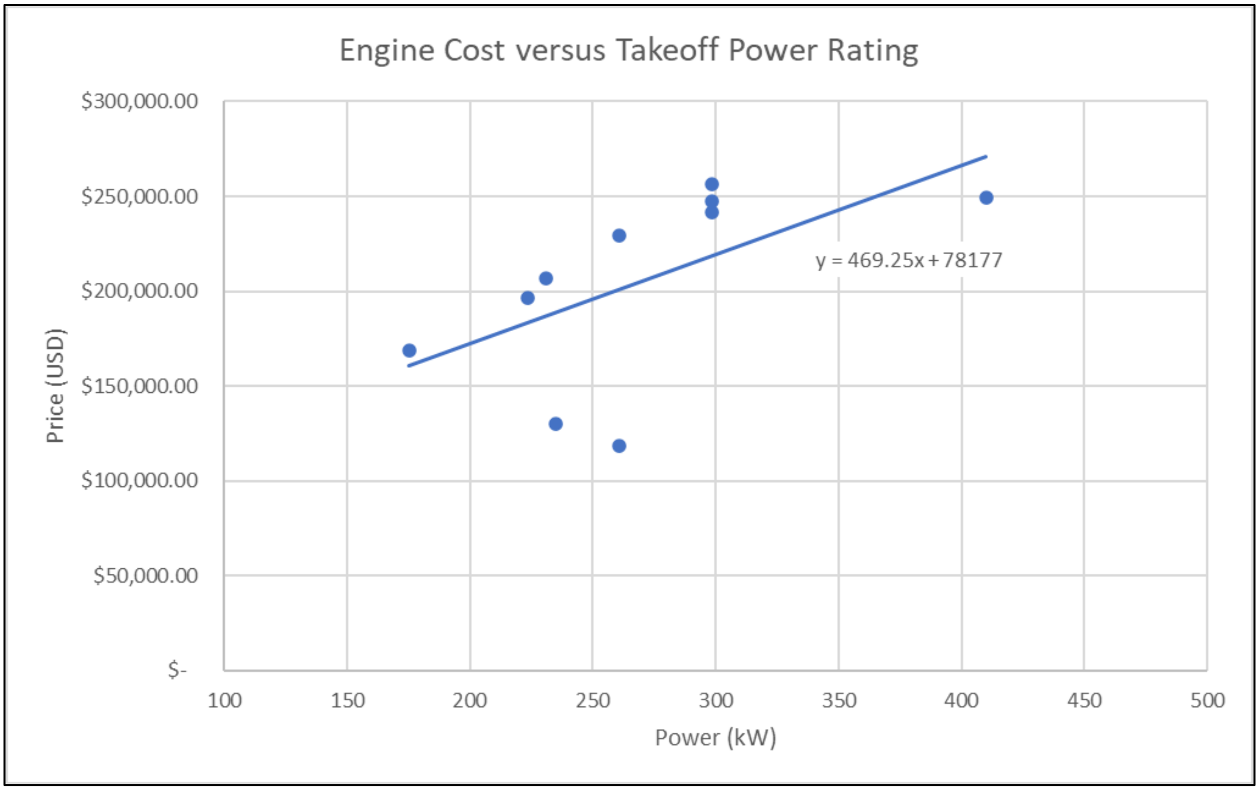

Figure 37 Turbocompounded Engine Cost versus Takeoff Power

Maintenance Costs

The Wright Turbo-Cyclone 18R-3350-TC engine achieved time between overhauls of approximately 4,000 hours in commercial airline service [67]. Aviation piston engines accrue a maintenance cost (including overhaul costs) of approximately 2/3 the cost of a new engine over that 4,000-hour service interval [76]. Although engines built with more modern materials and manufacturing processes are expected to have higher time between overhauls, for conservatism the 4,000 hour overhaul interval was maintained for this research activity.

Severity Factor

Since engines variants of this type were either in commercial service 75 years ago in the case of the Wright or were never put into commercial service in the case of the others, an extensive modern basis for predicting the severity factor is not available. However, these engines are expected to follow that same general behavior as the gas turbine, so for purposes of this study, the same ratio approach and equation was used.

Electrical Equipment

In Figures 6 & 14, several hybrid propulsion configurations were illustrated. These hybrid configurations use a variety of electrical elements including motors, motor drives, and generators, plus energy storage elements such as batteries.

Electric Motor

There are a wide variety of electric machine types in existence, and most have at least been considered for used in electrified aircraft propulsion. Figure 38 illustrates the various machine types that have either been used in, or are actively being investigated for, aircraft applications. Wound field synchronous machines are the predominant choice for both small (brushed/slip rings) and large (brushless) generator applications. Motors are a wide mix of permanent magnet, induction, or brushless DC, depending on aircraft system configuration (AC/DC), power level, and usage/life expectations. The reluctance machines see limited usage, with switched reluctance used on early F-35 aircraft, and synchronous reluctance still in the demonstration phase [78].

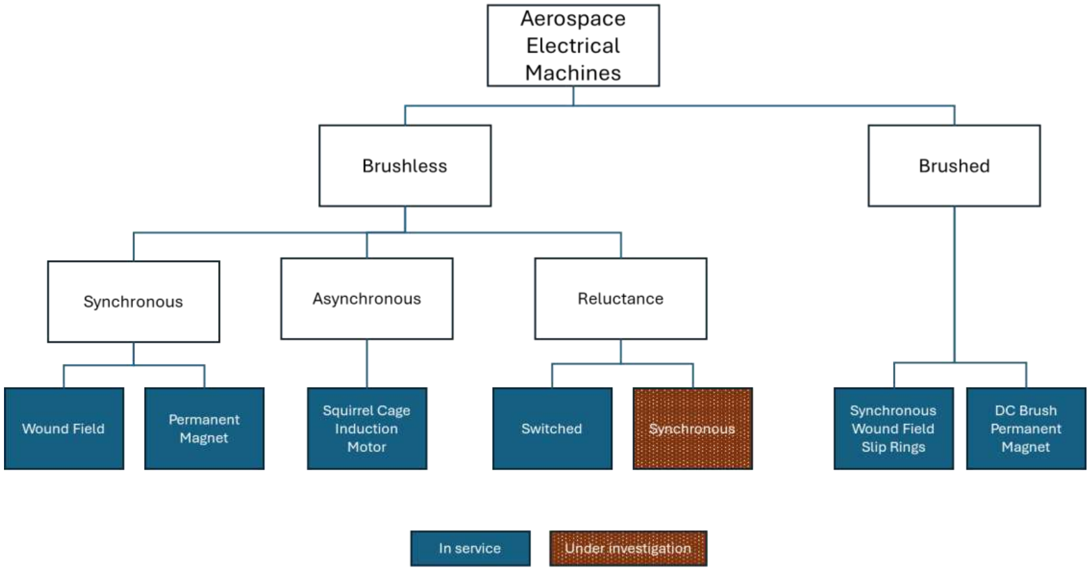

Figure 38 Electric Machine Types in Use and Under Investigation

To better illustrate these various machine types, Figure 39 below shows cross sections of a variety of these machine types [79].

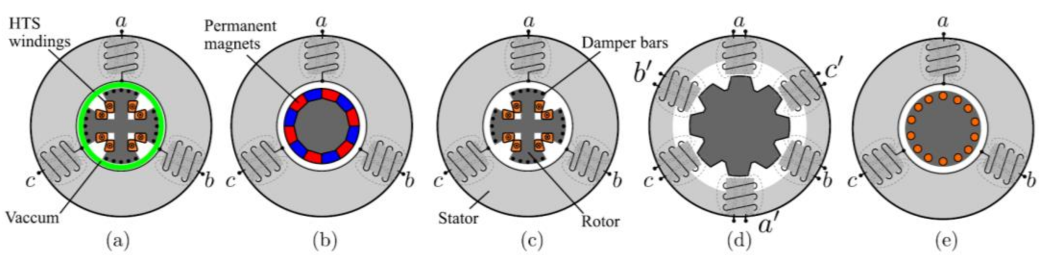

Figure 39 (a) HTS machines, (b) PMSMs, (c) WFSMs, (d) SRMs, and (e) IMs

Currently, permanent magnet synchronous motors (PMSM) are the predominant choice in propulsion applications due to their high specific power and efficiency, despite supply chain and cost concerns related to their rare earth magnets. Within permanent magnet machines, there are a variety of topologies, mechanical arrangements, and cooling approaches. One significant configuration choice is axial versus radial flux as shown in Figure 40 [80].

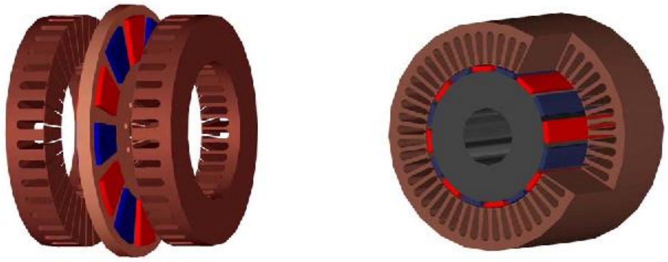

Figure 40 Axial (left) and Radial (right) Flux Permanent Magnet Machines

Various packaging and cooling arrangements have been considered for propulsion motors and the associated motor controllers. At one end of the spectrum is a direct drive, air-cooled system with an integrated motor controller. An example of this arrangement is the recently (2025) certified ENGINeUS^{TM} 125 from SAFRAN in France shown in Figure 41. This motor has a 125 kW power rating and is certified for use on small general aviation and sport aircraft [81].

Figure 41 SAFRAN ENGINeUS^{TM} Motor/Drive

The other end of the spectrum is represented by a superconducting electric machine such as the one designed by Hinetics illustrated in Figure 80. This is a 5 megawatt machine using a separate cryogenically cooled motor controller [82].

Figure 42 Hinetics Subscale Demo for 5 MW Motor

Experience with the design of parallel hybrid demonstrators for near term application in regional aircraft in this size range has shown that the predominant configuration is a radial flux, oil cooled configuration with separate motor controllers. Examples of this machine configuration are seen in the 1 MW motor from Collins Aerospace [83] shown in Figure 43 or the magni650 motor from Magnix [86] shown in Figure 44.

(a) Exterior view (b) Stator assembly

Figure 43 Collins Aerospace 1 MW Motor

Figure 44 Magnix magni650

Because of the predominance of this machine type in demonstrated applications, the metrics used in this analysis are those from that arrangement of permanent magnet machine, although any other machine could be used if comparable metrics were available.

Specific Power

Motor specific power claims from various industry and academic sources vary widely, since there is not a single universally used standard to define this value. Some of the pertinent variables are items such as:

1. Continuous power versus transient capability
2. Use of active weight only versus complete installed weight (housings, bearings, termination, etc.)
3. Coolant temperature limitations
4. Limitations on available supply voltage
5. Inclusion of Thermal Management System (TMS) elements

The author’s industry experience has shown that based on the assumptions included in the calculation, the same machine design can report specific powers that vary over a 3:1 range.

One of the most comprehensive surveys of existing machine specific powers and resulting future projections was performed by Pastr et.al. [84] in support of NASA electrified propulsion investigations. Results of this study are shown below as Figure 45.

TABLE IV
SPECIFIC POWER AND EFFICIENCY PROJECTIONS

Timeframe	Confidence Level	Specific Power (kW/kg)	Efficiency (%)
SoA	—	6	0.96
2030	Conservative	9.2	0.963
	Nominal	13.2	0.968
	Aggressive	16.1	0.974
2040	Conservative	10.8	0.967
	Nominal	20.4	0.975
	Aggressive	33	0.983
2050	Conservative	11.3	0.970
	Nominal	24.3	0.980
	Aggressive	50	0.989

F

Figure 45 Electric Machine Specific Power Projections

Internal industry work by the author shows reasonable alignment with 2030 projections but suggests the potential future projection tends to only align if a conservative/nominal case is considered.

One specific power characteristic that has traditionally appeared during industry electric machine sizing is the dependency of specific power on machine ratings. A study of designs performed by the author across a range of power levels under current consideration results in a specific power value versus maximum continuous power rating as shown in Figure 46 below.

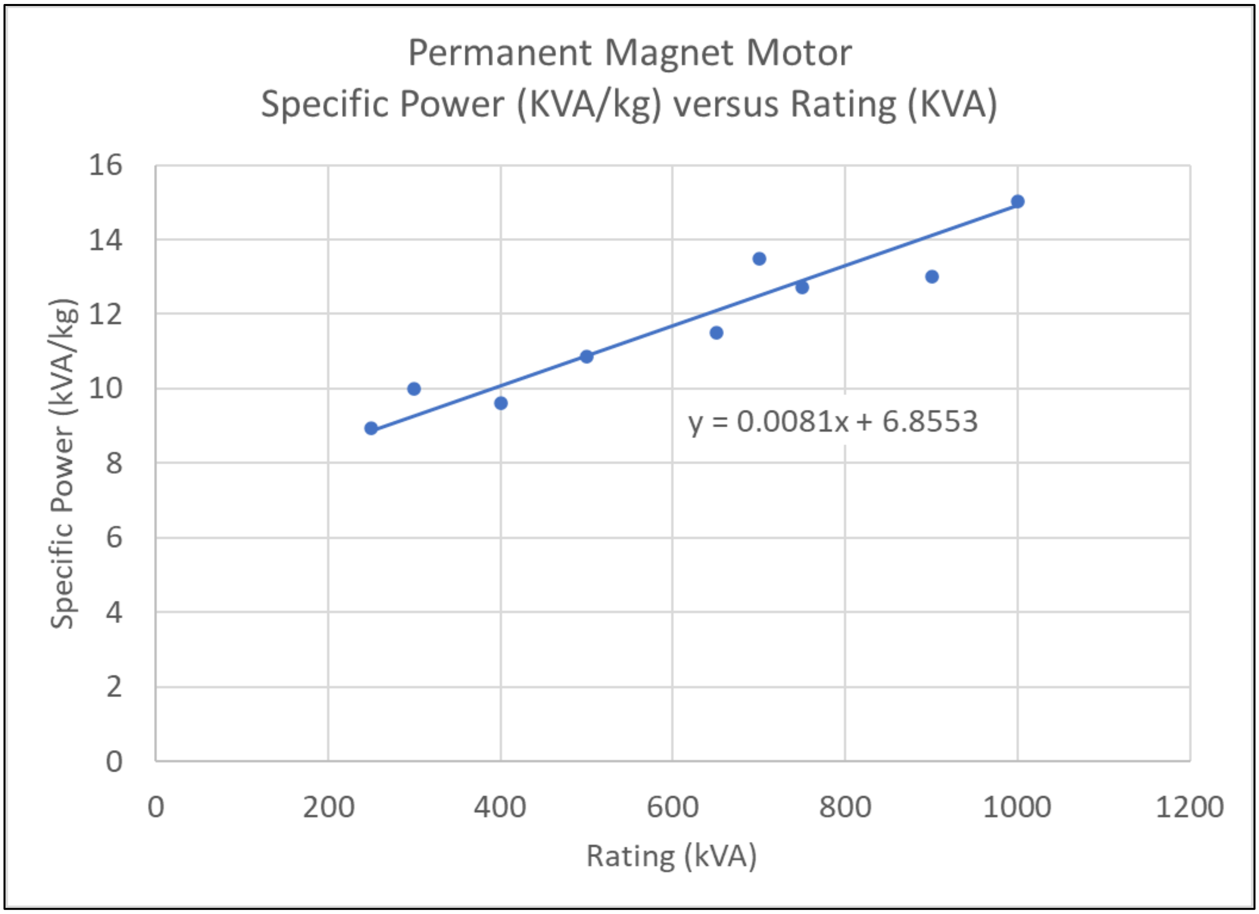

Figure 46 Motor Specific Power versus Maximum Continuous Rating

To fully capture the weight impacts associated with the addition of the electric motor, one must account for the associated added incremental weight of the thermal management system elements such as heat exchangers. Comparable aircraft studies [39] have recommended the addition of 0.5 kg of thermal management system mass for every kilowatt of motor losses.

Efficiency

Permanent magnet motors are well known for their high efficiency potential. Compared to other machine types such as induction or wound field, the near elimination of rotor losses in the permanent magnet machines brings significant advantage.

Efficiency does, however, vary across the operating range. Mechanical losses are present regardless of motor power output, and both iron and copper losses vary across the frequency and current range. A representative efficiency map from one of the authors designs is shown in Figure 47, showing an “island” of peak efficiency.

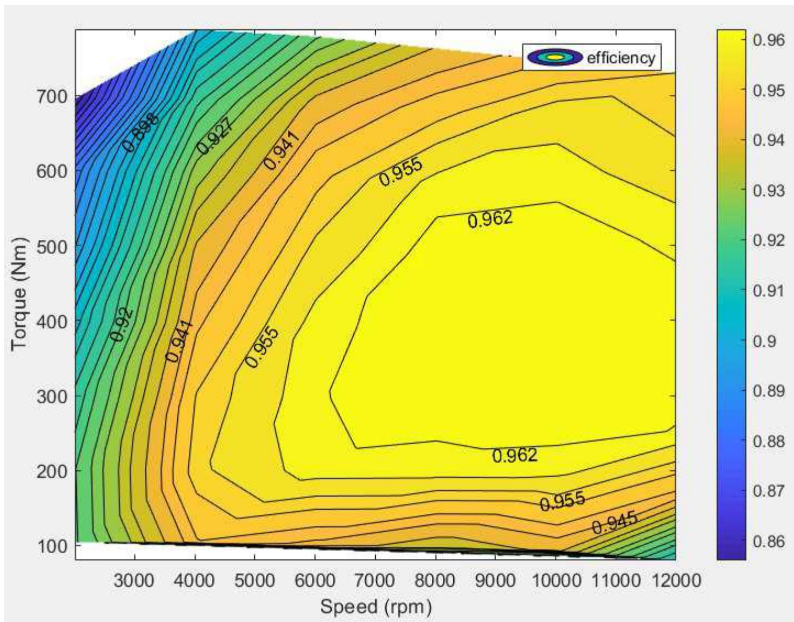

Figure 47 Representative Propulsion Motor Efficiency Map

Product Cost

Aircraft motors are significantly more expensive than industrial or automotive equipment of a similar power class. Low production rates discourage investment in automation, resulting in significant amounts of manual labor. Aerospace quality requirements limit supply chain options, and introduce added documentation, traceability, and testing requirements. Exotic materials such as high cobalt magnetic steel or titanium dramatically increase material and processing costs.

Total product costs consist of labor and material costs. Some costs scale with machine rating due to the increased quantity of raw materials, while others such as winding or testing costs may be relatively rating independent. The author's experience with electric machines in an aerospace environment resulted in the product cost comparisons illustrated in Figure 48 below.

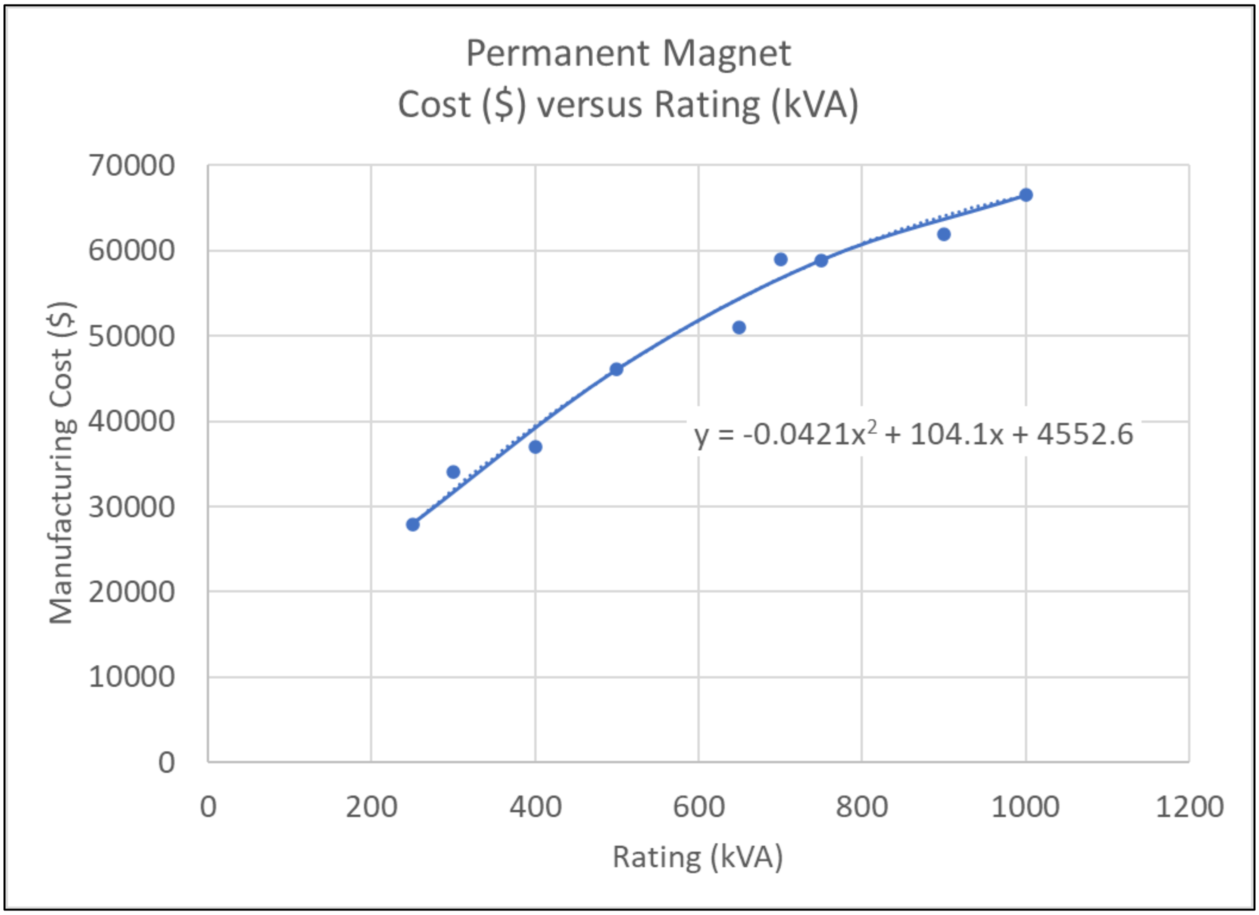

Figure 48 Aerospace Motor Manufacturing Cost versus Rating

Maintenance Cost

Unlike thermal engines which typically rely on periodic maintenance and hour or cycle-based overhauls, aircraft motors have typically operated "on condition" with maintenance beyond minor actions such as oil/filter changes only occurring if the motor is showing signs of actual or impending failure [87].

Industry experience with modern oil cooled and lubricated machines suggest that a 50,000 hour mean time between failure (MTBF) assumption is appropriate for a similar propulsion motor being operated in typical commercial airline service.

Motor Controls

Nearly every electrified propulsion concept uses variable speed motors and high voltage DC electrical networks, necessitating the use of motor controls. In some cases, these motor controls are unidirectional, acting in the motor only direction, but other system configurations are bidirectional, with the system serving both motor and generator functions.

As discussed in the previous paragraphs on electric motors, it is common for smaller rated, air-cooled propulsion systems to include physically integrated motor and motor controllers. While this arrangement may also prove ultimately workable in higher power pure electric series arrangements, its incorporation in the high vibration/temperature/thermal cycling environment of a parallel hybrid remains a significant reliability risk, at least for commercial airline service.

A more common configuration is to have a separate motor controller which may be installed in a less severe but still nearby location on the engine or nacelle. Liquid cooling of these motor controllers is typical due to the loss intensity and (relatively) low temperature limits within the motor controllers. Examples of this motor controller configuration are seen in the 1 MW motor controller from Collins Aerospace [83] shown in Figure 49 or the magni650 motor controllers from Magnix [86] shown in Figure 50.

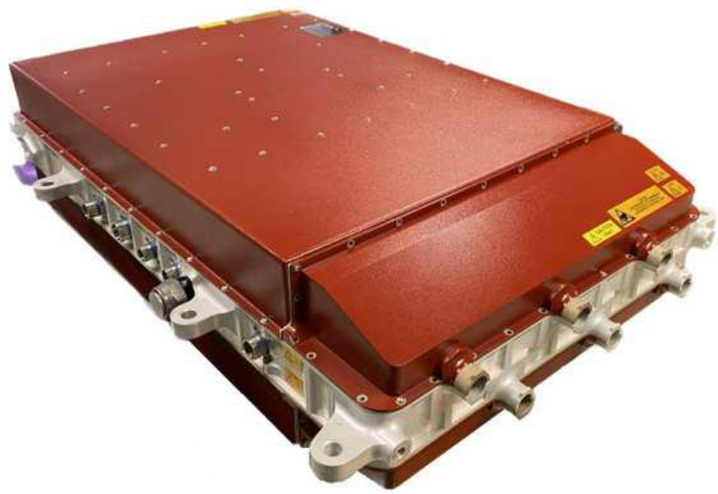

Figure 49 Collins Aerospace 1 MW motor controller

The magniDrive 100 is both an inverter and controller. It provides up to 170 kW of power and 400 A of current, and weighs 12 kg

Figure 50 Magnix motor controller

Specific Power

There are many application specific design configuration choices that make the determination of a generic motor controller specific power estimate difficult. Basic topology (2 vs multilevel), semiconductor device (Silicon, Silicon Carbide, GaN), voltage levels, and filtering/shielding are just some examples of technology choices that can significantly impact this metric.

One of the most comprehensive surveys of existing motor controller specific powers and resulting future projections was performed by Hall et.al. [88] in support of NASA electrified propulsion investigations. Results of this study are shown below as Figure 51.

TABLE IV
FINAL SPECIFIC POWER AND EFFICIENCY PROJECTIONS THROUGH 2050

Timeframe	Confidence Level	Specific Power (kW/kg)	Efficiency (%)
SoA	—	7.5	0.98
2030	Conservative	9.6	0.982
	Nominal	13.8	0.985
	Aggressive	17.3	0.988
2040	Conservative	11.4	0.985
	Nominal	21.1	0.989
	Aggressive	35.1	0.994
2050	Conservative	12	0.987
	Nominal	25.2	0.992
	Aggressive	52.9	0.997

Figure 51 Future Motor Controller Specific Power Projection

Internal sizing work has been performed on a number of motor controllers that are suitable for installation in an aircraft nacelle environment and are compatible with electrical network voltages of approximately 1 kilovolt. This characteristic as a function of power rating is illustrated in Figure 52 below.

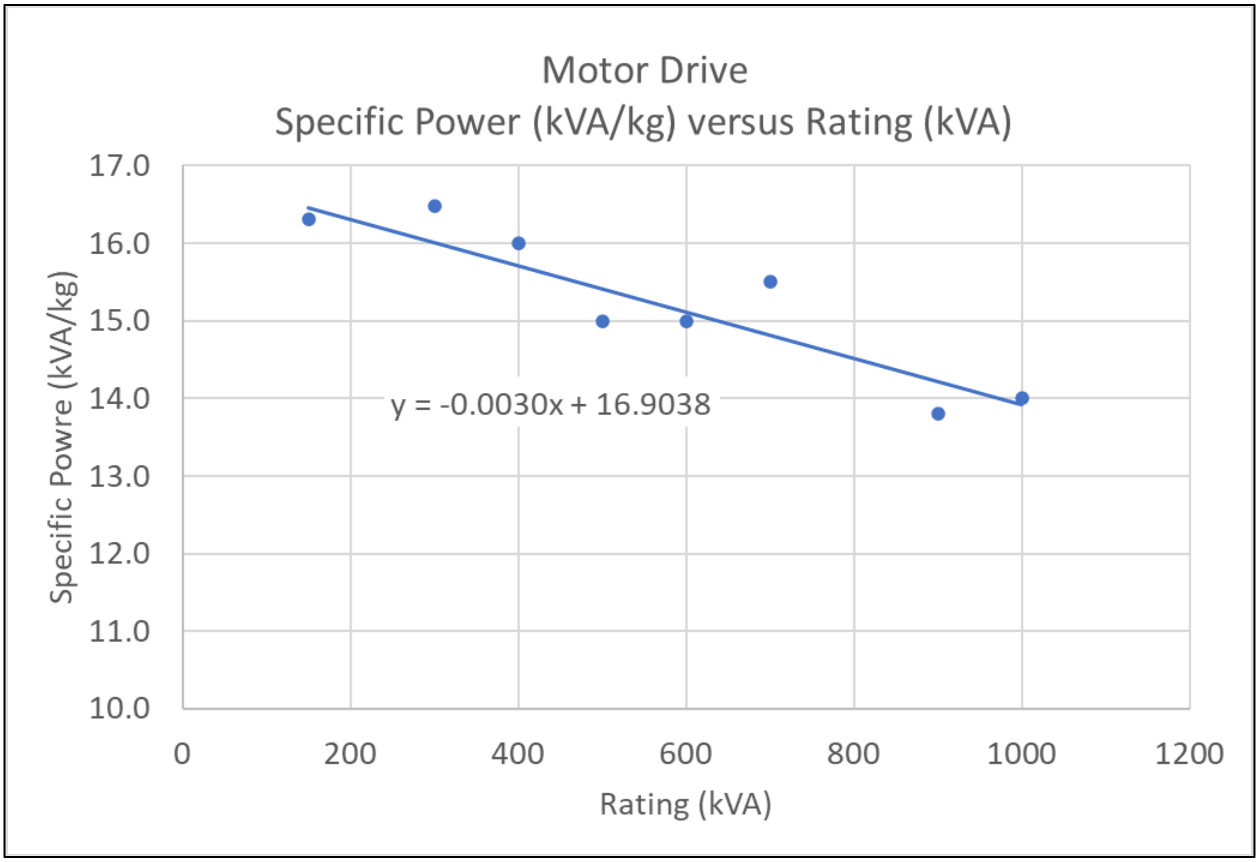

Figure 52 Motor Controller Specific Power versus Maximum Continuous Rating

To fully capture the weight impacts associated with the addition of the motor controller, one must account for the associated added incremental weight of the thermal management system elements such as heat exchangers. Comparable aircraft studies [39] have recommended the addition of 0.5 kg of thermal management system mass for every kilowatt of motor controller losses.

Efficiency

Experience has shown that the efficiency of a propulsion motor controller is relatively constant across the range of power levels in normal operation, so for this case the efficiency was assumed at a constant 98.5% value.

Product Cost

Aircraft motor controllers are significantly more expensive than industrial or automotive equipment of a similar power class. Low production rates discourage investment in automation, resulting in significant amounts of manual labor. Aerospace quality requirements limit supply chain options, and introduce added documentation, traceability, and testing requirements. Semiconductor devices using Silicon Carbide or GaN are significantly more expensive than their Silicon counterparts [89].

Total product costs consist of labor and material costs. Some costs scale with motor controller rating due to the increased quantity of raw materials, while others such as assembly or testing costs may be relatively rating independent. The author’s experience with motor controllers in an aerospace environment resulted in the product cost comparisons illustrated in Figure 53 below.

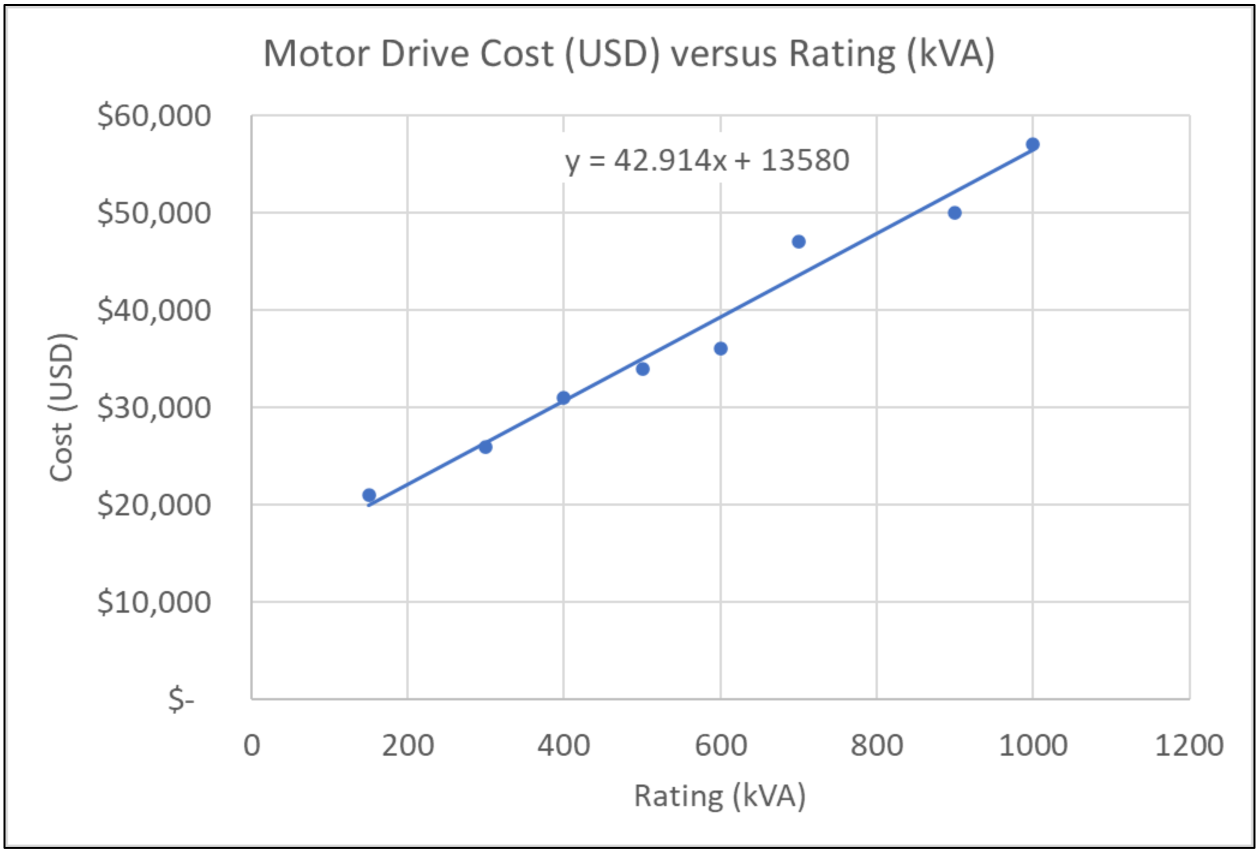

Figure 53 Aerospace Motor Controller Manufacturing Cost versus Rating

Maintenance Cost

Like the aircraft motor described previously, aircraft motor controllers are also typically operated "on condition" with maintenance only occurring if the motor controller is showing signs of actual or impending failure [87].

Internal experience with modern aircraft motor controllers suggest that a 50,000 hour mean time between failure (MTBF) assumption is appropriate to use as a base failure rate for a similar propulsion motor controller being operated in typical commercial airline service.

Battery

The key technology element that has enabled battery electric aircraft is advanced lithium-ion battery technologies. This section provides a comprehensive survey of existing battery chemistries, focusing on their energy density, cycle life, costs, and lifecycle carbon footprint.

This study focuses mainly on battery chemistries that are currently in commercial production and ready to be deployed on aircraft: namely LiFePO4 (LFP), LiNCoyAlO2 (NCA), LiNiMnCoO2 (NMC), and their variations. Each of these battery chemistries exhibit performance and cost tradeoffs. LFP batteries maintain performance over many cycles, exhibit low cost and have relatively low environmental impacts, yet have a low specific energy, which is not preferred in aircraft applications. NCA and NMC batteries exhibit higher specific energies yet have drawbacks in the form of life spans, environmental impact and pack cost [90].

Battery lifetimes have a significant impact on the viability of electric aircraft, as frequent battery replacement comes with a high cost. The lifetime of a battery, also defined as the number of full equivalent cycles the battery can go through before it loses significant capacity, is affected by multiple operational variables, including but not limited to depth of discharge, charging rate, and discharge rate [91].

For the purposes of this study, the performance factors used in this study based on an aggregation of data from multiple sources [91, 93, 94, 95, 96, 97, 98, 99]. The first five columns are based on existing chemistries, while the remaining two are based on optimistic future projections for NMC and LFP chemistries.

Specific Energy

Specific energy, often referred to as gravimetric energy density, is a measure of the energy capacity of a battery relative to its weight, typically expressed in watt-hours per kilogram (Wh/kg). It indicates how much energy a battery can store compared to its weight, making it a crucial factor in applications where weight is a critical consideration, such as in electric vehicles, portable electronics, and aerospace applications. Higher specific energy means that a battery can provide more power for a longer period without significantly increasing the weight of the device it powers. This parameter is essential for improving the efficiency and performance of battery-powered systems, directly impacting their range, usage duration, and overall effectiveness. The pack level gravimetric energy densities presented in Table 6 below reflect current and anticipated cell level energy densities including a 0.8 energy derating factor on cell level values to account for packaging overhead.

Table 6 Aviation Pack Level Specific Energy for Current and Future Chemistries

	NMC811	NCA	LFP	NMC532	NMC111	Opt2030 NMC	Opt2030LFP
W-hr/kg (pack level)	196.38	191.57	144.02	183.83	176.68	328	223

Product Cost

In addition to performance, cost continuously evolves for various battery chemistries. Costs of raw materials, and continuing advances in manufacturing process and efficiencies have resulted in changing relationships between the costs of differing chemistries. This data forms the basis of the cost optimizations that are discussed later in the paper. Cost premiums for aerospace applications (as compared to higher volume automotive or other commercial applications) also increase aviation battery cost and negatively impact electric aircraft adoption. This data used the expected prices of commercial automotive battery packs and then imposed a 4x multiplier to account for the lower quantities and more stringent quality/documentation requirements of the aerospace market [100]. Resulting projections for the pack level costs of an aviation battery are presented in Table 7.

Table 7 Aviation Pack Level Cost for Current and Future Chemistries

	NMC811	NCA	LFP	NMC532	NMC111	Opt2030 NMC	Opt2030LFP
$/kW-hr (pack level)	$ 506.80	$ 493.82	$ 387.95	$ 632.38	$ 506.80	$ 408.00	$ 324.00

Cycle Life

Figure 54 illustrates the cycle life behavior of the various lithium-ion battery chemistries considered in this analysis. Various electrochemical and physical mechanisms are the cause of reduced battery capacity as a function of its cycle-life and calendar life. For example, as the batteries are cycled during flights, the electrolyte and electrode react with one another to form a Solid Electrolyte Interface (SEI) layer that reduces the concentration of lithium ions, leading to reduced energy storage [92]. Mechanical cycling of electrodes can lead to physical breakdown of electroactive materials. This phenomenon can increase with higher depths of discharge and discharge rates. It is important to model this behavior when evaluating the battery energy storage system for electric aircraft, as it will have a deep impact on the design of energy storage for battery electric aircraft.

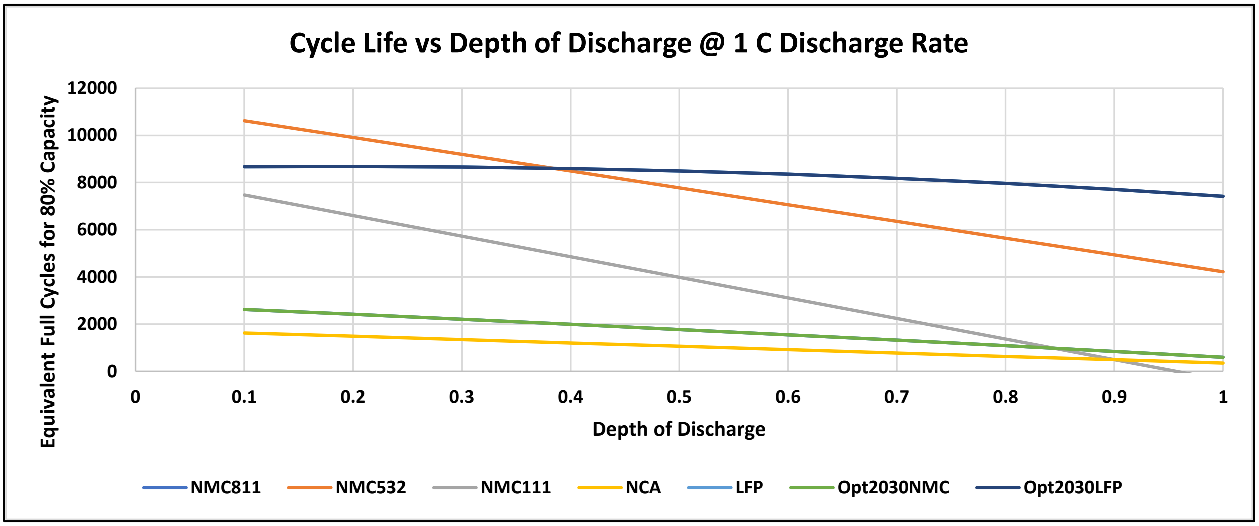

Figure 54 Battery Cycle Lives versus Discharge Depth

Lifecycle CO_2 Footprint

The lifecycle CO_2 emissions of a battery encompass the total amount of carbon dioxide released during its entire lifespan, from raw material extraction to manufacturing, usage, and end-of-life disposal or recycling. These emissions are influenced by several factors, including the type of materials used, the energy sources powering the manufacturing processes, the efficiency of the battery during its operational life, and the methods employed for its disposal or recycling. Additionally, advancements in recycling technologies can significantly reduce the environmental impact by reclaiming valuable materials and reducing the need for new raw material extraction. Understanding and minimizing lifecycle CO_2 emissions are critical for developing more sustainable battery technologies and reducing the overall carbon footprint of battery-powered systems.

The emissions related to usage are covered independently during the mission analysis, so the data presented in Figure 55 and Table 8 below focuses on the manufacturing-related emissions related to a variety of battery chemistries [101].

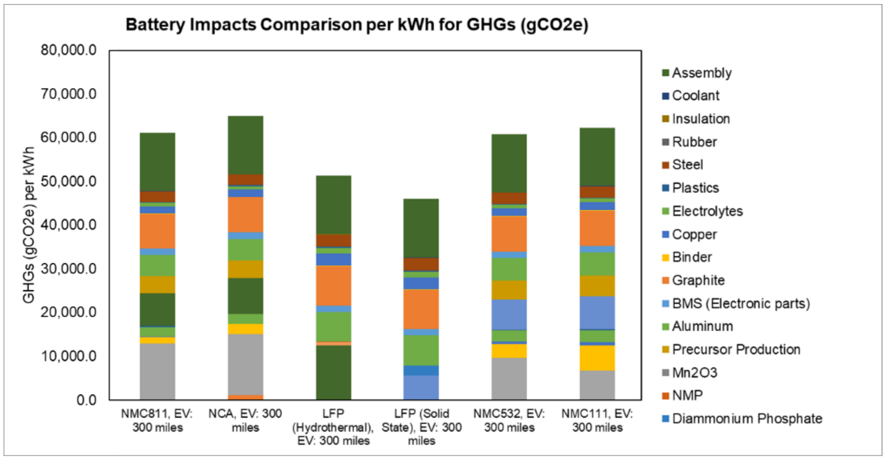

Figure 55 CO_2 Contribution Breakdown by Battery Type

Table 8 Pack Level Total CO_2 Contribution by Battery Type

	NMC811	NCA	LFP	NMC532	NMC111	Opt2030 NMC	Opt2030LFP
kg CO2/kW-hr	65.647	69.777	46.689	65.662	67.569	65	47

Airframe

As described in the introduction, there are several turboprop aircraft types within the scope of interest of this study. There are several airframe specific characteristics that must be specified to translate propulsion system metrics and behaviors to mission level results. From a performance viewpoint, this includes aerodynamic elements such as L/D for each mission segment, maximum takeoff weight, empty weight of the airframe minus the powertrain, and airframe maintenance costs. Seat count is also required to understand costs on a per-seat basis. These elements are all aircraft-specific and must be specified for the aircraft being considered. This can either be through the use of existing data for existing or derivative platforms, or through calculated or scaled values for new or novel airframes.

The ATR42 was selected as the platform for comparative analysis in this study due to its widespread usage and the availability of comprehensive data from both the manufacturer and airlines. This aircraft type provides a robust dataset that allows for a thorough examination of operational performance, cost efficiency, and other relevant metrics, making it an ideal candidate for the study's objectives.

An overview of the basic aircraft configuration is provided in Figures 56-58 below [102].

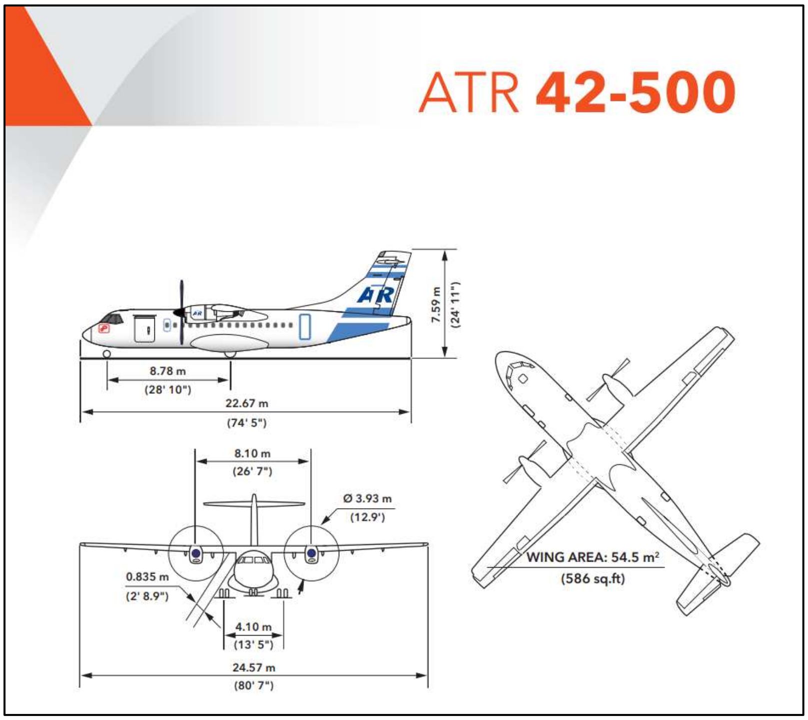

Figure 56 ATR42 External Dimensions

A key approach to normalize outputs across various aircraft types and sizes is to present that data per Available Seat Kilometer (ASK). The typical configuration of the ATR42 is a single class configuration with 48 passenger seats.

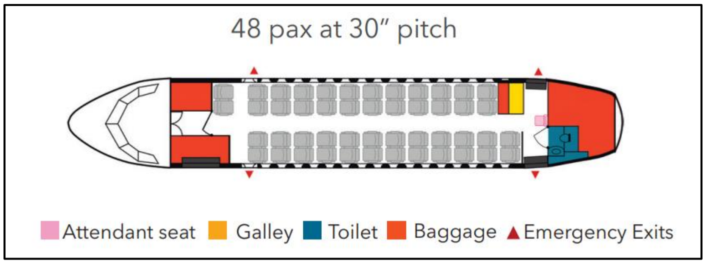

Figure 57 ATR42 Cabin Configuration

Some basic specifications and performance characteristics of this aircraft are shown below.

STANDARD CONFIGURATION	48 seats
Engines Pratt & Whitney Canada	**PW127E/M**
Take-off power	2,160 SHP
Take-off power - One engine	2,400 SHP
Max continuous	2,400 SHP
Max climb	2,160 SHP
Max cruise	2,132 SHP
Propellers Hamilton Standard	**568F**
Blades - diameter	6 - 3.93 m - 12.9 ft
Weights	
Max take-off weight (basic)	18,600 kg - 41,005 lb
Max landing weight (basic)	18,300 kg - 40,344 lb
Max zero fuel weight (basic)	16,700 kg - 36,817 lb
Max zero fuel weight (Option)	17,000 kg - 37,478 lb
Operational empty weight (Tech. Spec.)	11,250 kg - 24,802 lb
Operational empty weight (Typical in-service)	11,500 kg - 25,353 lb
Max payload (at typical in-service OEW)	5,500 kg - 12,125 lb
Max fuel load	4,500 kg - 9,921 lb
Airfield performance	
Take-off distance	
> Basic - MTOW - ISA - SL	1,165 m - 3,822 ft
> TOW for 300 NM - Max pax - SL - ISA	982 m - 3,221 ft
> TOW for 300 NM - Max pax - 3,000 ft - ISA +10	1,164 m - 3,818 ft
Take-off speed (V2 min @ MTOW)	112 KCAS
Landing field length (EASA Air Ops)	
> Basic MLW - SL	966 m - 3,169 ft
> LW (max pax + reserves) - SL	906 m - 2,972 ft
> Reference speed at landing	104 KIAS
En-route performance	
Optimum climb speed	160 KCAS
Rate of climb (ISA, SL, MTOW)	1,851 ft/min
Time to climb to FL170	12.7 min
One engine net ceiling (95% MTOW, ISA +10)	13,010 ft
Max Cruise speed (95% MTOW - ISA - Optimum FL)	300 KTAS - 556 km/h
Fuel flow at cruise speed	811 kg/hr - 1,788 lb/h
Range with max pax	703 NM
200 NM Block Fuel	584 kg - 1,287 lb
200 NM Block Time	60 min
300 NM Block Fuel	802 kg - 1,768 lb
300 NM Block Time	81 min

Figure 58 ATR42 Key Characteristics

Aerodynamic Performance

Aircraft fuel usage is intrinsically linked to the aircraft's lift-to-drag (L/D) ratio, which is a measure of aerodynamic efficiency, with fuel usage calculated using the Breguet range equation. An optimal lift-to-drag ratio means that the aircraft can generate the necessary lift with minimal drag. When the lift-to-drag ratio is high, the aircraft requires less thrust to overcome drag, thereby reducing the engine power output needed and ultimately lowering fuel usage. Conversely, a poor lift-to-drag ratio results in higher drag forces, necessitating increased thrust and, consequently, higher fuel consumption to maintain flight. L/D ratios vary by aircraft configuration (clean versus high lift devices deployed), airspeed, and altitude.

The L/D for the ATR42 aircraft used in this analysis was calculated by using data from the Flight Crew Operating Manual (FCOM), which includes propellor torque values for a variety of aircraft weight, altitude, and airspeed conditions [56]. These parameters are related by Equation 4:

$$Mass_{aircraft} * \mathrm{g} * \frac{V_{TAS}}{\frac{\mathrm{L}}{\mathrm{D}}} = 2 * P_{engine} * \eta_p \tag{Eq. 4}$$

Plotting the data for Indicated Airspeed (IAS) instead of Total Airspeed (TAS) was used to account for the air density differences across varying altitudes, resulting in the relationship illustrated in Figure 59 below.

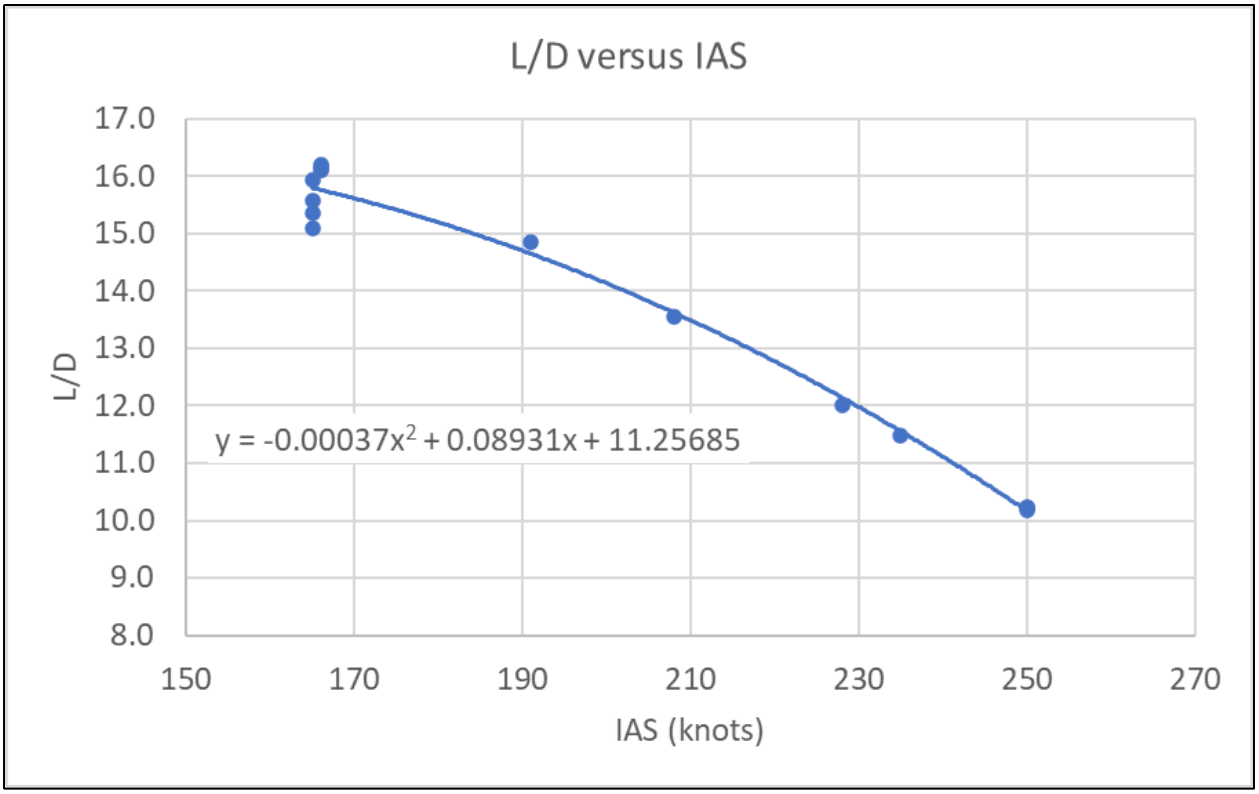

Figure 59 ATR42-500 L/D vs IAS (clean configuration)

Comparison with data from Roskam shows good correlation with typical historical values, with that reference citing L/D of 11-13 for cruise, and 14-16 for loiter [103].

The figure above represents the aircraft in a clean configuration. For operating conditions such as takeoff and landing, where high lift devices and landing gear are deployed, this calculated L/D was decreased by 20% for takeoff and 50% for landing [104].

Initial Cost

Two methodologies were considered to determine a metric for airframe cost as function of Operating Empty Weight (OEW) for aircraft in this size class. The first was to survey the information available for new aircraft costs, which were all referenced to

2023 dollars for aircraft that were no longer in production. This resulted in the following information as presented in Table 9 below [102, 106].

Table 9 New Aircraft Cost as a Function of Mass

	INCLUDING ENGINES					ENGINE DATA			AIRFRAME ONLY				
Aircraft	**OEW (kg)**	**MTOW (kg)**	**Cost (new)**	**$/kg (OEW)**	**$/kg (MTOW)**	**# of engines**	**Engine Mass Total (kg)**	**Engine Cost Total**	**OEW (kg)**	**MTOW (kg)**	**Cost (new)**	**$/kg (OEW)**	**$/kg (MTOW)**
Daher TBM 930	2097	3354	$ 4,000,000	$ 1,907	$ 1,193	1	$ 228	$ 955,000	1869	3126	$ 3,045,000	$ 1,629	$ 974
Cessna Caravan	2145	3969	$ 2,250,000	$ 1,049	$ 567	1	$ 228	$ 955,000	1917	3741	$ 1,295,000	$ 676	$ 346
Cessna Caravan EX	2145	3995	$ 2,750,000	$ 1,282	$ 688	1	$ 228	$ 955,000	1917	3767	$ 1,795,000	$ 936	$ 477
Pilatus PC12 NGX	3092	4750	$ 5,400,000	$ 1,746	$ 1,137	1	$ 228	$ 955,000	2864	4522	$ 4,445,000	$ 1,552	$ 983
Dehaviland Dash 6	3363	5670	$ 5,900,000	$ 1,754	$ 1,041	2	$ 456	$ 1,910,000	2907	5214	$ 3,990,000	$ 1,373	$ 765
King Air 250	4005	5670	$ 6,000,000	$ 1,498	$ 1,058	2	$ 456	$ 1,910,000	3549	5214	$ 4,090,000	$ 1,152	$ 784
king Air 350i	4516	6804	$ 7,500,000	$ 1,661	$ 1,102	2	$ 456	$ 1,910,000	4060	6348	$ 5,590,000	$ 1,377	$ 881
Beech 1900D	4932	7766	$ 8,469,826	$ 1,717	$ 1,091	2	$ 456	$ 1,910,000	4476	7310	$ 6,559,826	$ 1,466	$ 897
Cessna SkyCourier	5591	8618	$ 8,350,000	$ 1,493	$ 969	2	$ 456	$ 1,910,000	5135	8162	$ 6,440,000	$ 1,254	$ 789
Dehaviland Dash 8-100	10477	16466	$ 21,233,588	$ 2,027	$ 1,290	2	$ 964	$ 2,702,102	9513	15502	$ 18,531,486	$ 1,948	$ 1,195
ATR42-500	11250	18600	$ 19,000,000	$ 1,689	$ 1,022	2	$ 964	$ 2,702,102	10286	17636	$ 16,297,898	$ 1,584	$ 924
ATR72-600	13010	22800	$ 27,000,000	$ 2,075	$ 1,184	2	$ 964	$ 2,702,102	12046	21836	$ 24,297,898	$ 2,017	$ 1,113
Dehaviland Dash 8-400	17819	30481	$ 29,500,000	$ 1,656	$ 968	2	$ 1,434	$ 3,818,188	16385	29047	$ 25,681,812	$ 1,567	$ 884
AVERAGES FOR >4,500 KG OEW				$ 1,760	$ 1,089							$ 1,602	$ 955

A second data source was also considered [108] which used data from 2010 to determine a parametric cost as a function of OEW for aircraft up to 10,000 kg OEW. Note this equation was updated from the reference to account for inflation since that time.

$$Aircraft\ Cost\ (USD) = -.003584 * OEW^2 + 2616 * OEW - 2870140 \quad \text{(Eq. 5)}$$

The data from these two approaches is plotted as Figure 60 below. These two approaches show good correlation at masses of 5,000 kg or below but begin to diverge significantly at higher weights. Based on this, data based on current aircraft prices was used for further consideration in this study.

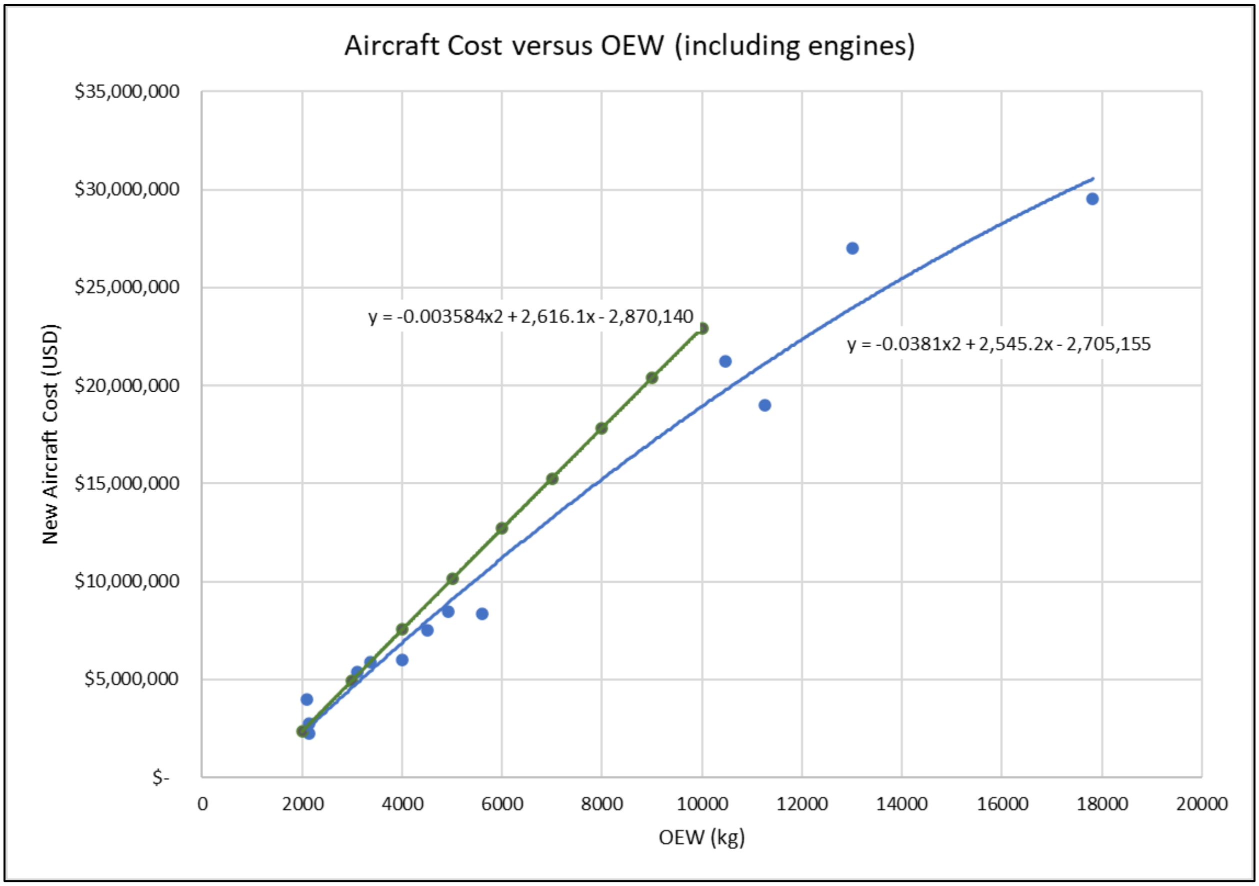

Figure 60 Aircraft Cost versus OEW (including engines)

Since this study will evaluate alternative powertrains, the data needed to be modified to remove the powerplant characteristics from the airframe mass and cost. Based on the cost models created for the gas turbines, the following average costs were used for each of the powerplant types used in these aircraft.

Engine Type	Per Engine Mass (kg)	Per Engine Cost (USD)
PT6	228	$ 955,000
PW120	482	$ 1,351,051
PW150	717	$ 1,909,094

The subtraction of these powerplant costs resulted in the airframe (minus engines) cost versus OEW relationship shown in Figure 61 below.

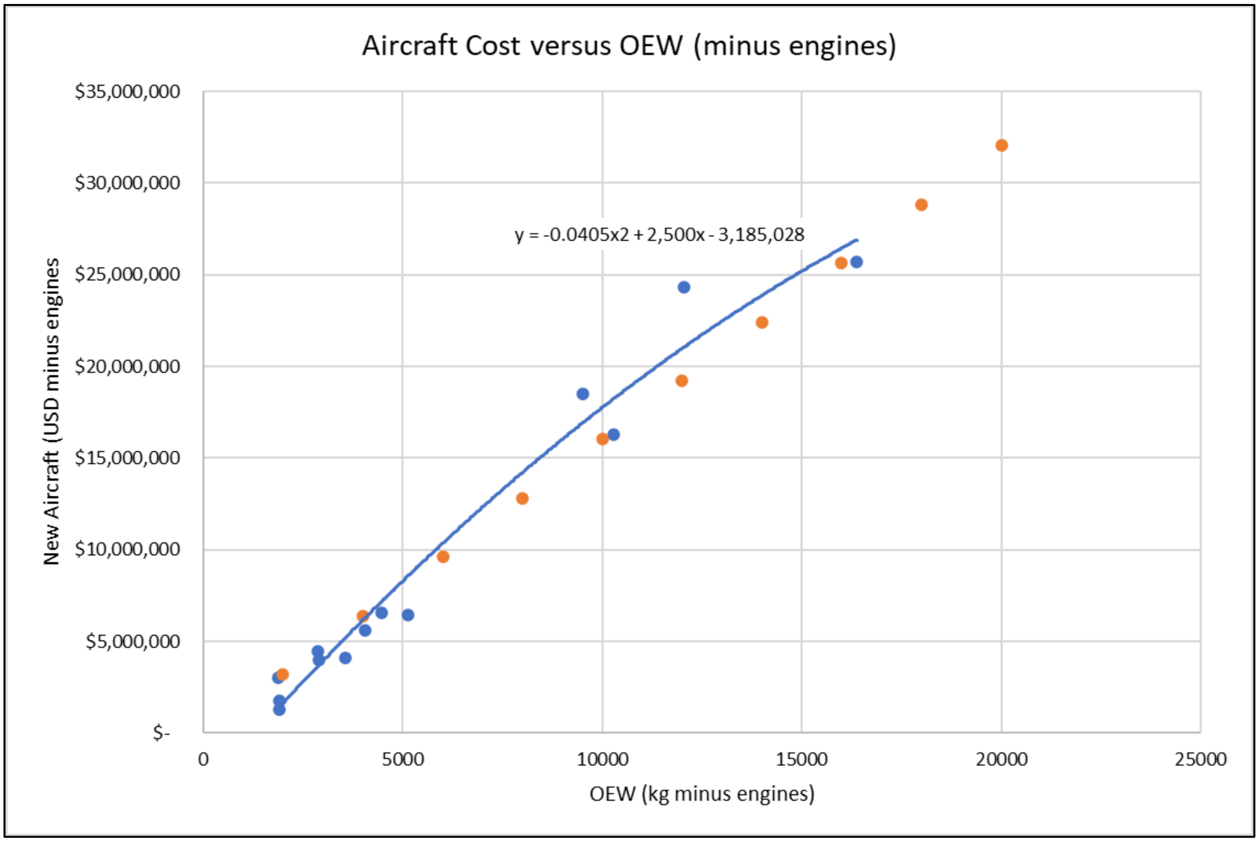

Figure 61 Airframe Cost versus OEW (minus engines)

Maintenance Cost

Airframe maintenance costs are a significant contributor to the total operating expenses for any aircraft. These costs are influenced by various factors and can be categorized into several key elements and consist of labor, parts/material, and consumables costs.

1. Scheduled Maintenance

- Routine Inspections: These are regular checks carried out at specified intervals to ensure the aircraft is in good working condition. This includes tasks such as visual inspections, functional tests, and minor repairs.

- Heavy Maintenance Checks: These are more extensive inspections and repairs performed less frequently. They include detailed examinations of the aircraft's structure, systems, and components and typically require the aircraft to be taken out of service for an extended period.

2. Unscheduled Maintenance

- Component Failures: Unexpected failures of various components such as avionics, landing gear, or fuselage components, leading to unscheduled maintenance and associated costs.

Since the ATR42 has been in service for many years with multiple airlines, maintenance costs for various airframe elements are well characterized [107]. Separating out the propulsion elements (engine, motor/drive, batteries) from the remainder of the aircraft, the resulting airframe Direct Maintenance Cost (DMC) used in this analysis was $545/hour.

Propellor Efficiency

Propeller efficiency is needed to calculate the engine power associated with the required thrust based on the particular aircraft mission segment. The main parameters that influence propeller efficiency are density, cruise speed and the propeller diameter [109]. Efficiency estimations may be based on either empirically derived diagrams or based on underlying theory. An example of an empirically based diagram is presented as Figure 62 below [110].

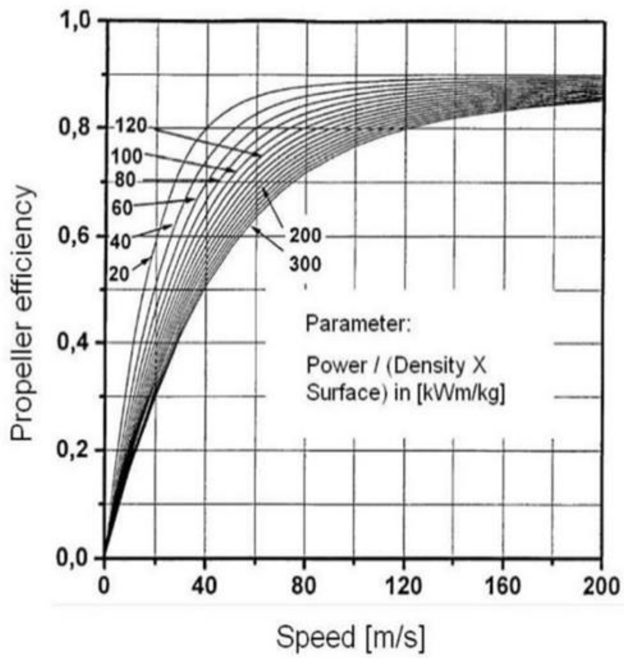

Figure 62 Estimation of Propellor Efficiency

A theoretical calculation was also proposed by Krull [112], as a modification of earlier work by Truckenbrodt [111]. This takes the form of Equation 6 presented below, and was the methodology used for calculations in this work.

$$\eta_p \approx 0.9 * \frac{2 - 2 * \lambda^2 * \ln\left(1 + \frac{1}{\lambda^2}\right)}{1 + \sqrt{1 + 2 * \frac{L_D}{V_{TAS}{}^3} - 2 * \lambda^2 * \ln\left(1 + \frac{1}{\lambda^2}\right)}} \quad \text{(Eq. 6)}$$

$\lambda = \frac{V_{TAS}}{u}$ with: $u = n * \pi * d_p$

Conclusions

This chapter sought to address the research problem identified as research question 2, which is repeated below:

Research Question 2) How can systems designers determine and characterize important hybrid electric configuration elements through empirical and physics-based models?

Now having performed the research activities documented in the above sections, we can answer the research question. The identification of existing information has allowed for the creation of the necessary powertrain and airframe models to characterize the elements that will be a part of a complete hybrid regional aircraft configuration.

Chapter 5 - Aircraft Evaluation and Optimization Methods and Tools

This chapter seeks to address the research problem identified as research question 3, which is repeated below:

Research Question 3) How do systems designers identify and create suitable analysis and optimization methods and tools?

To answer this question, this chapter presents the desired characteristics of the analytic and optimization toolset. Before the tool was created, the required characteristics of that tool were determined. User needs were evaluated and translated into a set of user requirements that must be satisfied by the new tool. A literature search and survey of industry and academia was performed to understand availability and characteristics of existing tools. A variety of analysis and MDO tools exist in industry and academia that may have been suitable for use in this activity. The current state of the art was researched and evaluated to identify any gaps that needed to be addressed. An analysis/optimization tool for aircraft and propulsion system design was then constructed and verified. Adaptation was needed to create a dedicated toolset that is tailored to this activity with the appropriate core functionality and peripheral functions/datasets required.

Introduction / Literature Search

As discussed in the work to address research question 1, the evaluation metrics of most important to regional aircraft operators are Direct Operating Costs and Lifecycle CO_2 emissions. A literature search was performed to understand the availability and capability of existing tools to quantify those metrics for a particular aircraft configuration and operational scenario.

Significant research efforts have been undertaken in the US related to electrified aircraft design, with significant funding sponsorship by NASA from the Electrified Aircraft Propulsion (EAP) project [113] and the Electrified Powertrain Flight Demonstration (EPFD) project [114]. These projects created and evaluated new electrified aircraft propulsion technologies and architectures and the challenges involved with integrating them into certifiable future aircraft concepts and inspired the creation of modern tools focused on the unique characteristics of these vehicles.

There are multiple examples of these types of tools created withing government, academia, and private industry. An example of government research comes from NASA, who has recently released AVIARY, a new platform for aircraft modeling that was derived from their Flight Optimization System (FLOPS) and General Aviation Synthesis Program (GASP). This tool looks at geometry, aerodynamics, propulsion, and mass, and then performs a mission analysis to evaluate the performance of the resulting aircraft [115]. Other studies by European Research & Technology Organizations such as ONERA, DLR, and NLR have also outlined methodologies to perform similar activities [116, 117, 119, 120].

Some of the earliest work in academia focused on Direct Operating Costs was performed by Scholz at HAW Hamburg [131]. This work captured the appropriate elements of the DOC, but elements such as powertrain maintenance costs were treated as operationally independent constants, which does not capture real world effects of thermal engine or motor/motor controller severity or battery cycle life. Other recent work is more focused on mission performance than overall operating costs. An example of this approach is the Future Aircraft Sizing Tool (FAST), created by the IDEAS lab at the University of Michigan [121]. This tool also uses a variety of parametric physics-based and data-driven models for both the airframe and propulsion system and provides mission level outputs. It is evolution of the earlier E-PASS toolset developed by Cinar while at Georgia Tech [122, 123, 124]. Another series of academic tools have evolved from Stanford University Aerospace Vehicle Environment (SUAVE), an open-source conceptual level aircraft design environment with similar functionality [125]. These include Library for Unified Conceptual Aircraft Synthesis (LUCAS) [126] and Research Community Aircraft Interdisciplinary Design Environment (RCAIDE) [127]. These tools have various levels of scope, fidelity, and optimization approaches. A summary of these characteristics is presented as Table 10 below.

Table 10 Key Characteristics of Existing Toolsets

Dimension	**FAST**	**RCAIDE**	**AVIARY**
Optimization Type	Parametric	Architecture-centric	Full MDO
Solver Style	Sweeps / heuristics, design space exploration	Hybrid continuous + discrete	Gradient-based nonlinear OpenMDAO
Objectives	DOC, block energy	Mission Energy, emissions	Block energy, MTOW
Variables	Wing loading, thrust-to-weight, tech factors	Propulsion layout, energy split	Geometry, structures, propulsion
Execution Speed	Very fast	Moderate	Slower

Lastly, an example of a tool created by private industry is the Piano suite of tools offered by Lyssys. This tool has widespread use by airframe and engine manufacturers and has progressively evolved to be able to accommodate the needs of evolving hybrid electric configurations [128].

These tools are all capable of providing detailed mission analysis, which is necessary for the calculation of fuel and energy usage and the associated carbon emissions, but they do not provide the wider information necessary to calculate Direct Operating Costs under actual operating conditions. This points to the need to create a more holistic evaluation method to meet that broader need.

Evaluation Approach Overview

In response to this need, an expanded methodology was developed that allowed the calculation of the metrics of interest for a particular configuration and operational scenario. The expanded methodology used to determine these metrics is presented in the flowchart shown in Figure 63 below. The information captured in the blue boxes to the left include configuration and performance information on the aircraft and powertrain, the aircraft mission that is being evaluated, and airport infrastructure information (including things like local energy costs).

The green boxes provide a summary of intermediate calculations, illustrating some high-level interrelationships across the various elements. This finally results in the actual metrics of interest shown at the right-hand side of the flowchart.

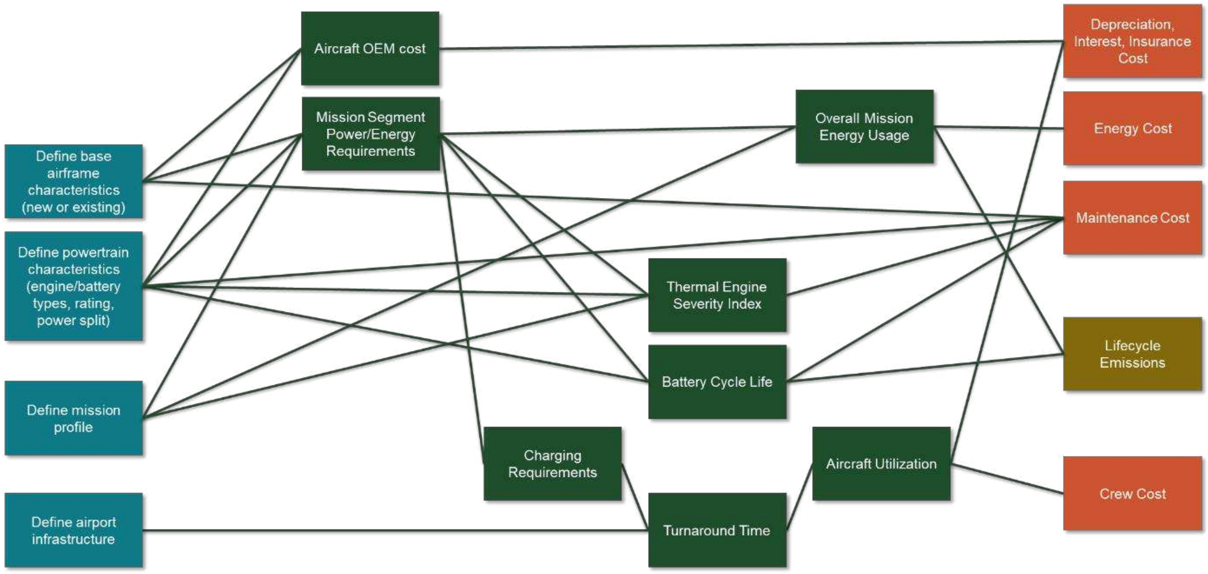

Figure 63 Evaluation Flowchart

The structure of the analysis process is more rigorously shown in the Design Structure Matrix illustrated in Figure 64.

	Direct Operating Cost	Maintenance cost	Lifecycle carbon emissions	Thermal engine severity index	Motor equivalent hours	Battery cycle life	Financing costs	Aircraft OEM cost	Energy cost	Crew cost	Aircraft utilization	Turnaround time	Charging requirements	Airport charging infrastructure	Fuel Type	Country of Operation	Aircraft empty weight	Takeoff weight	Mission segment power/energy	Mission profile	Thermal/electrical power split	Passenger and payload	Overall mission energy usage	Base airframe characteristics	Thermal engine power	Thermal engine type	Motor power rating	Battery capacity	Battery chemistry
Direct Operating Cost																													
Maintenance cost	X																												
Lifecycle carbon emissions																													
Thermal engine severity index		X																											
Motor equivalent hours		X																											
Battery cycle life		X	X																										
Financing costs	X																												
Aircraft OEM cost							X																						
Energy cost	X																												
Crew cost	X																												
Aircraft utilization							X			X																			
Turnaround time											X																		
Charging requirements												X																	
Airport charging infrastructure												X																	
Fuel Type									X																				
Country of Operation								X	X																				
Aircraft empty weight																		X											
Takeoff weight																			X										
Mission segment power/energy				X	X	X																	X						
Mission profile																			X										
Thermal/electrical power split																			X										
Passenger and payload																		X											
Overall mission energy usage			X						X				X					X											
Base airframe characteristics		X						X									X		X										
Thermal engine power		X		X				X									X												
Thermal engine type		X		X				X									X		X										
Motor power rating		X			X			X									X		X										
Battery capacity		X	X			X		X									X												
Battery chemistry		X	X			X		X									X												

Figure 64 Design Structure Matrix

The approach used in this research is Design Space Exploration (DSE). DSE identifies design solutions that best satisfy the metrics of interest from a space of possible design points. The DSE process searches through a large set of possible designs identify optimal configurations that best meet the desired metrics.

Each cycle of this DSM evaluates the metrics of interest for a single configuration and concept of operations. Exploration of the range of desired choices through multiple varied runs will result in the creation of a pareto frontier. This pareto frontier can then be examined to identify the option that achieves the maximization of the metric(s) of most interest to a particular customer. An automatic identification of the most preferred option through a weighted metric approach was initially considered and could ultimately be implemented, but insufficient quantified customer data was available to rigorously implement that approach at this time.

Careful consideration of the series of considered cases can be used to understand impacts of changing inputs such as fuel or electricity prices, or variation in some of the modelled characteristics such as battery specific energy, either due to uncertainty in the data or expected future technology advancements. This would be accomplished either through direct change in input values for single point values such as fuel price, or by application of a scaling factor to model parameters such as specific power.

One of the key inputs to this model is a fixed aircraft geometry and set of mission profiles. Once those characteristics have been fixed, the model calculates the required powertrain power at each specific mission point, and then determines the resulting component sizes, usage profiles, and nonrecurring and recurring costs. The toolset as it currently exists is populated with the aerodynamic, airframe weight/cost and mission profiles associated with an ATR42-500 aircraft. This was the aircraft used for generation of the results presented in Chapter 7, and for the validation presented in Chapter 6. The characteristics of a DeHavilland Dash8-100 were also used for the second Chapter 6 validation case. Use of this methodology for a different airframe or mission profile would require the creation/collection of corresponding data for that specific situation, and the tool is only limited by data availability to be able to represent various airframes/missions. The powertrain models and methodology, however, can be re-used without modification.

The basic procedure for setting up and executing the evaluation is as follows. The first step of the evaluation process is to populate the characteristics of the airframe of interest. As described previously, this includes information as described in Chapter 4 such as L/D, maximum takeoff weight, airframe weight minus powertrain, airframe maintenance costs, and passenger capacity. Once defined, these values remain constant throughout the exploration space.

The next step is defining the desired aircraft mission profile. This includes altitudes, airspeeds, climb rates, and overall mission lengths. Aircraft flight manuals include recommended values for existing aircraft, and these can be used as-is or can be modified as necessary (as an example, electric boost could be implemented to provide increased climb rate).

Physical characteristics of the powertrain such as power ratings and energy capacity must also be defined. This includes definition of thermal engine type, and desired battery chemistry. The concept of operation of the hybrid powertrain must also be defined, including which power source (thermal or electric) is providing the required power in what proportion for each mission segment.

Execution of the series of calculations described in detail in the following sections results in determination of the aircraft level metrics of interest. The detailed calculation methodologies were drawn from a variety of sources and consolidated into a single unified toolset.

Aircraft Mission Profile

For this study, design missions of both 200nm and 300nm were considered, based on published ATR mission data and advertised performance [102].

Figure 65 illustrates the mission length distribution of the ATR42 aircraft. It can be seen that most of the missions flown today are less than 200 nautical miles. A range of 200nm covers about 65% of all missions operated by regional turboprop aircraft, while 300nm covers 84% of all missions flown [42].

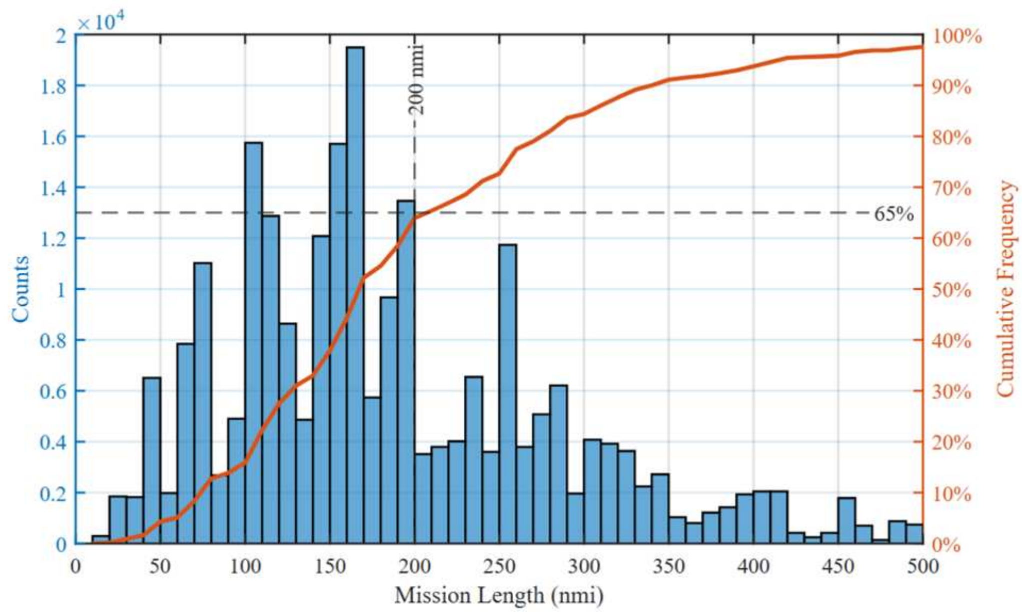

Figure 65 Worldwide mission length distribution for ATR42

Deutsche Aircraft data shows a similar trend as shown in Figure 66, particularly highlighting the shorter-range emphasis of the 30-seat turboprop compared to the 50-seat version [43].

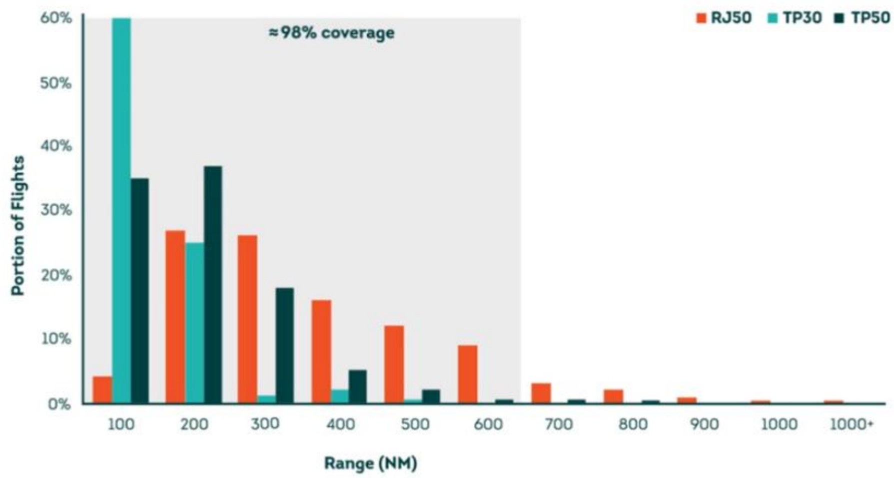

Figure 66 Deutsche Aircraft Data on Regional Aircraft Range Distribution

A survey of a typical day's flight of this aircraft type provides further insight of actual usage, varying from a low of 82nm to a high of 462nm, with an average of approximately 150nm [130]. The distribution of the typical flight distances is illustrated in Figure 67 below.

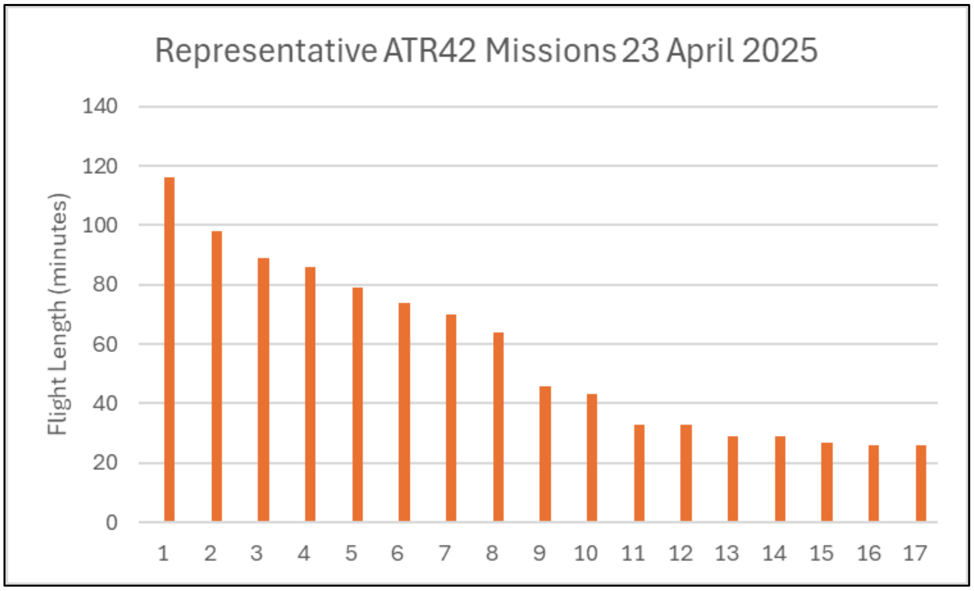

Figure 67 Example ATR Flight Length Distribution

The time/altitude/speed profile used for the mission analysis is illustrated in Figure 68 below. This mission profile was based on recommended operating characteristics as detailed in the ATR Flight Crew Operating Manual [56].

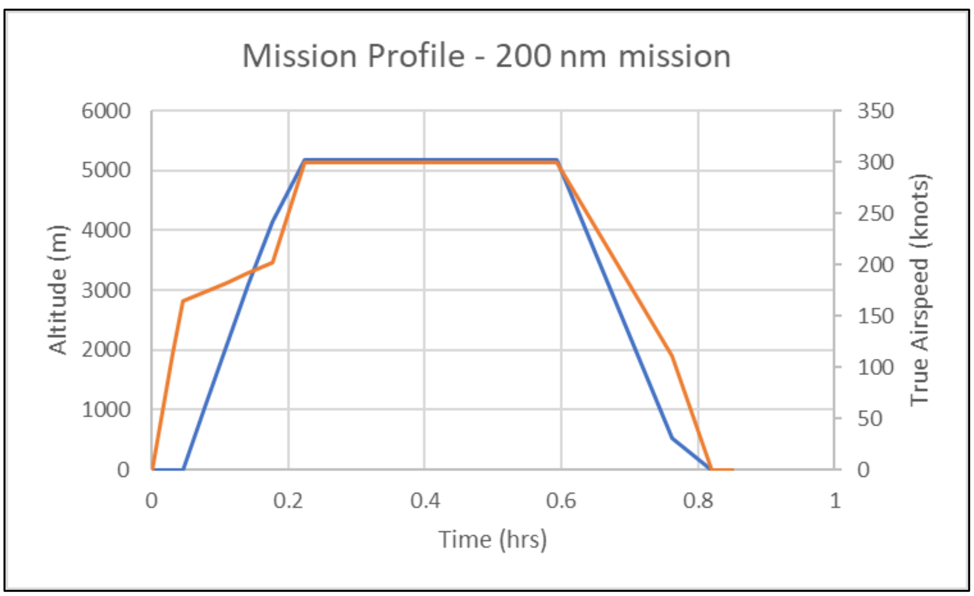

Figure 68 Example Analyzed Aircraft Mission (graphical form)

The same mission presented in tabular form is given in Table 11 below:

Table 11 Example Analyzed Aircraft Mission (tabular form)

Segment	Beginning Altitude (m)	Ending Altitude (m)	Time (hours)	Total Airspeed (km/hr)	Total Airspeed (knots)	Indicated Airspeed (knots)	Climb Rate (m/min)	Distance (km)	Distance (nm)
Constants (segment independent)									
Taxi Out	0	0	0.03	50					
Takeoff	0	0	0.02	209	113	113		3	2
Climb 20%	0	1036	0.03	304	164	160	530	10	5
Climb 40%	1036	2072	0.03	320	173	160	530	10	6
Climb 60%	2072	3108	0.03	336	181	160	530	11	6
Climb 80%	3108	4144	0.04	355	192	160	475	13	7
Climb 100%	4144	5180	0.05	375	202	160	375	17	9
Cruise	5180	5180	0.37	554	299	230		204	110
Descent	5180	518	0.17	530	286	248	-460	90	48
Approach/Landing	518	0	0.06	204	110	109	-150	12	6
Taxi In	0	0	0.03	50					
Overall Mission			0.85					370	200
Reserve	3000	3000	1	295	159	137		295	159

An example of an actual flight profile from a representative flight is shown in Figure 69, verifying the validity of the assumed idealized profile [130].

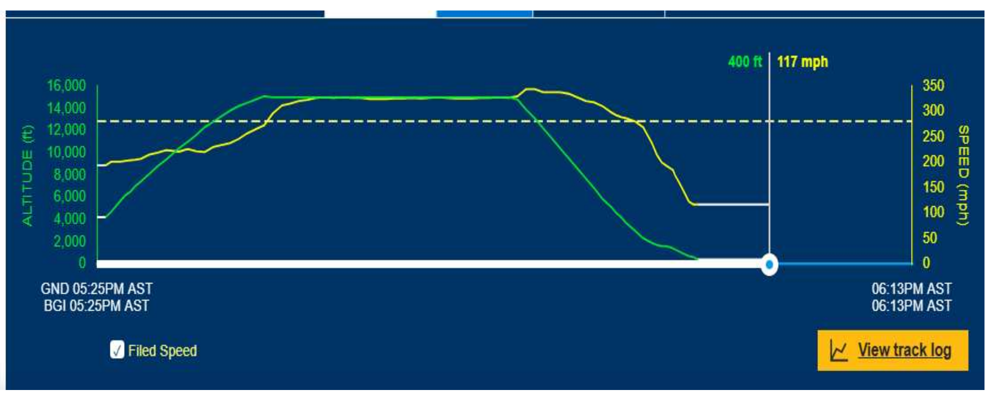

Figure 69 Example Flight Profile from an In-Service ATR42

Calculation Methodology Results

The calculation methodologies for each topic illustrated in the Design Structure Matrix in Figure 64 have been identified and are presented in the following section.

Depreciation/Interest/Insurance Cost

As was illustrated in Figure 13, Direct Operating Costs consist of Cash Operating Costs and Costs of Ownership (COO). COO includes depreciation, interest, and insurance costs. The base methodology used to calculate these costs is summarized in [131], with underlying factors collected from a variety of sources [132, 133, 134, 135], but has been modified to account for the added elements of the electrified powertrain, including batteries. It should be noted that these costs apply to airlines that purchase/own their own airplanes, and this cost would be replaced by a lease rate instead if the airline leased aircraft from another party instead. The price value for a particular configuration is aggregated from the choices made by the user on sizes and types/chemistries of the airframe and various powertrain elements, combined with the product cost curves presented in Chapter 4.

Depreciation

The depreciation is the allocation of the reduction in the value of an item over its useful service life. To calculate depreciation, you need to know the useful service life of the item and determine the reduction in its value over this period. The value of a new item is its total purchase price (P). After the end of its service life, the item can still be sold for its residual value (residual P). The reduction in value over the useful life (total reduction in value) is first calculated, then the annual depreciation expense is calculated by dividing the reduction in value by the useful service life. This formula gives the annual depreciation cost, which represents the yearly allocation of the reduction in the value of the item over its useful service life.

$$C_{DEP} = P_{total} * \frac{1 - \frac{P_{residual}}{P_{total}}}{n_{DEP}} \quad \text{(Eq. 7)}$$

The total purchase price of an aircraft P_{total} includes the delivery price $P_{delivery}$ and the price for the spares P_{spares} purchased with each aircraft.

$$P_{total} = P_{delivery} + P_{spares} \quad \text{(Eq. 8)}$$

The price for spares P_{spares} is calculated from a proportion $k_{spares,xx}$ of the prices of the airframe, engines, and major components such as motors and batteries, as applied to the incremental prices of each of those elements.

$$P_{spares} = k_{spares,airframe} * P_{airframe} + k_{spares,engine} * P_{engine} + k_{spares,motor} * P_{motor} + k_{spares,battery} * P_{battery} \quad \text{(Eq. 9)}$$

Table 12 Historical parameters for the calculation of depreciation [131]

Source	n_{DEP}	$\frac{P_{residual}}{P_{total}}$	$k_{S,AF}$	$k_{S,E}$
ATA 1967	12	0.00	0.10	0.10
NASA 1977			0.06	0.06
widebody [a]	16	0.10		
turbo fan [a]	14	0.02		
turbo jet [a]	10	0.05		
turbo prop [a]	10	0.15		
DLH 1982	14	0.00	calculated from necessary availability of spare parts in stock	
AEA 1989a	14	0.10	0.10	0.30
AEA 1989b	16	0.10	0.10	0.30
AI 1989	15	0.10	0.06	0.25
Fokker 1993	15	0.10	0.08	0.08

[a] Data in **NASA 1977** are quotes from the Hamurghden "Depreciation Guidelines" of the U.S. Civil Aeronautics Board (CAB).

Historical parameters for the calculation of depreciation are provided in Table 12 above. For purposes of this analysis the following values were used:

Table 13 Assumed Depreciation Factors for this Analysis

Parameter	airframe	engine	motor	battery
n_{DEP} - Depreciation Period (years)	10	10	10	10
$P_{residual}/P_{total}$	0.10	0.10	0.10	0.20
k_{spares}	0.10	0.30	0.10	0.20

Interest

The interest payable to the investor is calculated using the average interest rate. The annual interest cost can be determined by multiplying the total investment cost by the average interest rate (p_{av}). Since it is assumed that the investment for a new aircraft plus spares, is financed entirely from external sources, the total investment cost (k_0) is equal to the aircraft price (P_{total}). This provides the yearly interest expense that needs to be paid to the investor.

$$C_{INT} = p_{av} * k_0 = p_{av} * P_{total} \qquad \text{(Eq. 10)}$$

After the final payment year n_{PAY} a relative residual value k_n / k_0 of the outside capital may remain in the company. This relative residual value of the outside capital is independent of the relative residual value of the depreciation residual total $P_{residual}$ / P_{total} and may differ from this. This results in the following applied average interest rate.

$$p_{av} = \frac{\dfrac{\left((1+p)^{n}{}_{PAY} - \dfrac{k_n}{k_0}\right) * p * n_{PAY}}{(1+p)^{n}{}_{PAY} - 1} - \left(1 - \dfrac{k_n}{k_0}\right)}{n_{DEP}} \qquad \text{(Eq. 11)}$$

Table 14 Historical parameters for the calculation of interest [131]

source	p	$q = 1 + p$	n_{PAY}	$\frac{k_n}{k_0}$	n_{DEP}	p_{av}
ATA 1967	0.00	1.000	-	-	12	0.0000
NASA 1977 / AA 1980	0.00	1.000	-	-	-	0.0000
DLH 1982	0.09	1.09	14	0.0	14	0,0570
AEA 1989a	0.08	1.08	14	0.1	14	0.0529
AEA 1989b	0.08	1.08	16	0.1	16	0.0534
AI 1989	0.05	1.05	10	0.0	15	0.0197
Fokker 1993	0.08	1.08	15	0	15	0.0502

Historical parameters for the calculation of interest are provided in Table 14 above. For purposes of this analysis the following values were used:

Table 15 Assumed Interest Factors for this Analysis

p	n_{PAY}	k_n/k_0	n_{DEP}	p_{av}
0.04	10	0	10	0.0233

Insurance

COC also considers the insurance costs for the aircraft, which cover hull damage or hull loss. These insurance costs are calculated annually as a percentage of the aircraft's price for simplicity. Note that in this case the insurance cost is only applied to the operating equipment, not the associated spares.

$$C_{INS} = k_{INS} * P_{delivery} \qquad \text{(Eq. 12)}$$

Table 16 Historical parameters for the calculation of insurance [131]

Table 14.7 Parameters for the calculation of the insurance costs

	ATA 67	AA 1980	DLH 1982	AEA 1989a AEA 1989b	AI 1989	Fokker 1993
k_{INS}	0.0200	0.0100	0.0056	0.005	0.005	0.004

Historical parameters for the calculation of insurance are provided in Table 16 above. For purposes of this analysis the following values were used:

Table 17 Assumed Insurance Factors for this Analysis

k_{INS}	0.005

Energy Usage

Calculating aircraft mission fuel usage is a complex, multi-step process that involves multiple factors, each contributing to the overall efficiency and effectiveness of the aircraft's performance. To accurately estimate fuel consumption, one must consider various elements such as the aircraft's weight and aerodynamic characteristics, the flight plan, specific fuel consumption (SFC) of the engines, efficiency of the electrical powertrain (if present), and environmental conditions.

Starting with the aircraft's weight, it is essential to account for the total mass, which includes the aircraft's own weight (empty weight), the payload (passengers, cargo, and crew), and the fuel itself. The total weight significantly impacts the amount of fuel required for the mission. Heavier aircraft demand more thrust during takeoff, climb, cruise, and descent, leading to higher fuel consumption.

The flight plan is another critical factor in determining fuel usage. This includes the distance to be traveled, the chosen route, cruising altitude, and speed. The distance directly correlates with the amount of fuel needed, as longer flights require more fuel. However, the route taken can also influence fuel consumption. Selecting an optimal cruising altitude where the aircraft can operate most efficiently helps in reducing fuel consumption. The speed at which the aircraft flies also plays a role; while higher speeds can reduce travel time, they often result in increased fuel usage due to higher aerodynamic drag.

One of the most crucial parameters in fuel calculation is the specific fuel consumption (SFC) of the aircraft's engines. SFC is a measure of the fuel efficiency of an engine, defined as the amount of fuel needed to produce a specific amount of thrust for a specific period. Lower SFC values indicate more fuel-efficient engines. Different types of engines have varying SFC values, and this must be factored into the overall fuel consumption calculation. Modern engines are designed to optimize fuel efficiency, yet the SFC can still vary depending on the operating conditions such as altitude and throttle settings.

The flight profile, which includes the phases of climb, cruise, and descent, is addressed by segment to understand the overall mission fuel usage. Each phase has different fuel consumption characteristics. During the climb, engines operate at higher power settings to overcome gravity and gain altitude, leading to higher fuel consumption rates. The cruise phase is typically the most fuel-efficient part of the flight, as the aircraft operates at a steady altitude and speed where the engines can perform optimally. However, even within the cruise phase, slight adjustments in altitude and speed can further optimize fuel consumption. The descent phase generally requires less thrust as the aircraft descends primarily by gravity, but careful management is needed to ensure fuel is not wasted by excessive use of thrust or speed brakes.

Calculating the range for hybrid electric aircraft involves a detailed analysis of both the electric and conventional propulsion systems, as well as the integration between them.

The classic Breguet Range Equation has traditionally been used to calculate the range of a jet or propellor driven aircraft. This equation highlights the importance of factors such as aerodynamic efficiency (lift-to-drag ratio), engine efficiency (specific fuel consumption), and the weight ratio (initial to final weight) in determining the range of an aircraft. This equation [104, 136, 137] can be expressed as:

$$R = \eta_{gt} * \eta_p * \left(\frac{L}{D}\right) * \left(\frac{e_f}{g}\right) * \ln\left(\frac{W_{OE} + W_{PL} + W_f}{W_{OE} + W_{PL}}\right) \quad \text{(Eq. 13)}$$

The Breguet range equation for electric aircraft is adapted to account for the unique characteristics of electric propulsion systems. Unlike conventional jet or propeller-driven aircraft, electric aircraft rely on battery energy storage for energy storage as opposed to consumable fuel, resulting in a constant aircraft weight throughout the flight. The modified Breguet range equation [138, 139, 140, 141, 142, 143] for electric aircraft is given by:

$$R = \eta_m * \eta_p * \left(\frac{L}{D}\right) * \left(\frac{e_{bat}}{g}\right) * \left(\frac{W_{bat}}{W_{OE} + W_{PL} + W_{bat}}\right) \quad \text{(Eq. 14)}$$

Combining these two configurations into a series or parallel hybrid architecture results in the following generic powertrain diagram as shown in Figure 69 below.

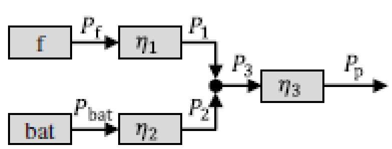

Figure 70 Generic Hybrid Powertrain Schematic

A necessary characteristic of a hybrid architecture is a power split parameter to define the amount of power coming from each energy source. This power ratio [144, 145] is defined as:

$$\Phi = \frac{P_{bat}}{P_{bat} + P_f} \quad \text{(Eq. 15)}$$

The full derivation of the resulting hybrid range equation is addressed in depth in [146, 147], with the following resulting equation:

$$R = \eta_3 * \left(\frac{L}{D}\right) * \left(\frac{e_f}{g}\right) * \left(\eta_1 + \eta_2 * \frac{\Phi}{1 - \Phi}\right) \quad \text{(Eq. 16)}$$

$$* \ln\left(\frac{W_{OE} + W_{PL} + \left(\frac{g}{e_{bat}}\right) * E_{0,bat} + \left(\frac{g}{e_f}\right) * E_{f(t_{start})}}{W_{OE} + W_{PL} + \left(\frac{g}{e_{bat}}\right) * E_{0,bat} + \left(\frac{g}{e_f}\right) * E_{f(t_{end})}}\right)$$

A key limitation of this equation is that it is only applicable for level flight. To compute the required thrust (and subsequent energy usage), a free body diagram of the aircraft is considered as shown in Figure 71.

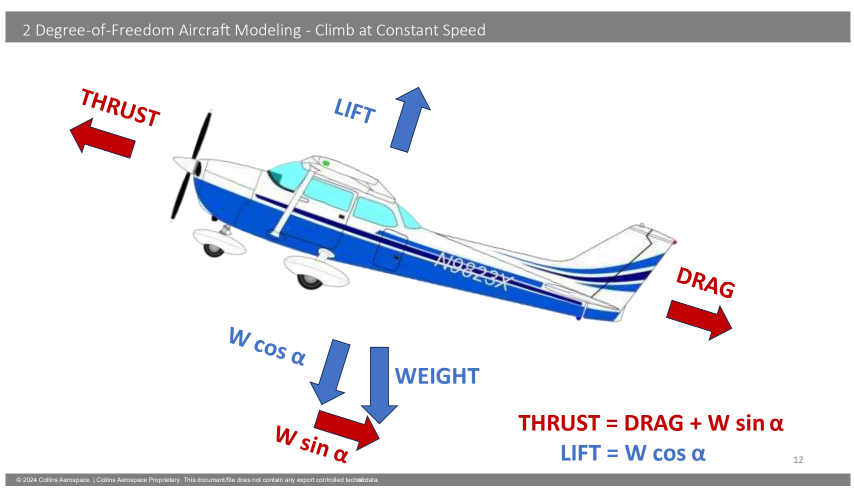

Figure 71 Free body diagram of climbing aircraft

As the diagram shows, this climb adds a weight component that is directly reacted by thrust, while also reducing the required lift, which relates to drag through the aircraft L/D ratio. This leads to a modification of Equation 16 as given as Equations 17 and 18 below.

$$R = \eta_3 * \left(\frac{L}{D}\right)^{modified} * \left(\frac{e_f}{g}\right) * \left(\eta_1 + \eta_2 * \frac{\Phi}{1-\Phi}\right) * \ln\left(\frac{W_{OE} + W_{PL} + \left(\frac{g}{e_{bat}}\right) * E_{0,bat} + \left(\frac{g}{e_f}\right) * E_{f(t_{start})}}{W_{OE} + W_{PL} + \left(\frac{g}{e_{bat}}\right) * E_{0,bat} + \left(\frac{g}{e_f}\right) * E_{f(t_{end})}}\right) \quad \text{(Eq. 17)}$$

where:

$$\left(\frac{L}{D}\right)^{modified} = \left(\frac{L}{D}\right) * \frac{1}{\cos(climb\ angle) + \sin(climb\ angle) * \left(\frac{L}{D}\right)} \quad \text{(Eq. 18)}$$

This range equation has the advantage of being a closed form equation-based solution, but it is limited in its flexibility to deal with changes in propulsive efficiency during the course of a mission due to varying power levels/splits, or with changes in L/D due to changes in configurations during flight (such as opening/closing of landing gear or high lift devices). A more refined method in this case is a stepwise approach where incremental fuel burn is calculated for each mission condition and summed to determine the overall mission fuel burn. This approach allows for individual performance factor changes to be included that change with base aircraft configuration or specific mission segment. This allows for each segment to be specifically tailored for power ratio, L/D and efficiencies, allowing for calculation of the fuel and battery energies used in each of those flight segments.

Energy Cost

To properly determine the values appropriate for use in this analysis, it is essential to understand the worldwide behaviors of jet fuel and electricity commodities. The cost of jet fuel is influenced by several factors, including crude oil prices, refining costs, supply and demand dynamics, geopolitical events, and regulatory policies. Jet fuel prices typically vary slightly between geographic regions, but can vary significantly over time.

Electricity costs, on the other hand, depend on factors such as the energy mix (renewables, coal, natural gas, nuclear, etc.), grid infrastructure, regional demand, governmental regulations, and market structures. Electricity prices can also fluctuate based on usage periods, as well as due to seasonal variations.

Analyzing historical data, market trends, and forecasts for both jet fuel and electricity will provide a more comprehensive understanding of their cost behaviors. This information can then be used to accurately model and compare the energy costs associated with different powertrain configurations.

Jet Fuel

Jet fuel costs have historically been one of the most volatile of the various contributors to direct operating costs. Over the period from 2000-2024, jet fuel prices on an inflation adjusted basis have varied from a low of $0.60/gallon to $5.60/gallon [148] as illustrated in Figure 72.

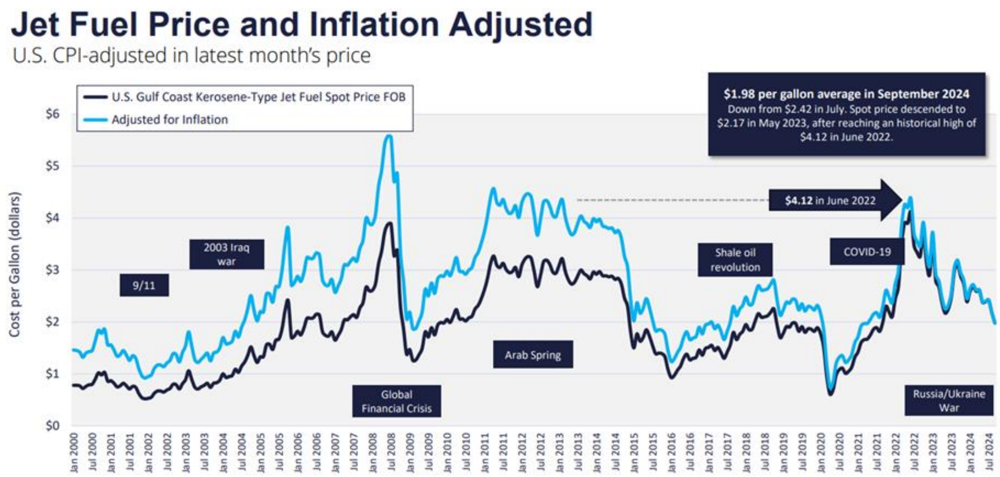

Figure 72 Inflation Adjusted Jet Fuel Prices

One of the primary near-term approaches to reduce net CO_2 emissions without fundamentally changing the aircraft engine has been to use Sustainable Aircraft Fuel (SAF). Sustainable Aviation Fuel is a type of renewable fuel specifically designed to power aircraft. It is produced from sustainable resources such as waste oils, agricultural residues, or other biomass sources, and can significantly reduce the carbon footprint of aviation compared to traditional fossil-based jet fuel. SAF is chemically similar to conventional jet fuel and can be blended with it, allowing it to be used in existing aircraft engines and fuel infrastructure without modifications. The use of SAF is a key strategy in the aviation industry's efforts to reduce greenhouse gas emissions and improve environmental sustainability. However, since SAF is not yet produced at industrial scale, its cost is significantly higher than petroleum-based jet fuel, with a current cost difference of 2.4:1 as shown in Figure 73 below [149].

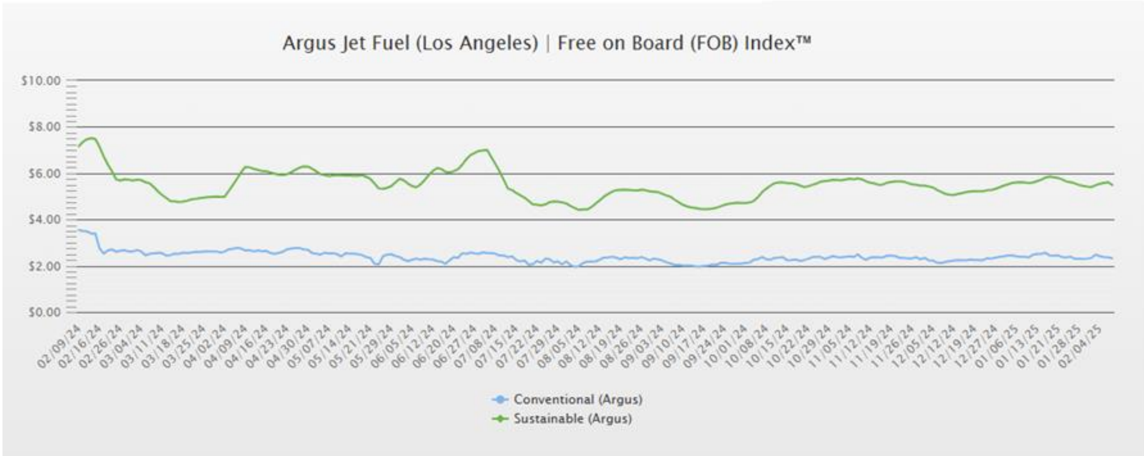

Figure 73 Price for SAF versus Conventional Jet Fuel

As baseline values for this work, the fuel costs shown in Table 18 were used in the overall economic analysis.

Table 18 Costs for Various Jet Fuel Types

Fuel Type	Fuel Cost ($/kg)	Fuel Cost ($/gallon)
Jet A	$0.76	$2.31
SAF (biomass)	$1.92	$5.50

Electricity

Electrical energy costs vary widely based on the area of the world where airline operations occur. The characteristics of the electrical grids in these countries vary widely from China or India using coal (low cost/high carbon footprint) to France using nuclear (high cost/low carbon footprint) to Norway using hydro (low cost/low carbon footprint). Examples of the 2022 cost of various national electric grids are presented in Table 19 below [150, 151].

Table 19 Selected Worldwide Electricity Costs

Region	2022 Cost ($USD/kWh)

World	$0.12
China	$0.09
Norway	$0.12
US	$0.15
India	$0.13
France	$0.21
Australia	$0.23
Brazil	$0.14

Maintenance Cost

The elements of maintenance cost that are addressed in this model include the airframe and powertrain components and systems. The powertrain includes the thermal engine, electric motors and motor controllers, and batteries.

In Chapter 4, the concept of the severity factor was presented. Experience has shown that the interval between engine maintenance actions is related to how closely the engine is operated to its design limits. This damage accumulation primarily occurs during the takeoff and climb phase of the mission. For each operating point, the thermal engine power being used is compared to the power available at the altitude condition. If the thermal engine is being operated below that available limit, it is considered “thrust derating” and is applied as described in equation 2. The mission length used for that severity factor is also based on the particular usage profile for the specific configuration, so if for example the thermal engine is only used for 10 minutes at the beginning and end of a 60-minute flight, it would be modelled as two cycles of ten minutes each instead of a single 60 minute cycle.

The maintenance costs for the motors and motor controllers are also addressed using this usage-based approach, although in a different way. Experience with secondary system motors and controllers reveals that failures occur even if the unit is not processing power due to stressors such as vibration, temperature cycling, and humidity. Because of this, a methodology is used that creates an “equivalent operating hours” based on the following formula:

$$Equivalent\ Operating\ Hours = X * Aircraft\ Block\ Hours + Y * Hours\ at > 50\%\ Power \quad \text{(Eq. 19)}$$

where X and Y for motors and motor controllers are as follows:

Table 20 Equivalent Operating Hours Factors for Motors and Motor Controllers

	X	Y
Motor	1.0	0.5
Motor Controller	0.5	1.0

These equivalent operating hours per aircraft block hour should then be used in conjunction with the replacement product cost and expected maintenance interval to calculate the maintenance cost per aircraft block hour.

The cycle life of the battery was discussed earlier in Chapter 4. The installed battery capacity and its usage during a particular mission cycle will determine the depth of discharge and C-rate, which will result in a percentage life used per block hour. The size/chemistry of the battery, its initial purchase price, and any residual battery value will then determine the battery related costs.

Crew Cost

The costs associated with pilots and flight attendants are a significant part of the operational expenses for regional airlines. These costs include salaries, benefits, training, and per-diem and travel expenses. Example salaries from Silver Airways [152], a large ATR42 operator are as follows:

<u>Salaries and Wages: (average total $254 per hour)</u>

First Officers: $63 - 71 per hour.

Captains: $120 - 184 per hour.

Flight Attendants: $20 - 50 per hour.

<u>Benefits: (average total 35% of wages)</u>

Health insurance, retirement plans, and travel benefits.

Per diem allowances for meals and other expenses during layovers.

<u>Training: (average total $17 per hour)</u>

Pilot training: $5,000 - 10,000 annually per pilot.

Flight attendant training: $1,000 – 2,000 annually per attendant.

Based on these values, a total crew cost of $360 per hour was assumed in this analysis.

Lifecycle CO_2 Emissions

Numerous elements contribute to the lifecycle CO_2 emissions of regional aircraft in operation. For purposes of this work, the focus is on emissions due to energy production and use (either fuel or electricity), and to battery manufacturing, since these are the primary differences when comparing various powertrain configurations. Other elements, such as airframe manufacture, are generally equivalent regardless of powertrain, and have been neglected for this work.

Fuel Based Emissions

The typical approach to characterize lifecycle CO_2 emissions is by using Well-to-Wake (WtWa) accounting methods. WtWa lifecycle CO_2 emissions for jet fuel refer to the total greenhouse gas emissions produced from the extraction of crude oil (the "well") through its processing, transportation, refinement into jet fuel, distribution, and finally its combustion in aircraft engines (the "wake"). This comprehensive assessment includes the following stages which are described below and illustrated in Figure 74 [153]:

1. Recovery, Extraction, and Movement: Emissions from extracting crude oil from the ground, including energy used in drilling and transporting the oil to refineries.

2. Jet Fuel Production (refining): Emissions from converting crude oil into jet fuel, involving various refining processes that consume energy and produce CO_2.

3. Fuel Transportation: Emissions from transporting refined fuel to airports and fueling aircraft.

4. Combustion: Emissions from burning fuel in aircraft engines during flight, which is the most significant source of CO_2 emissions in the lifecycle.

The WtWa approach provides a holistic view of the environmental impact of jet fuel.

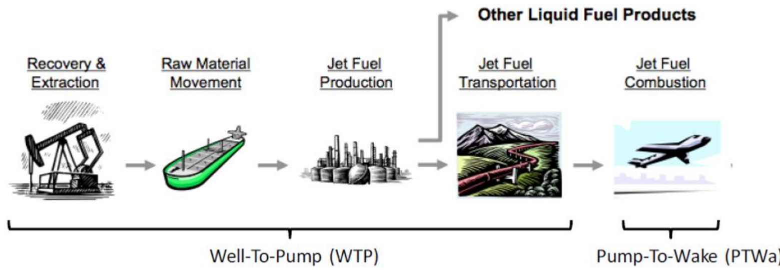

Figure 74 Illustration of Elements of WtWa Emissions

While this illustration is representative of petroleum-based jet fuels, a similar philosophy applies to Sustainable Aviation Fuel (SAF).

The Well-to-Pump (WtP) portion of the fossil fuel CO_2 lifecycle marginally varies across geographic regions, being lowest in the Middle East and highest in North America as shown in Figure 74 below [154].

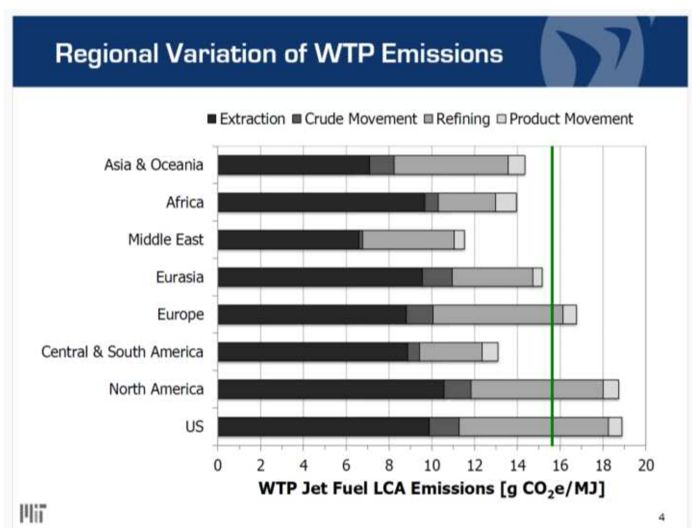

Figure 75 Regional Variation of WtP Emissions for Jet A

Using a worldwide average for the WTP values, the following WtWa values were used for Jet A and biomass-based SAF [155].

Table 21 WtWa Emissions for Various Jet Fuel Types

Fuel Type	GHG Emissions (gCO_2/MJ)	Fuel Carbon Intensity ($kg\ CO_2/kg$)
Jet A	88.7	3.965
SAF (biomass)	15.5	0.708

Electrical Grid Emissions

Like energy costs, carbon footprints attributable to electrical generation and transmission also vary widely based on the area of the world where airline operations occur. Examples of the 2022 carbon footprint of various national electric grids are presented in Table 22 below [156, 157]. A reduction in carbon intensities is expected in most world regions over the next decade, with estimated reductions of 20-40%.

Table 22 Selected Worldwide Electric Grid Carbon Footprints

Region	2022 Carbon Intensity ($kg\ CO_2/kWh$)
World	0.44
China	0.53
Norway	0.029
US	0.37
India	0.63
France	0.085
Australia	0.50
Brazil	0.10

Battery Manufacturing Emissions

The cycle life and manufacturing emissions characteristics of a variety of candidate battery chemistries were presented in an earlier chapter. To calculate the battery related CO_2 emissions characteristics of a particular use case, it is necessary to calculate the overall package size (in kW-hr), the cycle life (cycles) and manufacturing emissions related to the specific chemistry (g CO_2/kW-hr). Calculation of required battery package size for a desired depth of discharge was done using the same methodology as for the calculation of energy usage presented earlier and then applying it to the chemistry of the chosen battery.

Conclusions

This chapter sought to address the research problem identified as research question 3, which is repeated below:

Research Question 3) How do systems designers identify and create suitable analysis and optimization methods and tools?

Now having performed the research activities documented in the above sections, a complete analysis methodology has been designed and created to quantify the metrics of interest for a given configuration and set of operational considerations.

Chapter 6 - Validation of Models and Evaluation Toolset

This chapter seeks to address the research problem identified as research question 4, which is repeated below:

Research Question 4) How can the analytic tools and methodologies be validated for known configurations?

To answer this question, this chapter presents a cross section of published use cases across aircraft sizes, mission profiles, and powertrain configurations. The first step was to understand the work that has been done by others that can help validate the results of the tool. This used the results of the survey from research question 1 and a literature search of flight test results and analysis results and used that previous work to provide a cross section of tested and predicted vehicle performance. The new toolset was then used to determine consistency with previous studies, with tuning as necessary to achieve convergence. This task evaluated results across a range of aircraft sizes, hybridization configurations, mission profiles, and economic assumptions to replicate the results of others.

Introduction

Few examples of hybrid electric regional platforms have flown prior to this research being completed, but validation of the analytic model was needed to compare its output to data from other independent sources. This validation was performed for the legacy ATR42-500 aircraft, validating both mission fuel burn and DOC for a pure fuel powered gas turbine configuration, and for a parallel hybrid DeHavilland Dash 8, verifying the expected differences between the gas turbine and hybrid variants.

Results

The results of these comparisons are presented in the following section.

ATR42-500 Mission Fuel Burn

The first configuration to validate is the existing ATR42-500 aircraft with its current fuel engine only powertrain. The key model functionality to validate is the fuel that is used across a particular set of missions. The Flight Crew Operating Manual (FCOM) for this aircraft [56] includes a series of performance tables that allow the fuel usage to be calculated on a segment-by-segment basis as well as for a complete mission with a given flight profile.

Figure 76 illustrates the segment-by-segment fuel calculation methodology recommended in the FCOM. In this case, fuel usage during the climb, cruise, and descent phases are determined individually from the weight and speed conditions used for the particular mission.

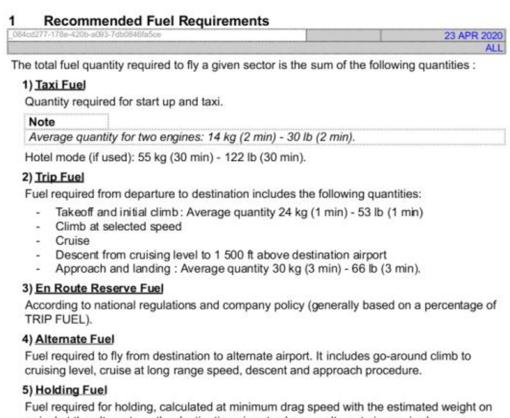
1 Recommended Fuel Requirements

084cd277-178e-420b-a093-7db0846fa5ce | 23 APR 2020 | ALL

The total fuel quantity required to fly a given sector is the sum of the following quantities :

1) <u>Taxi Fuel</u>

Quantity required for start up and taxi.

Note

Average quantity for two engines: 14 kg (2 min) - 30 lb (2 min).

Hotel mode (if used): 55 kg (30 min) - 122 lb (30 min).

2) Trip Fuel

Fuel required from departure to destination includes the following quantities:

- Takeoff and initial climb : Average quantity 24 kg (1 min) - 53 lb (1 min)
- Climb at selected speed
- Cruise
- Descent from cruising level to 1 500 ft above destination airport
- Approach and landing : Average quantity 30 kg (3 min) - 66 lb (3 min).

3) En Route Reserve Fuel

According to national regulations and company policy (generally based on a percentage of TRIP FUEL).

4) Alternate Fuel

Fuel required to fly from destination to alternate airport. It includes go-around climb to cruising level, cruise at long range speed, descent and approach procedure.

5) Holding Fuel

Fuel required for holding, calculated at minimum drag speed with the estimated weight on arrival at the alternate or the destination airport, when no alternate is required.

Figure 76 ATR42-500 FCOM mission fuel calculation methodology

A second approach is to use the graphical calculation method illustrated below in Figure 77 and 78. Note that these graphs are based on a particular aircraft weight (17,500 kg TOW) and cruise speed (max cruise).

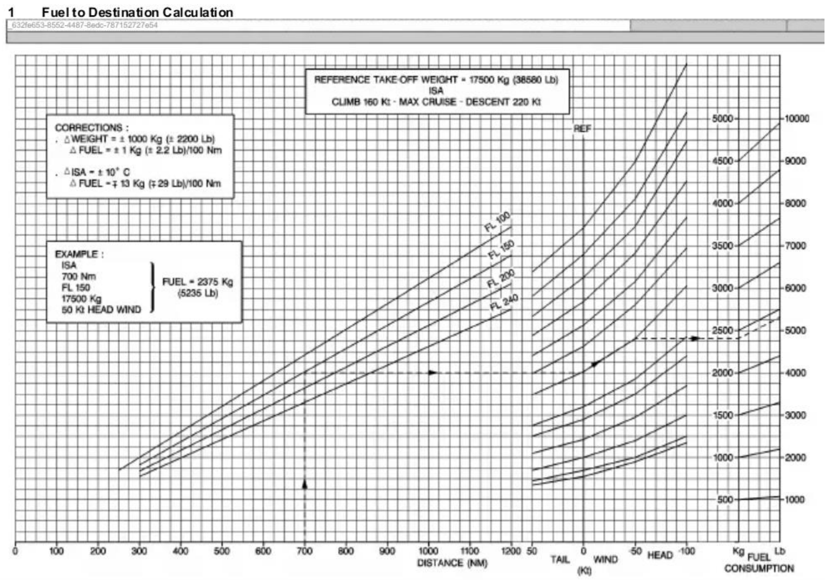

Figure 77 Fuel to destination calculation (17,500 kg TOW, max cruise)

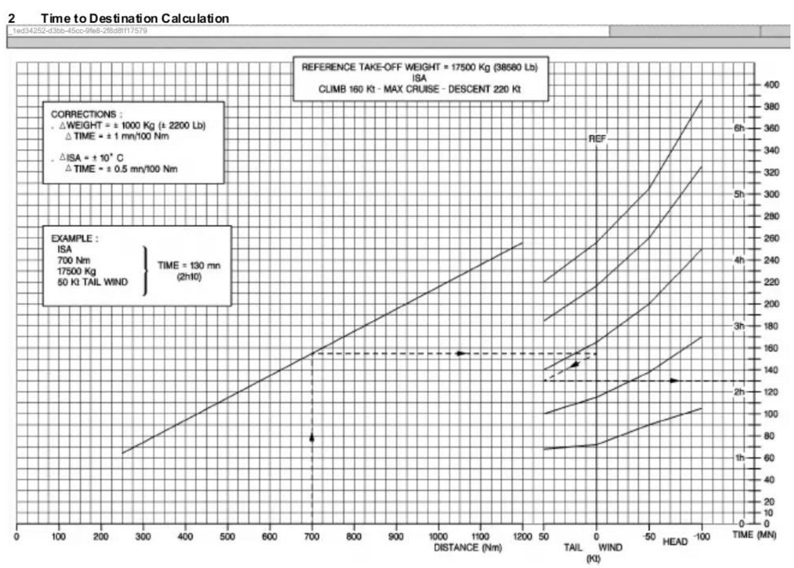

Figure 78 Time to destination calculation (17,500 kg TOW, max cruise)

A second graphical approach is also included in the FCOM which is more applicable to shorter missions and is presented in Figure 79.

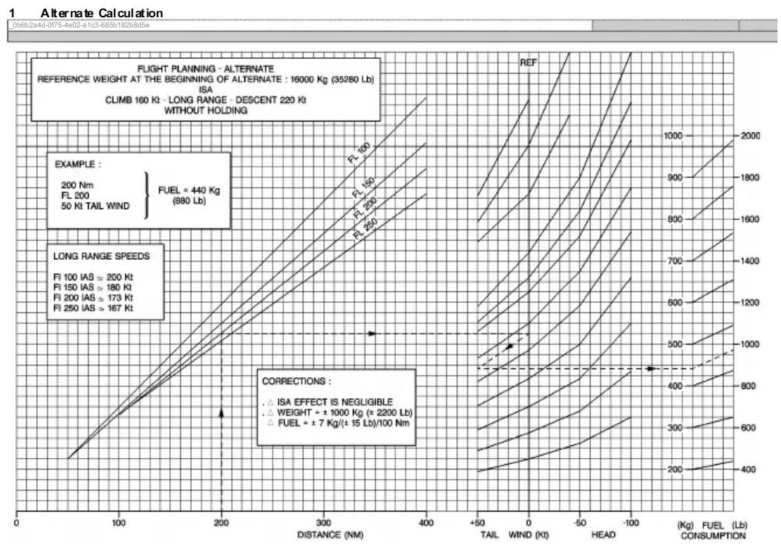

Figure 79 Fuel to destination calculation (16,000 kg TOW, long range cruise)

A comparison of the model outputs to each of these FCOM calculation methods is presented in Table 23. At an overall mission level, the model shows very good alignment to the FCOM values, with the worst-case overall mission fuel burn error of 6%.

Table 23 Fuel Burn Comparisons with FCOM methods

Mission Segment	Model 200 nm (kg)	FCOM 200 nm (kg)	% Error	Model 300 nm (kg)	FCOM 300 nm (kg)	% Error
Taxi	13.9	14	-0.7	13.9	14	-0.7
Takeoff	25.2	24	5.0	25.2	24	5.0
Climb	146.3	128	14.3	146.7	128	14.6
Cruise (230 knots IAS)	267.8	293.5	-8.8	510.0	561	-9.1
Descent	120.7	115	5.0	119.2	115	3.7
Approach/Landing	27.7	30	-7.7	27.4	30	-8.7
Taxi	13.9	14	-0.7	13.9	14	-0.7

Mission Segment	Model 200 nm (kg)	FCOM 200 nm (kg)	% Error	Model 300 nm (kg)	FCOM 300 nm (kg)	% Error
Total 230 knots IAS max cruise segment by segment method	**615.6**	**618.5**	**-0.5**	**856.3**	**886**	**-3.4**
Total 230 knots IAS max cruise graphical method	**615.6**	**600**	**-0.9**	**856.3**	**870**	**-2.7**
Total 178 knots IAS long range cruise	**569.5**	**537**	**6.1**	**766.3**	**750**	**2.2**

Further validation of the calculated fuel burn is seen in comparison to the information provided by Aircraft Commerce for various typical ATR42 routes [158]. Their data indicated 928 kg (305 USG) of fuel usage for a 318 nautical mile Vienna-Venice mission, which, when ratioed to a 300 nm mission, results in a fuel burn of 886 kg that compares well to the model outputs.

ATR42-500 Direct Operating Costs

In addition to mission fuel burn, validation was performed for the Direct Operating Costs for the baseline ATR42-500 aircraft. Figure 80 shows the economic analysis provided by ATR [159] for this aircraft for a 300 nautical mile mission (note that these values are in 2007 dollars), with the economic assumptions as shown in Figure 81.

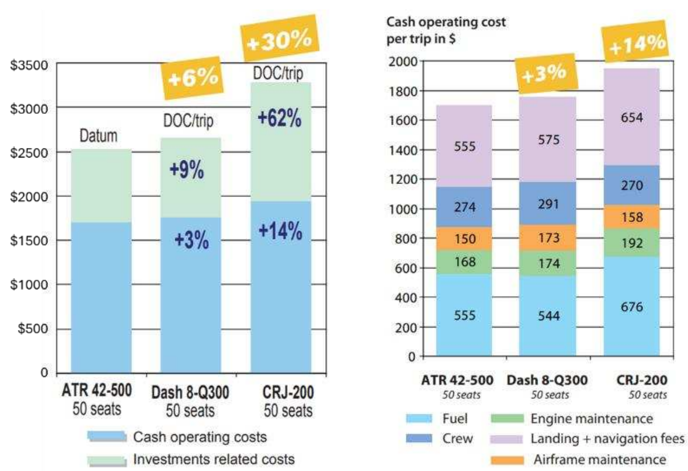

Figure 80 ATR DOC predictions

Economic Assumptions

European Environment, Standard Economics

- **Stage length**: 200 and 300Nm
- **Fuel price**: 2.06$/US gal
- **Aircraft prices**: As published by price catalog with 10% discount
- **Spares**: 10% aircraft price
- **Depreciation**: 12 years with 20% residual value
- **Financing**: 85% of investment over 10 years
- **Interest**: 5% per year
- **Insurance**: 1% of aircraft price/year
- **Block time & fuel**: Minimum time schedule (time allowance: 4 min taxi)
- **Annual utilisation**:
  - 300 Nm: 1800 flights
- **Crew** : Cockpit: statistical - Cockpit Jet: statistical - Cabin: 32$ BH/FA
- **Maintenance**
  - **ATR family**: as estimated by ATR
  - **Competitors**: estimated by ATR, based on manufacturers data
- **Maintenance labour rate**
  - In house: 30$/MH
  - Contracted: 63$/MH
- **Landing charges**: statistical

Figure 81 ATR DOC prediction assumptions

The analytic model was run using the economic assumptions from ATR, while the ATR predictions were scaled to account for 2025 economics and fuel prices. The comparison between the two is provided in Table 24 below. The primary difference between the results is in the maintenance costs for the airframe and powertrain, which is attributed to ATR using predicted values versus the in-service results used in the model.

Table 24 DOC validation comparison

Cost Element	**Model results for 300 nm mission**	**From ATR Brochure, scaled for fuel price and 2025 economics**
Fuel	$582	$616
Direct Maintenance Costs (powertrain)	$396	$260
Direct Maintenance Costs (airframe)	$771	$233
Crew Costs	$509	$425
Depreciation, Interest, Insurance	$1,215	$1,356
Total DOC	$3,473	$2,890

The other datapoint to validate the model DOC calculation was to compare it with data reported to the FAA in Form 41 Schedule P5.2, which captures operating expenses for US commercial airlines. Silver Airways, the only US commercial operator of ATR42 aircraft, reported total Direct Operating Costs of $47.2M with a total of 15,500 flight hours during 2024-2025 [160]. When ratioed to the flight duration of a 300 nm mission, this results in actual operating expenses of $3,501, closely matching the model prediction.

DeHavilland Dash 8 Hybrid Electric Study

A published study (Parallel Hybrid Propulsion System for a Regional Turboprop: Conceptual Design and Benefits Analysis, published in AIAA/IEEE Electric Aircraft Technologies Symposium Proceedings, 1 August 2019) was performed by Todd Spierling and Charles Lents to evaluate the cost benefits of a particular parallel hybrid architecture on a DeHavilland Dash 8 aircraft. Excerpts of this study are provided here, with the complete paper included as Appendix A. This study was used to validate the mission modeling approach for calculation of mission energy usage, which is a key subset of the more holistic overall modeling activity.

Study Baseline Vehicle and Engine

The study vehicle is a Bombardier Dash 8-100 turboprop powered by the standard installed PW121 gas turbine engines. Aircraft parameters are supplied in Table 25. Figure 82 provides a picture.

Table 25 Dash 8 Parameters

	Dash 8
Passengers/Class	37-39
Max Takeoff Gross Weight (lbm)	36,300
Operating Empty Weight (lbm)	24,000
Fuel Capacity (lbm)	5680
Wing Area (ft^2)	585
Aspect Ratio	12.4
Cruise L/D @ Long Range Cruise	15
Design Mission Range (nm)	1000
DOC Mission Range (nm)	250
Long Range Cruise Mach number	0.4

Figure 82 DeHavilland Dash 8-100

The Parallel Hybrid Electric Turboprop (PHEP) system-based vehicle has limited range due to system fixed weight (see Benefits section) and is limited to fly a 250 nm mission. Still, over half the missions flown by this vehicle class are < 250 nm. Thus, mission fuel burn for the baseline and PHEP based vehicles has been evaluated for a “standard mission” range of 250 nm. The 250 nm mission baseline vehicle and PW121 engine is provided in Table 26.

Table 26 Baseline Vehicle 250 nm Mission Fuel Consumption

	Duration (min)	Power per Engine (hp)	PSFC (lbm/hr) /hp	Fuel Burn (lbm)	Energy (kW-hr)
Taxi-Out	2	100	1.84	12	66
Takeoff	1	1950	0.53	35	186
Climb to Cruise	20	1362.5	0.46	418	2253
Cruise	33	960	0.46	486	2619
Descent	22	100	1.84	135	728
Approach & Land	2	630	0.53	22	120
Taxi-In	2	100	1.84	12	66
Total mission	82			1120	6039

Note: PSFC is based on an assumed gas turbine thermal efficiency of 30% at cruise, with a 15% PSFC increase at max power takeoff (past the typical gas turbine peak efficiency hook) and a 400% increase at idle conditions (Taxi and Descent)

Propulsion System Sizing and Performance Analysis

Notice that normal cruise power is ~1000 hp. A flat rated combustion core ideally sized for this application is then ~1000 hp. Such an engine, sized for cruise, will operate at peak efficiency during cruise. In order to provide make-up power for takeoff and climb, two 950 hp permanent magnet (PM) electric motors are required. Electric power to drive the motors is supplied by an electric drive train (EDT) comprised of two motor drives (1 for each motor), feeders, and a battery pack which is charged on the ground. At the on-wing propulsors, a combining gearbox (CGB) sums power from the motor and engine core to drive the propeller.

The system is operated as follows. At takeoff, 1950 hp is required (per propulsor). The flat-rated engine can only produce 1000 hp at any mission phase, thus the motor provides the remaining power (e.g. 950 hp at take-off). At cruise, the combustion engine is running at peak power (1000 hp) and at its highest efficiency, providing all the required power (no motor power). The power profile for both the core engine and motor are provided in Figure 82. Given the mission segment durations, power delivered to the propeller by the motor, the EDT efficiencies, and reserve energy requirement, the battery energy is determined at 500 kW-hr per aircraft.

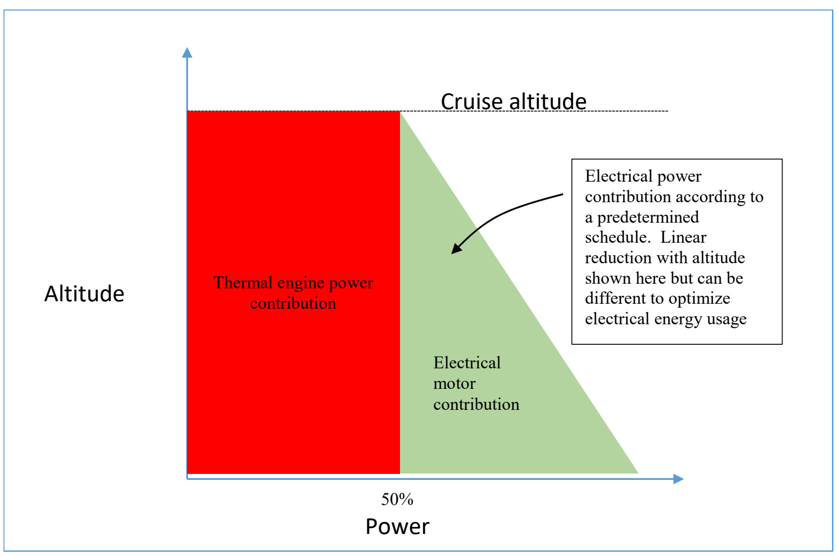

Figure 83 Power profile for Thermal Engine Core and Motor

If sized for the 1950 hp max takeoff (MTO) power, the core engine would have max power capability of 1950 hp at cruise, on account of the flat power rating, while only 1000 hp is required. Operating at only ~50% peak power, the engine cruise efficiency would drop significantly compared to peak efficiency at MTO. In addition, the core weight would be double of what is needed at cruise. Sized at cruise power (1000 hp), the core engine weight is cut in half. Most importantly, when operated at peak power throughout takeoff, climb and cruise as part of the PHET system, the core will operate at peak efficiency over most of the mission. A typical gas turbine for such an application will operate at ~ 30% thermal efficiency, while this flat rated core is projected to operate at ~ 40% thermal efficiency.

Figure 84 provides the rational for the PHET system. Fig 84c shows the mission profile. Fig 84b shows the power profile. The electric motor and core engine each cover half of the power at take-off whereas the core engine supplies all power at cruise. Motor power declines linearly between takeoff and cruise. Finally, Fig 84a shows the notional fuel burn of the PHET system compared to a conventional turboprop aircraft. Fuel flow is lower at the cruise condition due to the high efficiency PHET core. The fuel flow rate is significantly lower at takeoff and climb, where the motor is providing make-up power. This fuel flow reduction is realized only because the additional fuel flow required to carry EDT weight does not overcome the efficiency benefit.

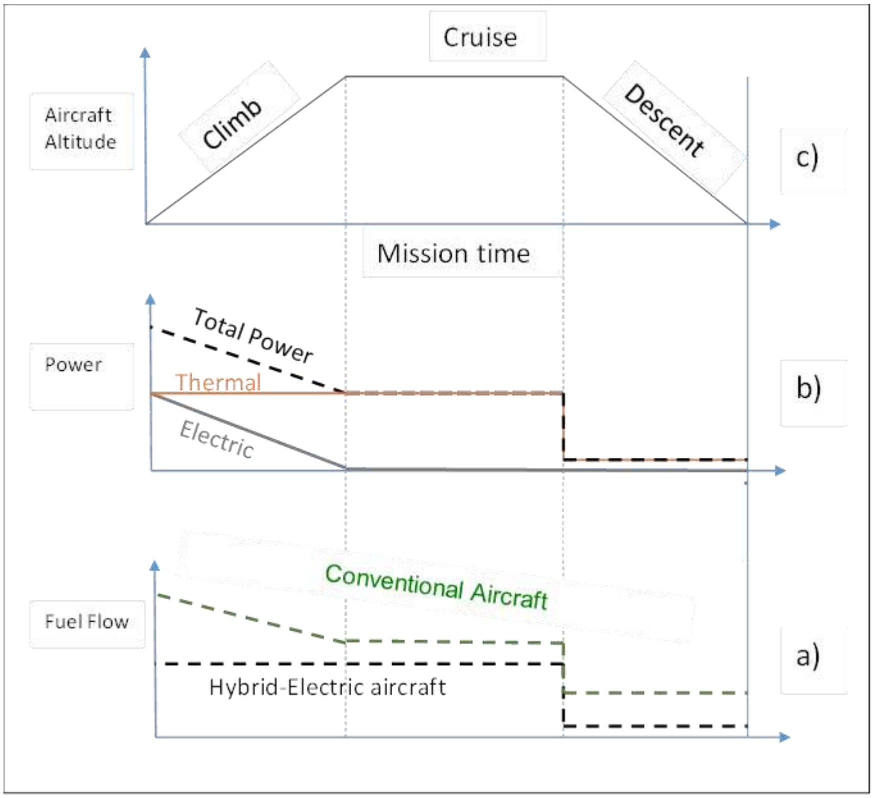

Figure 84 Typical mission illustration

The electrical component weight and performance parameters representing 5-10 year goals for the EDT components are provided in Table 27. The University of Illinois reports a power to weight ratio and a peak efficiency of 13 kW/kg and 0.97, respectively, for a motor being developed under NASA funding [28]. The motor drive parameters are reflective of ongoing work at Collins Aerospace and at NASA Glenn. The battery energy density of 355 Whr/kg is derived from a 500 W-hr/kg cell level energy density with 15% pack burden and max discharge of 90%. Motor drive and battery discharge efficiency are assumed fixed over their operating power range, while a typical motor efficiency vs part load characteristic is used for motor efficiency.

Table 27 PHET Electric Component Parameters

	Power to Weight (kW/kg)	Performance	Notes
Motor	13	Eff = 0.97 at full power, 0.8 at low power, and 0.89 average during climb	NASA supported motor development, at part power motor efficiency drops below peak efficiency
Motor Drive	20	0.98 eff	NASA supported inverter dev
Feeders	100	0.99 eff	Estimate
Battery	355 Whr/kg packaged	500 Whr/kg cell, 0.95 eff, 90% max discharge, 15% pack burden	Parameter targets laid out by Battery 500 consortium
TMS	2	NA	0.5 kg for every 1 kW of EDT heat rejection (2 kW/kg)

For this preliminary analysis, a fixed aircraft Takeoff Gross Weight (TGOW) is assumed. Thus, the propulsion system power requirements are identical for the conventional and PHET systems. The loss in aircraft range is discussed in the Benefits section.

System Weights

PHET system weight is derived for the power to weight values reported above. Table 28 provides a weight comparison to the conventional propulsion system.

Table 28 Weight Roll Up

Item	Dash -8 Baseline Weight, lbm	PHET Weight, lbm	Note
Operational Weight Empty (OWE)	24000	24000	
Power plant increase		55	Target, must be below this to make range
Gearbox		100	Weight increase due to CGB
Motor		253	eMotor 2x750kW @ 13 kW/kg
Motor Drive		165	eMotor drive, @ 20 kW/kg
Feeders		33	Feeders, @ 100kW/kg
Battery Pack		3099	500 kWh @ 355 Whr/kg
TMS		165	Estimate based on 2kW heat/kg
Passenger load (36 pax @ 200lb)	7200	7200	Passenger load
Fuel for 250 nm mission + Reserves	1680	1230	
Mission Takeoff Weight	32880	36300	
MTOW	36300	36300	

Benefits

Based on the above assumptions, Table 29 summarizes the PHET fuel burn and energy consumption. The system motor efficiency varies as a function of load (as described in Table 27) resulting in an average efficiency of 89% during boosted climb. This value is used in the calculation of climb energy. The improved thermal engine has an assumed efficiency of 40%. The cruise Power Specific Fuel Consumption (PSFC) is derived from this value, with the takeoff and idle PSFC increased in the same manner as the gas turbine engine baseline.

Table 29 PHET 250 nm mission Vehicle Fuel and Energy Consumption

	Duration (min)	Power per Propulsor (hp)	Thermal Engine Power (hp)	Motor Power (kW)	PSFC (lbm/hr) /hp	Fuel Burn (lbm)	Plug Energy (kW-hr)	Total Energy (kW-hr)
Taxi-Out	2	100	0	75			7	7
Takeoff	1	1950	1060	664	0.40	14	26	103
Climb to Cruise	26	1362.5	1060	226	0.35	322	252	1986
Cruise	28	960	960	0	0.35	314	0	1691
Descent	24	100	100	0	1.40	112	0	604
Approach & Land	2	630	630	0	0.40	17	0	92
Taxi-In	2	100	0	75			7	7
Total mission	85					778	293	4490

The reduction in on wing Jet-A fuel burn is 341 lbm (30%), however the plug energy for charging the PHET system batteries should also be considered. The baseline vehicle energy consumption is 6039 kW-hr of Jet-A (1120 lbm). The PHET vehicle energy consumption is 4197 kW-hr of Jet-A (778 lbm) and 293 kW-hr of plug energy (assuming a charging loss of 5%), for a total of 4490 kW-hr, a 26% reduction in energy consumption. A cost comparison is provided in Table 30.

Table 30 Energy Cost Comparison

	Conventional	PHET	Savings	Comment
Mission fuel burn, lbm	1120	778	341 lbm	
Electricity, kWh	0	293		
Fuel cost, $	432	300		5 year average 2.79 $/gal, $0.0716 $/kWhr
Electricity cost, $	0	33		Airport weight average, $0.1114 $/kWhr
Total costs, $	432	333	99	

Conclusion

Many previous studies of potential hybrid electric propulsion systems have failed to show fuel burn or energy consumption savings compared to conventional propulsion systems. This paper demonstrates that significant fuel burn and energy savings can be realized on a short-range propeller aircraft with a parallel hybrid propulsion system. Using only the core engine at cruise and using the parallel motor supplied by a battery stored electric energy for boosted takeoff and climb yields an on-wing fuel burn reduction of 30% and a total energy consumption reduction of 25% compared to a conventional turboprop engine. However, even with a 355 W-hr/kg battery pack energy density (estimated to be 10 years out), such a system would reduce the vehicle max range from ~ 1000 nm to 250 nm. The majority of flights executed by the study aircraft are 250 nm and less so there would still be wide application for such a vehicle.

Validation of these results was then performed against an independent calculation methodology [161]. Fuel burn estimates from a Jeppesen calculation of typical Dash 8 route structures predicted a fuel burn for the studied mission of 1190 lbs, which compared well with the 1120 lb value presented in Table 30.

Pure Electric General Aviation Aircraft Study

A published study (Battery Optimization for Sustainable Aviation: A Comprehensive Analysis for Battery Electric Aircraft, published in AIAA Journal of Aircraft 13 May 2025) was performed by Todd Spierling, Alexander Lynch and Thomas Bradley to evaluate the tradeoffs associated with different choices in battery chemistries and usage profiles for a pure electric general aviation aircraft. Excerpts of this study are provided here, with the complete paper included as Appendix B. This study focused specifically on the battery behavior when applied to the simplified case of a pure electric aircraft, enabling validation of that aspect of the model for the more complex hybrid electric propulsion case.

Battery Technology/Chemistry Overview

The key technology element that has enabled battery electric aircraft is advanced lithium-ion battery technologies. Most notably, improvements in energy density and cost have presented a competitive case for battery technology relative to less efficient internal combustion engine technology [11]. This section provides a comprehensive survey of existing battery chemistries, focusing on their energy density, cycle life, costs, and lifecycle carbon footprint.

This study focuses mainly on battery chemistries that are currently in commercial production and ready to be deployed on aircraft: namely $LiFePO_4$ (LFP), $LiNCo_yAlO_2$ (NCA), $LiNiMnCoO_2$ (NMC), and their variations. Each of these battery chemistries exhibit performance and cost tradeoffs. LFP batteries maintain performance over many cycles, exhibit low cost and have relatively low environmental impacts, yet have a low specific energy, which is not conducive to aircraft applications. NCA and NMC batteries exhibit higher specific energies yet have drawbacks in the form of life spans, environmental impact and pack cost [162].

Battery lifetimes have a significant impact on the viability of electric aircraft, as battery replacement comes with a high cost. The lifetime of a battery, also defined as the number of full equivalent cycles the battery can go through before it loses significant capacity, is affected by multiple operational variables, including but not limited to depth of discharge, charging rate, and discharge rate [90].

Various electrochemical and physical mechanisms are the cause of reduced battery capacity as a function of its cycle-life and calendar life. For example, as the batteries are cycled during flights, the electrolyte and electrode react with one another to form an SEI layer that reduces the concentration of lithium ions, leading to reduced energy storage [91]. Mechanical cycling of electrodes can lead to physical breakdown of electroactive materials. This phenomenon can increase with higher depths of discharge and discharge rates. It is important to model this behavior when evaluating the battery energy storage system for electric aircraft, as it will have a deep impact on the design of energy storage for battery electric aircraft.

In addition to performance, cost continuously evolves for various battery chemistries. Costs of raw materials, and continuing advances in manufacturing process and efficiencies have resulted in changing relationships between the costs of differing chemistries. This data forms the basis of the cost optimizations that are discussed later in the paper. Cost premiums for aerospace applications also play a role in electric aircraft adoption.

Table 31 Key Characteristics of Candidate Aerospace Battery Chemistries

	NMC 811	NCA	LFP	NMC 532	NMC 111	LFP 2030	NMC 2030
USD/kW-hr (pack level)	$506.80	$493.82	$387.95	$632.38	$506.80	$324.00	$408.00
W-hr/kg (pack level)	196	192	144	184	177	223	328
CO_2/kW-hr	65.6	69.8	46.7	65.7	67.6	47	65

For the purposes of this study, the preceding performance factors presented in Table 31 were used based on an aggregation of data from multiple sources [90, 92, 93, 94, 95, 96, 97, 98]. This data used the expected prices of commercial automotive battery packs and then imposed a 4x multiplier to account for the lower quantities and more stringent quality/documentation requirements of the aerospace market. The first five columns are based on existing chemistries, while the remaining two are based on optimistic future projections for NMC and LFP chemistries.

Methodology

Battery Powered Electric Aircraft Range Equation

While the potential benefits of electric aviation are immense, challenges abound. The weight considerations of batteries directly impact aircraft performance, and the achievable energy density poses constraints both on the achievable range and the energy required to achieve a given mission. This relationship is typically captured by the Breguet range equation, modified as appropriate to reflect the fixed mass of a battery electric aircraft throughout the mission, as opposed to the decreasing mass of a fuel powered aircraft [99]. This modified equation also includes the depth of battery discharge during a flight, or the percentage of battery capacity used. The Breguet range equation for the level flight range of a full electric aircraft is given as Equation 20:

$$R = 3.6\left(\frac{L}{D}\right)\left(\frac{e_{bat} * \eta_{b2s}\eta_p}{g}\right)\left(\frac{DoD * m_b}{m_b + m_p + m_e}\right) \quad \text{(Eq. 20)}$$

Where:

L/D – lift to drag ratio (16 for this analysis)

e_{bat} – battery specific energy (W-hr/kg)

η_{b2s} – system efficiency battery to motor output shaft (90% for this analysis)

η_p – propeller efficiency (85% for this analysis)

g – acceleration due to gravity (9.81 m/s^2)

DoD – depth of battery discharge

m_b – battery mass (kg)

m_p – payload mass (kg)

m_e – aircraft empty mass (kg)

An example of the results seen with variations for the battery specific energy and battery mass fraction is illustrated in Figure 85 below. Increasing the battery mass fraction (battery weight as a percentage of overall aircraft weight and/or increasing the battery specific energy results in corresponding increases in aircraft range.

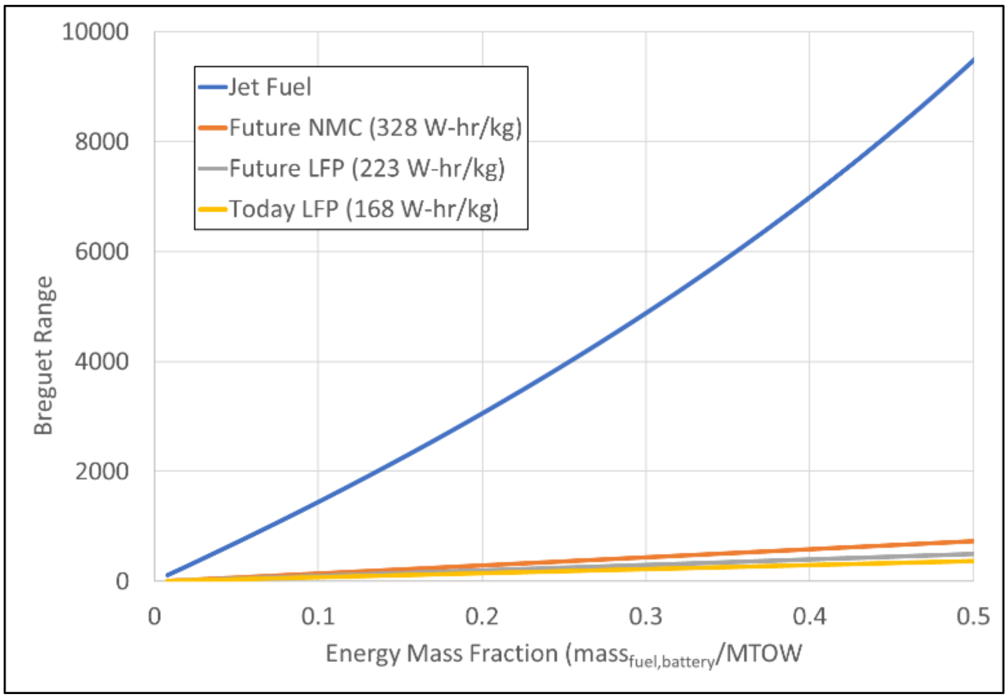

Figure 85 Breguet Range Behavior Example

Optimizing Battery Design for Target Aircraft Range Across a Range of Chemistries and Use Cases:

The Breguet range equation was used to optimize the battery size for a theoretical 9 passenger small commuter electric aircraft at a target range of 250km. Examples of this aircraft type in turboprop form include the Cessna Caravan or Pilatus PC-12 in the single-engine configuration, or a Beech King Air in the two-engine configuration. These aircraft have ranges over 1600 km yet often service routes of less than 500 km [163, 164, 165].

The candidate aircraft for this analysis assumed the characteristics presented in Table 32:

Table 32 Analyzed Aircraft Characteristics

Characteristic	Assumed Value
Cruise Lift-to Drag Ratio	16
Operating Empty Weight	2050 kg
Payload Weight (@ 86 kg/pax)	777 kg
Cruise Speed	186 knots
Loiter Speed	135 knots
Normal Cruise Range	250 km
Max Cruise Range	377 km

A key consideration in this range analysis is the differentiation between normal operational range and absolute maximum range. Regulations require that the aircraft have enough fuel (in this case batteries) to divert to an alternate landing location and then be able to loiter for a given time period. This analysis assumes daytime VFR conditions which require no alternate and 30 minutes of loiter time, which is less stringent than night VFR (no alternate/45 minutes loiter) or IFR (nearest alternate/45 minutes loiter) [166].

The trade-offs in battery chemistry and usage profiles are central to achieving optimal performance in electric aircraft. Low depths of discharge can potentially result in high levels of mission cost and CO_2 emissions due to excessive battery pack size and weight, resulting in higher energy usage and increased manufacturing costs. In contrast, high depths of discharge can potentially result in lighter batteries and lower mission energy usage yet have unacceptably short battery lifetimes and high replacement costs. Initial calculations utilizing Equation 20 consider these complex relationships to produce a range of pack sizes and energy requirements based on different DoDs and battery chemistries.

We analyze the economic and environmental influences of battery chemistry and depth of discharge in both normal mission and diversion cases. Calculations are performed to determine the cost of operation on a per mission basis, given in Equation 21, and the carbon intensity per mission, given in Equation 22. These equations consider cost and carbon impacts of various operational factors like battery service life and replacement intervals and the increased electricity usage of larger battery packs.

$$Cost_m = \frac{(m_b e_{bat})\frac{\$}{kWh_{batt}}}{c_{battery}} + (DoD * m_b e_{bat})\frac{\$}{kWh_{elec}} \quad \text{(Eq. 21)}$$

$$Carbon_m = \frac{(m_b e_{bat})\frac{CO_2}{kWh_{batt}}}{c_{battery}} + (DoD * m_b e_{bat})\frac{CO_2}{kWh_{elec}} \quad \text{(Eq. 22)}$$

Where:

m_b – battery mass (kg)

e_{bat} – battery specific energy (W-hr/kg)

$c_{battery}$ – total number of battery cycles before replacement

DoD – battery depth of discharge

$\frac{\$}{kWh_{batt}}$ - cost of the battery per kWh

$\frac{\$}{kWh_{elec}}$ - cost of electricity per kWh

$\frac{CO_2}{kWh_{elec}}$ - carbon intensity of electricity production per kWh

$\frac{CO_2}{kWh_{batt}}$ - carbon intensity of battery manufacturing per kWh

The airplane design is iterated with various battery chemistries and depths of discharge to calculate the amount of installed battery capacity, the required electrical energy levels for the mission, and the associated costs and carbon footprints associated with both manufacturing and operation.

Geographic Sensitivity

The relative tradeoffs related to energy costs and carbon footprints vary widely based on the area of the world where airline operations occur. The characteristics of the electrical grids in these countries vary widely from China or India using coal (low cost/high carbon footprint) to France using nuclear (high cost/low carbon footprint) to Norway using hydro (low cost/low carbon footprint). Examples of the 2022 cost and carbon footprint of various national electric grids are presented in Table 33 below [150, 151, 156, 157].

Table 33 Electrical Grid Cost and Carbon Intensity

Region	2022 Carbon Intensity (kg CO_2/kWh)	2022 Cost ($USD/kWh)
World	0.44	$0.12
China	0.53	$0.09
Norway	0.029	$0.12

US	0.37	$0.15
India	0.63	$0.13
France	0.085	$0.21
Australia	0.50	$0.23
Brazil	0.10	$0.14

Operational Sensitivity

An additional area that must also be addressed in how to best operate the aircraft is mission usage, specifically for missions shorter than the design range of the aircraft. As an example, an aircraft may have a design range of 250 km but only be operated on a 50 km route. This gives the airline the option to charge a 250 km capable battery between every flight, operate up to five flights between charges, or to even potentially just install less batteries in the aircraft and only have a 50 km range. This choice may result in very different mission costs and carbon footprints depending on the battery chemistry. There are also additional airline operational efficiency and economic implications due to considerations such as aircraft turnaround times between flights, but those are beyond the scope of this paper.

Results

Battery Optimization for Candidate Aircraft

Figures 86 and 87 below show the outputs of the battery optimization process that includes Equations 20, 21, and 22. Figure 85 presents the relationship between depth of discharge and overall mission cost, taking into account cost of electricity in the U.S. per mission and battery replacement cost over its lifetime. While low depths of discharge require less replacement cost over the lifetime of the aircraft, the per mission energy cost is higher due to its higher battery pack mass. Inversely, higher depths of discharge require more frequent battery pack replacement, offsetting the cost savings from per-mission electricity usage. Note that while these examples illustrate behavior all the way to 100% depth of discharge, that is not a reasonable operating condition for normal flight due to the need to reserve battery capacity for diversion conditions, this is shown by the maximum DoD line at 0.63.

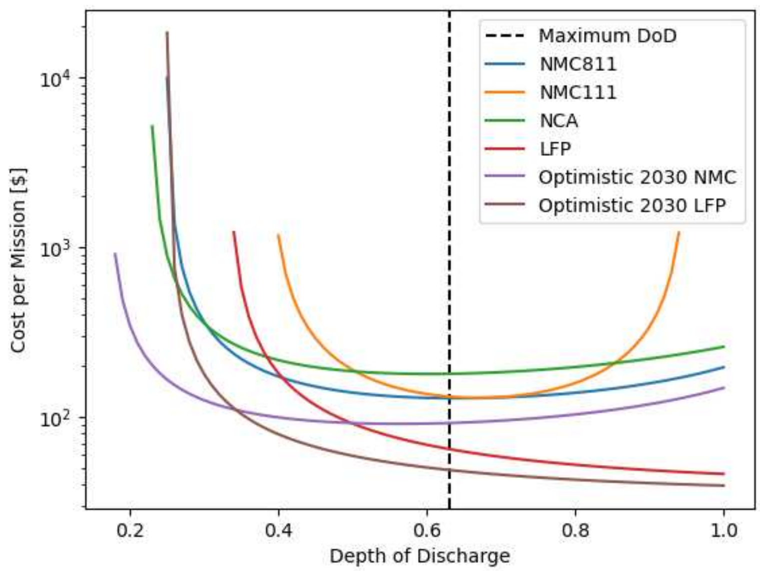

Figure 86 Total Mission Cost versus Depth of Discharge for Normal Flight

Figure 86 displays the relationship between DoD and the total carbon dioxide emissions per mission. These emissions come from US based electricity generation. In this metric, the carbon impact of battery manufacturing far outweighs the carbon impact of increased electricity need. For all battery chemistries, carbon impact is minimized at the highest possible depth of discharge.

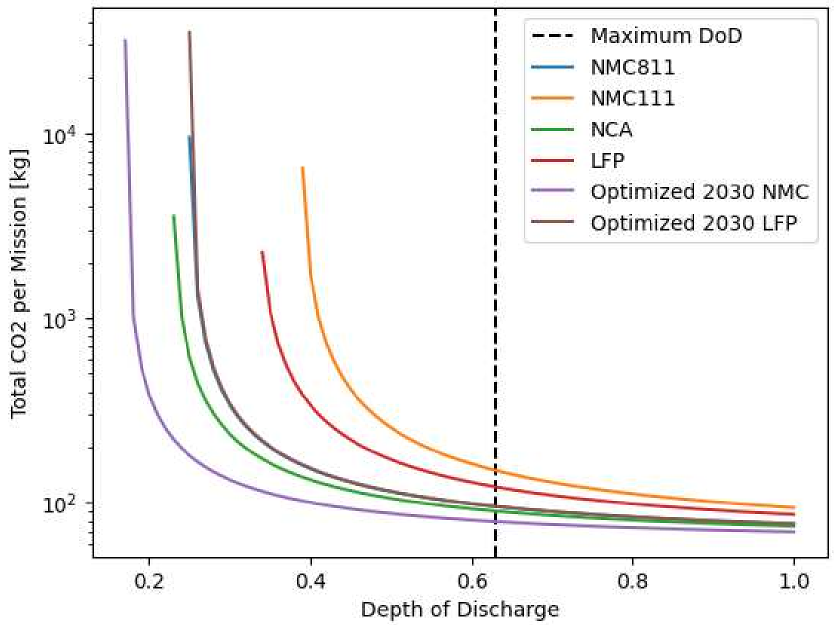

Figure 87 Total Mission CO_2 versus Depth of Discharge for Normal Flight

As expected, the behaviors vary between different battery chemistries, as each has its own specific energy density, cycle life, manufacturing cost, and manufacturing carbon footprint. Based on these results, you would then choose the preferred chemistry, battery mass, and depth of discharge at design mission range based on the optimization parameter of interest (operating $/$CO_2$, battery replacement intervals, etc).

Cost and Carbon Impact when Considering Geographic Sensitivities

The first analysis was performed for a 250 km usable range case across a variety of countries, with the minimum mission level electricity + battery costs and carbon footprints tabulated below for each of the preferred nickel and non-nickel-based battery chemistries. In some cases, multiple minimums (as a function of depth of discharge) occurred depending on whether mission cost or mission carbon was the parameter being minimized. Results of this analysis are presented as Table 34.

Table 34 Mission Results by Geographic Region

Country	Chemistry (DoD)	Mission Cost	Mission Carbon Footprint
China	LFP (.63)	**$33.90**	142 kg
China	NMC (.63)	$79.78	**131 kg**
China	NMC (.56)	$78.20	136 kg
Norway	LFP (.63)	**$41.45**	**10 kg**
Norway	NMC (.63)	$86.02	22 kg
Norway	NMC (.55)	$84.73	22 kg
USA	LFP (.63)	**$48.75**	98 kg
USA	NMC (.63)	$92.05	**95 kg**
USA	NMC (.56)	$91.07	98 kg
France	LFP (.63)	**$64.38**	**25 kg**
France	NMC (.63)	104.97	34 kg
France	NMC (.58)	104.48	34 kg

*For reference jet-A fueled aircraft consumes 101 kg of fuel for comparable mission, with fuel only cost of $149.50 and CO_2 emissions of 321 kg

As is evident in these results, mission operating costs and carbon footprints can vary dramatically for an aircraft with the same characteristics and range across a variety of countries. Across the four countries and two best chemistries considered, there is a >3x range in the $/mission cost, and a >14x range on the per-mission carbon footprint. In every case, the configuration using the LFP battery was significantly less expensive than the NMC alternative, primarily due the much smaller battery cost/mission cycle for the LFP which more than offset the weight increase (and correspondingly higher electricity usage) of the LFP battery. When considering carbon footprint, however, the opposite effect often became apparent. In countries with a high grid carbon footprint, the increased electricity usage due to the heavier battery penalized the LFP battery, resulting in a preference for the more energy dense NMC chemistries in countries with more carbon intensive electrical grids. In those countries, however, the cost penalty for that carbon savings is high, with a >2x cost penalty to achieve a <8% carbon reduction.

Another interesting behavior was observed when determining which parameter (cost or carbon footprint) to use for optimization. In the case of the LFP chemistry, both parameters continued to improve up to the maximum depth of discharge constraint set by the diversion criteria. In the case of the NMC chemistry, however, the cost minimum was reached at an intermediate depth of discharge, while the carbon minimum was reached at the diversion-driven maximum depth of discharge constraint.

Cost and Carbon Impact when Considering Operational Sensitivities

The next situation considered was operation of the aircraft at shorter segments than the design range of the aircraft. In the preceding analysis, costs and carbon footprint were considered for a 250 km operating cruise range. Consider instead an airline operating 50 km missions. Using the China case from the earlier analysis and calculating overall cost and carbon footprint for 5 x 50 km legs generates the results presented in Table 35.

Table 35 Mission Results by Operational Scenario

Operating Scenario	**Chemistry (DoD)**	**Mission Cost**	**Mission Carbon Footprint**
China (250 km battery, charge every 250 km)	LFP (.63)	**$33.90**	142 kg
China (250 km battery, charge every 50 km)	LFP (.13)	**$33.34**	141 kg
China (50 km battery, charge every 50 km)	LFP (.27)	**$25.10**	105 kg
China (250 km battery, charge every 250 km)	NMC (.63)	$79.78	**131 kg**
China (250 km battery, charge every 50 km)	NMC (.13)	$53.95	**124 kg**

China (50 km battery, charge every 50 km)	NMC (.27)	$47.00	**104 kg**

In this situation, maintaining the 250 km capability battery pack but charging every flight has minimal impact on the cost or carbon footprint of the LFP battery pack, but significant favorable impacts on both cost and carbon footprint of the 250 km capability NMC pack. Taking the next step and installing a smaller 50 km capability battery pack has significant additional favorable cost/carbon impacts for the LFP pack, with lesser favorable gains on the NMC pack.

Conclusion

In conclusion, this paper provides a panoramic view of the intricate landscape surrounding battery optimization for electric aircraft. The synthesis of technological advancements, operational considerations, economic analyses, and real-world case studies paints a comprehensive picture of the challenges and opportunities in this dynamic field. As the aviation industry navigates towards a sustainable future, the role of battery optimization emerges as a linchpin for realizing the full potential of electric aircraft.

This study validated the portion of the model that dealt with battery behavior. The results seen in this study were consistent with behavioral expectations for the battery system, providing confidence in its applicability for the more complex hybrid electric use case.

Conclusions

This chapter sought to address the research problem identified as research question 4, which is repeated below:

Research Question 4) How can the analytic tools and methodologies be validated for known configurations?

Now having performed the research activities documented in the above sections, the analysis methodology has been compared to an existing aircraft configuration and operational mission to validate its ability to generate appropriate outputs, as well as to a simplified use cases of both parallel hybrid and pure battery electric configurations from previously presented studies.

Chapter 7 - Example Results of Architecture Exploration on Hybrid Aircraft

This chapter seeks to address the research problem identified as research question 5, which is repeated below:

Research Question 5) What needs to be done to perform optimization exercises on a variety of use cases to demonstrate the costs and benefits of the proposed optimization approach?

To answer this question, this chapter presents a series of analyses to identify trends and optimums and demonstrates that the tool can be used to search for an optimum solution for a desired prioritized metric of interest. This was done by performing analysis activities on several candidate aircraft configurations and operating scenarios to determine possible benefits and robustness of particular solutions to changes in usage, cost elements, or progressions/shortfalls in technology.

Introduction

A design space exploration was performed to understand the behavior of the results to varying configuration and operational scenarios. Parameters varied included:

1. Thermal engine type

Both gas turbine and turbocompounded engine types were evaluated during this research. The differing specific powers, efficiencies, durability and costs were considered across the full range of architecture and operational scenarios.

2. Thermal engine power rating

There are a variety of thermal engine power ratings that could be considered based on the degree of electrification and the desire for increased thermal engine durability. Takeoff, climb, and cruise can all be sizing points for a traditional aircraft powertrain, based on the desired aircraft performance and altitude lapse rate of the engine.

3. Fuel type

Both conventional kerosene (Jet A) and biomass based synthetic aviation fuels were considered. Synthetic fuels have very lower net CO_2 generation compared to Jet A but currently come at a significant price premium.

4. Country of operation

In chapter 5, the differences in electricity cost and grid emissions across a wide range of countries of operation was presented. These differences result in varying degrees of cost and lifecycle emissions benefits due to hybrid implementation depending on where the airline is operating. The countries of operation included China, Norway, United States, India, France, Australia, and Brazil.

5. Battery chemistry and depth of discharge

The choice of battery chemistry and depth of discharge (battery capacity) have a significant impact on the operating economics and emissions of the hybrid configuration. Multiple competing trends drive the variation in results across the spectrum of battery choices. Using a chemistry with a lower specific energy or using that battery to a lower depth of discharge increases the weight of the aircraft. This increases the engine power requirements, increasing fuel burn and engine maintenance costs. In some cases, this can also result in MTOW limitations for the aircraft, reducing passenger count and increasing cost and emissions on an available seat kilometer basis, even if overall gross aircraft values do not increase.

6. Segment/magnitude/profile of electric augmentation

There are several portions of the mission where electric augmentation can be implemented. This could be done for a variety of reasons such as reducing mission fuel burn, reducing system maintenance costs, or reducing either ground or whole-mission emissions. For purposes of this study, the designs were considered under a set of three high level use cases: an electric taxi use case, a descent/electric taxi use case, and a takeoff/climb use case. These use cases will be illustrated in the series of following figures. In each figure, the left-hand column in each of the clustered sets is the current baseline ATR42 platform, while the right hand is the particular use case under discussion.

The first example of this is electric taxi shown in Figure 88. Here, the engine mounted electric motor is used to drive the propellor without the gas turbine being ignited. This use case includes both taxi in and taxi out segments.

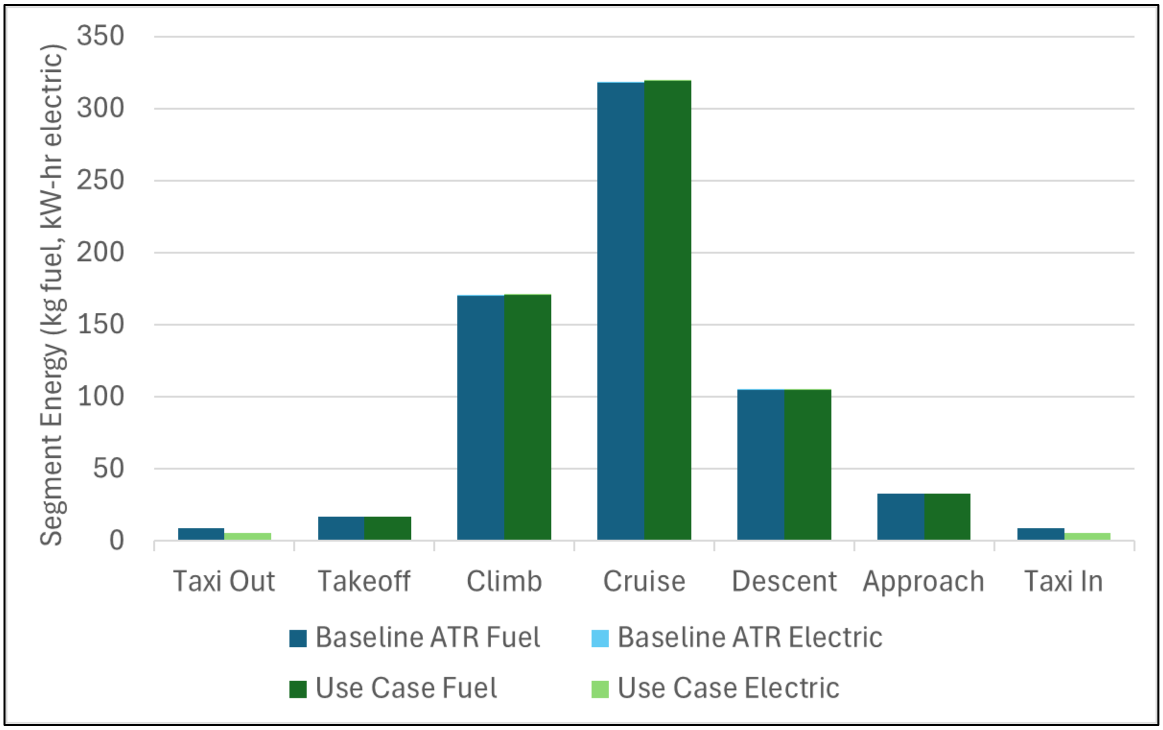

Figure 88 Energy Consumption Profile for the Electric Taxi Use Case

A further extension to this approach is to also incorporate electric operation during descent as shown in Figure 89. This use case addresses the mission points where the thermal engine is at its lowest power settings and operates at its lowest thermal efficiency.

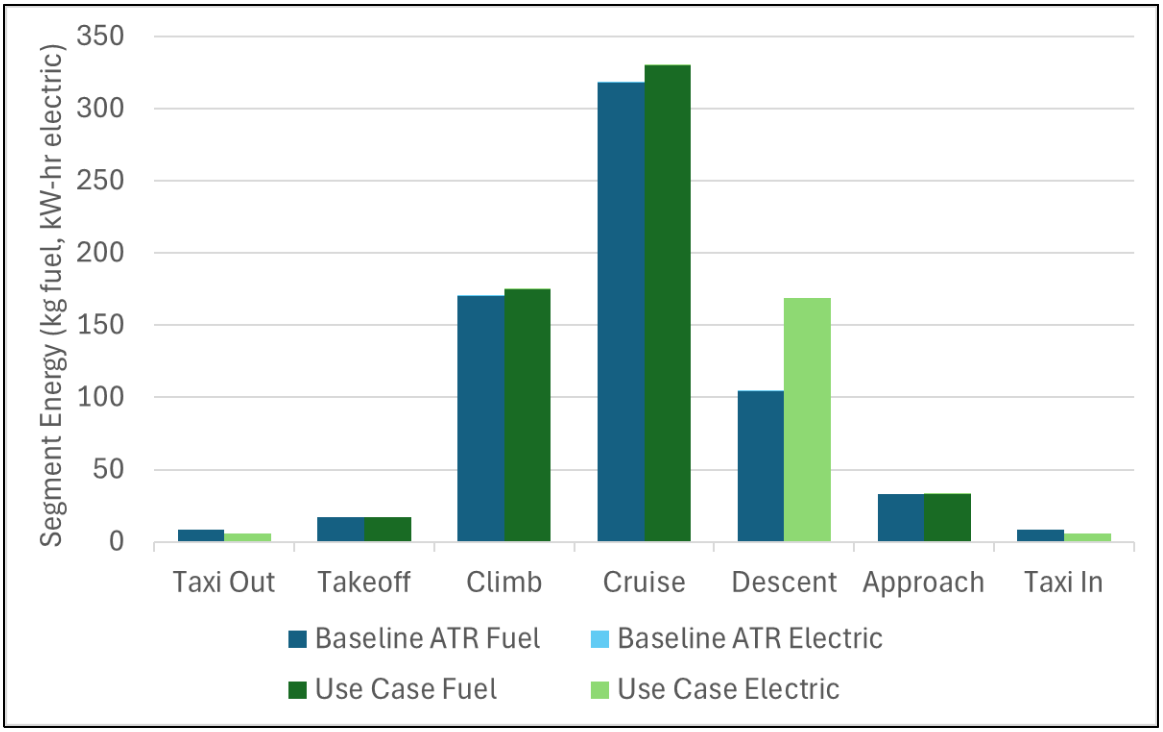

Figure 89 Energy Consumption Profile for the Electric Taxi and Descent Use Case

Another popular implementation of electric augmentation is to use electricity to either replace or supplement the thermal engine power during takeoff and climb. These phases of operation are very damaging to the thermal engine and off-loading the engine during these operating segments can show substantial durability benefits. It can also allow the thermal engine to be downsized if these segments were a sizing point in the particular application. Alternatively, the electric power can be used to supplement the thermal engine and provide an overall increased size powertrain which could allow for expanded operations from short runways or during hot/high conditions. Figures 90 and 91 illustrate two different percentage level examples of takeoff and climb injection.

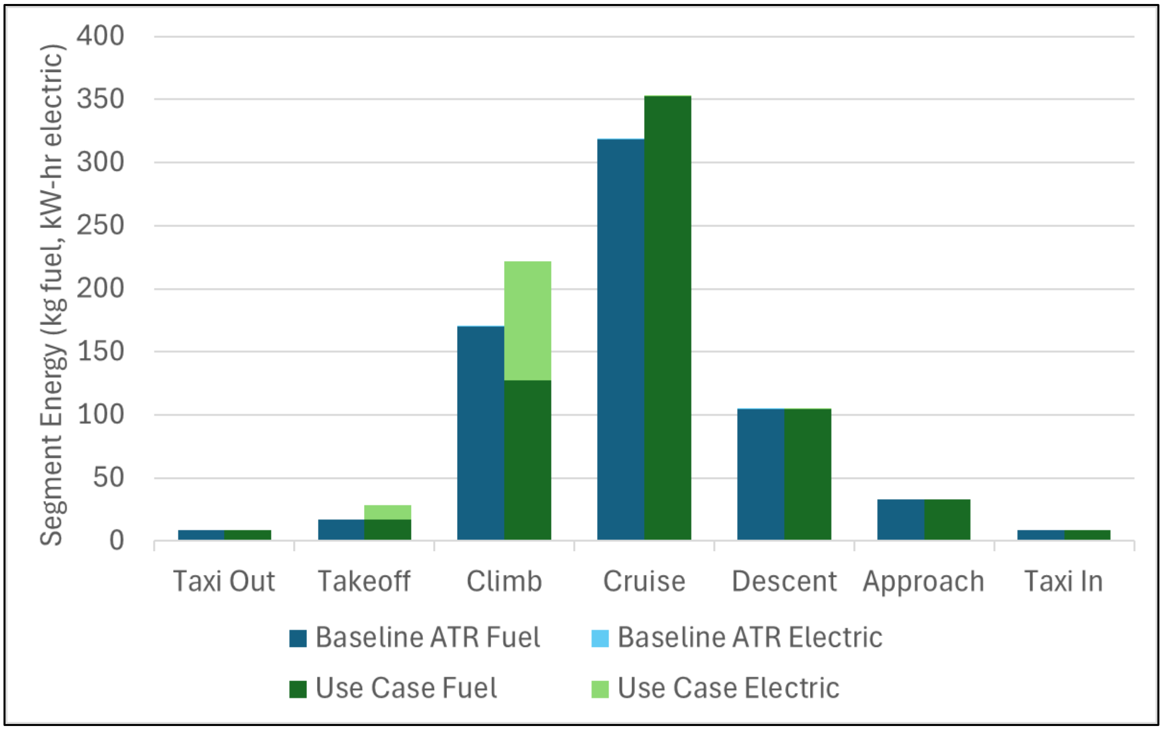

Figure 90 Energy Consumption Profile for the ~20% Takeoff and Climb Injection Use Case

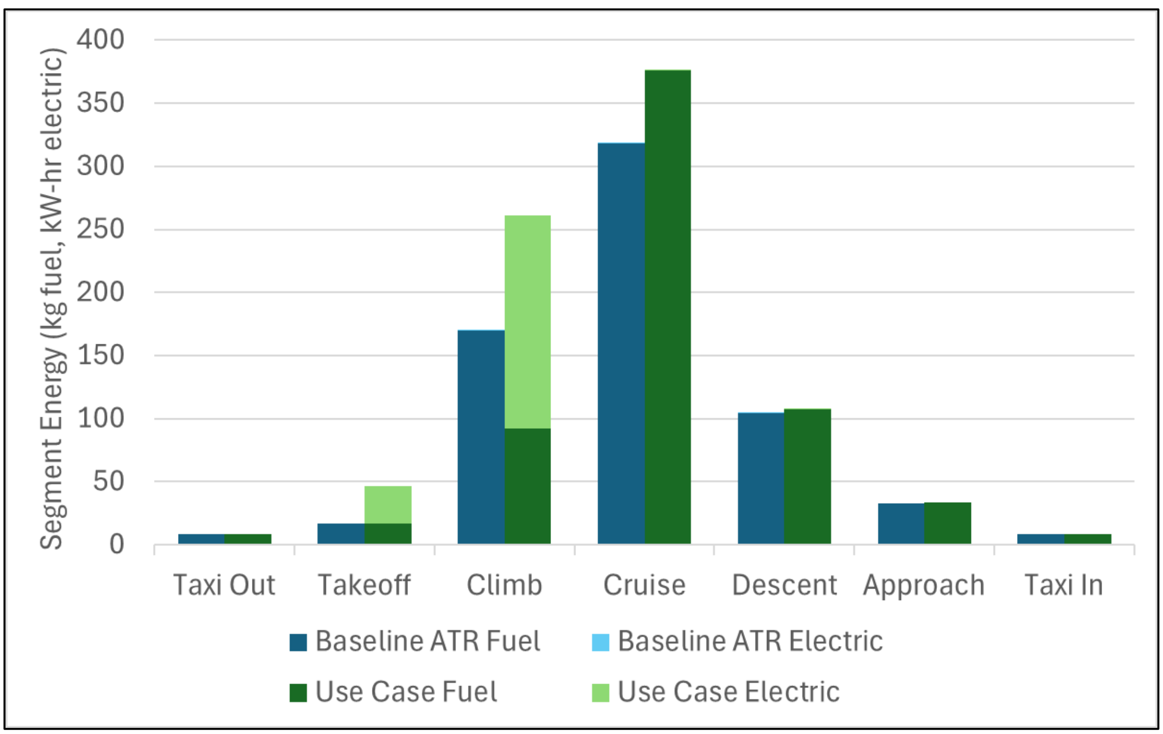

Figure 91 Energy Consumption Profile for the ~50% Takeoff and Climb Injection Use Case

Beyond the raw level of electric power injection, there are also variations in how that power can be profiled. Figure 92 below illustrates various offset and addition options as applied to the climb segment. The impacts of these injection scenarios vary. Full electric offset reduces stress on the thermal engine, prolonging its life. Tapered electric addition minimizes electric energy and battery size, while full electric addition provides additional climb performance at higher altitudes.

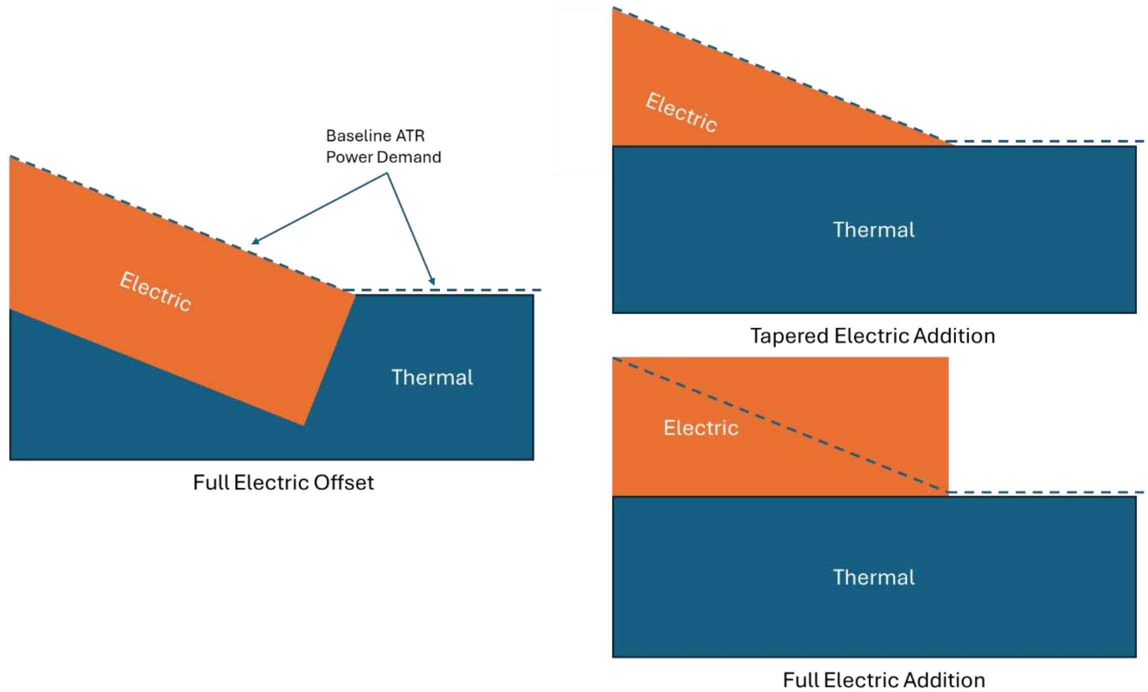

Figure 92 Electric Offset/Addition Options - Climb

7. Mission Length

A variation in mission length can have a variety of implications on the results of the analysis. As the mission length increases, the cruise segment gets longer while the other mission segments are roughly unchanged and overall mission fuel burn increases. In this case, implementation of a strategy such as electric taxi may result in the same absolute fuel burn reduction, but a reduced percentage decrease due to the greater overall mission fuel burn. Other strategies such as takeoff or climb assist will also be impacted because the aircraft may be at a higher weight (due to increased cruise fuel) during the early mission stages. Lastly, many of the hybrid configurations add weight to the aircraft which puts it at its MTOW limits. In that case, the need to fly increased range will result in the need to remove passengers with the associated negative impact on CASK.

Exploration Summary Results

The results of this comparison are presented in the following section. The first set of presented results includes a complete view of the overall landscape, followed by specific sensitivity studies to illustrate the outcomes of specific design choices.

Design Space Exploration Results

Figure 93 provides an overview of the spread of results across a range of both conventional non-hybrid and hybrid solutions. These results are for a 200 nautical mile mission being operated in China. The points designated by red stars are the non-hybrid alternatives for both gas turbine and turbocompound powerplants.

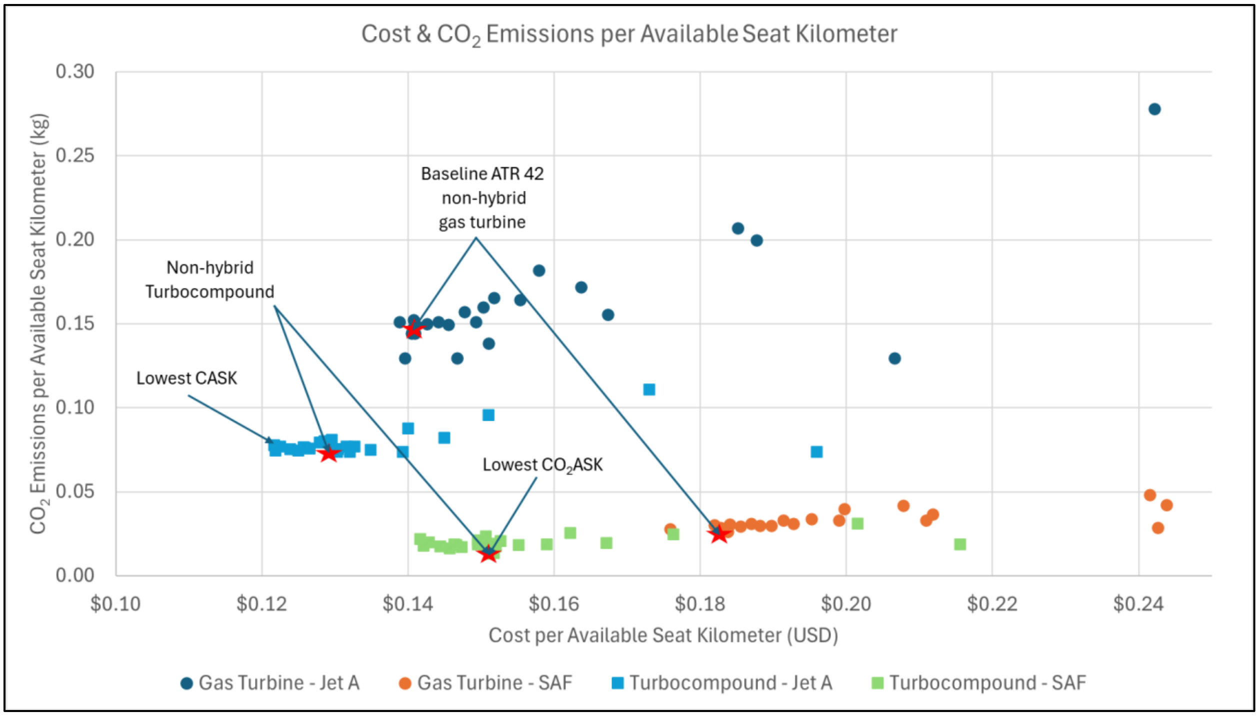

Figure 93 Summary View - Cost & CO_2 Emissions per Available Seat Kilometer

Several general trends can be seen in these results. For the gas turbine configuration using Jet A, the non-hybrid version was extremely attractive from a cost perspective compared to the hybrid alternates with only two hybrid configurations showing marginally superior cost values, but there were several hybrid alternates that were superior from an emissions perspective. For the gas turbine configuration using SAF, there was at least one hybrid configuration with noticeably superior costs, but the non-hybrid had the lowest emissions. For the turbocompound configuration using Jet A, multiple hybrid version had superior costs to the non-hybrid, but nearly all the hybrids had higher emissions. For the turbocompound configuration using SAF, a similar situation applied, although the spread in emissions was even lower.

A few of the key use case results are captured in Table 36 below. This table details the configuration and performance results for non-hybrid gas turbine and turbocompound configurations using both Jet A and SAF fuels and also captures the hybrid-electric configurations with the same options of engine and fuel types that result in the lowest cost and emissions per available seat kilometer.

Table 36 Key Use Case Results with Configuration Descriptions

Use Case Definition	**Baseline ATR non hybrid gas turbine**	**Hybrid gas turbine 100% taxi & 100% descent offset jet**	**Hybrid gas turbine 20% takeoff climb offset**	**Baseline ATR non hybrid TC**	**Hybrid TC 100% taxi offset**	**Hybrid TC 50% takeoff climb offset**	**Baseline ATR non hybrid gas turbine SAF**	**Hybrid gas turbine 100% taxi offset SAF**	**Hybrid gas turbine 100% taxi & 100% descent offset SAF**	**Baseline ATR non hybrid TC SAF**	**Hybrid TC 50% takeoff climb offset SAF**
Mission Length (km)	370	370	370	370	370	370	370	370	370	370	370
Complete Powertrain Mass (including battery) (kg)	954	1944	1664	1133	1221	2622	954	1042	1944	1133	2622
Fuel Engine (kg)	954	954	954	1133	1133	952	954	954	954	1133	952
Takeoff Mass (kg)	17657	18554	18378	17141	17228	18515	17657	17733	18554	17141	18515
Passenger Count	48	48	48	48	48	47	48	48	48	48	47
Payload Mass (kg)	500	500	500	500	500	500	500	500	500	500	500
Thermal Engine Thermo Rating (kW)	2457	2457	2457	1900	1900	1320	2457	2457	2457	1900	1320
Thermal Engine Mech. Rating (kW)	1790	1790	1790	1900	1900	1320	1790	1790	1790	1900	1320
Electric Motor Rating (kW)		430	340		90	780		90	430		780
Installed Battery Energy (kW-hr)		190	133		12	322		12	190		322
Battery Chemistry		Opt2030 LFP	Opt2030 LFP		Opt2030 LFP	Opt2030 LFP		Opt2030 LFP	Opt2030 LFP	Opt2030 NMC	Opt2030 LFP
Fuel Type	Jet A	Jet A	Jet A	Jet A	Jet A	Jet A	SAF	SAF	SAF	SAF	SAF
Operating Country	China	China	China	China	China	China	China	China	China	China	China
Charging Power (kW)	90	400	270	90	90	650	90	90	400	400	650
Battery Depth of Discharge		95%	96%		95%	95%		95%	95%		95%
Total Fuel (kg)	660.2	555.6	658.8	331.9	328.6	299.7	660.2	645.8	555.6	331.9	299.7
Total Electricity (kW-hr)	0.0	181.4	127.8	0.0	11.4	306.8	0.0	11.4	181.4	0.0	306.8
Taxi Out Fuel (kg)	8.8	0.0	8.8	2.4	0.0	1.8	8.8	0.0	0.0	2.4	1.8
Taxi Out Electricity (kW-hr)	0.0	5.7	0.0	0.0	5.7	0.0	0.0	5.7	5.7	0.0	0.0
Takeoff Fuel (kg)	16.8	16.8	15.2	10.9	10.9	6.2	16.8	16.8	16.8	10.9	6.2
Takeoff Electricity (kW-hr)	0.0	0.0	12.0	0.0	0.0	26.1	0.0	0.0	0.0	0.0	26.1
Climb Fuel (kg)	170.1	175.5	157.5	97.5	98.0	56.7	170.1	171.0	175.5	97.5	56.7
Climb Electricity (kW-hr)	0.0	0.0	115.9	0.0	0.0	280.8	0.0	0.0	0.0	0.0	280.8
Cruise Fuel (kg)	318.1	329.5	329.0	170.8	171.7	183.0	318.1	319.6	329.5	170.8	183.0
Cruise Electricity (kW-hr)	0.0	0.0	0.0	0.0	0.0	0.0	0.0	0.0	0.0	0.0	0.0
Descent Fuel (kg)	104.6	0.0	106.4	36.2	36.4	38.0	104.6	105.1	0.0	36.2	38.0
Descent Electricity (kW-hr)	0.0	170.0	0.0	0.0	0.0	0.0	0.0	0.0	170.0	0.0	0.0
Approach Fuel (kg)	33.1	33.6	33.1	11.6	11.6	12.3	33.1	33.2	33.6	11.6	12.3
Approach Electricity (kW-hr)	0.0	0.0	0.0	0.0	0.0	0.0	0.0	0.0	0.0	0.0	0.0
Taxi In Fuel (kg)	8.8	0.0	8.8	2.4	0.0	1.8	8.8	0.0	0.0	2.4	1.8
Taxi In Electricity (kW-hr)	0.0	5.7	0.0	0.0	5.7	0.0	0.0	5.7	5.7	0.0	0.0
New Aircraft Cost (million USD)	$21.370	$21.578	$21.539	$20.213	$20.279	$19.986	$21.370	$21.435	$21.578	$20.213	$19.986
New Complete Powertrain Cost (including battery) (million USD)	$3.097	$3.305	$3.266	$1.940	$2.006	$1.713	$3.097	$3.162	$3.305	$1.940	$1.713
New Fuel Engine Cost (million USD)	$3.097	$3.097	$3.097	$1.940	$1.940	$1.395	$3.097	$3.097	$3.097	$1.940	$1.395
Mission Energy Cost (USD)	$502	$438	$512	$252	$251	$254	$1,268	$1,241	$1,083	$637	$602
Fuel Engines Only DMC (USD)	$364	$381	$302	$462	$464	$254	$364	$366	$381	$462	$254
Mission Powertrain DMC (USD)	$364	$399	$315	$462	$466	$284	$364	$368	$399	$462	$284
DOC per Block Hour (USD)	$2,863	$2,840	$2,826	$2,636	$2,642	$2,425	$3,741	$3,717	$3,578	$3,077	$2,823
Costs per Available Seat Kilometer (USD)	$0.1407	$0.1395	$0.1388	$0.1295	$0.1298	$0.1217	$0.1838	$0.1826	$0.1758	$0.1512	$0.1417
Emissions per Available Seat Kilometer (kg)	0.1474	0.1296	0.1510	0.0741	0.0737	0.0780	0.0263	0.0261	0.0277	0.0132	0.0218
CASK Percentage Reduction from Baseline	Baseline	0.8%	1.3%	7.9%	7.7%	13.5%	-30.7%	-29.8%	-25.0%	-7.5%	-0.7%
Emissions Percentage Reduction from Baseline	Baseline	12.1%	-2.5%	49.7%	50.0%	47.1%	82.2%	82.3%	81.2%	91.0%	85.2%

Stakeholder Needs-driven Results

The survey results presented in Chapter 3 showed that 7 of the 10 respondents did not consider CO_2 emissions directly when considering future aircraft purchases. These airlines would gravitate towards the hybrid turbocompound configurations using Jet A since they have the lowest CASK values, with the absolute lowest CASK configuration incorporating 50% takeoff/climb electric augmentation. This configuration features a 14% CASK improvement and 47% CO_2ASK reduction compared to the baseline airplane. For the airlines that prioritize CO_2 reductions, two options are available. Option 1 would be to use the same hybrid configuration described above, but use SAF instead of Jet A, resulting in a 1% CASK increase with an 85% CO_2ASK reduction compared to baseline. Option 2 uses a SAF-fueled non-hybrid turbocompound engine, with a 91% CO_2ASK reduction and an 8% CASK increase as compared to baseline. Since even the airlines that showed sensitivity to CO_2 emissions also highly prioritized operating costs, the expectation would be that they would choose Option 1 and then make tactical usage choices on Jet A versus SAF based on relative cost and availability.

Impact of Electrification on Powertrain Metrics of Interest

In Chapter 4, various metrics were presented for traditional thermal engine powertrains, such as specific power, efficiency, and cost. Examination of the results of this evaluation with a variety of hybrid powertrain configurations shows how these metrics are impacted at a complete “black box” powertrain level with the introduction of electrification. Data presented in Table 36 is used to draw these conclusions.

Specific power – the addition of electrification has an unfavorable impact on the specific power of the overall powertrain, particularly in the case of the gas turbine-based architectures. The addition of the electrical equipment adds mass, and the sizing points for the powertrain do not allow any offsetting size/mass reduction of the gas turbine, increasing overall powertrain weight. This impact is exaggerated even further if battery mass is included in the powertrain mass for purposes of specific power calculations, with overall mass for electrified powertrains up to 2x the mass of the non-electrified baseline for the same total power level.

Efficiency – the efficiency of the electrical powertrain is much higher than the fuel burning engine, roughly 90% versus 30%, depending on the particular operating condition. This results in the creation of a family of efficiency curves based on various thermal/electrical power splits, with the lower bound being the fuel only operation, the upper bound being electric only operations, with intermediate values as the electrical portion of the power split increases. It should be noted that this research work only accounts for changes in the power rating of the thermal engine and does not account for any engine cycle design changes that could be enabled by electrification. An example of this could include changes in compressor efficiency due to changes in surge margin requirements or clearance changes due to differing transient behavior. Exploitation of these gas turbine enhancement opportunities could result in additional efficiency benefits for the engines used in the hybrid configurations.

Acquisition cost – the acquisition cost behavior will be similar to the specific power, with the addition of electrical elements not being offset by reduction on the fuel engine elements, resulting in generally higher costs for the hybrid electric powertrains.

Durability – the durability of the hybrid powertrain is highly dependent on the configuration and usage profiles, so it is difficult to draw specific conclusions. From a parts count perspective, the additional electrical elements increase the possibility of failures and increase maintenance requirements, but if electrification is targeted to the most damaging portions of the flight, the thermal engine life can be increased to offset that result.

In summary, the relationships between traditional airplane metrics and the associated propulsion system “black box” metrics are demonstrated here to be not severed in design of hybrid electric aircraft. Instead, the addition of hybridization requires a shift in thinking and allocation of these traditional metrics because the powerplant now needs to be considered as a combined thermal engine/electrical system that can have multiple configurations and operating modes.

CO_2 Contributions of Battery Manufacturing

The initial research gap analysis highlighted that existing study methodologies did not address chemistry and usage-based CO_2 emissions embedded in the battery system (including emissions due to battery mining, manufacturing, and transportation). This effect has been captured in the well-to-wake evaluation methodology contained in this work and allows for quantification of this effect to determine its relative contribution.

This effect is shown in Figures 94-97 below, which illustrate CO_2 emissions due to fuel, electricity production, and battery manufacturing. This data was captured for a variety of engine types, fuel types, country of operation, and battery chemistry. Figure 94 illustrates the summative well-to-wake per-mission CO_2 emissions from all sources.

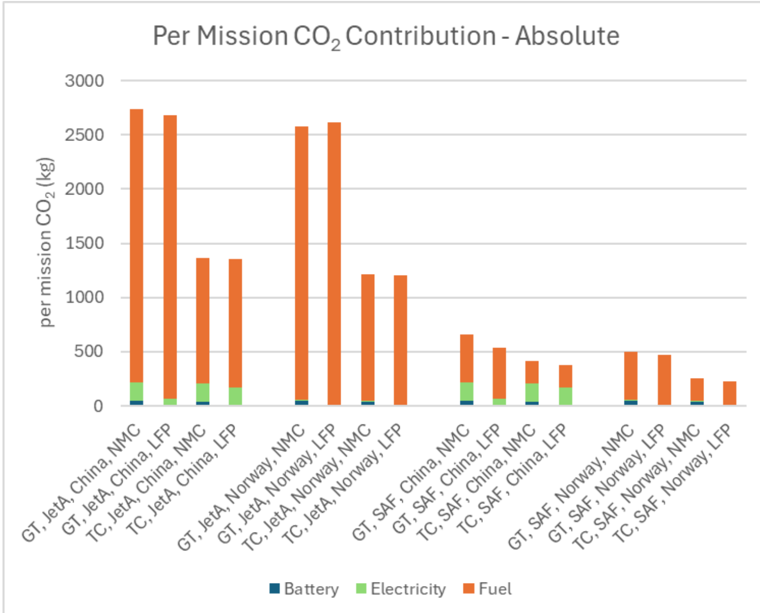

Figure 94 Summative “well-to-wake” CO_2 Emissions - all sources

The relative well-to-wake CO_2 contribution from each source is presented in Figure 95.

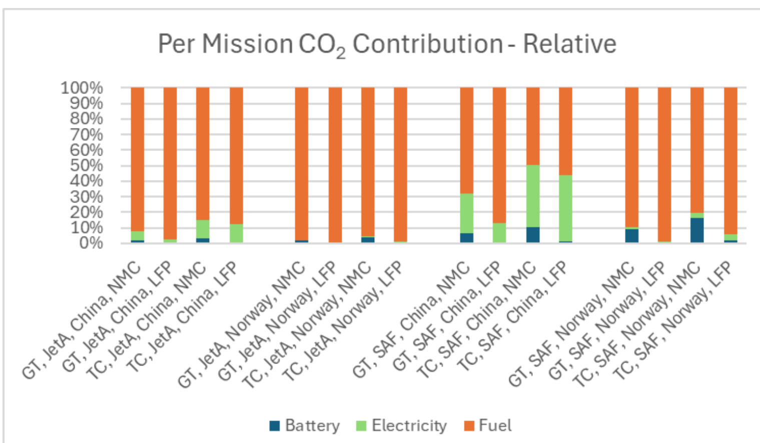

Figure 95 Relative “well-to-wake” CO_2 Emissions - all sources

These figures illustrate that when Jet A is used as the fuel source, the emissions from burning fuel dominate overall CO_2 emissions. When SAF is used, however, electricity and battery emissions play a more prominent role.

To better illustrate the value of including battery emissions in addition to the electricity emissions, the fuel contribution was removed and only the battery and electricity were considered. Figure 96 illustrates the summative well-to-wake CO_2 emissions.

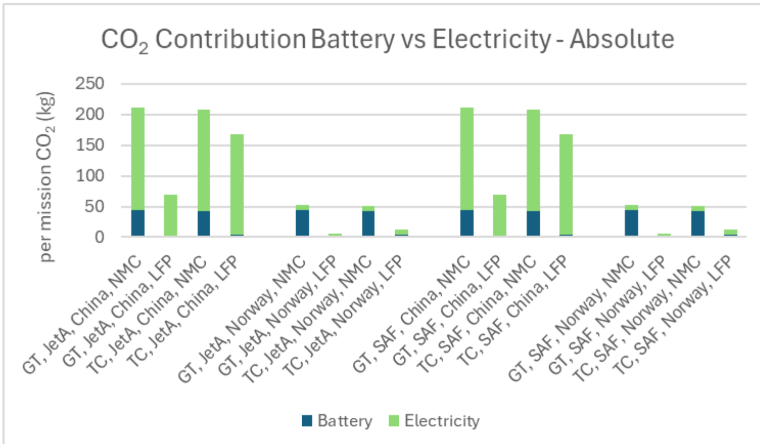

Figure 96 Summative "well-to-wake" CO_2 Emissions - battery/electricity only

Comparable relative values are presented in Figure 97.

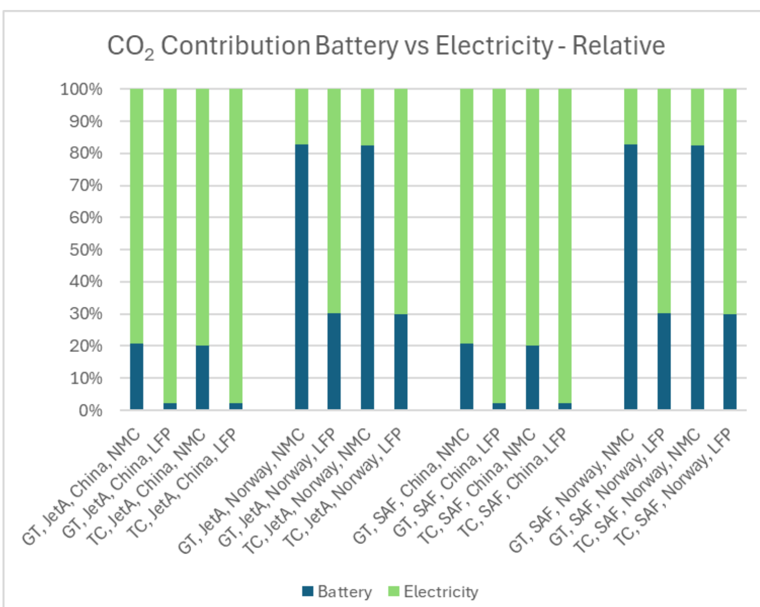

Figure 97 Relative "well-to-wake" CO_2 Emissions - battery/electricity only

As expected, operations in countries with very clean electric grids reduce CO_2 emissions due to electricity and increase the relative impact of the battery.

These results show that consideration of the emissions related to battery lifecycle can be at least as important as the CO_2 emissions from the electrical grid, accounting for up to 16% of the overall emissions in certain scenarios.

Sensitivity/Uncertainty Analysis

The results presented in Figure 93 and Table 36 were generated based upon a particular set of model characteristics (specific power, efficiency, cost, durability) and financial (fuel cost, electricity cost, financing rates) metrics. It is necessary to examine the impact of the variation of these values to understand the robustness of the overall conclusions. This was accomplished by performing a One-Variable-at-a-Time sensitivity analysis on both the baseline non-hybrid configuration presented as tornado plots in Figure 98 as well as the hybrid configuration with the lowest CASK presented in Figure 99. For reference, the nominal CASK for the non-hybrid is $0.1407 and $0.1217 for the hybrid. Engine specific power, Engine BSFC, Motor/Drive specific power, and Battery Specific Energy were varied over a +/- 20% range, while the others were varied over a +/- 50% range from their nominal values.

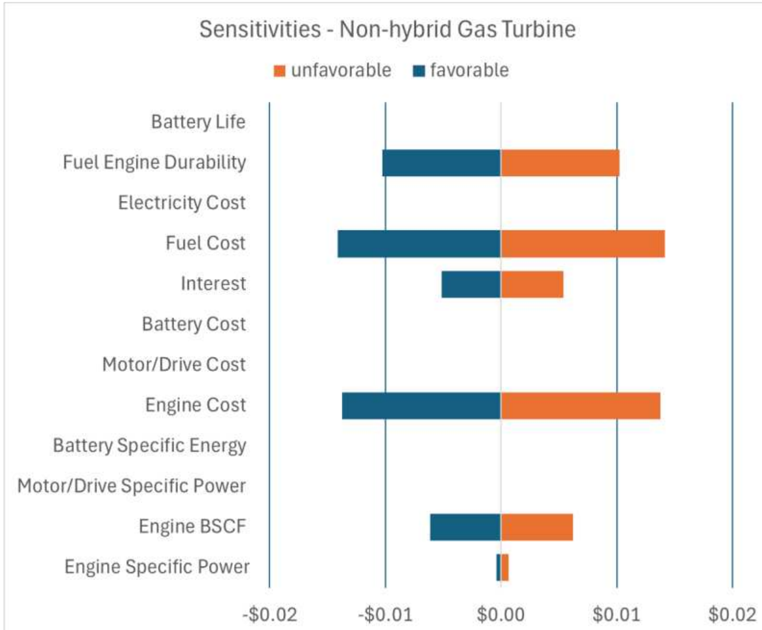

Figure 98 CASK Sensitivity for Non-Hybrid Configuration

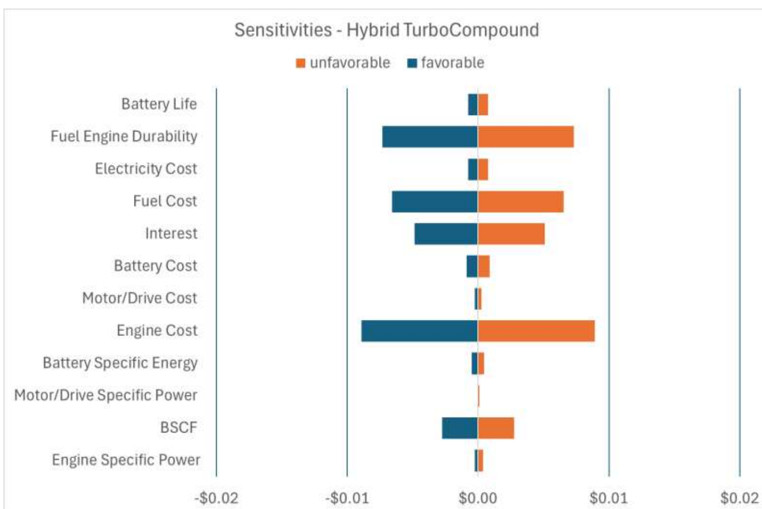

Figure 99 CASK Sensitivity for Hybrid Configuration

As expected, the addition of electrical elements in the hybrid configuration increases the impact of changes in those elements while decreasing the impact of changes to the fuel burning elements. Examples of this include engine durability, where a 50% variation results in a $0.010 change in CASK for the non-hybrid version, while the same variation in the hybrid only results in a $0.007 change. Another example would be sensitivity to engine cost, with a $0.014 change for the non-hybrid versus $.0085 for the hybrid with the same variation level. Higher levels of hybridization would increase the magnitude of this behavior as compared to these results at a relatively low degree of hybridization in this configuration. Uncertainty in some input elements such as fuel costs or interest rates will impact all configurations in the same direction (although to different degrees), while uncertainty in other elements such as engine durability may differ independently across the range of options since different configurations may use entirely different engine types that can have technology-unique characteristics.

Several of the specific configuration and operating characteristics were then looked at individually to understand the sensitivity of the outcome to changes.

1. Thermal engine type

To understand the impact of thermal engine type, a family of analyses was performed for both non-hybrid and a wide variety of hybrid approaches. Results of this analysis are shown in Figure 100. In can be seen that in every approach considered, the turbocompound approach results in lower cost per available seat kilometer, although the magnitude of benefit is highly dependent on the particular hybrid powertrain approach.

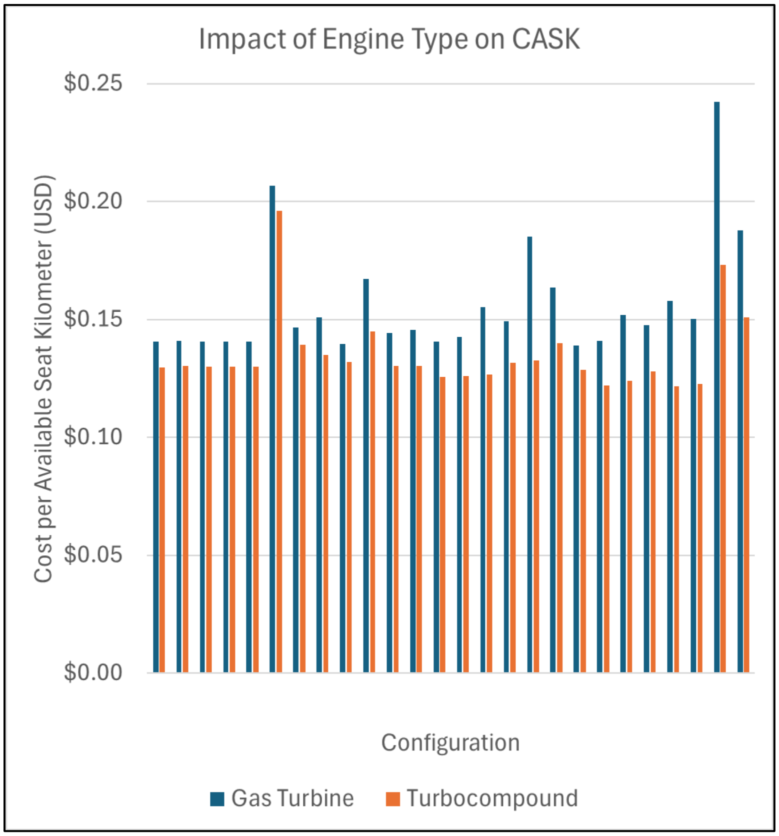

Figure 100 Impact of Engine Type on CASK for a set of 26 aircraft configurations

2. Thermal engine power rating

This sensitivity of this parameter was investigated by using the case of the non-hybrid thermal engine only configuration. Basic engine sizing was performed to determine the minimum engine power for takeoff, climb, or cruise. For the gas turbine, the primary sizing criteria was the top of climb performance, since the gas turbine engine power lapses with altitude. In contrast, the turbocompound engine does not exhibit this lapse behavior, and the takeoff/initial climb segment became the sizing criteria. For each configuration, the engine was then upsized by 25% and 50% to determine the sensitivity.

Overall, this results in the behavior shown below in Figure 101, with an increase in thermal engine size for a given configuration resulting in an increase in cost per available seat kilometer. Fuel costs increase due to increased engine weight, and due to the engine operating at part throttle and consequently at a lower efficiency point. The larger engines are more expensive, increasing the OEM financing costs. While the engine is run at a less severe operating point and therefore has a longer interval between overhauls, the increased engine overhaul cost nearly offsets that gain, resulting in almost identical powerplant direct maintenance costs. Since the engine costs are lower for the turbocompound engine, the magnitude of the overall cost increases is less than that of the gas turbine, although the general behavior remains consistent.

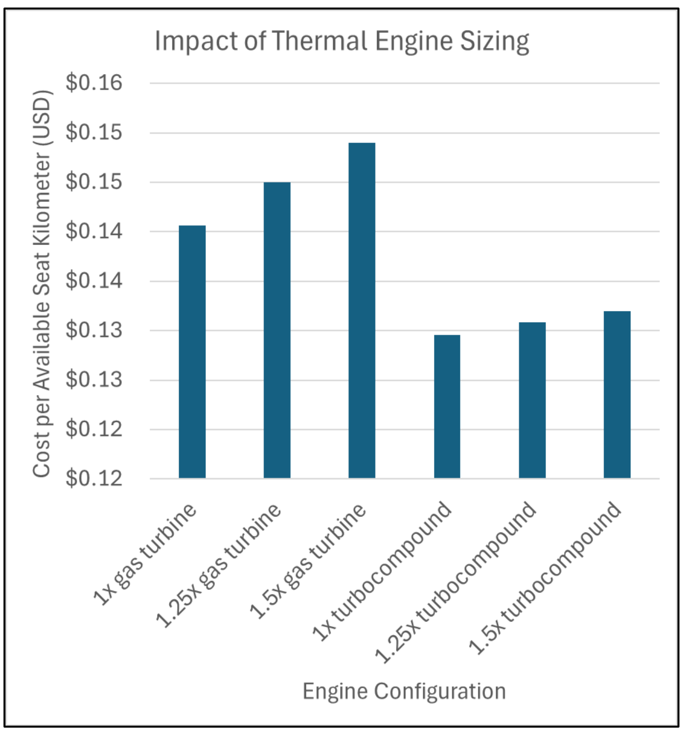

Figure 101 Impact of Thermal Engine Sizing on CASK

3. Fuel type

Both conventional kerosene (Jet A) and biomass based synthetic aviation fuels were considered. Synthetic fuels have much lower net CO_2 emissions compared to Jet A but come at a significant price premium. Figure 102 illustrates the impact of this fuel choice on a family of hybrid configuration choices using both gas turbine and turbocompound engines. It should be noted that both families show a significant reduction when moving to SAF, but the turbocompound configurations are less impacted due their lower overall fuel usage as compared to the gas turbine.

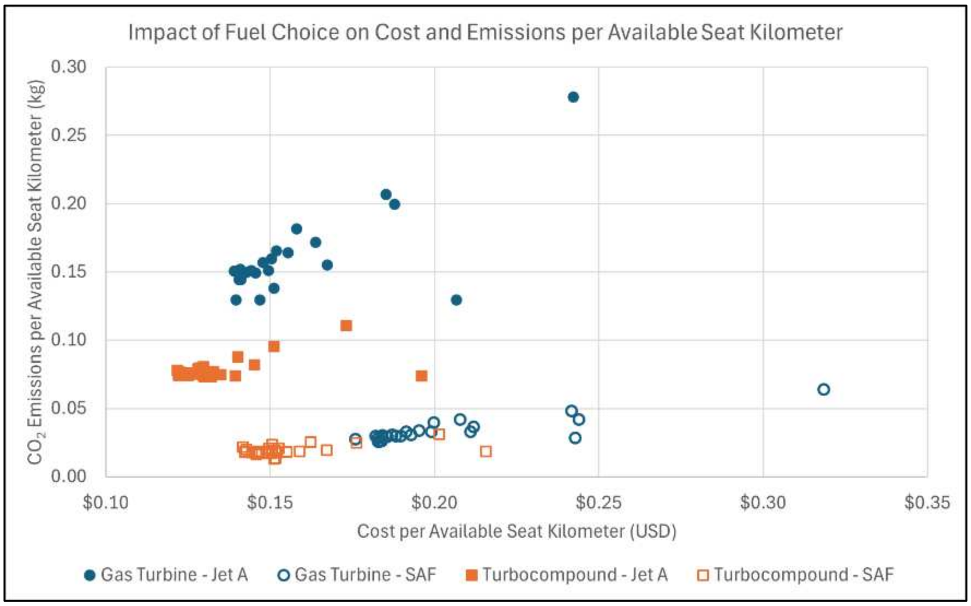

Figure 102 Impact of Fuel Choice on Cost and Emissions

4. Country of operation

Two sets of use cases were evaluated to demonstrate the impact of operating country on the performance of a hybrid configuration compared to the baseline ATR42 aircraft. This evaluation was performed for both gas turbine and turbocompounded configurations at the hybrid configuration with the lowest cost per available seat kilometer.

The first case is the gas turbine-based configuration shown in Figure 103. In this instance, the operating case with the lowest cost per available seat kilometer used a 20% electrical offset during the climb phase. When compared with the baseline legacy ATR42 case (first column), in every country considered the cost remained below the legacy baseline, while the direction and magnitude of emission impact varied strongly by country. In most cases, overall CO_2 emissions increased with the introduction of hybrid, even though overall mission jet fuel usage decreased. This was due to the high electrical grid CO_2 footprint in some countries as well as the added CO_2 footprint due to battery lifecycle manufacturing emissions.

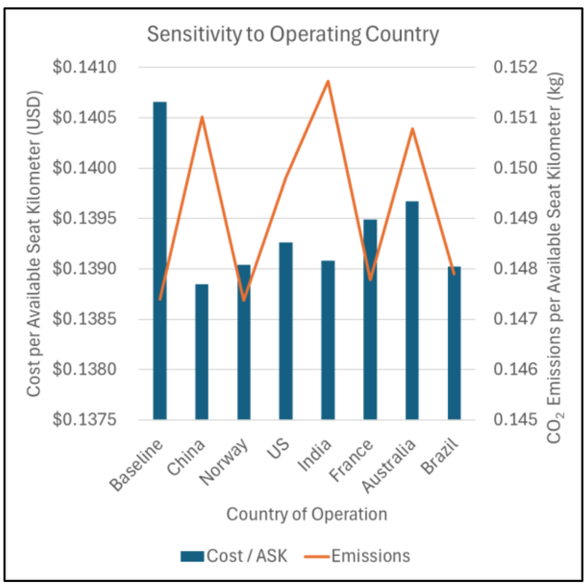

Figure 103 Cost and Emissions by Operating Country (gas turbine)

Contrast this, however, with the second case, which is the turbocompound-based configuration shown in Figure 104. In this instance, the operating case with the lowest cost per available seat kilometer used a 50% electrical offset during the climb phase. When compared with the baseline legacy ATR42 case (first column), in every country both cost and emission impacts were below the legacy baseline, although the magnitude of decrease varied on a country-by-country basis. In this case, the significant decrease in overall mission jet fuel usage overwhelmed the impacts of the high electrical grid CO_2 footprint in some countries as well as the added CO_2 footprint due to battery lifecycle manufacturing emissions.

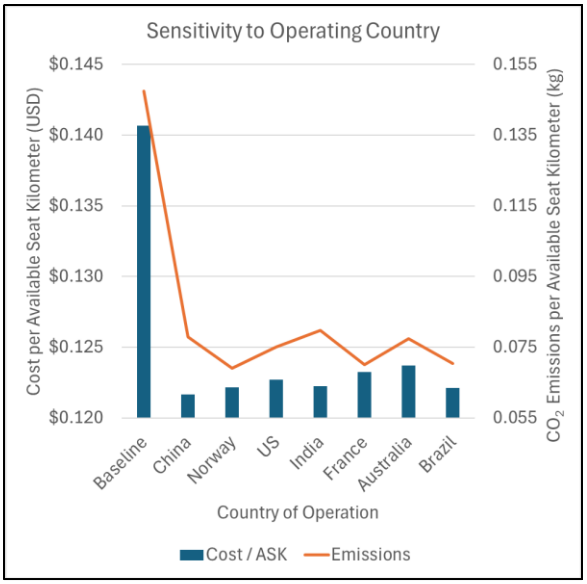

Figure 104 Cost and Emissions by Operating Country (turbocompound)

5. Battery chemistry and depth of discharge

For this study, two different chemistries were considered (NMC and LFP) with both 50% and 95% depths of discharge. Additionally, who different levels of electric augmentation during climb were evaluated to illustrate how this impacts the results. Results are presented for the turbocompounded hybrid configuration, but the same trends are present in the gas turbine hybrid configuration. The mission length chosen for this comparison was 200 nautical miles.

The first set of results is for a 30% electric augmentation during takeoff/climb. In Figure 105 two opposing trends are apparent. When looking at block hour aircraft costs, the configuration using NMC battery chemistry shows a cost decrease as the depth of discharge moves from 95% to 50%. This is because the high specific energy of the NMC chemistry drives a smaller negative weight impact, but the high cost and cycle life sensitivity of this chemistry to depth of discharge results in comparatively larger battery maintenance cost advantages relative to the fuel burn and engine life disadvantages. In contrast, the lower specific energy, cost and depth of discharge sensitivity of LFP results in the opposite result, where the battery gains are outweighed by the fuel burn and engine life reductions.

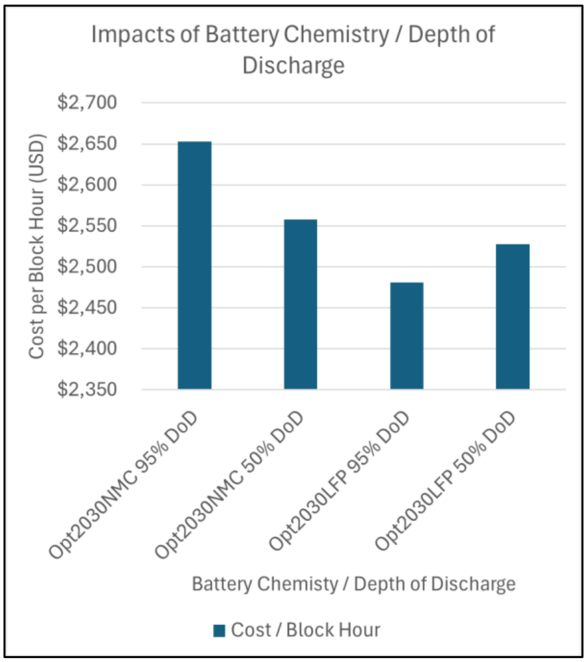

Figure 105 Battery Impact (Cost / Block Hour) – 30% Augmentation

Figure 106 examines the cost and lifecycle emissions on an available seat kilometer basis. On the cost side, the available seat kilometer costs illustrate the same general behavior as the block hour costs, although the impact is amplified for the 50% DoD LFP case, since MTOW limitations result in the removal of two available passenger seats from service. Emissions, however, demonstrate a slightly different behavior. At the electric augmentation levels being used here, the emissions due to fuel usage are more impactful than those due to battery manufacturing/replacement, so moving to lower depths of discharge (with resulting weight increases) penalizes overall emissions levels. In addition, like the costs on an available seat kilometer basis, the 50% DoD LFP case is also additionally penalized by the loss of two available passenger seats.

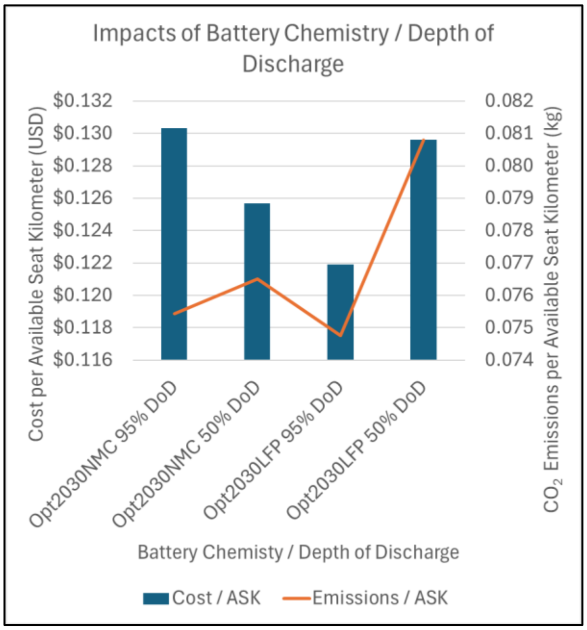

Figure 106 Battery Impact (Cost/ASK, Emissions/ASK) – 30% Augmentation

The use case with 50% electric augmentation shown in Figure 107 demonstrates a slightly different block cost behavior, due primarily to the higher levels of aircraft weight with this configuration. Here, in all cases, the aircraft is operating near or at its MTOW limits in all cases but the NMC/95% DoD case, with varying levels of passenger seat count reduction to offset the increasing battery weight due to lower specific energy chemistries or depths of discharge. In these cases, since the aircraft weight is not significantly changing, fuel burn and engine maintenance costs remain relatively constant, while battery costs vary due to cycle life variations with depth of discharge.

Again, this figure illustrates the high cycle life sensitivity of NMC to depth of discharge and the comparatively lower sensitivity of LFP.

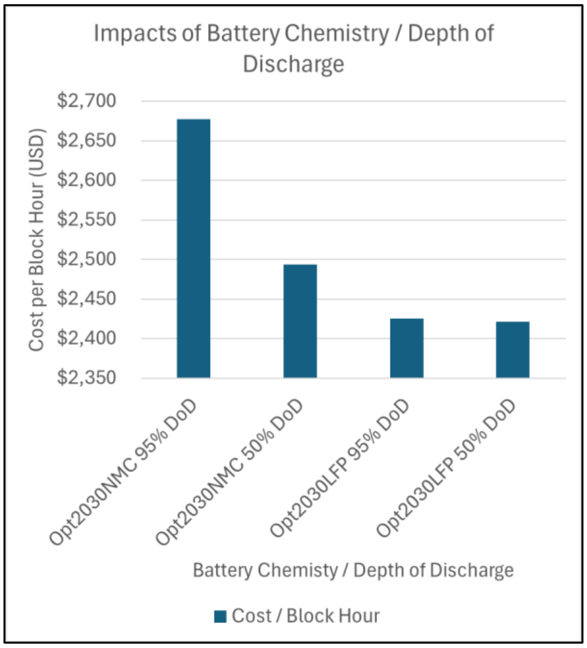

Figure 107 Battery Impact (Cost/Block Hour) – 50% Augmentation

The impact of the loss of available seats is seen much more strongly for this use case as illustrated in Figure 108. For the NMC, the costs on an available seat kilometer basis increase, even though the costs per block hour decrease, reflective of the loss of six seats at the lower depths of discharge. For the LFP case, the effect is even more dramatic due to the loss of 14 seats (almost 30% of baseline seating capacity) when moving to the lower depth of discharge.

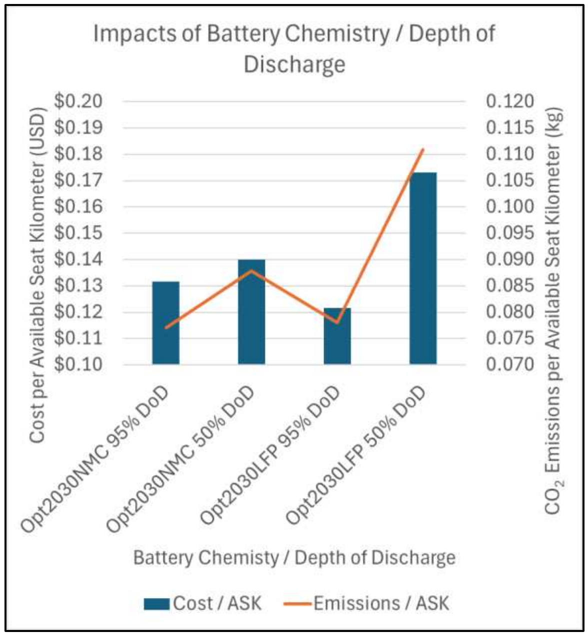

Figure 108 Battery Impact (Cost/ASK, Emissions/ASK) – 50% Augmentation

These results show that it is difficult to draw general conclusions as to the best battery choice. Low battery cost, high specific energy, and low cycle life sensitivity to depth of discharge all make a particular battery choice more attractive, but specific behavior is very tied to an aircraft configuration and operational profile.

6. Segment/magnitude/profile of electric augmentation

There are many ways that electric augmentation can be applied in the hybrid configurations. The flight segment where the augmentation is applied, and the magnitude of that augmentation can significantly impact the performance of the hybrid configurations.

Figure 109 shows the cost and emissions for both the gas turbine and turbocompound with augmentation applied in different segments.

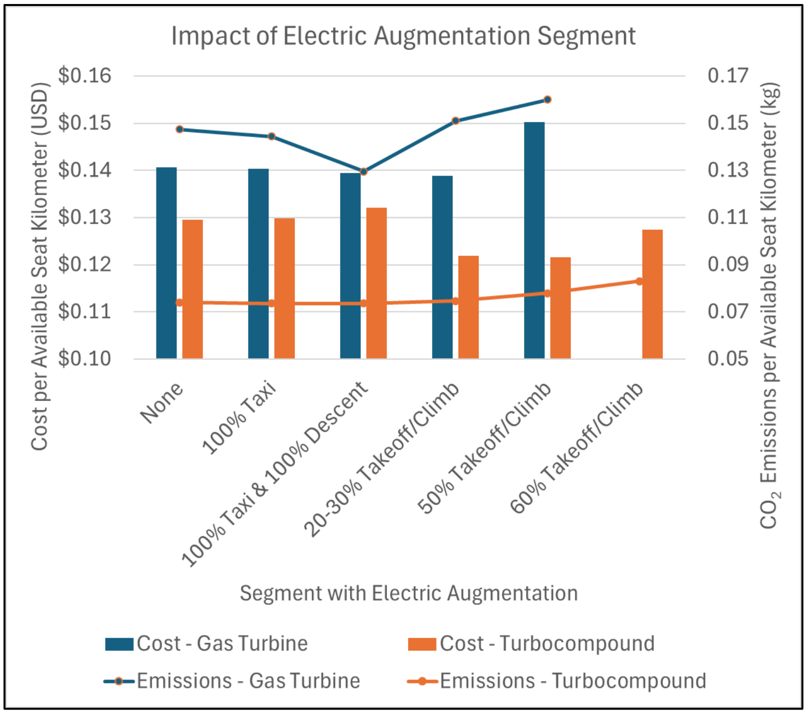

Figure 109 Impact of Electric Augmentation Segment

For the gas turbine configuration, the greatest benefit occurs at approximately 20% level of takeoff/climb augmentation but then shows noticeable deterioration as the augmentation level is further increased. The turbocompound configuration shows a similar characteristic, although the benefit increase continues to the 50% takeoff/climb augmentation level before reducing as augmentation levels further increase, primarily due to a loss in passenger capacity due to the increased battery and electrical equipment weight.

Also, as described in the previous section, the profile of electric augmentation during climb can be varied. Figure 110 shows the behavior of the system to these various augmentation approaches. It can be seen that both cost and emissions are impacted by this change in approach, although the associated trend varies depending on which one is being emphasized.

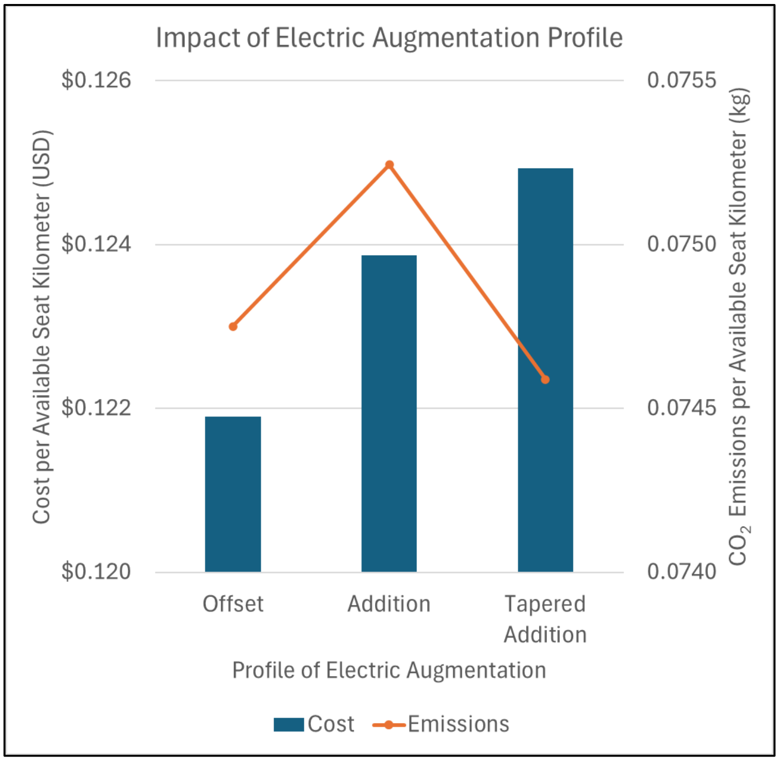

Figure 110 Impact of Electric Augmentation Profile

7. Mission length

A sensitivity study was performed to characterize how mission length contributes to operating cost results. The two configurations used were the baseline ATR configuration with a non-hybrid gas turbine, and a hybrid turbocompound powertrain with 50% electric takeoff/climb augmentation and LFP batteries.

Figure 111 characterizes the impact of mission length on the cost per block hour. The block hour cost advantage maintains a clear advantage across the range of mission lengths and increases at shorter mission ranges, since a greater portion of the mission energy comes from the lower cost electrical source as opposed to Jet A.

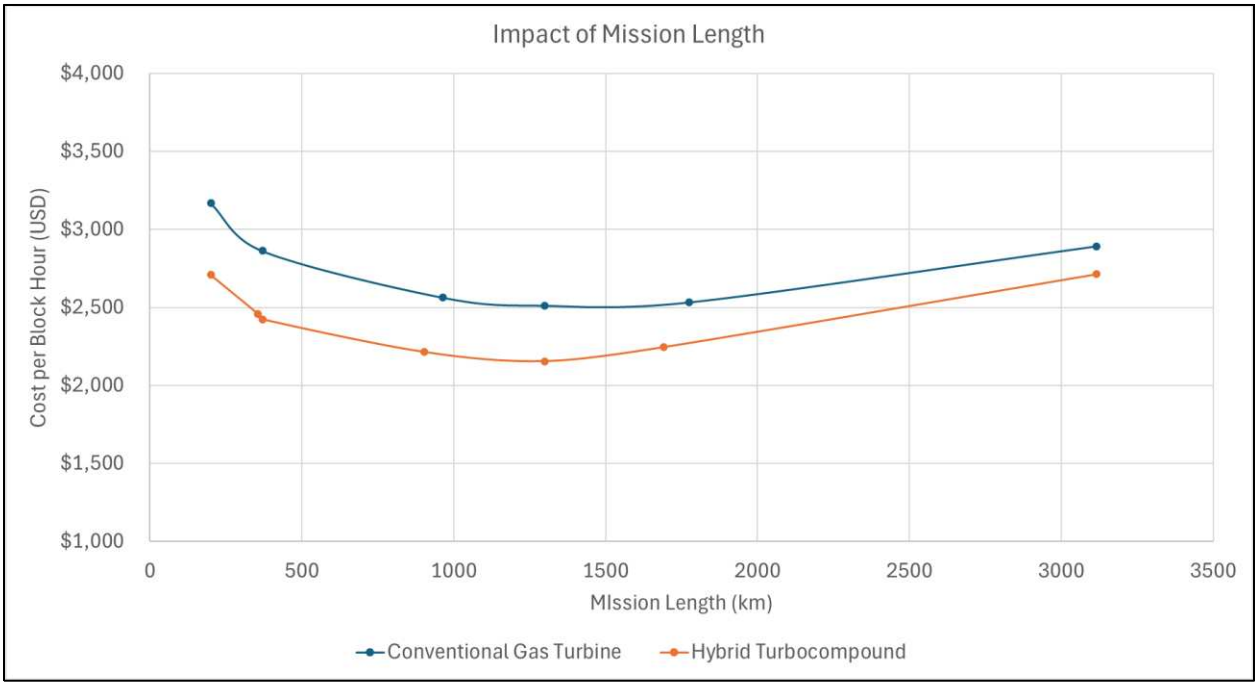

Figure 111 Sensitivity of Block Hour Cost to Mission Length

This situation changes, however, when costs are evaluated based on available seat kilometers, as shown in Figure 112. Since the hybrid aircraft is heavier than the baseline ATR42, it more quickly reaches a range threshold where you must start removing passengers in favor of fuel to maintain the aircraft MTOW. While hybrid maintains a cost advantage at short or very long mission ranges, missions in the 1000-1500 km range show almost identical costs per available seat kilometer.

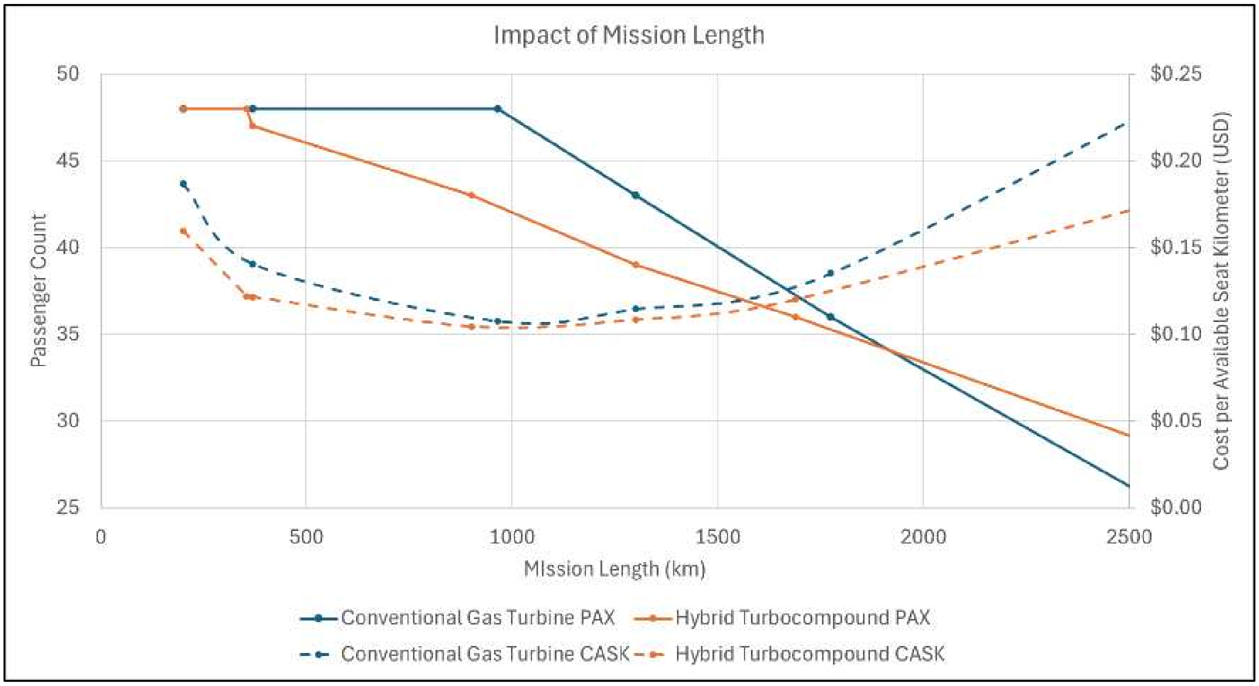

Figure 112 Sensitivity of Passenger Count and Cost per Available Seat Kilometer to Mission Length

CO_2 emissions per available seat kilometer also show a similar behavior as shown in Figure 113.

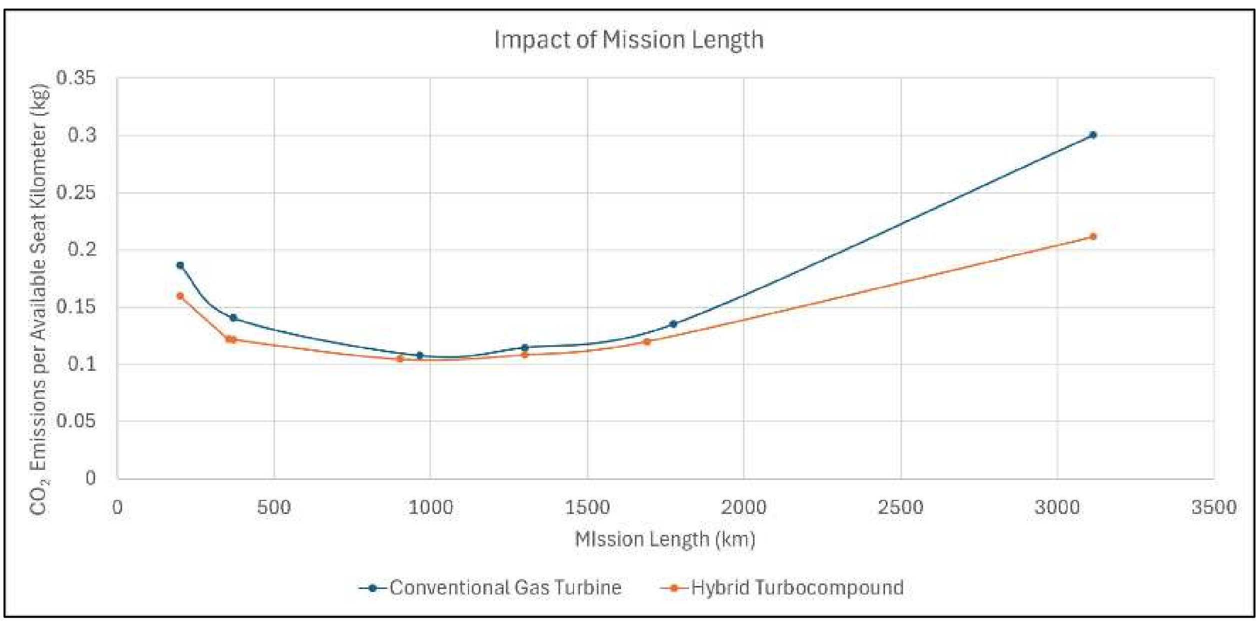

Figure 113 Sensitivity of CO_2 Emissions per Available Seat Kilometer to Mission Length

Overall, this shows that the hybrid turbocompound configuration is most advantageous for shorter (<750 km) routes or longer (>1500 km) routes, with only moderate advantage at medium mission ranges.

Conclusions

This chapter sought to address the research problem identified as research question 5, which is repeated below:

> **Research Question 5) What needs to be done to perform optimization exercises on a variety of use cases to demonstrate the costs and benefits of the proposed optimization approach?**

Now having performed the research activities documented in the above sections, we can answer the research question. The results of the optimization exercise have demonstrated the ability of the analysis methodology to address variations in configuration and operational considerations and has generated a family of optimum solutions based on the desired metric of interest. It has been shown that hybrid-electric can bring benefits (particularly cost benefits) to both gas turbine and turbocompound configurations, although turbocompound configurations are consistently better.

Overall, the best turbocompounded hybrid solution has a 13.5% cost per available seat kilometer and a 47% CO_2 emissions per available seat kilometer advantage when compared to the baseline ATR42 aircraft with both using Jet A, or can achieve a 23% cost per available seat kilometer and a 17% CO_2 emissions per available seat kilometer advantage when compared to the baseline ATR42 aircraft with both using SAF. If emissions reduction were the primary goal, using a SAF-fueled turbocompound hybrid can result in a 91% emissions decrease, with only a 7.5% cost increase compared to today’s ATR42 using Jet A.

Chapter 8 - Conclusions, Contributions, and Future Work

This research investigates a systematic approach to identify future customer needs for next generation regional aircraft powertrains and to develop an approach for evaluating configurations and operating scenarios to best satisfy those needs.

Conclusions

This research executed a series of tasks to address the primary research challenges associated with optimization of regional aircraft hybrid electric powertrains to maximize customer defined value. Existing modeling approaches are focused on fuel burn or carbon emissions, and do not adequately capture the impacts of electrification on turbine engine design and operating costs. This activity considered customer value inputs, component and system performance and cost characteristics, and design/optimization approaches to create a novel holistic system engineering approach to powertrain design. The result of this proposed research is an improved understanding of driving factors, and a corresponding tool to perform the optimization process and understand sensitivity to input variation more effectively.

Contributions

Collectively, there is an identified industry need for a methodology and toolset to be able to consider this wide range of system-level airline operator metrics, and to be able to assess the comparative values of these metrics to determine the relative value of differing potential configurations. The ability of the toolset to perform efficient parameterized evaluation would be valued to reduce the design time needed to converge on a preferred solution subject to a particular unique set of input and weightings. This is a current gap in industry and forms the value statement for these research results. Specific research contributions include:

1. The construction of a novel value-based assessment of the characteristics that are important to mid-sized regional airline customers. This allowed the identification of the value (economic, environmental, societal) of an optimized hybrid electric configuration to these commercial aviation stakeholders, supported by surveys of potential users in a market space not addressed in prior research.
2. Creation and validation of novel performance, reliability, and cost models/relationships for current and future electrical, thermal engine, and energy storage elements of a hybrid electric system. Previous research is focused on performance characteristics impacting fuel burn but does not account for how changes in configuration and operational scenarios can also impact acquisition and maintenance costs and aircraft efficiency.
3. A validated holistic regional aircraft model and evaluation technique that efficiently identifies a preferred solution across a range of inputs and customer value gauges. This model calculates the interactions between the various elements to determine the metrics of interest, and then quantifies those metrics to define the optimum powertrain configuration for a particular customer situation.
4. Evaluation of the new process versus those from literature which define a series of point designs or heuristic methods to validate the effectiveness of

the proposed approach and its benefits to the powertrain designer. The ultimate measure of the success of this activity is that it creates configurations of maximum value to the customer in the quickest possible manner.

5. An in-depth analysis of a particular powertrain architecture (parallel hybrid with turbocompounded engine), demonstrating the output of the methodology and potential value to the airline customer.

Future Work

The work presented in this dissertation could be further expanded and improved in several areas. This would result in the more efficient and comprehensive exploration of the full range of potential configuration and operational choices and allow for faster understanding of the impact of variation of inputs such as fuel prices or evolution of technical attributes such as energy density. Today, each use case is a dedicated manual run and the modification of the tool to allow for scripting of alternatives would allow for much quicker exploration across an expanded potential space and allow for better understanding of uncertainties within the model, either as a single characteristic or in combination with others.

Another improvement would be to expand the architectural range that the tool addresses, Due to the alignment with my industrial activities, and the perceived near-term utility of a parallel hybrid architecture, the analysis methodology and collected model data focused on information of value to that specific architecture. Future work would expand this methodology to capture additional propulsion architectures such as series hybrid and/or distributed propulsion, as well as additional component level model data for technologies such as fuel cells, superconducting/cryogenic motors and motor controllers, and advanced battery chemistries.

Lastly, this tool and methodology exist as a self-contained toolset without any connection to other higher level aircraft or mission design and optimization MDO tools. Further work should be done to understand how the novel characteristics of this work could either be embedded or connected to more detailed aircraft modeling tools to add fidelity to the mission analysis, or broader airline-level operations and route analysis models to understand the full airline fleet level impacts.

Chapter 9 - References

1. Machinery Market (2019, July 12). Rolls Royce Focuses on “Third Era” of Aviation. Retrieved from https://www.machinery-market.co.uk/news/24305/Rolls-Royce-focuses-on-%E2%80%98the-third-era-of-aviation.
2. Roser, M., Ritchie, H., Ortiz-Ospina, E. (2019). World Population Growth. Retrieved from https://ourworldindata.org/world-population-growth
3. Graver, B., Polishing my Crystal Ball: Airline Traffic in 2050. International Council on Clean Transportation Retrieved from https://theicct.org/global-aviation-airline-traffic-jan22/
4. Shulz, E. Global Market Forecast 2018-2037. Global Networks, Global Citizens. Airbus, 2018.
5. ATR (2022, July) Turboprop Market Forecast 2022-2041. Retrieved from https://www.google.com/url?sa=i&url=https%3A%2F%2Fwww.atr-aircraft.com%2Fwp-content%2Fuploads%2F2022%2F07%2FATR_Market-Forecast_2022_Digital_HD.pdf&psig=AOvVaw366ZCR8Nj340z4jOFz4pqC&ust=1739637404678000&source=images&cd=vfe&opi=89978449&ved=0CAQQn5wMahcKEwjwy6zx0MOLAxUAAAAAHQAAAAAQBA
6. Ritchie, H. (2020, October 22) Climate change and flying: what share of global CO2 emissions come from aviation?. Retrieved from https://ourworldindata.org/co2-emissions-from-aviation#:~:text=Flying%20is%20a%20highly%20controversial,impacts%20on%20climate%20into%20account
7. DLR.; BDLI. Zero Emission Aviation - Emissionsfreie Luftfahrt: German Aviation Research White Paper 2020.
8. Kharina, A.; Rutherford, D. Fuel efficiency trends for new commercial jet aircraft: 1960 to 2014. Whitepaper of the International Council on Clean Transportation, 2015.
9. Timperley, J, (2019, September 9). Why ‘flight shame’ is making people swap planes for trains. BBC. Retrieved from https://www.bbc.com/future/article/20190909-why-flight-shame-is-making-people-swap-planes-for-trains.
10. Antcliff, K., Borer, N., “Regional Air Mobility: Leveraging Our National Investments to Energize the American Travel Experience,” National Aeronautics and Space Administration Whitepaper NASA/CR–20210014033, 2021.
11. Saxon, S., Weber, M. (2013, July 17). A better approach to airline costs. Retrieved from https://www.mckinsey.com/industries/travel-logistics-and-infrastructure/our-insights/a-better-approach-to-airline-costs
12. Hameed, M., & Rutherford, D. (2025). *Fuel burn of new commercial jet aircraft: 1960 to 2024* (ICCT Working Paper No. 287). International Council on Clean Transportation. https://theicct.org/publication/fuel-burn-of-new-commercial-jet-aircraft-1960-to-2024-feb25

13. European Commission: Directorate-General for Mobility and Transport and Directorate-General for Research and Innovation. Flightpath 2050 – Europe's vision for aviation – Maintaining global leadership and serving society's needs. Publications Office, 2011. doi:https://data.europa.eu/doi/10.2777/50266.
14. IATA. A global approach to reducing aviation emissions. First stop: carbon-neutral growth from 2020, 2009.
15. ICAO. Environmental report 2016. Aviation and climate change 2016.
16. Drake, A. NASA environmentally responsible aviation (ERA) N+ 2 advanced vehicle study. 50th AIAA Aerospace Sciences Meeting, 2012.
17. van der Sman, E.; Peerlings, J.; Kos, J.; Lieshout, R.; Boonekamp, T. Destination 2050 - A route to net zero European aviation. Destination2050, 2021.
18. ATAG. (2021). Waypoint 2050. Geneva: ATAG
19. NASA Electric Propulsion System Studies. Available online: https://ntrs.nasa.gov/api/citations/20160009274/downloads/20160009274.pdf (accessed on 30 March 2022).
20. Hoogreef, M., Vos, R., de Vries, R., Veldhuis, L., "Conceptual Assessment of Hybrid Electric Aircraft with Distributed Propulsion and Boosted Turbofans," AIAA Science and Technology Conference, San Diego, 2019, 10.2514/6.2019-1807.
21. Schiltgen, B. and Freeman, J., "ECO-150-300 Design and Performance: A Tube-and-Wing Distributed Electric Propulsion Aircraft," AIAA Sci Tech Forum, San Diego CA, 2019
22. Jansen, R. H., Duffy, K. P., Felder, J. L., Brown, G. V, "Turboelectric Aircraft Drive Key Performance Parameters and Functional Requirements," AIAA Propulsion and Energy Forum, AIAA 2015-3890, Orlando FL, 2015.
23. Jansen, R. H., Duffy, K. P., Brown, G. V., "Partially Turboelectric Aircraft Drive Key Performance Parameters," AIAA Propulsion and Energy Conference, Atlanta, 2017, AIAA-2017-4702.
24. Bradley, M. K., and Droney, C. K., "Subsonic Ultra Green Aircraft Research Phase I Final Report," National Aeronautics and Space Administration Contractor Report NASA/CR–2011-216847, 2011.
25. Bradley, M. K., and Droney, C. K., "Subsonic Ultra Green Aircraft Research Phase II: N+4 Advanced Concept Development," National Aeronautics and Space Administration Contractor Report NASA/CR-2012-217556, 2012.
26. Lents, C. E., Hardin, L.W., Rheaume, J.M, and Kohlman, L., "Parallel Hybrid Gas-Electric Geared Turbofan Engine Conceptual Design and Benefits Analysis," AIAA Propulsion and Energy Conference, Salt Lake City, 2016, p. 4610
27. Gladin, J. C., et. al., "Fundamentals of Parallel Hybrid Turbofan Mission Analysis with Application to the Electrically Variable Engine," AIAA/IEEE Electric Aircraft Technology Symposium, Cincinnati, 2018, 10.2514/6.2018-5024.
28. Haran, K., "High Speed, High Frequency Air-core Machine and Drive," NASA Grant Number: NNX14AL79A, Annual Review, October 5, 2016.
29. Bradley, M. K., and Droney, C. K., "Subsonic Ultra Green Aircraft Research Phase II Volume II Hybrid Electric Design Exploration," National Aeronautics and Space Administration Contractor Report NASA/CR–2015-218704, 2015.

30. Cinar, G., et. Al., “Sizing and Optimization of Novel General Aviation Vehicles and Propulsion System Architectures,” AIAA Aviation Technology, Integration, and Operations Conference, Atlanta, 2018, doi.org/10.2514/6.2018-3974
31. Cinar, G., Garcia, E., Mavris, D. N., “A Framework for Electrified Propulsion Architecture and Operation Analysis,” Journal of Aircraft Engineering and Aerospace Technology, August 19, 2019. 10.1108/AEAT-06-2019-0118.
32. Antcliff, K. R., et. al., “Mission Analysis and Aircraft Sizing of a Hybrid Electric Regional Aircraft,” 54th Annual AIAA Aerospace Sciences Meeting, Sand Diego, 2016, doi.org/10.2514/6.2016-1028.
33. Fornaro,E., Cardone, M., and Dannier, A., "A Comparative Assessment of Hybrid Parallel, Series, and Full-Electric Propulsion Systems for Aircraft Application," in IEEE Access, vol. 10, pp. 28808-28820, 2022, doi: 10.1109/ACCESS.2022.3158372.
34. Plötner, K., et. al., ”Operating Cost Estimation for Electric-Powered Transport Aircraft,” 2013 Aviation Technology, Integration, and Operations Conference. 10.2514/6.2013-4281.
35. Hoelzen, J., et. al., “Conceptual Design of Operation Strategies for Hybrid Electric Aircraft,” Energies. 2018; 11(1):217. https://doi.org/10.3390/en11010217
36. Scholz, A,. Trifonov, D., Hornung, M., “Environmental life cycle assessment and operating cost analysis of a conceptual battery hybrid-electric transport aircraft,” CEAS Aeronautical Journal, 2021. 10.1007/s13272-021-00556-0.
37. Kavvalos, M. D., et. al., "Exploring Design Trade-Offs For Installed Parallel Hybrid Powertrain Systems," 2021 AIAA/IEEE Electric Aircraft Technologies Symposium (EATS), 2021, pp. 1-16, doi: 10.23919/EATS52162.2021.9704836.
38. Ribeiro, R. F. G., Trapp, L. G., Lacava, P. T., "Economical Aspects of Aircraft Propulsion Electrification," 2021 AIAA/IEEE Electric Aircraft Technologies Symposium (EATS), 2021, pp. 1-18, doi: 10.23919/EATS52162.2021.9704846.
39. Spierling, T.A., Lents, C.E., “Parallel Hybrid Propulsion System for a Regional Turboprop: Conceptual Design and Benefits Analysis,” AIAA Propulsion and Energy Forum, Indianapolis, 2019, 10.2514/6.2019-4466.
40. Harish, Anusha & Perron, Christian & Bavaro, Daniel & Ahuja, Jai & Ozcan, Melek & Justin, Cedric & Briceno, Simon & German, Brian & Mavris, Dimitri. (2016). Economics of Advanced Thin-Haul Concepts and Operations. 10.2514/6.2016-3767.
41. Aviation Week Intelligence Network. Fleet by Operator, Accessed February 2025.
42. Guzhva, V. S., Curtis, T., & Borodulin, V. (2013). Market Analysis for Small and Mid-Size Commercial Turboprop Aircraft. Retrieved from https://commons.erau.edu/publication/71
43. Deutsche Aircraft, (2023) D328eco: The Turboprop (R)evolution. [brochure]
44. Trimble, S. (2023, October 11). Emerging markets both spur and limit Embraer’s E3 turboprop potential. The Air Current. https://theaircurrent.com/analysis/emerging-markets-both-spur-and-limit-embraers-e3-turboprop-potential/
45. Eisenhut, D., Moebs, N., Windels, E., Bergmann, D., Geiß, I., Reis, R., & Strohmayer, A. (2021). Aircraft Requirements for Sustainable Regional Aviation. Aerospace, 8(3), 61. https://doi.org/10.3390/aerospace8030061

46. Clean Aviation. (2024). Clean Aviation Strategic Research and Innovation Agenda (SRIA). Clean Aviation. https://clean-aviation.eu/sites/default/files/2024-09/2024-Clean-Aviation-SRIA.pdf
47. Merlin, P. W. (2020). *Green Light for Green Flight*. National Aeronautics and Space Administration. https://www.nasa.gov/wp-content/uploads/2020/07/green-light-for-green-flight-tagged.pdf?emrc=670e84
48. Yan, R., Tang, B.-J., Hu, Y.-J., Ji, C.-J., Lin, K.-B., & Shen, M. (2025). Sustainable aviation fuel and next-generation aircraft: Low-carbon pathway for China's civil aviation industry. *Journal of Environmental Management, 391*, 126493. https://doi.org/10.1016/j.jenvman.2025.126493
49. Avions de Transport Regional (2005). ATR42-500 A New Standard of Excellence [Brochure]. DC/E Marketing-Commercial Directorate
50. European Union Aviation Safety Agency. (n.d.). *Type certificate data sheet: Pratt & Whitney Canada PW100 series*. Retrieved October 2023, from https://www.easa.europa.eu/en/document-library/type-certificates/engine-cs-e/easaime041-pratt-and-whitney-canada-pw100-series
51. RTX. (2024, July 23) RTX's Pratt & Whitney Canada Celebrates 40 Years of PW100 Engine Family [Press Release], https://www.prattwhitney.com/en/newsroom/news/2024/07/23/rtxs-pratt-whitney-canada-celebrates-40-years-of-pw100-engine-family
52. Pratt & Whitney. (2023, February 23) Pratt & Whitney Canada Celebrates One Billion Flying Hours and 60 Years of PT6 Innovation [Press Release], https://www.prattwhitney.com/en/newsroom/news/2023/02/23/pwc-celebrates-one-billion-flying-hours-and-60-years-of-pt6-innovation
53. Meier, N., (2021), Jet Engine Specification Database, https://jet-engine.net/
54. Pratt & Whitney (2024) Q4 2024 Engine Card [Brochure]. Pratt & Whitney Canada
55. Avions de Transport Regional. (2001, July). ATR: The Optimum Choice for a Friendly Environment. Avions de Transport Regional
56. Avions de Transport Regional. (1998). ATR42-500 Flight Crew Operating Manual. Avions de Transport Regional
57. Forecast International. (2023). The market for aviation turboprop engines. Forecast International.
58. CFM International. (2017, August 8) ALC finalizes $348 million CFM LEAP-1B engine order [Press Release], https://www.cfmaeroengines.com/press-articles/alc-finalizes-348-million-cfm-leap-1b-engine-order/
59. GE Reports. (n.d.). The art of engineering: The world's largest jet engine shows off composite curves. GE. Retrieved from https://www.ge.com/news/reports/the-art-of-engineering-the-worlds-largest-jet-engine-shows-off-composite-curves
60. Sasso, M. (2011, December 14). JetBlue to buy Pratt & Whitney engines. Bloomberg. Retrieved from https://www.bloomberg.com/news/articles/2011-12-14/jetblue-to-buy-pratt-whitney-engines
61. Aircraft Commerce (2006), ATR 42 & 72 maintenance analysis & budget, Issue 49 December 2006/January 2007

62. Standard Aero. (2024). PW 100 SMART Program. Retrieved from https://standardaero.com/engines-3/prattwhitneycanada/pw100/pw100smartprogram/
63. Ackert, S. (2010), Engine Maintenance Concepts for Financiers, Macquarie AirFinance. Dublin, 2010
64. Seemann, R., Langhans, S., Schilling, T., & Gollnick, V. (2011). MODELING THE LIFE CYCLE COST OF JET ENGINE MAINTENANCE.
65. Hanumanthan, H. (2009). Severity estimation and shop visit prediction of civil aircraft engines.
66. Chiles, P. (2011), “When Less is More”, FlightSafety Foundation, Retrieved from https://flightsafety.org/asw-article/when-less-is-more/
67. Aviation Week. (1954, May 17). Compound diesel engine design analyzed. Aviation Week, 60(20), 30–32, 34.
68. Curtiss-Wright Corporation, Wright Aeronautical Division. (1956, October). Facts about the Wright Turbo Compound. Wood Ridge, NJ.
69. Kuhns, C. (n.d.). Turbocompounds. Aircraft Engine Historical Society. Retrieved Novem 18, 2024, from https://www.enginehistory.org/Piston/Wright/Kuhns/CurtissWrightTC18/TurboCompounds.shtml
70. National Air and Space Museum. (n.d.). Wright turbo cyclone 18R-3350 TC-972 (TC18DA2), 2-row radial engine. Smithsonian Institution. Retrieved November 18, 2024, from https://airandspace.si.edu/collection-objects/wright-turbo-cyclone-18r-3350-tc-972tc18da2-2-row-radial-engine/nasm_A19660150000
71. Wiegand, F. J., & Eichberg, W. R. (1954). Development of the Turbo Compound Engine. SAE Transactions, 62, 265–279. http://www.jstor.org/stable/44547322
72. Gunston, Bill (30 April 1954). "Napier Nomad: An engine of outstanding efficiency". Flight: 543–551.
73. Sammons, H., & Chatterton, E. (1955). Napier Nomad Aircraft Diesel Engine. SAE Transactions, 63, 107–131. http://www.jstor.org/stable/44468553
74. Bobula, G.A., Wintucky, W.T., & Castor, J.G. (1986). Compound cycle engine program.
75. Bromers, Alex P., “Lightweight Diesel Engine Designs for Commuter Type Aircraft” National Aeronautics and Space Administration Contractor Report NASA/CR 165470, 1981
76. Air Power Inc. (n.d.). 500 series. Retrieved December 4, 2024, from https://www.airpowerinc.com/500-series?viewmode=grid&orderby=11
77. AVweb. (12 April 2019). 500-horsepower V-12 turbo-diesel engine from Germany. Retrieved December 10, 2024, from https://www.avweb.com/news/500-horsepower-v-12-turbo-diesel-engine-from-germany/
78. E. Ganev, "Selecting the Best Electric Machines for Electrical Power-Generation Systems: High-performance solutions for aerospace More electric architectures," in IEEE Electrification Magazine, vol. 2, no. 4, pp. 13-22, Dec. 2014, doi: 10.1109/MELE.2014.2364731.

79. Sayed, E., Abdalmagid, M., Pietrini, G., Sa'adeh, N., Callegaro, A.D., Goldstein, C., & Emadi, A. (2021). Review of Electric Machines in More-/Hybrid-/Turbo-Electric Aircraft. IEEE Transactions on Transportation Electrification, 7, 2976-3005.
80. Parviainen, A., Niemela, M., Pyrhonen, J.J., & Mantere, J. (2005). Performance comparison between low-speed axial-flux and radial-flux permanent-magnet machines including mechanical constraints. IEEE International Conference on Electric Machines and Drives, 2005., 1695-1702.
81. Perry, D. (2025, February 4). Safran seals certification for EngineUs 100 electric motor. FlightGlobal. https://www.flightglobal.com/aerospace/safran-seals-certification-for-engineus-100-electric-motor/161656.article
82. Warwik, G. (2025, May 6). Hinetics runs first cryogen-free superconducting electric motor. Aviation Week. https://aviationweek.com/aerospace/advanced-air-mobility/hinetics-runs-first-cryogen-free-superconducting-electric-motor
83. T. Sawata and S. Minshull, "Development of 1 MW Hybrid Electric Propulsion Drive System," 2024 IEEE International Conference on Electrical Systems for Aircraft, Railway, Ship Propulsion and Road Vehicles & International Transportation Electrification Conference (ESARS-ITEC), Naples, Italy, 2024, pp. 1-6, doi: 10.1109/ESARS-ITEC60450.2024.10819918.
84. C. L. Pastra, C. Hall, G. Cinar, J. Gladin and D. N. Mavris, "Specific Power and Efficiency Projections of Electric Machines and Circuit Protection Exploration for Aircraft Applications," 2022 IEEE Transportation Electrification Conference & Expo (ITEC), Anaheim, CA, USA, 2022, pp. 766-771, doi: 10.1109/ITEC53557.2022.9813927.
85. European Union Aviation Safety Agency. (n.d.). EASA.E.251: Engineus 100 engine series. Retrieved June 11, 2025, from https://www.easa.europa.eu/en/document-library/type-certificates/engine-cs-e/easae251-engineus100-engine-series
86. e-Mobility Engineering. (n.d.). MagniX magni350/650 and magniDrive 100. e-Mobility Engineering. Retrieved June 13, 2025, from https://www.emobility-engineering.com/magnix-magni350-650-and-magnidrive-100/
87. Author unknown. (2023, February 6). *Preventive vs. on-condition maintenance: Comparing & contrasting aircraft maintenance strategies*. SimpleFlying. https://simpleflying.com/preventive-on-condition-maintenance-comparison/
88. Hall, Christopher & Pastra, Chrysoula Lydia & Burrell, Andrew & Gladin, Jonathan & Mavris, Dimitri. (2022). Projecting Power Converter Specific Power Through 2050 for Aerospace Applications. 760-765. 10.1109/ITEC53557.2022.9813991.
89. Ahmad, M. (2023, April 18). *Silicon carbide's wafer cost conundrum and the way forward*. EDN. https://www.edn.com/silicon-carbides-wafer-cost-conundrum-and-the-way-forward/
90. Buchmann, I., "BU-205: Types of Lithium-Ion." Battery University, 2017, URL: https://batteryuniversity.com/article/bu-205-types-of-lithium-ion

91. Preger, Y., Barkholtz, H. M., Fresquez, A., Campbell, D. L., Juba, B. W., Romàn-Kustas, J., Ferreira, S. R., and Chalamala, B. “Degradation of Commercial Lithium-Ion Cells as a Function of Chemistry and Cycling Conditions.” Journal of The Electrochemical Society, Vol. 167, No. 12, 2020, p. 120532. URL: https://doi.org/10.1149/1945-7111/abae37
92. Edge, J. S., O’Kane, S., Prosser, R., Kirkaldy, N. D., Patel, A. N., Hales, A., Ghosh, A., Ai, W., Chen, J., Yang, J., Li, S., Pang, M.-C., Bravo Diaz, L., Tomaszewska, A., Marzook, M. W., Radhakrishnan, K. N., Wang, H., Patel, Y., Wu, B., and Offer, G. J. “Lithium Ion Battery Degradation: What You Need to Know.” Physical Chemistry Chemical Physics, Vol. 23, No. 14, 2021, pp. 8200–8221.URL: https://doi.org/10.1039/d1cp00359c
93. Burzyński, D., and Kasprzyk, L. “A Novel Method for the Modeling of the State of Health of Lithium-Ion Cells Using Machine Learning for Practical Applications.” Knowledge-Based Systems, Vol. 219, 2021, p. 106900. URL: https://doi.org/10.1016/j.knosys.2021.106900
94. Olmos, J., Gandiaga, I., Saez-de-Ibarra, A., Larrea, X., Nieva, T., and Aizpuru, I. “Modelling the Cycling Degradation of Li-Ion Batteries: Chemistry Influenced Stress Factors.” Journal of Energy Storage, Vol. 40, 2021, p. 102765. URL: https://doi.org/10.1016/j.est.2021.102765
95. Krishna, M. “LFP Batteries: The Electric Vehicle Battery Chemistry Debate Just Got More Complicated.” Fastmarkets, Jul 21, 2022.
96. Silva, E., and Chen, A. “Batteries: Emerging Chemistries Create Trade-Offs in Cost, Performance.” S&P Global Market Intelligence, Jun 08, 2023.
97. Hasselwander, S., Meyer, M., and Österle, I. “Techno-Economic Analysis of Different Battery Cell Chemistries for the Passenger Vehicle Market.” Batteries, Vol. 9, No. 7, 2023, p. 379. URL: https://doi.org/10.3390/batteries9070379
98. Campagnol, N., Erriquez, M., Schwedhelm, D., Wu, J., and Wu, T. “Building Better Batteries: Insights on Chemistry and Design from China.” McKinsey & Company, Apr 22, 2021.
99. Venditti, B. “Visualized: What Is the Cost of Electric Vehicle Batteries?” Elements by Visual Capitalist, Oct 14, 2023.
100. Naor, J. (2024, February 16). Opinion: Will eVTOLs disrupt traditional aircraft values? Aviation Week Network. https://aviationweek.com/business-aviation/aircraft-propulsion/opinion-will-evtols-disrupt-traditional-aircraft-values?
101. Argonne National Laboratory. (n.d.). GREET Battery Model. Retrieved October 26, 2023, from https://greet.anl.gov/greet_battery
102. Avions de Transport Regional (2020). ATR42-500 [Brochure]. DC/E Marketing-Commercial Directorate, https://www.atr-aircraft.com/wp-content/uploads/2020/07/42-500.pdf
103. Roskam, D. (2005). Airplane Design Part I through VIII. Design, Analysis and Research Corporation (DARcorporation).Lawrence, Kansas: DARcorporation.

104. Gunnam, R. (2019). Design of a regional hybrid transport aircraft [Master's thesis, San Jose State University]. https://www.sjsu.edu/ae/docs/project-thesis/Rupa.Gunnam-S19.pdf.
105. Schoenberg, A. (2023, June). Turboprop Market Report. TrueNoord. Retrieved from https://www.truenoord.com/wp-content/uploads/2023/06/Turboprop_report_onscreen.pdf
106. BoltFlight. (n.d.). Turboprops. Retrieved October 15, 2023, from https://boltflight.com/category/aircraft/turboprops/
107. Aircraft Commerce. (2006). ATR 42/72 Maintenance Costs. Retrieved from https://www.aircraft-commerce.com/wp-content/uploads/aircraft-commerce-docs/Aircraft%20guides/ATR%2042%2072/ISSUE49_ATR42%2072MTCE.pdf
108. Al-Shamma, O., & Ali, R. (2014). A Comparative Study of Cost Estimation Models used For Preliminary Aircraft Design. Global Journal of Researches In Engineering: B Automotive Engineering, 14(4). https://globaljournals.org/GJRE_Volume14/2-A-Comparative-Study.pdf
109. JOHANNING, Andreas, SCHOLZ, Dieter, 2013. Propeller Efficiency Calculation in Conceptual Aircraft Design. Hamburg. Available from: https://bit.ly/37GOZjE. Achived at: https://perma.cc/UW2Z-WJNQ
110. MARCKWARDT, Klaus, 1998. Unterlagen zur Vorlesung Flugmechanik I. Hamburg University of Applied Sciences.quoted in Johanning (2013)
111. TRUCKENBRODT, Erich, 1999. Fluidmechanik: Band 2: Elementare Strömungsvorgänge dichteveränderlicher Fluide sowie Potential- und Grenzschichtströmungen. 4th Edition, Berlin, Heidelberg: Springer.Available from: https://doi.org/10.1007/978-3-540-79024-2 (closed)Xxx
112. Krull, Marlis. 2024. “Preliminary Sizing of Propeller Aircraft (Part 25).” Digital Library - Projects and Theses - Prof. Dr. Scholz. Harvard Dataverse. https://doi.org/doi:10.7910/DVN/ET4ZKV.
113. National Aeronautics, and Space Administration, “Electrified Aircraft Propulsion (EAP),” https://www1.grc.nasa.gov/aeronautics/eap/, 2024.
114. National Aeronautics, and Space Administration, “About Electrified Powertrain Flight Demonstration Project,” https://www.nasa.gov/directorates/armd/integrated-aviation-systems-program/armd-iasp-epfd/about-electrified-powertrain flight-demonstration-project/, 2022.
115. Recine, C., Kirk, J., Jasa, J., Gratz, J., (2024). *Oshkosh Aviary Presentation* (Report No. 20240009217). National Aeronautics and Space Administration. https://ntrs.nasa.gov/api/citations/20240009217/downloads/Oshkosh_Aviary_Presentation.pdf.
116. Michael Iwanizki, Max Arzberger, Martin Plohr, Daniel Silberhorn and Tobias Hecken. "Conceptual Design Studies of Short Range Aircraft Configurations with Hybrid Electric Propulsion," AIAA 2019-3680. AIAA Aviation 2019 Forum. June 2019.

117. Zill, T., Iwanizki, M., Schmollgruber, P., Defoort, S., Döll, C., Hoogreef, M., Vries, R.D., Vankan, J.M., & Lammen, W.F. (2020). An Overview of the Conceptual Design Studies of Hybrid Electric Propulsion Air Vehicles in the Frame of Clean Sky 2 Large Passenger Aircraft.
118. Joksimoviă, Aleksandra and Carbonneau, Xavier and Crabé, Charline and Benichou, Emmanuel Generalised Methodology for Sizing of Air Vehicles with Hybrid-Electric Propulsion. (2019) In: NATO AVT-RSY-323 Research Symposium on Hybrid/Electric Aero-Propulsion Systems for Military Applications, 7 October 2019 - 9 October 2019 (Trondheim, Norway)
119. Vincenzo Palladino, Nathalie Bartoli, Sylvain Dubreuil, Emmanuel Bénard, Valérie Pommier-Budinger, et al. A comparative study of different propulsion models for hybrid electric aircraft. 3AF Aerospace Europe Conference 2020, Feb 2020, Bordeaux, France. ⟨hal-02904367⟩
120. Peter Schmollgruber, David Donjat, Michael Ridel, Italo Cafarelli, Olivier Atinault, et al. Multi disciplinary Design and performance of the ONERA Hybrid Electric Distributed Propulsion concept (DRAGON). AIAA Scitech 2020 Forum, Jan 2020, Orlando, United States. ff10.2514/6.2020-0501ff. ffhal-03125217
121. Mokotoff, P. R., Arnson, M., & Cinar, G. (2025). “FAST: A Future Aircraft Sizing Tool for Advanced Aircraft and Propulsion System Design”, in press, *AIAA Scitech Forum*, 2025.
122. Cinar, G., “A methodology for dynamic sizing of electric power generation and distribution architectures,” Ph.D. thesis, Georgia Institute of Technology, 2018.
123. Cinar, G., Cai, Y., Chakraborty, I., and Mavris, D. N., “Sizing and optimization of novel general aviation vehicles and propulsion system architectures,” 2018 Aviation Technology, Integration, and Operations Conference, 2018, p. 3974. https://doi.org/https://doi.org/10.2514/6.2018-3974. 40
124. Cinar, G., Cai, Y., Bendarkar, M. V., Burrell, A. I., Denney, R. K., and Mavris, D. N., “System analysis and design space exploration of regional aircraft with electrified powertrains,” Journal of Aircraft, Vol. 60, No. 2, 2023, pp. 382–409. https://doi.org/https://doi.org/10.2514/1.C036919
125. Lukaczyk, T. W., Wendorff, A. D., Colonno, M., Economon, T. D., Alonso, J. J., Orra, T. H., and Ilario, C., “SUAVE: an open-source environment for multi-fidelity conceptual vehicle design,” 16th AIAA/ISSMO Multidisciplinary Analysis and Optimization Conference, 2015, p. 3087. https://doi.org/https://doi.org/10.2514/6.2015-3087
126. Kruger, M., “The Challenges and Potential Benefits of Electrified Propulsion for Aircraft,” Ph.D. thesis, University of Southern California, 2022.
127. RCAIDE. (n.d.). *RCAIDE — Research Community Aircraft Interdisciplinary Design Environment*. https://www.rcaide.leadsresearchgroup.com/
128. Lissys. (n.d.). *Lissys: Aircraft design software*. Lissys. https://lissys.uk/
129. Morejón Ramírez, L., Decroix, J., Justin, C. Y., Payan, A., and Mavris, D., “Design and Operation Considerations for the Integration of Fleets of Regional Air Mobility

Aircraft at Large Hubs," AIAA AVIATION 2021 FORUM, American Institute of Aeronautics and Astronautics, 2021. https://doi.org/10.2514/6.2021-3178.
130. FlightAware. (n.d.). Aircraft type AT43. FlightAware. Retrieved April 23, 2025, from https://www.flightaware.com/live/aircrafttype/AT43
131. SCHOLZ, Dieter, 2015. Aircraft Design. Lecture Notes. Hamburg University of Applied Sciences. Available from: http://LectureNotes.AircraftDesign.org.
132. ATA, "Standard method of estimating comparative direct operating costs of turbine powered transport airplanes", ATA, December 1967.
133. AEA, "Short-Medium range aircraft – AEA requirements", December 1989.
134. AEA, "Long range aircraft – AEA requirements", December 1989.
135. American Airlines, "A New Method for Estimating Current and Future Transport Aircraft Operating Economics," NASA CR-145190(rev), March 1978. (N78-20094)
136. Raymer, D. P. Aircraft Design: A Conceptual Approach. American Institute of Aeronautics and Astronautics Incorporated, 2018.
137. Torenbeek, E., Synthesis of Subsonic Airplane Design, Delft University Press, Delft, the Netherlands, 1982, Chap. 5.
138. Hepperle, M., "Electric Flight—Potential and Limitations," NATO Rept. STO-MP-AVT-209, 2012.
139. Traub, L. W., "Range and Endurance Estimates for Battery-Powered Aircraft," Journal of Aircraft, Vol. 48, No. 2, 2011, pp. 703–707.https://doi.org/10.2514/1.C031027
140. Avanzini, G., and Giulietti, F., "Maximum Range for Battery-Powered Aircraft," Journal of Aircraft, Vol. 50, No. 1, 2013, pp. 304–307. https://doi.org/10.2514/1.C031748
141. Patterson, M. D., German, B. J., and Moore, M. D., "Performance Analysis and Design of On-Demand Electric Aircraft Concepts," 12th AIAA Aviation Technology, Integration, and Operations Conference, AIAA Paper 2012-5474, Sept. 2012. https://doi.org/10.2514/6.2012-5474
142. Kuhn, H., Falter, C., and Sizmann, A., "Renewable Energy Perspectives for Aviation," Proceedings of the 3rd CEAS Air & Space Conference and 21st AIDAA Congress, Council of European Aerospace Societies, Brussels, Belgium, 2011, pp. 24–28.
143. Brelje, B. J., and Martins, J. R. R. A., "Electric, Hybrid, and Turboelectric Fixed-Wing Aircraft: A Review of Concepts, Models, and Design Approaches," Progress in Aerospace Sciences, Vol. 104, Jan. 2019, pp. 1–19.
144. Isikveren, A. T., Kaiser, S., Pornet, C., and Vratny, P. C., "Pre-Design Strategies and Sizing Techniques for Dual-Energy Aircraft," Aircraft Engineering and Aerospace Technology: An International Journal, Vol. 86, No. 6, 2014, pp. 525–542.
145. de Vries, R., Brown, M., and Vos, R., "Preliminary Sizing Method for Hybrid-Electric Distributed-Propulsion Aircraft," Journal of Aircraft, Vol. 56, No. 6, 2019, pp. 2172–2188.

146. de Vries, R., Hoogreef, M. F. M., & Vos, R. (2020). Range equation for hybrid-electric aircraft with constant power split. Journal of Aircraft, 57(3), 552-557. https://doi.org/10.2514/1.C035734
147. Batra, A., Raute, R., & Camilleri, R. (2023). On the Range Equation for Hybrid-Electric Aircraft. Aerospace, 10(8), 687. https://doi.org/10.3390/aerospace10080687
148. Aviation Week Network. (2025). 2025 Market Summary Report. Aviation Week.
149. Airlines for America. (n.d.). SAF vs. Jet Fuel Comparison. Retrieved February 12, 2025, from https://www.airlines.org/dataset/saf-vs-jet-fuel-comparison/#jet-fuel-prices
150. Electricity Prices." GlobalPetrolPrices.com, 2024, URL: https://www.globalpetrolprices.com/electricity_prices/
151. Statistica Research Department, "Household Electricity Prices Worldwide in December 2023, by Select Country." Statista, July 10, 2024, URL: https://www.statista.com/statistics/263492/electricity-prices-in-selected-countries/
152. Airline Pilot Central. (n.d.). Silver Airways. Retrieved June 10, 2025, from https://www.airlinepilotcentral.com/airlines/regional/silver_airways
153. Elgowainy, A., Han, J., Wang, M., Carter, N., Stratton, R., Hileman, J., Malwitz, A., & Balasubramanian, S. N. (2012). Life-Cycle Analysis of Alternative Aviation Fuels in GREET (Report No. ANL/ESD/12-8). Argonne National Laboratory. https://rosap.ntl.bts.gov/view/dot/35807
154. Speth, R. L., Rosen, C. V., Azadi, P., & Malina, R. (2016, September 14-15). LCA of Current & Future GHG Emissions from Petroleum Jet Fuel. DOE BETO Alternative Aviation Fuel Workshop. https://www.energy.gov/sites/prod/files/2016/09/f33/speth_alternative_aviation_fuel_workshop.pdf
155. Jing, L., El-Houjeiri, H., Monfort, J.-C., Littlefield, J., Al-Qahtani, A., Dixit, Y., Speth, R., Brandt, A., Masnadi, M. S., Maclean, H., Peltier, W., Gordon, D., & Bergerson, J. (2022). Understanding variability in petroleum jet fuel life cycle greenhouse gas emissions to inform aviation decarbonization. Nature Communications, 13, 7853. https://doi.org/10.1038/s41467-022-35392-1
156. Tiseo, I., "Power Generation CO2 Intensity Outlook by Region 2050." Statista, June 20, 2023, URL: https://www.statista.com/statistics/1257765/global-emission-intensity-electricity-generation-region/
157. Ember and Energy Institute, "Carbon Intensity of Electricity Generation." Our World in Data, 2024, URL: https://ourworldindata.org/grapher/carbon-intensity-electricity?tab=table
158. Aircraft Commerce. (2006). *ATR 42/72 fuel burn performance* (Issue 49). https://www.aircraft-commerce.com/wp-content/uploads/aircraft-commerce-docs1/Aircraft%20guides/ATR%2042%2072/ISSUE49_ATR42%2072FUEL.pdf
159. ATR. (2007). ATR 42-500 [Brochure]. Retrieved from https://www.aerocontact.com/public/img/aviaexpo/produits/catalogues/76/depliant_atr_42_500_2007_31.pdf

160. Bureau of Transportation Statistics. (2024-2025). Air carrier operating expense data (Form 41, Schedule P-5.2) [Data set]. U.S. Department of Transportation. https://www.transtats.bts.gov
161. Aircraft Commerce. (2009, April–May). *Dash 8 & Q Series fuel burn performance* (Aircraft Operator's & Owner's Guide, Issue No. 63). Aircraft Commerce. Retrieved from https://www.aircraft-commerce.com/wp-content/uploads/aircraft-commerce-docs/Aircraft%20guides/DASH%208%20%26%20Q%20SERIES/ISSUE63_DASH8FUEL.pdf
162. Norris, G., *Tecnam Pulls Plug On Electric P-Volt Project*, Aviation Week Network, New York, June 2023.
163. Filippone, A., and Parkes, B., "Evaluation of Commuter Airplane Emissions: A European Case Study., Transportation Research Part D," *Transport and Environment*, Vol. 98, 2021, Paper 102979. https://doi.org/10.1016/j.trd.2021.102979
164. Cessna Caravan, "Cessna Caravan, 2024, https://cessna.txtav.com/en/turboprop/caravan [retrieved 14 May 2024].
165. PC-12 NGX, "Pilatus Aircraft Ltd.," 2024, https://www.pilatusaircraft.com/en/fly/pc-12 [retrieved 14 May 2024].
166. 14 CFR Part 91, *General Operating and Flight Rules, Code of Federal Regulations*, 2024, https://www.ecfr.gov/current/title-14/chapter-I/ subchapter-F/part-91 [retrieved 15 May 2024].

Parallel Hybrid Propulsion System for a Regional Turboprop: Conceptual Design and Benefits Analysis

Authors:

Todd Spierling[1] and Charles Lents[2]
United Technologies Corporation, Farmington, CT, 06108

A conventional, high-wing, regional aircraft in the 30-50 passenger class with a parallel hybrid electric turboprop propulsion (PHET) system has been studied. The PHET system is comprised of 2 under-wing engines assisted by 750 kW motors, each integrated by a combining gearbox (CGB) driving the PHET propeller. The electric drive train (EDT) further consists of 2 motor drives, a 1000 V electric distribution system, a 500 kW-hr battery pack capable of 1500 kW discharge (c-rate of 3) and a thermal management system (TMS) capable of maintaining component temperatures at levels required for high life. The flat rated PHET system core engines, sized for cruise power are significantly undersized for take-off and climb; thus the make-up power comes from the CBG mounted motors fed by a ground-charged battery pack. The EDT and TMS weight and performance analysis as well as the overall propulsion system performance analysis is described. One mission concept of operations (CoO) is analyzed with the resultant fuel and energy consumption quantified and compared to a conventional propulsion system-based aircraft. The 250 nm mission CoO carries only the battery pack mass required for boosted take-off and climb, with all energy for cruise supplied by on board fuel. A fuel burn reduction of 30% and energy reduction of 25% are predicted for this CoO.

Nomenclature

Alt – Altitude,
CBG – Combining Gearbox
CoO – Concept of Operations
EDT – Electric Drive Train
ETAC – Core thermal efficiency
L/D – Lift over Drag ratio
Mach – Mach number
MTO – Maximum Takeoff
PSFC – Power Specific Fuel Consumption
PHET – Parallel Hybrid Electric Turboprop
PM – Permanent Magnet
RGB – Reduction Gearbox
TMS – Thermal Management System

I. Introduction

Hybrid electric aircraft have been widely studied, with the promise of significant reduction in fuel burn, energy consumption and CO_2 emissions compared to a conventional aircraft. The series turbo-electric architecture (Figure 1) in which a prime mover drives a generator to create electric power distributed to electrically driven propulsors has been shown to provide little to no fuel burn benefit due to the electric drive train (EDT) weight and losses [1-2]. Even with the potential for improved propulsive efficiency and aircraft L/D with distributed propulsion and propulsion airframe integration, there have been few concepts proposed that could provide an overall aircraft level benefit. Jansen [3-4] provides a parametric study showing the EDT power density and efficiency necessary for a single-aisle aircraft turbo-electric [3] or partial turbo-electric [4] (gas turbine provides direct propulsion and electric power) based distributed propulsion system to provide an overall aircraft energy consumption reduction. This work shows that very high power density and efficiency will be required compare to an under-wing gas turbine if there is no efficiency improvement in the EDT prime mover.

[1] United Technologies Advanced Projects, Director, Systems Integration
[2] United Technologies Research Center, Associate Director, Thermal Management

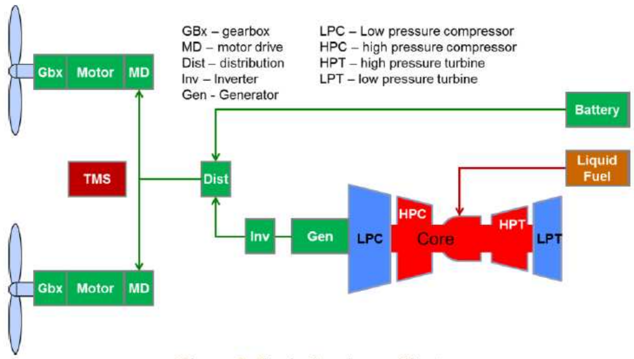

Figure 1: Typical series architecture

In contrast, several studies have shown the potential benefits of a parallel hybrid propulsion system [4-8], in which the propulsor is powered by a gas turbine core and by an electric motor (Figure 2). These studies have focused on single aisle class aircraft. Motivated by these benefits, the current research has investigated the parallel hybrid architecture for a turboprop 30-50 passenger class aircraft. As shown in Figure 2, the parallel hybrid turboprop propulsion (PHET) system is comprised of a combustion engine and an electric motor integrated on a combining gearbox (CGB) that drives the propeller. A reduction stage may be integrated into the CBG or could be incorporated into a separate reduction gearbox (RGB). Fuel and a fuel system feed the combustion engine, while an electric drive train (EDT) comprised of a battery pack, distribution system and motor drive feed the motor.

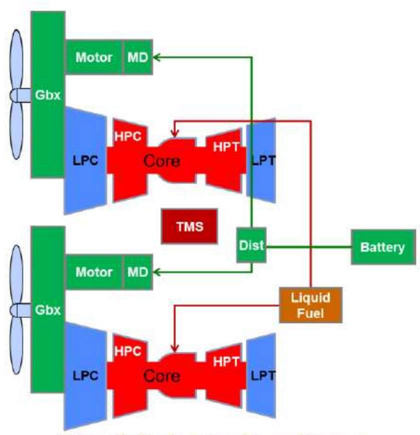

Figure 2: Typical parallel architecture

II. Study Baseline Vehicle and Engine

The study vehicle is a Bombardier Dash 8-100 turboprop powered by the standard installed PW121 gas turbine engines. Aircraft parameters are supplied in Table 1. Figure 3 provides a picture.

Table 1: Dash-8 Parameters

	Dash 8
Passengers/Class	37-39
Max Takeoff Gross Weight (lbm)	36,300
Operating Empty Weight (lbm)	24,000
Fuel Capacity (lbm)	5680
Wing Area (ft^2)	585
Aspect Ratio	12.4
Cruise L/D @ Long Range Cruise	15
Design Mission Range (nm)	1000
DOC Mission Range (nm)	250
Long Range Cruise Mach number	0.4

Figure 3

The PW121 represents a modern gas turbine engine with world class performance, thus providing a good baseline for comparison to the PHET system. The baseline propulsion system weight is 960 lbm per engine, or 1920 lbm per aircraft. Table 2 provides the normalized performance parameters.

The PHEP system based vehicle has limited range due to system fixed weight (see section V), and is limited to fly a 250 nm mission. Still, over half the missions flown by this vehicle class are < 250 nm. Thus mission fuel burn for the baseline and PHEP based vehicles has been evaluated for a "standard mission" range of 250 nm. The 250 nm mission baseline vehicle and PW121 engine is provided in Table 2.

Table 2: Baseline Vehicle 250 nm Mission Fuel Consumption

	Duration (min)	Power per Engine (hp)	PSFC (lbm/hr) /hp	Fuel Burn (lbm)	Energy (kW-hr)
Taxi-Out	2	100	1.84	12	66
Takeoff	1	1950	0.53	35	186
Climb to Cruise	20	1362.5	0.46	418	2253
Cruise	33	960	0.46	486	2619
Descent	22	100	1.84	135	728
Approach & Land	2	630	0.53	22	120
Taxi-In	2	100	1.84	12	66
Total mission	82			1120	6039

Note: PSFC is based on an assumed gas turbine thermal efficiency of 30% at cruise, with a 15% PSFC increase at max power takeoff (past the typical gas turbine peak efficiency hook) and a 400% increase at idle conditions (Taxi and Descent)

III. Propulsion System Sizing and Performance Analysis

Notice that normal cruise power is ~1000 hp. A flat rated combustion core ideally sized for this application is then ~1000 hp. Such an engine, sized for cruise, will operate at peak efficiency during cruise. In order to provide make-up power for takeoff and climb, two 950 hp permanent magnet (PM) electric motors are required. Electric power to drive the motors is supplied by an EDT comprised of two motor drives(1 for each motor), feeders, and a battery pack which is charged on the ground. At the on-wing propulsors, a CGB sums power from the motor and engine core to drive the propeller.

The system is operated as follows. At takeoff, 1950 hp is required (per propulsor). The flat-rated engine can only produce 1000 hp at any mission phase, thus the motor provides the remaining power (e.g. 950 hp at take-off). At cruise, the combustion engine is running at peak power (1000 hp) and at its highest efficiency, providing all the required power (no motor power). The power profile for both the core engine and motor are provided in Figure 5. Given the mission segment durations, power delivered to the propeller by the motor, the EDT efficiencies, and reserve energy requirement, the battery energy is determined at 500 kWhr per aircraft.

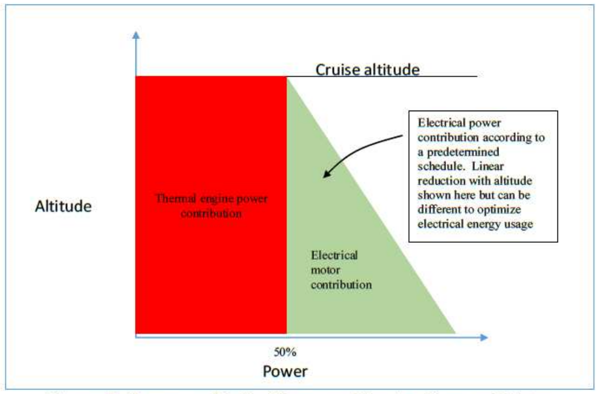

Figure 5: Power profile for Thermmal Engine Core and Motor

If sized for the 1950 hp max takeoff (MTO) power, the core engine would have max power capability of 1950 hp at cruise, on account of the flat power rating, while only 1000 hp is required. Operating at only ~50% peak power, the engine cruise efficiency would drop significantly compared to peak efficiency at MTO. In addition, the core weight would be double of what is needed at cruise. Sized at cruise power (1000 hp), the core engine weight is cut in half. Most importantly, when operated at peak power throughout takeoff, climb and cruise as part of the PHET system, the core will operate at peak efficiency over most of the mission. A typical gas turbine for such an application will operate at ~ 30% thermal efficiency, while this flat rated core is projected to operate at ~ 40% thermal efficiency.

Figure 6 provides the rational for the PHET system. Fig 6c shows the mission profile.Fig 6b shows the power profile. The electric motor and core engine each cover half of the power at take-off whereas the core engine supplies all power at cruise. Motor power declines linearly between takeoff and cruise. Finally Fig 6a shows the notional fuel burn of the PHET system compared to a conventional turboprop aircraft. Fuel flow is lower at the cruise condition due to the high efficiency PHET core. The fuel flow rate is significantly lower at takeoff and climb, where the motor is providing make-up power. This fuel flow reduction is realized only because the additional fuel flow required to carry EDT weight does not overcome the efficiency benefit.

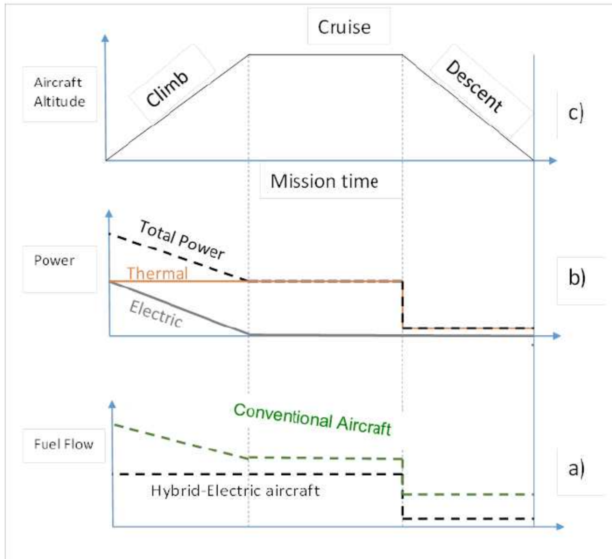

Figure 6: Typical mission illustration

The electrical component weight and performance parameters representing 5-10 year goals for the EDT components are provided in Table 3. The University of Illinois reports a power to weight ratio and a peak efficiency of 13 kW/kg and 0.97, respectively, for a motor being developed under NASA funding [9]. The motor drive parameters are reflective of ongoing work at Collins Aerospace and at NASA Glenn. The battery energy density of 355 Whr/kg is derived from a 500 Whr/kg cell level energy densitywith 15% pack burden and max discharge of 90%. Motor drive and battery discharge efficiency are assumed fixed over their operating power range, while a typical motor efficiency vs part load characteristic is used for motor efficiency.

Table 3: PHET Electric Component Parameters

	Power to Weight (kW/kg)	Performance	Notes
Motor	13	Eff = 0.97 at full power, 0.8 at low power, and 0.89 average during climb	NASA supported motor development, at part power motor efficiency drops below peak efficiency
Motor Drive	20	0.98 eff	NASA supported inverter dev
Feeders	100	0.99 eff	Estimate
Battery	355 Whr/kg packaged	500 Whr/kg cell, 0.95 eff, 90% max discharge, 15% pack burden	Parameter targets laid out by Battery 500 consortium
TMS	2	NA	0.5 kg for every 1 kW of EDT heat rejection (2 kW/kg)

For this preliminary analysis, a fixed aircraft TOGW is assumed. Thus the propulsion system power requirements are identical for the conventional and PHET systems. The loss in aircraft range is discussed in Section V.

IV. System Weights

PHET system weight is derived for the power to weight values reported above. Table 4 provides a weight comparison to the conventional propulsion system.

Table 4: Weight Roll Up

Item	Dash -8 Baseline Weight, lbm	PHET Weight, lbm	Note
Operational Weight Empty (OWE)	24000	24000	
Power plant increase		55	Target, must be below this to make range
Gearbox		100	Weight increase due to CGB
Motor		253	eMotor 2x750kW @ 13 kW/kg
Motor Drive		165	eMotor drive, @ 20 kW/kg
Feeders		33	Feeders, @ 100kW/kg
Battery Pack		3099	500 kWh @ 355 Whr/kg
TMS		165	Estimate based on 2kW heat/kg
Passenger load (36 pax @ 200lb)	7200	7200	Passenger load
Fuel for 250 nm mission + Reserves	1680	1230	
Mission Takeoff Weight	32880	36300	
MTOW	36300	36300	

V. Benefits

Based on the above assumptions, Table 5 summarizes the PHET fuel burn and energy consumption. The system motor efficiency varies as a function of load (as described in Table 3) resulting in an average efficiency of 89% during boosted climb. This value is used in the calculation of climb energy. The improved thermal engine has an assumed efficiency of 40%. The cruise PSFC is derived from this value, with the takeoff and idle PSFC increased in the same manner as the gas turbine engine baseline.

Table 5: PHET 250 nm mission Vehicle Fuel and Energy Consumption

	Duration (min)	Power per Propulsor (hp)	Thermal Engine Power (hp)	Motor Power (kW)	PSFC (lbm/hr)/hp	Fuel Burn (lbm)	Plug Energy (kW-hr)	Total Energy (kW-hr)
Taxi-Out	2	100	0	75			7	7
Takeoff	1	1950	1060	664	0.40	14	26	103
Climb to Cruise	26	1362.5	1060	226	0.35	322	252	1986
Cruise	28	960	960	0	0.35	314	0	1691
Descent	24	100	100	0	1.40	112	0	604
Approach & Land	2	630	630	0	0.40	17	0	92
Taxi-In	2	100	0	75			7	7
Total mission	85					778	293	4490

The reduction in on wing Jet-A fuel burn is 341 lbm (30%) However the plug energy for charging the PHET system batteries should also be considered. The baseline vehicle energy consumption is 6039 kWhr of Jet-A (1120 lbm). The PHET vehicle energy consumption is 4197 kWhr of Jet-A (778 lbm) and 293 kWhr of plug energy (assuming a charging loss of 5%), for a total of 4490 kWhr, a 26% reduction in energy consumption. A cost comparison is provided in Table 6.

Table 6: Energy Cost Comparison

	Conventional	PHET	Savings	Comment
Mission fuel burn, lbm	1120	778	341 lbm	
Electricity, kWh	0	293		
Fuel cost, $	432	300		5 year average 2.79 $/gal, $0.0716 $/kWhr
Electricity cost, $	0	33		Airport weight average, $0.1114 $/kWhr
Total costs, $	432	333	99$	

VI. Conclusion

Many previous studies of potential hybrid electric propulsion systems have failed to show a fuel burn or energy consumption savings compared to a conventional propulsion systems. This paper demonstrates that a significant fuel burn and energy savings can be realized on a short range propeller aircraft with a parallel hybrid propulsion system. Using only the core engine at cruise and using the parallel motor supplied by a battery stored electric energy for boosted takeoff and climb yields an on-wing fuel burn reduction of 30% and a total energy consumption reduction of 25% compared to a conventional turboprop engine. However, even with a 355 Whr/kg battery pack energy density (estimated to be 10 years out), such a system would reduce the vehicle max range from ~ 1000 nm to 250 nm. The majority of flights executed by the study aircraft are 250 nm and less so there would still be wide application for such a vehicle.

Acknowledgements

The authors wish to acknowledge the contribution of Pierre Bertrand, Pratt and Whitney Canada, Staff Engineer, Aero/Thermodynamics who executed the early aircraft performance analysis.

References

[1]Maurice F. M. Hoogreef, Roelof Vos, Reynard de Vries and Leo L. M. Veldhuis, "Conceptual Assessment of Hybrid Electric Aircraft with Distributed Propulsion and Boosted Turbofans," AIAA Science and Technology Conference, San Diego, 2019, 10.2514/6.2019-1807.

[2]Schiltgen, B. and Freeman, J., "ECO-150-300 Design and Performance: A Tube-and-Wing Distributed Electric Propulsion Aircraft," AIAA Sci Tech Forum, San Diego CA, 2019

3 Jansen, R. H., Duffy, K. P., Felder, J. L., Brown, G. V, "Turboelectric Aircraft Drive Key Performance Parameters and Functional Requirements," AIAA Propulsion and Energy Forum, AIAA 2015-3890, Orlando FL, 2015.

[4]Jansen, R. H., Duffy, K. P., Brown, G. V., "Partially Turboelectric Aircraft Drive Key Performance Parameters," AIAA Propulsion and Energy Conference, Atlanta, 2017, AIAA-2017-4702.

[5]Bradley, M. K., and Droney, C. K., "Subsonic Ultra Green Aircraft Research Phase I Final Report," National Aeronautics and Space Administration Contractor Report NASA/CR–2011-216847, 2011.

[6]Bradley, M. K., and Droney, C. K., "Subsonic Ultra Green Aircraft Research Phase II: N+4 Advanced Concept Development," National Aeronautics and Space Administration Contractor Report NASA/CR-2012-217556, 2012.

[7]Lents, C. E., Hardin, L.W., Rheaume, J.M, and Kohlman, L., "Parallel Hybrid Gas-Electric Geared Turbofan Engine Conceptual Design and Benefits Analysis," AIAA Propulsion and Energy Conference, Salt Lake City, 2016, p. 4610

[8]Gladin, J. C., et. al., "Fundamentals of Parallel Hybrid Turbofan Mission Analysis with Application to the Electrically Variable Engine," AIAA/IEEE Electric Aircraft Technology Symposium, Cincinnati, 2018, 10.2514/6.2018-5024.

Chapter 11 - Appendix B – Full Journal of Aircraft Paper

Battery Optimization for Sustainable Aviation: A Comprehensive Analysis for Battery Electric Aircraft

Todd A. Spierling,* Alexander Lynch,† and Thomas H. Bradley‡
Colorado State University, Fort Collins, Colorado 80523

https://doi.org/10.2514/1.C038197

The aviation industry is entering a transformative era with the introduction of electrified aircraft, driven by the imperative to reduce reliance on legacy fossil fuels and to mitigate the industry's environmental impact. Battery systems are an enabling technology of this revolution, and an appropriate balance between performance, efficiency, and cost becomes critically important to the viability and acceptance of this new propulsion paradigm. This paper provides a comprehensive set of considerations for battery system optimization for the application of electric aircraft. We leverage the relationship between depth of discharge, *C*-rate, and cycle life of multiple battery chemistries to enable the design of efficient and cost-effective energy storage systems. The paper will analyze the operational, economic, and environmental implications of battery use, considering factors such as mission lengths, operating conditions, and battery life cycle and energy production costs and emissions. The results and discussion contribute to a framework for battery electric aircraft design for a variety of mission requirements.

I. Introduction

AVIATION has long been an area where worldwide forces and technology innovations have come together to drive fundamental changes within the industry. Many have argued that we are now in the "Third Era of Aviation"—the first being the original piston engine aircraft, the second being gas turbine-powered aircraft, and the third being the introduction of electrification to aircraft propulsion [1].

There are several trends that are driving the innovation of this new era. The trends of population growth/urbanization and increased focus on sustainability and environmental issues have resulted in new and increasing demands on the aviation sector. Continuing commercial pressures on airlines cause challenges to airline profitability and motivation to provide affordable air service in many areas, particularly in the absence of government incentives and/or mandates.

The first major trend is the growth in world population, which, along with increasing affluence, results in the continuing growth of travel demand and aviation. World population has doubled in the last 50 years, with most of this growth (at least in absolute terms) occurring in Asia. Much of this growth has occurred in urban areas. The annual population growth rate has averaged 1 and 2% for much of the late 20th and early 21st centuries [2]. The growth rate of air travel, however, has exceeded that of the population at large. As illustrated in Fig. 1, air travel has grown at an annual rate of 4 and 5% over the last 25 years, and it is expected to continue at 3.7% for the next 25 years. [3].

This increased air traffic, however, comes at an environmental price, which is related to the second trend of environmental sustainability. While carbon emissions due to aviation have held steady at approximately 2.5% of overall carbon emissions worldwide, the absolute level of aviation carbon emissions has steadily increased and now stands at approximately 1 billion tons $CO_{2\text{-eq}}$/year [4]. If aviation carbon emissions continue to increase at their current rates, and expected carbon reduction measures occur in other sectors, aviation could account for up to 22% of the worldwide carbon emissions by 2050 [5]. This carbon footprint has become more of a social issue in recent years, and "flight shaming" threatens to impact future airline growth, most pointedly in European and North American markets [6]. In response, aviation industry stakeholders have committed to achieving net zero carbon emissions by 2050.

The last trend driving change is the commercial pressure on airlines, impacting the routes that they can profitably serve. Currently, 0.6% of U.S. airports support over 70% of domestic air travel [7], resulting in large numbers of locations that are not being served to their full potential. As illustrated in Fig. 2, the airline industry is intensely competitive, with very small (sometimes negative) differences between revenue and cost [8]. As seen in this graph, profit margins are historically approximately 3–5%, illustrating the extreme competitiveness of the commercial airline industry and the poor returns of airlines relative to other industries.

In combination, these trends illustrate that to meet demand, the global aviation sector will need to become bigger (in terms of higher seat-km per year), cleaner (in terms of absolute greenhouse gases despite rising seat-km), and more economically efficient (in terms of $ per seat-km). This is a substantial, complex technological/economic problem that needs to be addressed through the application of advanced systems engineering approaches.

Electrification of aviation is asserted to be a key component of realizing these contradictory and challenging characteristics of a future aviation system. Electric aircraft have the potential to eliminate direct and indirect CO_2 impacts if paired with renewable power generation and can provide efficiency improvements over conventional aircraft [9]. Although in its nascent stages, all-electric urban air mobility (UAM) aircraft have shown to be more efficient than internal combustion aircraft for ranges from 50 to 300 miles [10], paving the way for the implementation of electric aircraft in the regional sector [9]. With improvements to battery technology, specifically specific energy, this will expand to the electrification of regional jets.

Unfortunately, the technical feasibility of the electrification of aviation does not necessarily equate with economic viability/attractiveness. A recent example of this was the recent deferral of the *P-Volt* project between Tecnam, Rolls Royce, and Wideroe. This program was initiated in 2021, based on a fully battery-electric version of the Tecnam P2012 aircraft as shown in Fig. 3. By 2023, however, further technical and economic analyses highlighted emerging issues with this approach. Rolls Royce acknowledged that "while the initial range is sufficient for key applications, energy storage lifecycle performance results in business cases that do not lend themselves to broad market adoption" [11].

This case study and the broad state of the field highlight the need for a more holistic look at the analysis of battery electric propulsion systems, considering a wider range of measures to evaluate and optimize the configuration and usage of these propulsion systems.

Presented as Paper 2024-3622 at the AIAA AVIATION Forum and Exposition, Las Vegas, NV, July 28–Aug. 2, 2024; received 5 September 2024; accepted for publication 15 April 2025; published online 9 May 2025.

*Student, Systems Engineering; gte466x@colostate.edu (Corresponding Author).

†Student, Systems Engineering.

‡Department Head, Systems Engineering.

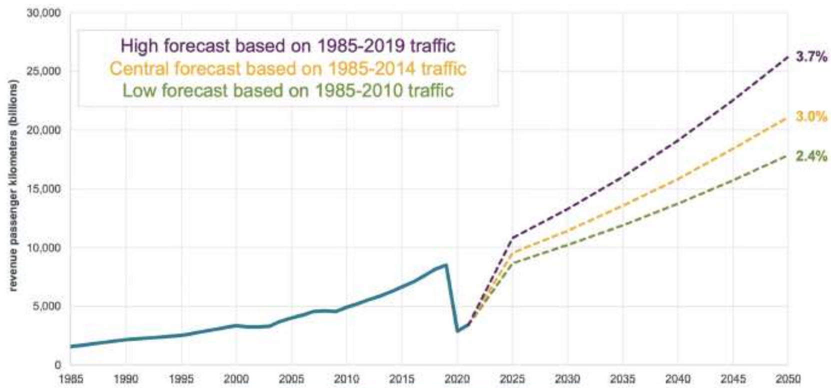

Fig. 1 Historical and projected future air traffic levels.

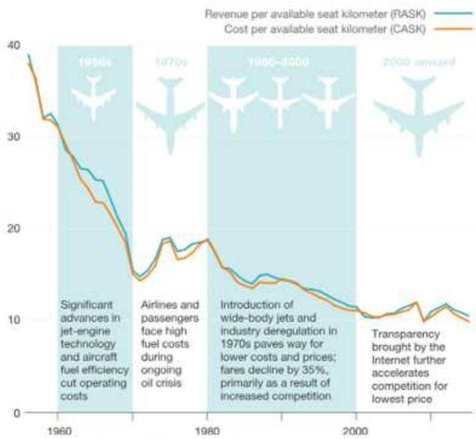

Fig. 2 Historical airline costs and revenue.

II. Battery Technology/Chemistry Overview

The key technology element that has enabled battery electric aircraft is advanced lithium-ion battery technologies. Most notably, improvements in energy density and cost have presented a competitive case for battery technology relative to less efficient internal combustion engine technology [9]. This section provides a comprehensive survey of existing battery chemistries, focusing on their energy density, cycle life, costs, and lifecycle carbon footprint.

This study focuses mainly on battery chemistries that are currently in commercial production and ready to be deployed on aircraft: namely $LiFePO_4$ (LFP), $LiNCo_yAlO_2$ (NCA), $LiNiMnCoO_2$ (NMC), and their variations. Each of these battery chemistries exhibits performance and cost tradeoffs. LFP batteries maintain performance over many cycles, exhibit low cost, and have relatively low environmental impacts, yet have a low specific energy, which is not conducive to aircraft applications. NCA and NMC batteries exhibit higher specific energies yet have drawbacks in the form of life spans, environmental impact, and pack cost [12].

Battery lifetimes have a significant impact on the viability of electric aircraft, as battery replacement comes with a high cost. The lifetime of a battery, also defined as the number of full equivalent cycles the battery can go through before it loses significant capacity, is affected by multiple operational variables, including but not limited to depth of discharge, charging rate, and discharge rate [13]. Figure 4 illustrates the cycle life behavior of the various lithium-ion battery chemistries considered in this analysis.

Various electrochemical and physical mechanisms are the cause of reduced battery capacity as a function of its cycle life and calendar life. For example, as the batteries are cycled during flights, the electrolyte and electrode react with one another to form a solid electrolyte interface (SEI) layer that reduces the concentration of lithium ions, leading to reduced energy storage [14]. Mechanical cycling of electrodes can lead to physical breakdown of electroactive

Fig. 3 Tecnam P-Volt aircraft.

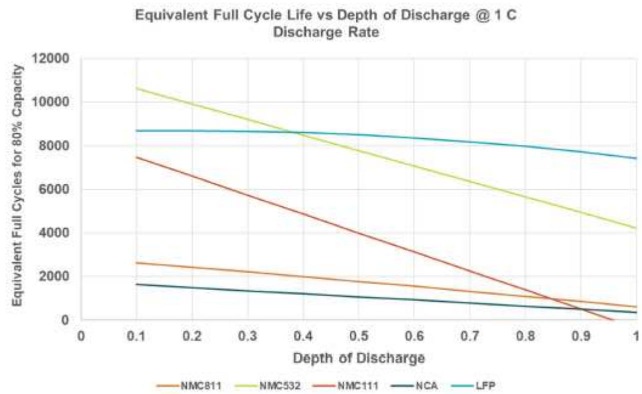

Fig. 4 Battery cycle life behavior.

Table 1 Key characteristics of candidate aerospace battery chemistries

Parameter	NMC 811	NCA	LFP	NMC 532	NMC 111	LFP 2030	NMC 2030
USD/kW-h (pack level)	\$506.80	\$493.82	\$387.95	\$632.38	\$506.80	\$324.00	\$408.00
W-h/kg (pack level)	196	192	144	184	177	223	328
CO_2/kW-h	65.6	69.8	46.7	65.7	67.6	47	65

materials. This phenomenon can increase with higher depths of discharge and discharge rates. It is important to model this behavior when evaluating the battery energy storage system for electric aircraft, as it will have a deep impact on the design of energy storage for the battery electric aircraft.

In addition to performance, cost continuously evolves for various battery chemistries. Costs of raw materials and continuing advances in manufacturing processes and efficiencies have resulted in changing relationships between the costs of differing chemistries. This data forms the basis of the cost optimizations that are discussed later in the paper. Cost premiums for aerospace applications (as compared to higher-volume automotive or other commercial applications) also increase aviation battery costs and negatively impact electric aircraft adoption.

For the purposes of this study, the preceding performance factors presented in Table 1 were used based on an aggregation of data from multiple sources [13,15–21]. This data used the expected prices of commercial automotive battery packs and then imposed a 4x multiplier to account for the lower quantities and more stringent quality/documentation requirements of the aerospace market. The first five columns are based on existing chemistries, while the remaining two are based on optimistic future projections for NMC and LFP chemistries. The pack-level gravimetric energy densities reflect current and anticipated cell energy densities with a 0.8 energy derating factor to account for pack overhead.

III. Methodology

A. Battery-Powered Electric Aircraft Range Equation

While the potential benefits of electric aviation are immense, challenges abound. The weight considerations of batteries directly impact aircraft performance, and the achievable energy density poses constraints both on the achievable range and the energy required to achieve a given mission. This relationship is typically captured by the Breguet range equation, modified as appropriate to reflect the fixed mass of a battery electric aircraft throughout the mission, as opposed to the decreasing mass of a fuel-powered aircraft [22]. This modified equation also includes the depth of battery discharge during a flight, or the percentage of battery capacity used. The Breguet range equation for a full electric aircraft is given as Eq. (1):

Level Flight Range (km):

$$R = 3.6\left(\frac{L}{D}\right)\left(\frac{E_{sb} * \eta_{b2s}\eta_p}{g}\right)\left(\frac{DoD * m_b}{m_b + m_p + m_e}\right) \quad (1)$$

where

3.6—accounts for unit conversions (hours to seconds, meters to kilometers)

L/D—lift-to-drag ratio (16 for this analysis)

E_{sb}—battery specific energy (W-h/kg)

η_{b2s}—system efficiency battery to motor output shaft (90% for this analysis)

η_p—propeller efficiency (85% for this analysis)

g—acceleration due to gravity (9.81 m/s^2)

DoD—depth of battery discharge

m_b—battery mass, kg

m_p—payload mass, kg

m_e—aircraft empty mass, kg

An example of the results seen with variations for the battery specific energy and battery mass fraction is illustrated in Fig. 5. Increasing the battery mass fraction (battery weight as a percentage of overall aircraft weight and/or increasing the battery specific energy) results in corresponding increases in aircraft range. Note that these data account for the relative efficiency differences between electric and fuel-based powertrains.

B. Optimizing Battery Design for Target Aircraft Range Across a Range of Chemistries and Use Cases

The Breguet range equation was used to optimize the battery size for a theoretical nine-passenger small commuter electric aircraft at a target range of 250 km. Examples of this aircraft type in turboprop form include the Cessna Caravan or Pilatus PC-12 in the single-engine configuration, or a Beech King Air in the two-engine configuration. These aircraft have ranges over 1600 km, yet often service routes of less than 500 km [23–25].

The candidate aircraft for this analysis assumed the characteristics presented in Table 2.

A key consideration in this range analysis is the differentiation between normal operational range and absolute maximum range. Regulations require that the aircraft have enough fuel (in this case

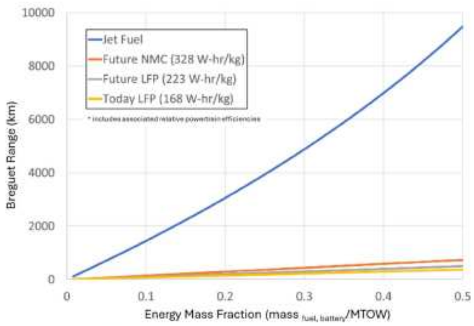

Fig. 5 Breguet range behavior example.

Table 2 Analyzed aircraft characteristics

Characteristic	Assumed value
Cruise lift-to drag ratio	16
Operating empty weight	2050 kg
Payload weight (@ 86 kg/pax)	777 kg
Cruise speed	186 knots
Loiter speed	135 knots
Normal cruise range	250 km
Max cruise range	377 km

batteries) to divert to an alternate landing location and then be able to loiter for a given time period. This analysis assumes daytime VFR conditions, which require no alternate and 30 min of loiter time, which is less stringent than night VFR (no alternate/45 min loiter) or IFR (nearest alternate/45 min loiter) [26].

The tradeoffs in battery chemistry and usage profiles are central to achieving optimal performance in electric aircraft. Low depths of discharge can potentially result in high levels of mission cost and CO_2 emissions due to excessive battery pack size and weight, resulting in higher energy usage and increased manufacturing costs. In contrast, high depths of discharge can potentially result in lighter batteries and lower mission energy usage, yet have unacceptably short battery lifetimes and high replacement costs. Initial calculations utilizing Eq. (1) consider these complex relationships to produce a range of pack sizes and energy requirements based on different DoDs and battery chemistries.

We analyze the economic and environmental influences of battery chemistry and depth of discharge in both normal mission and diversion cases. Calculations are performed to determine the cost of operation on a per-mission basis, given in Eq. (2), and the carbon intensity per mission, given in Eq. (3). These equations consider the cost and carbon impacts of various operational factors like battery service life and replacement intervals and the increased electricity usage of larger battery packs.

$$\mathrm{Cost}_m = \frac{(m_b E_{sb})\frac{\$}{\mathrm{kWh_{batt}}}}{c_{\mathrm{battery}}} + (DoD * m_b E_{sp})\frac{\$}{kWh_{\mathrm{elec}}} \quad (2)$$

$$\mathrm{Carbon}_m = \frac{(m_b E_{sb})\frac{\mathrm{CO_2}}{\mathrm{kWh_{batt}}}}{c_{\mathrm{battery}}} + (DoD * m_b E_{sp})\frac{\mathrm{CO_2}}{\mathrm{kWh_{elec}}} \quad (3)$$

where

m_b—battery mass (kg)
E_{sb}—battery specific energy (W-h/kg)
c_{battery}—total number of battery cycles before replacement
DoD—battery depth of discharge
$\$/\mathrm{kWh_{batt}}$—cost of the battery per kWh
$\$/\mathrm{kWh_{elec}}$—cost of electricity per kWh
$\mathrm{CO_2/kWh_{elec}}$—carbon intensity of electricity production per kWh
$\mathrm{CO_2/kWh_{batt}}$—carbon intensity of battery manufacturing per kWh

Table 3 Electrical grid cost and carbon intensity

Region	2022 carbon intensity, kg CO_2/kWh	2022 cost ($USD/kWh)
World	0.44	$0.12
China	0.53	$0.09
Norway	0.029	$0.12
United States	0.37	$0.15
India	0.63	$0.13
France	0.085	$0.21
Australia	0.50	$0.23
Brazil	0.10	$0.14

The airplane design is iterated with various battery chemistries and depths of discharge to calculate the amount of installed battery capacity, the required electrical energy levels for the mission, and the associated costs and carbon footprints associated with both manufacturing and operation.

C. Geographic Sensitivity

The relative tradeoffs related to energy costs and carbon footprints vary widely based on the area of the world where airline operations occur. The characteristics of the electrical grids in these countries vary widely, from China or India using coal (low cost/high carbon footprint) to France using nuclear (high cost/low carbon footprint) to Norway using hydro (low cost/low carbon footprint). Examples of the 2022 cost and carbon footprint of various national electric grids are presented in Table 3 [27–30]. A reduction in carbon intensities is expected in most world regions over the next decade, with estimated reductions of 20–40%.

D. Operational Sensitivity

An additional area that must also be addressed in how to best operate the aircraft is mission usage, specifically for missions shorter than the design range of the aircraft. As an example, an aircraft may have a design range of 250 km but only be operated on a 50 km route. This gives the airline the option to charge a 250-km-capable battery between every flight, operate up to five flights between charges, or even potentially just install fewer batteries in the aircraft and only have a 50 km range. This choice may result in very different mission costs and carbon footprints depending on the battery chemistry. There are also additional airline operational efficiency and economic implications due to considerations such as aircraft turnaround times between flights, but those are beyond the scope of this paper.

IV. Results

A. Battery Optimization for Candidate Aircraft

Figures 6 and 7 show the outputs of the battery optimization process that includes Eqs. (1), (2), and (3). Figure 6 presents the relationship between depth of discharge and overall mission cost, considering the cost of electricity in the U.S. per-mission and battery replacement cost over its lifetime. Details of the electrical grid inputs are per Table 3, aircraft characteristics per Table 2, and battery characteristics per Table 1 and Fig. 4. While low depths of discharge require less replacement cost over the lifetime of the aircraft, the per-mission energy cost is higher due to its higher battery pack mass. Inversely, higher depths of discharge require more frequent battery pack replacement, offsetting the cost savings from per-mission electricity usage. Note that while these examples illustrate behavior all the way to 100% depth of discharge, that is not a reasonable operating condition for normal flight due to the need to reserve battery capacity for diversion conditions; this is shown by the maximum DoD line at 0.63. For nickel-based chemistries, the per-mission replacement costs of the batteries are approximately 2x and 3x the per-mission electrical costs, while the two are roughly equal for LFP chemistries.

Figure 7 displays the relationship between DoD and the total carbon dioxide emissions per mission. These emissions come from U.S.-based electricity generation per Table 3, aircraft characteristics per Table 2, and battery characteristics per Table 1 and Fig. 4. In this metric, the

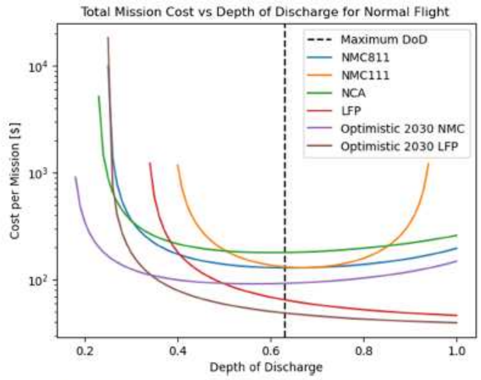

Fig. 6 Total cost behavior versus depth of discharge.

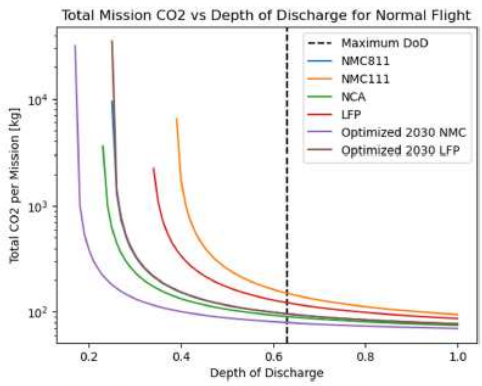

Fig. 7 Total mission CO_2 versus depth of discharge.

carbon impact of the increased electrical energy need far outweighs the carbon impact of battery manufacturing. For all battery chemistries, carbon impact is minimized at the highest possible depth of discharge.

As expected, the behaviors vary between different battery chemistries, as each has its own specific energy density, cycle life, manufacturing cost, and manufacturing carbon footprint. Based on these results, you would then choose the preferred chemistry, battery mass, and depth of discharge at the design mission range based on the optimization parameter of interest (operating $/$CO_2$, battery replacement intervals, etc.).

B. Cost and Carbon Impact When Considering Geographic Sensitivities

The first analysis was performed for a 250 km usable range case across a variety of countries, with the minimum mission level electricity + battery replacement costs and carbon footprints tabulated below for each of the preferred nickel and non-nickel-based battery chemistries. In some cases, multiple minimums (as a function of depth of discharge) occurred depending on whether mission cost or mission carbon was the parameter being minimized. Results of this analysis are presented as Table 4.

As is evident in these results, mission operating costs and carbon footprints can vary dramatically for an aircraft with the same characteristics and range across a variety of countries. Across the four countries and two best chemistries considered, there is $a > 3x$ range in the $/mission cost, and $a > 14x$ range on the per-mission carbon footprint. In every case, the configuration using the LFP battery was significantly less expensive than the NMC alternative, primarily due

Table 4 Mission results by geographic region

Country	Chemistry (DoD where minimum occurred)	Total mission cost (energy + battery)	Mission carbon footprint
China	LFP (.63)	**$33.90**	142 kg
China	NMC (.63)	$79.78	**131 kg**
China	NMC (.56)	$78.20	136 kg
Norway	LFP (.63)	**$41.45**	**10 kg**
Norway	NMC (.63)	$86.02	22 kg
Norway	NMC (.55)	$84.73	22 kg
USA	LFP (.63)	**$48.75**	98 kg
USA	NMC (.63)	$92.05	**95 kg**
USA	NMC (.56)	$91.07	98 kg
France	LFP (.63)	**$64.38**	**25 kg**
France	NMC (.63)	104.97	34 kg
France	NMC (.58)	104.48	34 kg

^a^For reference, a jet-A-fueled aircraft consumes 101 kg of fuel for a comparable mission, with a fuel-only cost of $149.50 and CO_2 emissions of 321 kg.
Bold implies minimum value for particular operational scenario.

to the much smaller battery cost/mission cycle for the LFP, which more than offset the weight increase (and correspondingly higher electricity usage) of the LFP battery. When considering carbon footprint, however, the opposite effect often became apparent. In countries with a high grid carbon footprint, the increased electricity usage due to the heavier battery penalized the LFP battery, resulting in a preference for the more energy-dense NMC chemistries in countries with more carbon-intensive electrical grids. In those countries, however, the cost penalty for that carbon savings is high, with $a > 2x$ cost penalty to achieve $a < 8\%$ carbon reduction.

Another interesting behavior was observed when determining which parameter (cost or carbon footprint) to use for optimization. In the case of the LFP chemistry, both parameters continued to improve up to the limit of the maximum depth of discharge constraint set by the diversion criteria. In the case of the NMC chemistry, however, the cost minimum was reached at an intermediate depth of discharge, while the carbon minimum was reached at the diversion-driven maximum depth of discharge constraint.

C. Cost and Carbon Impact When Considering Operational Sensitivities

The next situation considered was the operation of the aircraft at shorter segments than the design range of the aircraft. In the preceding analysis, mission costs attributable to energy + battery replacement and carbon footprint were considered for a 250 km operating cruise range. Consider instead an airline operating 50 km missions. Using the China case from the earlier analysis and calculating the overall mission cost and carbon footprint for 5×50 km legs generates the results presented in Table 5.

In this situation, maintaining the 250-km-capability battery pack but charging every flight has minimal impact on the cost or carbon footprint of the LFP battery pack but significant favorable impacts on both the cost and carbon footprint of the 250-km-capability NMC

Table 5 Mission results by operational scenario

Operating scenario	Chemistry (DoD)	Total 250 km mission cost	Total 250 km carbon footprint
China (250 km battery, charge every 250 km)	LFP (.63)	**$33.90**	142 kg
China (250 km battery, charge every 50 km)	LFP (.13)	**$33.34**	141 kg
China (50 km battery, charge every 50 km)	LFP (.27)	**$25.10**	105 kg
China (250 km battery, charge every 250 km)	NMC (.63)	$79.78	**131 kg**
China (250 km battery, charge every 50 km)	NMC (.13)	$53.95	**124 kg**
China (50 km battery, charge every 50 km)	NMC (.27)	$47.00	**104 kg**

Bold implies minimum value for particular operational scenario.

pack. Taking the next step and installing a smaller 50-km-capability battery pack has significant additional favorable cost/carbon impacts for the LFP pack, with lesser favorable gains on the NMC pack.

V. Future Prospects and Research Directions

Consideration of the major driving factors in this analysis (energy grid cost/carbon, battery characteristics, operational considerations) reveals many potential extensions of this research. A future definition of the electrical grid, as each geographic area/country evolves its mix of renewable electricity, either country-wide or specific to the aviation sector, could indicate a changing emphasis on the importance of energy usage versus battery behavior. Batteries have historically shown dramatic progressions in performance and cost, and future batteries, such as solid-state could similarly have a dramatic effect on the analysis outcome. Lastly, the operational considerations only considered the impacts on battery lifecycle costs. Charging the batteries every flight (whether needed or not) showed cost and emissions benefits but did not attempt to characterize the negative impacts on maintenance costs, infrastructure, or turnaround time (aircraft productivity). A more comprehensive look at that airline operating ecosystem would be beneficial to better consider the full lifecycle impacts of those choices.

VI. Conclusions

This paper provides a panoramic view of the intricate landscape surrounding battery optimization for electric aircraft. The synthesis of technological advancements, operational considerations, economic analyses, and real-world case studies paints a comprehensive picture of the challenges and opportunities in this dynamic field. As the aviation industry navigates toward a sustainable future, the role of battery optimization emerges as a linchpin for realizing the full potential of electric aircraft.

Acknowledgments

The authors would like to thank Colorado State University and Collins Aerospace for providing inspiration for the research problem statement and support for the execution and presentation of this work.

References

[1] Hunter, J., *Rolls-Royce Focuses on 'the Third Era' of Aviation*, Machinery Market, July 2019, https://www.machinery-market.co.uk/news/24305/Rolls-Royce-focuses-on-%E2%80%98the-third-era-of-aviation.

[2] Ritchie, H., Rodés-Guirao, L., Mathieu, E., Gerber, M., Ortiz-Ospina, E., Hasell, J., and Roser, M., *Population Growth*, Our World in Data, 2023, https://ourworldindata.org/world-population-growth.

[3] Graver, B., *Polishing My Crystal Ball: Airline Traffic in 2050*, International Council on Clean Transportation, Washington, D.C., Jan. 2022.

[4] Ritchie, H., *What Share of Global CO2 Emissions Come from Aviation?*, Our World in Data, April 2024, https://ourworldindata.org/global-aviation-emissions#:~:text=Aviation%20accounts%20for%202.5%25%20of,to%20global%20warming%20to%20date.

[5] Cames, Martin, Graichen, Jakob, Siemons, Anne, and Cook, Vanessa, *Emission Reduction Targets for International Aviation and Shipping*, European Parliament, Europe, 2015, p. 9, https://www.europarl.europa.eu/RegData/etudes/STUD/2015/569964/IPOL_STU(2015)569964_EN.pdf.

[6] Timperley, J., *Why Flight Shame Is Making People Swap Planes for Trains*, BBC, London, Sep. 2019.

[7] Antcliff, K., Borer, N., Sartorius, S., Saleh, P., Rose, R., Gariel, M., Oldham, J., Courtin, C., Bradley, M., Roy, S., et al., *Leveraging Our National Investments to Energize the American Travel Experience.*, *NASA*, NASA, Washington, D.C., 2021, p. 4.

[8] Saxon, S., and Weber, M., *A Better Approach to Airline Costs*, McKinsey & Company, New York, July 2017.

[9] Schäfer, A. W., Barrett, S. R. H., Doyme, K., Dray, L. M., Gnadt, A. R., Self, R., O'Sullivan, A., Synodinos, A. P., and Torija, A. J., "Technological, Economic and Environmental Prospects of All-Electric Aircraft," *Nature Energy*, Vol. 4, No. 2, 2018, pp. 160–166.
https://doi.org/10.1038/s41560-018-0294-x

[10] Sripad, S., and Viswanathan, V., "The Promise of Energy-Efficient Battery-Powered Urban Aircraft," *Proceedings of the National Academy of Sciences of the United States of America*, Vol. 118, No. 45, 2021, Paper e2111164118.
https://doi.org/10.1073/pnas.2111164118

[11] Norris, G., *Tecnam Pulls Plug On Electric P-Volt Project*, Aviation Week Network, New York, June 2023.

[12] Buchmann, I., *BU-205: Types of Lithium-Ion*, Battery Univ., Durant OK, 2017, https://batteryuniversity.com/article/bu-205-types-of-lithium-ion.

[13] Preger, Y., Barkholtz, H. M., Fresquez, A., Campbell, D. L., Juba, B. W., Romàn-Kustas, J., Ferreira, S. R., and Chalamala, B., "Degradation of Commercial Lithium-Ion Cells as a Function of Chemistry and Cycling Conditions," *Journal of the Electrochemical Society*, Vol. 167, No. 12, 2020, Paper 120532.
https://doi.org/10.1149/1945-7111/abae37

[14] Edge, J. S., O'Kane, S., Prosser, R., Kirkaldy, N. D., Patel, A. N., Hales, A., Ghosh, A., Ai, W., Chen, J., Yang, J., et al., "Lithium Ion Battery Degradation: What You Need to Know," *Physical Chemistry Chemical Physics*, Vol. 23, No. 14, 2021, pp. 8200–8221.
https://doi.org/10.1039/D1CP00359C

[15] Burzyński, D., and Kasprzyk, L., "A Novel Method for the Modeling of the State of Health of Lithium-Ion Cells Using Machine Learning for Practical Applications," *Knowledge-Based Systems*, Vol. 219, 2021, Paper 106900.
https://doi.org/10.1016/j.knosys.2021.106900

[16] Olmos, J., Gandiaga, I., Saez-de-Ibarra, A., Larrea, X., Nieva, T., and Aizpuru, I., "Modelling the Cycling Degradation of Li-Ion Batteries: Chemistry Influenced Stress Factors," *Journal of Energy Storage*, Vol. 40, 2021, Paper 102765.
https://doi.org/10.1016/j.est.2021.102765

[17] Krishna, M., *LFP Batteries: The Electric Vehicle Battery Chemistry Debate Just Got More Complicated*, Fastmarkets, July 2022.

[18] Silva, E., and Chen, A., *Batteries: Emerging Chemistries Create Trade-Offs in Cost, Performance*, S&P Global Market Intelligence, New York, June 2023.

[19] Hasselwander, S., Meyer, M., and Österle, I., "Techno-Economic Analysis of Different Battery Cell Chemistries for the Passenger Vehicle Market," *Batteries*, Vol. 9, No. 7, 2023, p. 379.
https://doi.org/10.3390/batteries9070379

[20] Campagnol, N., Erriquez, M., Schwedhelm, D., Wu, J., and Wu, T., *Building Better Batteries: Insights on Chemistry and Design from China*, McKinsey & Company, Chicago, April 2021.

[21] Venditti, B., "Visualized: What Is the Cost of Electric Vehicle Batteries?, *Elements by Visual Capitalist*, Oct. 2023, https://elements.visualcapitalist.com/cost-of-electric-vehicle-batteries/.

[22] Raymer, D. P., *Aircraft Design: A Conceptual Approach*, AIAA, Reston, VA, 2018, p. 757.

[23] Filippone, A., and Parkes, B., "Evaluation of Commuter Airplane Emissions: A European Case Study., Transportation Research Part D," *Transport and Environment*, Vol. 98, 2021, Paper 102979.
https://doi.org/10.1016/j.trd.2021.102979

[24] Cessna Caravan, "Cessna Caravan, 2024, https://cessna.txtav.com/en/turboprop/caravan [retrieved 14 May 2024].

[25] PC-12 NGX, "Pilatus Aircraft Ltd.," 2024, https://www.pilatus-aircraft.com/en/fly/pc-12 [retrieved 14 May 2024].

[26] 14 CFR Part 91, *General Operating and Flight Rules*, *Code of Federal Regulations*, 2024, https://www.ecfr.gov/current/title-14/chapter-I/subchapter-F/part-91 [retrieved 15 May 2024].

[27] Electricity Prices, "GlobalPetrolPrices.com," 2024, https://www.globalpetrolprices.com/electricity_prices/.

[28] Statistica Research Department, "Statistica Research Department, Household Electricity Prices Worldwide in December 2023, by Select Country," Statista, Germany, July 2024, https://www.statista.com/statistics/263492/electricity-prices-in-selected-countries/.

[29] Tiseo, I., *Power Generation CO2 Intensity Outlook by Region*, Statista, Germany, June 2023, https://www.statista.com/statistics/1257765/global-emission-intensity-electricity-generation-region/.

[30] Ember and Energy Institute, *Carbon Intensity of Electricity Generation*, Our World in Data, 2024, https://ourworldindata.org/grapher/carbon-intensity-electricity?tab=table.

B. Stanford
Associate Editor